# A FIELD CONSOLIDATION STUDY OF HIGH ASH PAPERMILL SLUDGE

Thesis for the Degree of Ph. D.
MICHIGAN STATE UNIVERSITY
ROBERT P. VALLEE
1973



This is to certify that the

thesis entitled

A FIELD CONSOLIDATION STUDY OF HIGH ASH

PAPERMILL SLUDGE

presented by

Robert P. Vallee

has been accepted towards fulfillment of the requirements for

Ph.D. degree in <u>Civil Engin</u>eering

O.B. Wandersolans.

Date 19,1913

0-7639

LIBRARY
Michigan State
University

3 433

#### ABSTRACT

# A FIELD CONSOLIDATION STUDY OF HIGH ASH PAPERMILL SLUDGE

Вy

#### Robert P. Vallee

An experimental papermill sludge landfill was constructed and monitored to obtain engineering information essential to the development of guidelines and recommendations for the design and operation of solid papermill waste landfills. Papermill sludge is an organic clay material consisting of 32 to 59% kaolinite and having an initial water content of about 260%. The non-clay fraction is primarily organic cellulose fibers. The experimental landfill consisted of 2 sludge layers, each initially 10 ft. thick, with sand drainage blankets at the top, middle, and bottom. An earth dike provided lateral confinement of the soft sludge both during and after construction. A surface load, consisting of 3 ft. of natural soil, was placed immediately after construction. The landfill was instrumented with 32 settlement plates, 16 piezometers, 3 total pressure cells, and 10 thermistors. Field data obtained during the first year included settlements, pore water pressures, vertical and lateral earth pressures, temperatures, sludge unit weights, specific gravities, and water contents. Laboratory work included consistency limits, ash contents, and consolidation tests run on both fresh and undisturbed samples of sludge. A detailed description of the field

behavior is given in the thesis along with predictions based on laboratory results and soil mechanics theory. For each sludge layer the ultimate settlement, time-rate of settlement, and pore pressure dissipation are discussed in detail. Several theories that include secondary compression throughout the consolidation process are included in the analyses, along with Terzaghi's theory. The lower sludge layer was loaded gradually (by the upper layer) with time, and its consolidation behavior is modeled using a computer program to account for the slow loading. Pore pressures generated during construction and those existing at the end of primary compression (residual) are analyzed and discussed. Laboratory consolidation data from the undisturbed samples are discussed in detail.

It is shown that soil mechanics theory can be used to accurately model the sludge consolidation behavior for different conditions of loading. Ultimate primary settlements can be reasonably estimated if appropriate pore pressure changes and void ratio considerations are included in the settlement analysis. Secondary compression is difficult to predict from laboratory parameters. The hydrodynamic portion of the time-settlement relation is accurately modeled by Terzaghi's (1943) theory, Gibson and Lo's (1961) theory, and Wahls's (1962) theory, when a representative value for the coefficient of consolidation is used. Laboratory consolidation tests underestimated this parameter by a factor of four or more. Consolidation theory can be used to predict pore pressures up to about 70 percent dissipation. Residual pore pressures were observed in the sludge at the completion of primary compression. Pore pressures generated during construction were in general agreement

with predicted values based on Gibson's (1958) theory. The coefficient of lateral stress decreased from an initial value close to 0.65 immediately after sludge placement to about 0.32 for the final stages of consolidation.

# A FIELD CONSOLIDATION STUDY OF HIGH ASH PAPERMILL SLUDGE

Ву

Robert P. Vallee

# A THESIS

Submitted to
Michigan State University
in partial fulfillment of the requirements
for the degree of

DOCTOR OF PHILOSOPHY

Department of Civil Engineering

G god is L

To Lindsa

who helped me discover the joy of learning

#### **ACKNOWLEDGEMENTS**

The writer wishes to express his appreciation to his major professor, Dr. O. B. Andersland, Professor of Civil Engineering, whose initiative and hard work resulted in the realization of this project, and who provided valuable guidance during the preparation of this thesis. Thanks go also to the members of the writer's doctoral committee: Dr. R. R. Goughnour, former Professor of Civil Engineering; Dr. W. A. Bradley, Professor of Metallurgy, Mechanics, and Materials Science; and to Dr. M. M. Mortland, Professor of Soil Science. The writer also owes his appreciation to: Dr. John M. Paloorthekkathil for performing the Atterberg Limit tests; Mr. Wayne A. Charlie for obtaining the undisturbed sludge samples; Mr. Tom Danis Sr. of the B. G. Danis Co., Dayton, Ohio for his help and cooperation during construction of the landfill; and to my wife, Lindsa, who helped type the manuscript and gave me encouragement throughout my graduate work. Special appreciation is also given to my parents and Lindsa's parents for their continuing support and interest in my work.

Thanks are also due to the U. S. Environmental Protection

Agency and the National Council of the Paper Industry for Air and Stream

Improvement, Inc. for their financial assistance and cooperation which

made this research possible.

# TABLE OF CONTENTS

																				Page
DEDIC	AT	ION .	•	•	•	•		•	•			•				•	•	•	•	ii
ACKNO	WL:	EDGMEN	TS		•	•		•				•			•	•	•	•	•	iii
LIST	OF	TABLE	S	•	•	•	•	•	•			•	•			•	•	•	•	vii
LIST	OF	FIGUR	ES			•		•	•			•				•	•	•	•	viii
LIST	OF	SYMBO	LS	•		•	•	•		•			•	•	•	•			•	xii
Chapt	er																			
I.		INTROD	UCTI	ON				•								•	•			1
		1.1 1.2		ed E			-	Stud	• Iv	•	•		•	•	•	•	•	•	•	1 2
II.	]	PAPERM		•					-		•	•	•	•	•	•	•	•	•	_
	]	LITERA	TURE	E RE	VII	EW	•	•	•	•	•	•	•	•	•	•	•	•	•	5
		2.1 2.2						ce Theo	-						•	•	•	•	•	5 7
III.		EVALUA CHARAC						ENGI	NEE	ERIN	•			•			•	•	•	25
		3.1						rtie		•	•	•	•	•	•	•	•			25
				L.1 L.2	Ur	nit	We	onte ight	:	•	•		•	•	•	•	•	•		25 27
				L.3 L.4				c Gr tent					onte			•	•	•	•	28 28
				L.5				ency					•			•	•	•	•	29
		3.2						tion						s	•	•	•	•	•	30
				2.1				dati						•	•	•	•	•	•	30
			3.2	2.2	Ur	ndra	aine	ed S	hea	ar S	Stre	ngt	h		•		•	•		33

Chapte	r			Page
IV.		RUCTION, INSTRUMENTATION ONITORING	•	38
	4.1	Construction of the Experimental Landfill	•	38
		4.1.1 Site Preparation and Dike Construction .		38
		4.1.2 Sludge Placement		40
		4.1.3 Drainage Blanket Placement		41
		4.1.4 Earth Surcharge Placement		42
	4.2			43
		4.2.1 Settlement Plates		43
		4.2.2 Piezometers		45
		4.2.3 Total Pressure Cells		46
		4.2.4 Temperature Sensors		47
		4.2.5 Vane Shear Tests	•	47
V.	EXPERI	MENTAL RESULTS		58
	5.1	Physical Properties of the Papermill Sludge		58
	5.2	• •		59
	3.2	5.2.1 Laboratory Consolidation		59
		5.2.2 In-place Vane Shear Tests		61
	5.3	Field Monitoring		62
		5.3.1 Settlement		62
		5.3.2 Pore Water Pressures		63
		5.3.3 Temperature		64
		5.3.4 Lateral Sludge Pressures	•	64
VI.	DISCUS	SSION AND INTERPRETATION OF RESULTS	•	105
	6.1	Sludge Placement	•	105
	6.2	Engineering Characteristics of the		
		Papermill Sludge	•	106
		6.2.1 Physical Properties	•	106
		6.2.2 Consolidation Behavior	•	108
		6.2.3 Undrained Shear Strength	•	113
		6.2.4 Stress State in the Sludge	•	114
		6.2.5 Temperature	•	115
	6.3	Settlement Behavior of the Landfill	•	116
		6.3.1 Upper Sludge Layer	•	117
		6.3.1.1 Loading and Field Observations		117
		6.3.1.2 Ultimate Settlement		120
		6.3.1.3 Time-rate of Settlement		124
		6.3.1.4 Pore Pressure Dissipation	•	128
		6.3.2 Lower Sludge Layer	•	133
		6.3.2.1 Loading and Field Observations		133
		6.3.2.2 Ultimate Settlement		134
		6.3.2.3 Time-rate of Settlement		135
		6.3.2.4 Pore Pressure Dissipation		139

Chapte	r				Page
VII.	SUMMARY AND CONCLUSIONS	•	•	•	163
	7.1 Field Consolidation		•	•	163
	7.1.1 Settlement			•	164
	7.1.2 Pore Pressures		•	•	165
	7.1.3 Stress and Temperature Conditions				166
	•				200
REFERE	NCES	•	•		168
APPEND:	ICES	•	•	•	172
Α.	Settlement Data			•	173
В.	Piezometer Data			•	177
C.	Pressure Cell Data	•	•	•	179
D.	Temperature Data		•	•	180
Ε.	Vane Shear Strength Data		_		181
F.	Consolidation Data	•		-	183
G.	Computer program for load increasing linearly	•	•	•	103
•	with time followed by an instantaneous surcharge				
	application				204
н.	Computer program for the solution to the	•	•	•	204
11.	equations in the theory of Gibson and Lo (1961)				207

# LIST OF TABLES

Table				Page
5.1	Physical properties of the papermill sludge		•	66
5.2	Sludge placement water contents	•	•	67
5.3	Summary of consolidation characteristics, fresh sludge	•		68
5.4	Summary of consolidation characteristics, undisturbed samples	•		71
6.1	Comparison of actual and calculated settlements	•		141
A-1	Settlement plate elevations at the bottom sand blanket	•	•	173
A-2	Settlement plate elevations at the midpoints of the lower and upper sludge layers	•	•	174
A-3	Settlement plate elevations at the middle sand blanket	•	•	175
A-4	Settlement plate elevations at the top sand blanket .	•	•	176
B-1	Pore water pressures for the bottom sand blanket and lower sludge layer	•		177
B-2	Pore water pressures for the middle sand blanket and upper sludge layer	•	•	178
C-1	Total pressure cell data	•	•	179
D-1	Temperature data for the papermill sludge landfill .	•	•	180
E-1	Undisturbed vane shear strengths	•	•	181
E-2	Remolded vane shear strengths	•	•	182
F-1 t	o 7 Conventional consolidation data	•	•	183
F-8 t	o 12 Bishop consolidation data	•	•	190
F-13	& 14 Single increment Bishop consolidation data	•	•	195
F-15	to 19 Undisturbed sample consolidation data	•	•	198

# LIST OF FIGURES

Figure			Page
2.1	The settlement problem: (a) Section through a sludge landfill (b) Volume-void ratio relationships		22
2.2	Models for the consolidation process: (a) Gibson and Lo (1961) (b) Wahls (1962)	•	23
2.3	Void ratio - effective stress relationships for a normally consolidated clay	•	24
3.1	Time-compression curves: (a) Primary and secondary compression (b) Definitions		35
3.2	(a) Consolidation machine and recorder (b) Fixed ring consolidation unit and sludge sample		36
3.3	Vane shear apparatus	•	37
4.1	Pre-construction map of existing gravel pit area including dike layout	•	50
4.2	Experimental landfill and instrument group locations, plan view		51
4.3	Section of landfill (typical), north dike at end of construction		52
4.4	Sludge placement: (a) Dragline operation (b) Dumping over the dike sides	•	53
4.5	Experimental sludge landfill during placement of the lower sludge layer	•	54
4.6	Settlement plate: (a) Installation in a sand blanket (b) Placement in the sludge, carpenters level shown on plate	•	55
4.7	Distribution of settlement plates, piezometers, and total pressure cells in the instrument groups	•	56
4.8	Piezometer: (a) Pore pressure transducer (b) Installation in a small sand pocket in the sludge		57

Figure		Page
5.1	Water contents of the sludge in the landfill at the end of consolidation	73
5.2	Consolidation characteristics for sludge sample U-5: (a) Void ratio (b) Coefficient of consolidation, c (c) Primary compression ratio, r	74
5.3	Compression dial reading versus logarithm of time: (a) Load increment $0.1\text{-}0.2~\text{kg/cm}^2$ (b) Load increment $0.4\text{-}0.8~\text{kg/cm}^2$	75
5.4	Coefficient of secondary compression, $C_{\alpha}$ : (a) $C_{\alpha}$ versus $\log \bar{p}$ (b) $C_{\alpha}/\Delta p$ versus $\log \bar{p}$	76
5.5	Void ratio-effective stress relationships, undisturbed sludge samples	77
5.6	Consolidation characteristics for the undisturbed sludge samples: (a) Coefficient of consolidation, c (b) Primary compression ratio, r (c) Coefficient of secondary compression, C  ,	78
5.7	Vane shear strengths of the sludge in the landfill:  (a) After completion of each sludge layer and after partial consolidation, hand driven vane test  (b) Immediately prior to slope excavation, vane test run with pre-augered hole	79
5.8	Settlement-time curves: (a) Group 1 (b) Group 2 (c) Group 3 (d) Group 4 (e) Group 5 (f) Group 6 (g) Group 7 (h) Group 8	81
5.9	Settlement versus square root of time curves, upper sludge layer: (a) Groups 1 through 4 (b) Groups 5 through 8	89
5.10	Settlement-logarithm of time curves, upper sludge layer: (a) Groups 1 through 3 and 7 (b) Groups 4 through 6 and 8	91
5.11	Settlement-logarithm of time curves, lower sludge layer after surcharge placement: (a) Groups 1, 2, 3, and 4 (b) Groups 5, 6, 7, and 8	93
5.12	Pore pressure versus time curves: (a) Group 5, piezometers 3 and 6 (b) Group 5, piezometers 2 and 7 (c) Group 5, piezometers 4 and 8 (d) Group 6 (e) Group 7, piezometers 3 and 6 (f) Group 7,	
	piezometers 4 and 7 (g) Group 5, piezometers 5	95

Figure			Page
5.13	Temperature versus time: (a) Thermistors 1, 3, 5, 7, and 9 (b) Thermistors 2, 4, 6, 8, and 0	•	102
5.14	Horizoncal and vertical total stresses, lower sludge layer	•	104
6.1	Typical stress-strain curves for papermill sludge at 43% and 50% organic contents (Andersland and Laza, 1971).	•	142
6.2	Comparison between the measured leachate flow rate and the flow rate calculated from time-settlement curves.	•	143
6.3	Estimated effective stress changes and strain distribution in the upper sludge layer: (a) initial stresses (b) Final stresses (c) Strain distribution .	•	144
6.4	Parameter determination for the method of Gibson and Lo	•	145
6.5	Measured residual excess pore pressures versus depth .	•	146
6.6	Comparison of actual and predicted time-settlement curves, upper sludge layer: (a) Terzaghi (1943) theory, settlement vs. time (b) Terzaghi (1943) theory, settlement vs. logarithm of time (c) Theory of Gibson and Lo (1961), settlement vs. logarithm of time (d) Wahls's (1962) theory, settlement vs. logarithm of time		147
6.7	Pore pressure increase due to application of the upper sand blanket and surcharge: (a) Group 5, upper layer (b) Groups 6 and 7, upper layer (c) Group 5, lower layer (d) Groups 6 and 7, lower layer	•	151
6.8	Comparison of measured and predicted initial pore pressures, upper sludge layer	•	152
6.9	Comparison of measured and predicted pore pressure, mid-point of upper sludge layer: (a) Terzaghi's (1943) theory (b) Theory of Gibson and Lo (1961)	•	153
6.10	Theoretical final pore pressure distribution at the end of consolidation if a threshold gradient exists	•	155
6.11	Comparison of initial, maximum, and residual pore pressures, upper sludge layer		155
6.12	Estimated effective stress changes and strain distri- bution in the lower sludge layer: (a) Initial stresses (b) Final stresses (c) Strain distribution .	•	156

Figure		Page
6.13	Load increasing linearly with time followed by an instantaneous surcharge application	157
6.14	Estimates of ultimate settlement of the lower sludge layer for different elevations of the upper sludge layer	158
6.15	Comparison between the predicted and measured time- settlement curves, lower sludge layer: (a) Finite difference solution (b) Terzaghi procedure for a linearly increasing load	159
6.16	Comparison between predicted and measured pore pressures at the mid-point of the lower sludge layer	161
6.17	Measured and estimated initial excess pore pressures in the lower sludge layer	162

#### LIST OF SYMBOLS

- a = Primary Compressibility of the soil skeleton, in 2/1b
- a = Coefficient of compressibility
- b = Secondary compressibility of the soil skeleton,  $in^2/1b$
- c = Distance to the mid-point of a doubly drained clay layer at t = 0
- C = Compression index
- c = Coefficient of consolidation
- $C_{\alpha}$  = Coefficient of secondary compression
- $C_F = (1 + e_0)/(1 + e) \cdot c_v$
- D = Total oedometer compression for an increment of load
- d, = Initial compression in oedometer for an increment of load
- d = Primary compression in oedometer for an increment of load
- d = Secondary compression in oedometer for an increment of load
- e = Void ratio
- $G_s$  = Specific gravity of the soil solids
- H = Thickness of sludge layer or sample
- H = Thickness of sludge layer or sample at the end of primary consolidation
- i = Hydraulic gradient
- i = Threshold hydraulic gradient
- k = Coefficient of permeability
- K = Ratio of horizontal effective stress to vertical effective
   stress
- L = Liquid limit

m = Coefficient of volume compressibility

p = Pressure

p = Effective pressure

p<sub>u</sub> = Plastic limit

q = Applied surface load

0 = Leachate flow rate from drain pipe

r = Primary compression ratio, <sup>d</sup>p/D

S(t) = Settlement as a function of time

t = Time

t = Time assumed for the end of primary compression

 $t_s$  = Time of surcharge application

T. = Time factor

u = Excess hydrostatic pore pressure

U = Percent consolidation

 $u_r$  = Residual excess pore pressure

v = Nominal flow rate of pore fluid

V = Volume

w = Water content

z = Depth to a point in a soil layer

 $\gamma_{w}$  = Unit weight of water

 $\gamma_d$  = Dry unit weight

 $\Delta$  = Increment

 $\delta_1$  = Settlement at time  $t_1$ 

 $\delta_2$  = Settlement at time  $t_2$ 

 $\varepsilon$  = Strain at a point

g = Effective normal stress

 $1/\lambda$  = Viscosity of the soil structure, lb-sec/in<sup>2</sup>

#### CHAPTER I

#### INTRODUCTION

#### 1.1 Need for Study

Solid wastes resulting from the pulp or paper making process are removed from effluent streams by treatment devices designed to protect the nation's surface water resources. An estimated 2,500,000 dry tons of solid residue are removed annually (Gillespie, Gellman, and Janes, 1970) giving a sludge cake volume close to 200 million cubic yards. The great majority of these sludges are disposed of on land. A survey (Gillespie, 1969) by the National Council of the Paper Industry for Air and Stream Improvement, Inc., indicated that more than 1100 acres of land are in use as sludge depositories. Sludge disposal on land, in most cases, lacks long range planning, hence it is achieved on a temporary rather than a permanent basis. Thorough planning would include the application of sound engineering principles to all stages of site selection, design, operation, and completed use of the landfill.

To facilitate this planning, it is essential to have an understanding of the many variables that will affect landfill volume change, settlement, slope stability and bearing capacity. In anticipation of the industry's need for information on satisfactory disposal practices, the National Council of the Paper Industry for Air and Stream Improvement conducted both a questionnaire survey of current land disposal practices (Gillespie, 1969) and a core sampling investigation of existing sludge

deposits (Gillespie, Mazzola, and Gellman, 1970). The core sampling program showed that in situ sludge water contents were higher than those normally encountered in clay soils, with large variations occurring in the vertical direction. These high water contents suggest that large settlements can be expected under surface loads. Field vane shear strengths ranged from 0.12 to 0.37 kg/cm<sup>2</sup> indicating low in-situ sludge stability. Experimental laboratory data (Andersland and Laza, 1971; Andersland and Paloorthekkathil, 1972) have demonstrated the influence of a number of variables on the shear strength, permeability, and consolidation behavior of papermill sludge. The task remained to verify, with field observations, the accuracy of predictions (based on laboratory data) of settlement, drainage, and stability for a constructed landfill.

# 1.2 Objectives of Study

The general objective of the study is to contribute—through field observations on an experimental landfill, laboratory work, and analysis—basic information, relative to the sludge behavior, which is needed for developing guidelines and recommendations for the design and operation of solid papermill waste landfills. It is desirable that the completed sludge landfill be stable and have the potential for a number of uses, including use as a recreational area or as a foundation for light construction. Pursuant to this general objective the research program was directed at the consolidation behavior of the landfill. Specific items relative to consolidation behavior include:

1. Dewatered pulp and papermill sludges from different mills may have consistencies which require different placement techniques.

Effectiveness of placement methods used at the experimental site will be summarized.

- 2. Consolidation parameters, which include the compression index, coefficient of consolidation, and coefficient of secondary compression, are useful in prediction of settlement in soils. Comparisons will be made between the observed field behavior and predictions based on these experimental sludge parameters. These predictions have implications relative to landfill capacity, settlement of future structures built on the landfill, and flow rate and volume of drainage effluent. Various theories used to mathematically model the consolidating sludge will be reviewed and their application to the sludge landfill discussed. The laboratory parameters will be determined for both fresh sludge samples and for undisturbed samples obtained from the landfill at the completion of consolidation.
- 3. Surcharge loads used in combination with drainage blankets are an effective means for improving the drainage of certain peat and clay soils. Use of this method in the experimental sludge landfill will be evaluated as to its potential for obtaining better sludge drainage. This should result in increased sludge shear strength and improved landfill stability. In-situ vane shear tests will be run to determine the increase in shear strength with consolidation.
- 4. The magnitude of effective lateral stresses has implications relative to stability analyses involving bearing capacity and slope stability.

  The observed change in lateral stresses during sludge placement, surcharge loading, and consolidation will provide insight as to the actual stress distribution existing in the sludge.

The field research site was selected in collaboration with the

National Council of the Paper Industry for Air and Stream Improvement, Inc., and the host papermill. The experimental landfill site, the dewatered sludge (including hauling to the site), and field laboratory space were provided by the host papermill. A local contractor constructed the earth dikes and placed the dewatered papermill sludge and sand drainage blankets during the summer and fall of 1971. The author supervised construction of the landfill, took initial sludge samples, installed instrumentation, and initiated field monitoring of the landfill. Physical properties and certain stress-deformation characteristics of the sludge were obtained using the soil mechanics laboratory facilities at Michigan State University.

#### CHAPTER II

#### LITERATURE REVIEW

Information directly oriented to the design and operation of papermill sludge landfills is very limited. Most of the literature concerns the separation and concentration of solids from the papermill waste, with very limited planning and application of engineering principles to disposal of the sludge cake on land. Current practices depend on land available, haul distance, nuisance condition, and local requirements for sanitary landfills. Settlement data for these sludge landfills is essentially nonexistent except for some laboratory research.

# 2.1 Current Practice

Sludge disposal procedures followed at a particular mill are dependent, to some extent, on the quantity and nature of the sludge produced. Sludge removed from a primary clarifier may range from 1 to 15 percent solids by weight and have an ash content as high as 70 percent. This low consistency undewatered sludge is in some cases pumped to earthen basins, lagoons, or drying beds for natural dewatering. The earthen basins or drying beds require adjacent soils which are relatively permeable, such as sands or gravels. After dewatering by natural drainage, the sludge cake may be covered with soil and left in place indefinitely, or may be excavated and hauled to some more distant landfill. Gillespie (1969) states that data available for drying beds are

too erratic to allow meaningful conclusions to be drawn on the performance of this type of dewatering. In some cases long pipelines have been constructed to transport these fluid sludges to large abandoned pits, especially when the calculated use period exceeds five years. The life of these pits was usually extended by the construction of dikes to retain more sludge. Very often, odors emanating from the lagoons or drying beds during warm weather have become a nuisance to local residents and property owners. The practice of pumping clarifier sludge to earthen basins is limited to smaller mills where the volume of sludge production is low and where land is available. In most instances this practice lacks long range planning and solves the disposal problem on a temporary rather than a permanent basis.

More recent disposal developments (Follet and Gehm, 1966) include the dewatering of the clarifier sludge by means of centrifugation, vacuum filtration, or mechanical pressing. The resulting sludge cake may have a solids content as high as 40 percent (equivalent to 150 percent water content) for the high ash sludges. The dewatered sludge is hauled by truck to the disposal site, in some cases as far as five miles from the mill. The disposal sites often are abandoned gravel pits, low lying areas, or other such lands depreciated through use. The sludge is dumped at the site and distributed with suitable earth moving equipment. In a few instances, a cell type of landfill with individual compartments separated horizontally and vertically with a porous material has been used. The resulting slow drainage has helped to decrease the volume occupied by the residue. Limited information on sludge stability and sludge drainability has hindered the development of this approach to organized landfill operations. This project is intended to provide

information relative to the field consolidation of dewatered sludge so that the necessary guidelines and recommendations for the design and operation of papermill sludge landfills can be developed.

# 2.2 Consolidation Theory

Natural drainage of water from sludge deposits results in a decrease in volume with an accompanying settlement of the surface. This volume change may occur almost entirely in the vertical direction, approximating one-dimensional compression. The application of surface loads from additional sludge, soil cover, or construction serves to increase this volume change or settlement. This phenomenon has been observed for existing sludge deposits containing high in-situ water contents. For organized landfill operations it is desirable to predict this volume change so as to permit the estimation of total sludge capacity of a landfill and to predict the settlement of any constructed facilities placed on the sludge landfill.

Very little published information is available regarding the settlement of papermill sludge landfills. Accordingly, one goes to related areas, such as soil mechanics, and borrows those theories which appear to describe the sludge behavior. Consolidation theory involves the development of an equation from which pressure and void ratio values may be computed at any point and time in a stratum of consolidating material. From such an equation the change in overall thickness of the strata after any interval of time may be determined by integration or numerical computation. To illustrate the application of certain consolidation concepts, consider a section through a sludge landfill as shown in Figure 2.1a. If it is assumed that leachate drainage results in one-dimensional compression, i.e. volume change occurs only in the vertical

direction as settlement, then the change in sludge layer thickness,  $\Delta H$ , per unit of thickness,  $H_o$ , equals the change in volume,  $\Delta V$ , per unit of original volume  $V_o$ . It is convenient to work with a small sludge sample, which can be represented as shown in Figure 2.1b. Volume-void relationships show that  $\Delta V/V_o = \Delta e/(1+e_o)$ , where  $\Delta e$  is the change in void ratio and  $e_o = V_v/V_s$  is the initial void ratio expressed in terms of the initial void volume,  $V_v$ , and the solids volume,  $V_s$ . Now the settlement,  $\Delta H$ , can be computed as

$$\Delta H = H_0 \frac{\Delta e}{1 + e_0} \tag{2.1}$$

The initial sludge layer thickness,  $\rm H_{0}$ , and the average initial void ratio,  $\rm e_{0}$ , can be determined. The problem now becomes one of determining the relationship between void ratio and effective normal stress (loads) and how effective normal stress changes with drainage of water from the sludge. The theory and procedures needed are given in various references (Lambe and Whitman, 1969; Leonards, 1962; Lambe, 1951).

These procedures are based entirely on Terzaghi's (1943) one-dimensional consolidation theory, and although this theory is widely accepted, it includes certain assumptions that may not apply to papermill sludge. To determine the significance of these assumptions, several theories are reviewed below which include one or several of the assumptions in their mathematical formulation. The theories of Wahls (1962) and Gibson and Lo (1961) are included in the settlement analysis of the sludge landfill and are discussed in detail. Among Terzaghi's assumptions are: (1) the time lag of compression is caused exclusively by the low permeability of the material (ignores secondary compression), (2) constant soil compressibility during the load increment (assumes a linear

stress-strain relation), (3) Darcy's law is valid at low hydraulic gradients (no threshold gradient), and (4) small strain theory is valid.

A theory proposed by Gibson and Lo (1961) for the consolidation of soils exhibiting secondary compression involves the representation of the soil skeleton by the mathematical model shown in Figure 2.2a. In this rheological model, primary compression is represented by the transfer of stress from the pore water to the soil skeleton resulting in an effective stress,  $\sigma(t)$ , which causes compression of the Hookean spring a. This effective stress is also applied to the Kelvin element, but its compression is retarded because of the presence of the dashpot ' $\lambda$ '. The effective stress is thus initially carried entirely by the viscous dashpot, but as time passes the stress is transferred to spring b, resulting in secondary consolidation. Since the transference of stress from pore water to soil skeleton is delayed due to the low permeability of the soil, the effective stress  $\sigma(t)$  increases gradually and hence the compression of spring a is also gradual. Secondary compression is controlled by the viscous resistance of the soil skeleton and can occur simultaneously with primary compression, thus eliminating assumption (1) above.

Gibson and Lo (1961) consider stress and compatibility conditions in the Kelvin element, yielding

$$\frac{f}{b} + \frac{1}{\lambda} \frac{df}{dt} = \overline{\sigma}(t) \tag{2.2}$$

where b is the secondary compressibility, f is the strain in spring b,  $\frac{1}{\lambda}$  is the viscosity of the soil structure (dashpot '\lambda'), and t is the time after load application. Solving this equation helps to yield the

stress-strain relationship

$$\varepsilon = a\overline{\sigma}(t) + \int_{0}^{t} \frac{-\lambda}{\sigma(\tau)} e^{\frac{\lambda}{b}(t - \tau)} d\tau$$
 (2.3)

where a is the primary compressibility, and  $\tau$  is a dummy variable. Considering continuity of flow of water through an element of soil, Gibson and Lo (1961) write

$$\frac{k}{\gamma_W} \frac{\partial^2 \overline{\sigma}(t)}{\partial Z^2} = \frac{\partial \varepsilon}{\partial t}$$
 (2.4)

where k is the permeability of the soil,  $\epsilon$  is the vertical strain at a point,  $\gamma_w$  the unit weight of water, and Z is the distance from the surface of a soil layer with an impermeable base. Combining equations 2.3 and 2.4 yields the one-dimensional equation of consolidation

$$\frac{k}{\gamma_w} \frac{\partial^2 \overline{\sigma}(t)}{\partial z^2} = a \frac{\partial \overline{\sigma}(t)}{\partial t} + \lambda \overline{\sigma}(t) - \frac{\lambda^2}{b} \int_0^t \overline{\sigma}(Z, \tau) e^{-\frac{\lambda}{b}(t - \tau)} d\tau \qquad (2.5)$$

Gibson and Lo (1961) solve this equation, for the appropriate boundary conditions, by the use of Laplace Transforms and the Convolution Theorem. The solution for a step (instantaneous) load,  $\mathbf{q}_0$ , yields the following expression for settlement:

$$S(t) = (a + b)q_0H \left(1 + \frac{8}{\pi^2} \sum_{n=odd}^{\infty} \frac{1}{n^2} \left[ \left(\frac{K-x_1}{x_1-x_2}\right) e^{-x_2t} - \left(\frac{K-x_2}{x_1-x_2}\right) e^{-x_1t} \right] \right)$$
(2.6)

where H = thickness of the soil layer,  $K = \frac{a}{a+b} K_1$ ,  $K_1 = \frac{n^2 \pi^2 c_v}{4H^2}$ ,

$$c_{v} = \frac{k}{a\gamma_{w}}, \quad \frac{x_{1}}{x_{2}} = \frac{(\alpha + K_{1})^{2} + \sqrt{[(\alpha + K_{1})^{2} - 4\beta K_{1}]}}{2}, \quad \alpha = (\frac{1}{a} + \frac{1}{b})\lambda, \text{ and}$$

 $\beta = \frac{\lambda}{b}$  . The pore pressure is given by the expression

$$u = \frac{4}{\pi} \frac{a+b}{a} q_0 \sum_{n=odd}^{\infty} \frac{1}{n} \left( \frac{x_1 \left(\frac{a}{a+b} - \frac{x_2}{K_2}\right) - x_1 t}{x_1 - x_2} e^{-x_1 t} - \frac{x_2 \left(\frac{a}{a+b} - \frac{x_1}{K_1}\right) - x_2 t}{x_1 - x_2} e^{-x_2 t} \right) \sin \frac{n\pi Z}{2H}$$
(2.7)

For a soil which is infinitely viscous  $(\lambda \rightarrow 0)$  or exhibits no secondary compression (b $\rightarrow 0$ ) the above equations reduce to those of the classical solution of Terzaghi.

These equations have been programmed for solution by computer and the program is given in appendix H. The program assumes that the soil layer is doubly drained and solves for the settlement and pore pressures (at the eighth points of the layer) for each specified time. The thickness of the layer is adjusted after each settlement computation to maintain the appropriate length of drainage path.

For large values of time the settlement becomes

$$S(t) = q_0 H \left[ a + b \left( 1 - e^{\frac{\lambda}{b}t} \right) \right] \qquad t \ge t_a$$
 (2.8)

and in the limit  $t\rightarrow 0$ , the ultimate settlement of the layer is given as

$$S_{ult} = (a + b)q_0H$$
 (2.9)

To determine the parameters a, b, and  $\lambda$  it is necessary to plot a graph of  $\log_{10}(\delta_2 - \delta_1)$  vs.  $t_1$ , where  $\delta_2$  and  $\delta_1$  are the settlements at times  $t_2$  and  $t_1$ , respectively, and  $t_2 - t_1 = \Delta t = \text{constant}$ . Using equation

2.8 the following expression is derived.

$$\log(\delta_2 - \delta_1) = \log I - .434 \frac{\lambda}{b} t_1$$
 (2.10)

where I =  $q_0Hb(1 - e^{-\frac{\lambda}{b}}\Delta t)$ . The intercept of the graph represents log I, thus

$$b = \frac{I \times 10^{-4}}{\frac{-\lambda}{b} \Delta t}$$

$$q_0 H (1 - e^{-\lambda})$$
(2.11)

The slope of the line is given by .434  $\frac{\lambda}{b}$ . The value of a can be found from

$$a = \frac{\varepsilon(t_a)}{q_0} - b(1 - e^{-\frac{\lambda}{b}t_a})$$
 (2.12)

where  $\varepsilon(t_a)$  represents the strain at time  $t=t_a$ . Figure 6.4 shows a plot of  $\log (\delta_2 - \delta_1)$  vs  $t_1$  for papermill sludge.

The rheological model proposed by Wahls (1962) for the analysis of primary and secondary consolidation is shown in Figure 2.2b. Here primary compression is represented by the Kelvin elements and secondary compression is represented by the secondary dashpots. The time dependent transfer of stress from the pore fluid to the soil skeleton is mathematically modeled by the transfer of stress from the viscous dashpot to the Hookean spring in the Kelvin element. Thus, for an increment of load,  $\Delta p$ , we can write for the nth element,

$$\Delta p = \frac{R_n}{A_n} + \frac{dR_n}{dt} \frac{1}{B_n}$$
 (2.13)

where  $R_n$  is the compression of the nth Kelvin body,  $A_n$  is the spring constant for the nth elastic spring, and  $B_n$  is the dashpot constant for the nth viscous dashpot. By solving equation 2.13 for  $R_n$  and summing over all the elements to obtain the total primary compression,  $R_1$ , at time t, Wahls (1962) arrived at

$$R_{1} = \sum_{n=0}^{\infty} R_{n} = \Delta p \sum_{n=0}^{\infty} A_{n} (1 - e^{\frac{-B_{n}}{A}} t)$$
 (2.14)

Since the Terzaghi solution for primary compression provides a good representation of the hydrodynamic effect, Wahls (1962) chose his constants  $A_n$  and  $B_n$  to make equation 2.14 identical to the Terzaghi equation, arriving at the following deformation equation of the rheological model for primary compression,

$$R_1 = A_p \Delta p \ f(T_v)$$
 (2.15)

where 
$$f(T_v) = 1 - \frac{8}{\pi^2} \sum_{n=0}^{\infty} \frac{1}{(2n+1)^2} \exp \left\{-\frac{(2n+1)\pi}{2}\right\}^2 T_v$$
,

$$A_p = \sum_{n=0}^{\infty} A_n = \text{coefficient of compressibility, } T_v = \frac{c_v t}{H^2}$$
, and  $c_v =$ 

coefficient of consolidation.

Certain assumptions made by Wahls (1962) concerning secondary compression lead to its representation by the viscous dashpots linked

in series with each Kelvin body as shown in Figure 2.2b. The deformation equation of the nth secondary dashpot is assumed to be

$$\frac{dR_n}{dt} = \frac{C_n}{1 + \frac{B_n}{A_n}t} (p_o + \Delta p)$$
 (2.16)

where  $R_n$  is the compression of the nth secondary dashpot and  $C_n$  is the dashpot constant of the nth secondary dashpot. Solving this equation for  $R_n$  and summing to determine the total secondary deformation, Wahls (1962) arrives at the equation

$$R_2 = \sum_{n=0}^{\infty} R_n = C_{\alpha} h(T)$$
 (2.17)

where

$$h(T) = 1.08516 \frac{8}{\pi^2} \sum_{n=0}^{\infty} \frac{1}{(2n+1)^2} \log_{10} \left[ 1 + \left( \frac{2n+1}{2} \pi \right)^2 T_v \right] \text{ for } T_v \le 7$$

and h(T) = .8353 +  $\log_{10} T_v$  for  $T_v > 7$  and  $C_\alpha = \Delta H/H_p/\Delta \log t = strain$  per cycle log time. Thus the total compression,  $R_T$ , caused by a pressure increment,  $\Delta p$ , is

$$R_T = R_1 + R_2 = A_p \Delta p \ f(T_v) + C_{\alpha} H_p \ h(T_v)$$
 (2.18)

where  $A_p \Delta p = \Delta H_p$  = total estimated primary compression, and  $H_p$  = thickness of the layer at the end of primary compression. Wahls (1962) has determined values of the functions  $f(T_v)$  and  $h(T_v)$  for different values of  $T_v$  and these have been used to determine theoretical

time-settlement curves for the papermill sludge. It should be noted that  $\Delta H_p$  represents primary compression only, and any estimate of primary compression based on field piezometer readings or laboratory  $C_c$  values must have the appropriate theoretical amount of secondary compression subtracted from it. This is discussed further in Chapter VI. Wahls's (1962) theory provides no estimate of pore pressures.

Garlanger (1972) bases his theory on a soil model described by Bjerrum (1967), and replaces the Terzaghi equation

$$\frac{\partial e}{\partial t} = -a_{V} \frac{\partial \overline{p}}{\partial t} \tag{2.19}$$

where e is the void ratio, t the time,  $\overline{p}$  the effective normal stress, and  $a_{\overline{V}}$  the coefficient of compressibility equal to  $\partial e/\partial \overline{p}$ , a constant which assumes a time-independent linear relationship between void ratio and pressure, with the equation

$$\frac{\partial e}{\partial t} = \frac{\partial e}{\partial p} \frac{\partial \overline{p}}{\partial t} + \left(\frac{\partial e}{\partial t}\right)_{c}.$$
 (2.20)

In this equation the compressibility,  $\frac{\partial e}{\partial \overline{p}}$  , and creep rate,  $(\frac{\partial e}{\partial t})$  , are

assumed to be functions of both void ratio and pressure. To obtain numerical values for these relations, the appropriate coefficients are determined from a plot of logarithm of void ratio versus logarithm of the effective normal stress. Garlanger (1972) solves equation 2.20 simultaneously with two Terzaghi equations, by a numerical process, to give the void ratio-time and the pore pressure-time relationships at every point within the consolidating soil. Although this model eliminates assumptions (1) and (2) above, it was found to be

inapplicable to the sludge landfill because the necessary e vs. log p relationships could not be realized from the undisturbed samples. The theories discussed thus far require the assumption of a value for the coefficient of consolidation,  $\mathbf{c}_{\mathbf{v}}$ , and as is discussed in Chapter VI, the time-settlement relation is quite sensitive to this value. Therefore it might be concluded that although these theories more accurately model the consolidating soil, the determination of a proper value for  $\mathbf{c}_{\mathbf{v}}$  may be a far more important consideration in the settlement analysis.

Janbu (1965) and Davis and Raymond (1965) have included the nonlinear stress-strain relation of equation 6.2 into the consolidation development to replace Terzaghi's assumed linear relation.

Janbu formulates the differential equation of consolidation in terms of strain, i.e.

$$\frac{\partial \varepsilon}{\partial t} = c_{v} \frac{\partial^{2} \varepsilon}{\partial z^{2}} - \frac{\partial v_{o}}{\partial z}$$
 (2.21)

where  $\epsilon$  is the strain at a point,  $c_V$  the coefficient of consolidation,  $v_O$  the nominal flow rate associated with a threshold gradient  $i_O$ , and solves the equation based on different assumed final strain-depth distributions. Since his model can account for the decrease in strain with depth shown in Figure 6.3c, it allows consolidation to take place more rapidly than it would in a solution obtained on the basis of constant additional stress. Since the laboratory parameters in Terzaghi's theory underestimate the rate of settlement, such a rate increase would be desirable. However, there are problems involved in assuming a proper analytical final strain distribution for use in the

theory. As seen above, this theory allows for the formation of a residual pore pressure in the soil based on the concept of a threshold gradient.

Davis and Raymond (1965) use the non-linear relation of equation 6.2 in a different method of formulation, based on continuity and stress conditions, and arrive at the conclusion that Terzaghi's theory accurately predicts the time-rate of settlement but overestimates the rate of pore pressure dissipation. This theory, along with Janbu's (1965), involves the assumption of a value of  $\mathbf{c}_{\mathbf{v}}$  in its application, and thus is subject to the same explanation given previously on its limitation in predicting time rate of settlement. There are also certain contradictions between the conclusions of the two theories, which makes it difficult to assess which would be the most applicable to papermill sludge.

Gibson et al. (1967) have attempted to take into account the variability of the coefficient of consolidation, and have also eliminated the assumption of small strains. In so doing they have formulated the governing differential equation for a thin clay layer subjected to large deformations. The solution is obtained for both a constant  $\mathbf{C}_F$  and a  $\mathbf{C}_F$  linearly related to the void ratio, where  $\mathbf{C}_F$  is a coefficient closely related to the familiar coefficient of consolidation  $\mathbf{c}_V$ . In the solution of the former case, the linear differential equation is

$$C_{F} \frac{\partial^{2} e}{\partial c^{2}} = \frac{\partial e}{\partial t}$$
 (2.22)

where  $C_F$  is the term  $\frac{(1+e_o)}{(1+e)}$   $c_v$ , e the void ratio, and c the distance from the midpoint of a doubly drained clay layer (at t = 0). This equation holds without restriction on the form of the relation between effective stress and void ratio. It also assumes only  $C_F$  as constant, with no such restriction being placed on the coefficient of permeability, k, and compressibility,  $(d\sigma'/de)$ , as in Terzaghi's (1943) theory. Upon solution of equation 2.22, the effective stresses can be found by application of a suitable stress strain relation (void ratio vs. effective normal stress) and the pore pressures obtained from the effective stresses (constant total stress). The resulting pore pressures will in general not correspond to those obtained by Terzaghi's theory, however the early part of settlement will, as in the Terzaghi case, behave like  $t^{1/2}$ . Such a result would indicate that Terzaghi's theory should adequately predict the time-settlement relation for papermill sludge even though it undergoes large deformation.

Gibson (1958) has developed a theory which describes the progress of consolidation in a clay layer increasing in thickness with time. From this theory it is possible to estimate the pore pressures that develop in a clay layer or embankment that is being constructed at a constant rate on soil which is either permeable or impermeable. Gibson initially considers the case of sedimentation taking place through still water of depth H(t) to the bottom, the current thickness of the deposit being h(t). The total vertical stress at a point a distance  $\times$  from the bottom is

$$\sigma_{xx} = \gamma(h - x) + \gamma_{w}(H - h) = \overline{\sigma}_{xx} + p_{w}$$
 (2.23)

where p is the pore water pressure,  $\gamma$  is the total unit weight of the deposit material, and  $\sigma_{xx}$  is the vertical effective stress. The continuity equation for one dimensional compression is

$$c_{\mathbf{v}} \frac{\partial^{2} \mathbf{p}_{\mathbf{w}}}{\partial \mathbf{x}^{2}} = -\frac{\partial \overline{\sigma}_{\mathbf{x}\mathbf{x}}}{\partial \mathbf{t}}$$
 (2.24)

Combining 2.23 and 2.24, Gibson obtained the equation governing the pore water pressure in the sediment,

$$c_{v_{\partial x}^{2}}^{\frac{\partial p_{w}}{\partial t}} = \frac{\partial p_{w}}{\partial t} - \gamma_{w} \frac{dH}{dt} + \gamma' \frac{dh}{dt}$$
 (2.25)

where  $\gamma' = \gamma - \gamma_w$ . In bank or landfill construction problems with saturated fill, H(t) = h(t) and equation 2.25 becomes

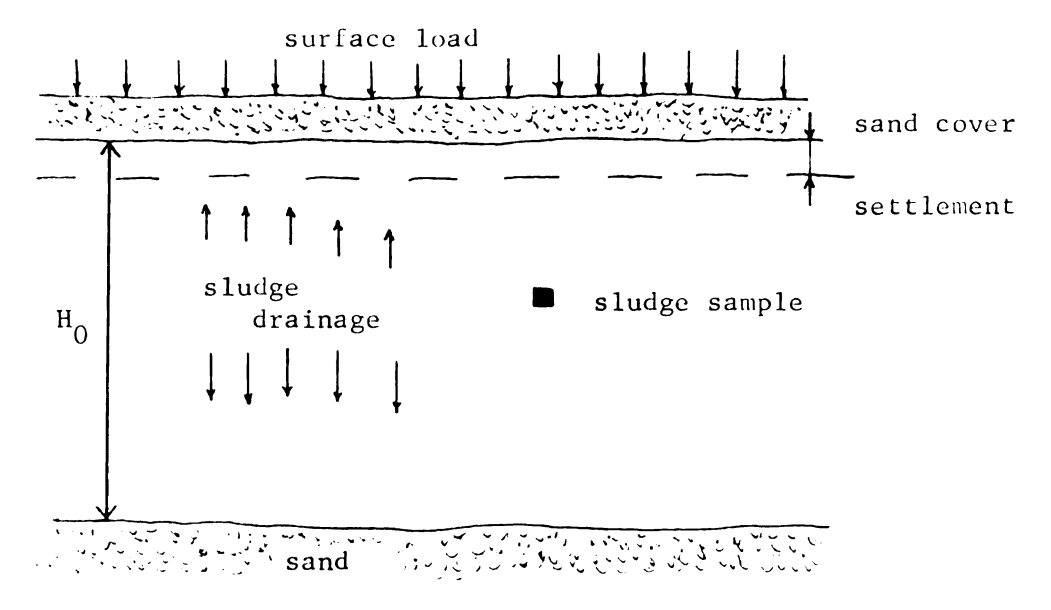
$$c_{\mathbf{v}} \frac{\partial^{2} \mathbf{p}_{\mathbf{w}}}{\partial \mathbf{x}^{2}} = \frac{\partial \mathbf{p}_{\mathbf{w}}}{\partial \mathbf{t}} - \gamma \frac{d\mathbf{H}}{d\mathbf{t}}$$
 (2.26)

For a permeable base the boundary conditions are  $p_w = 0$  at x = 0 and  $p_w = 0$  at x = H. Gibson solves equation 2.26, subject to the preceding boundary conditions, for the case of deposition occurring at a constant rate (H = mt). He presents the solution as a series of curves of x/H versus  $p_w/\gamma H$  for five values of  $\frac{m^2 t}{c_v}$ . Using these curves, pore pressures generated during construction of a sludge layer can be estimated.

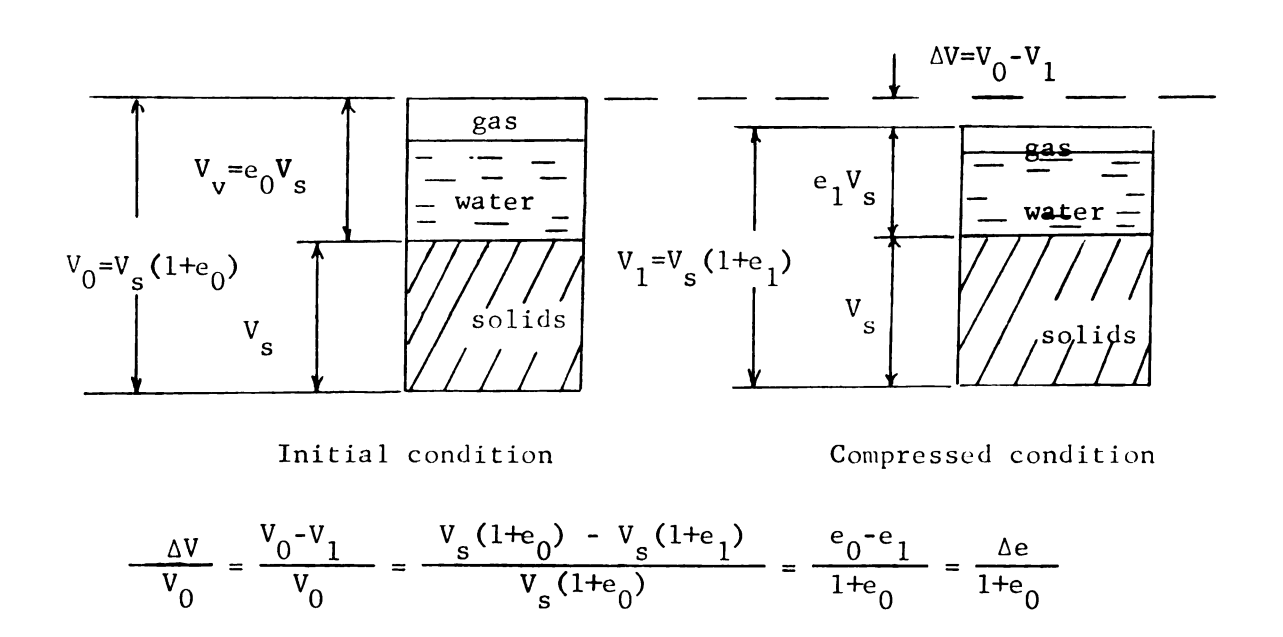
A soil deposit is said to be normally consolidated if the present effective overburden pressures are the maximum pressures to which the deposit has ever been consolidated at any time in its

history. Leonards (1962) discusses in detail the void ratio-effective stress relationships for normally consolidated soil samples, and these concepts are used in the interpretation and analysis of consolidation tests performed on "undisturbed" samples of sludge taken from the landfill. Figure 2.3 illustrates typical e - log p relationships for a normally consolidated clay subjected to various loading conditions and degrees of disturbance. It can be seen that the curve obtained using small load increments best defines the in-situ void ratioeffective stress relationship, and that this relationship can be substantially affected by sample disturbance. There is a sharp break in the e -  $\log p$  curve at a stress level equal to the effective overburden pressure for soils that have experienced little secondary compression. Bjerrum (1967) and Leonards and Ramiah (1959) discuss the increase in  $\overline{\sigma}$  (effective stress at which in-situ consolidation begins) as a result of long term secondary compressions. An increase in  $\sigma$  can also occur from thixotropic and cementation effects. For soils that have been substantially disturbed during sampling, there is no well defined break in the  $e - \log p$  curve and it is difficult to accurately determine  $\overline{p}$ . In the analysis of the consolidation tests on papermill sludge, the Casagrande (1936) procedure was used to backcompute  $\overline{p}$  from the laboratory e vs.  $\log \overline{p}$  curves. Since this procedure was designed for use with overconsolidated clays, it could be in error in estimating  $\overline{p}$  for normally consolidated deposits. This is because the initial portion of a normally consolidated e vs. log p curve does not represent a true reload portion as is assumed in the Casagrande construction. This is discussed further in Chapter VI.

The application of consolidation theory to pulp and papermill sludges does have certain limitations, as shown by Andersland and Paloorthekkathil (1972). They conducted a series of one-dimensional compression tests on an integrated pulp and papermill sludge and two secondary fiber mill sludges. Most of their results are relevant to this study. For example, the composition and solids content of the dewatered sludge produced at a given mill will vary from day to day. Since the consolidation parameters are dependent on these factors, the problem arises as to how much sampling and testing is required to obtain representative consolidation data for the sludge being placed into the landfill. Data presented by Andersland and Laza (1972) show the influence of gas bubbles trapped in the sludge on its permeability. Hydraulic pressures existing in most sludge landfills will not be large enough to eliminate this factor, hence the problem of predicting consolidation rates becomes more complicated. Energy released during sludge decomposition will alter the temperature of sludge landfills. Andersland and Paloorthekkathil (1972) show that temperature change alters the equilibrium void ratio as well as the coefficient of consolidation. The observed settlements in the experimental sludge landfill will permit comparisons with predicted settlements based on laboratory data, thereby helping to delineate possible limitations of the application of consolidation theory to papermill sludges.



a) Section through a sludge landfill.



b) Volume-void ratio relationships.

Figure 2.1. The settlement problem.

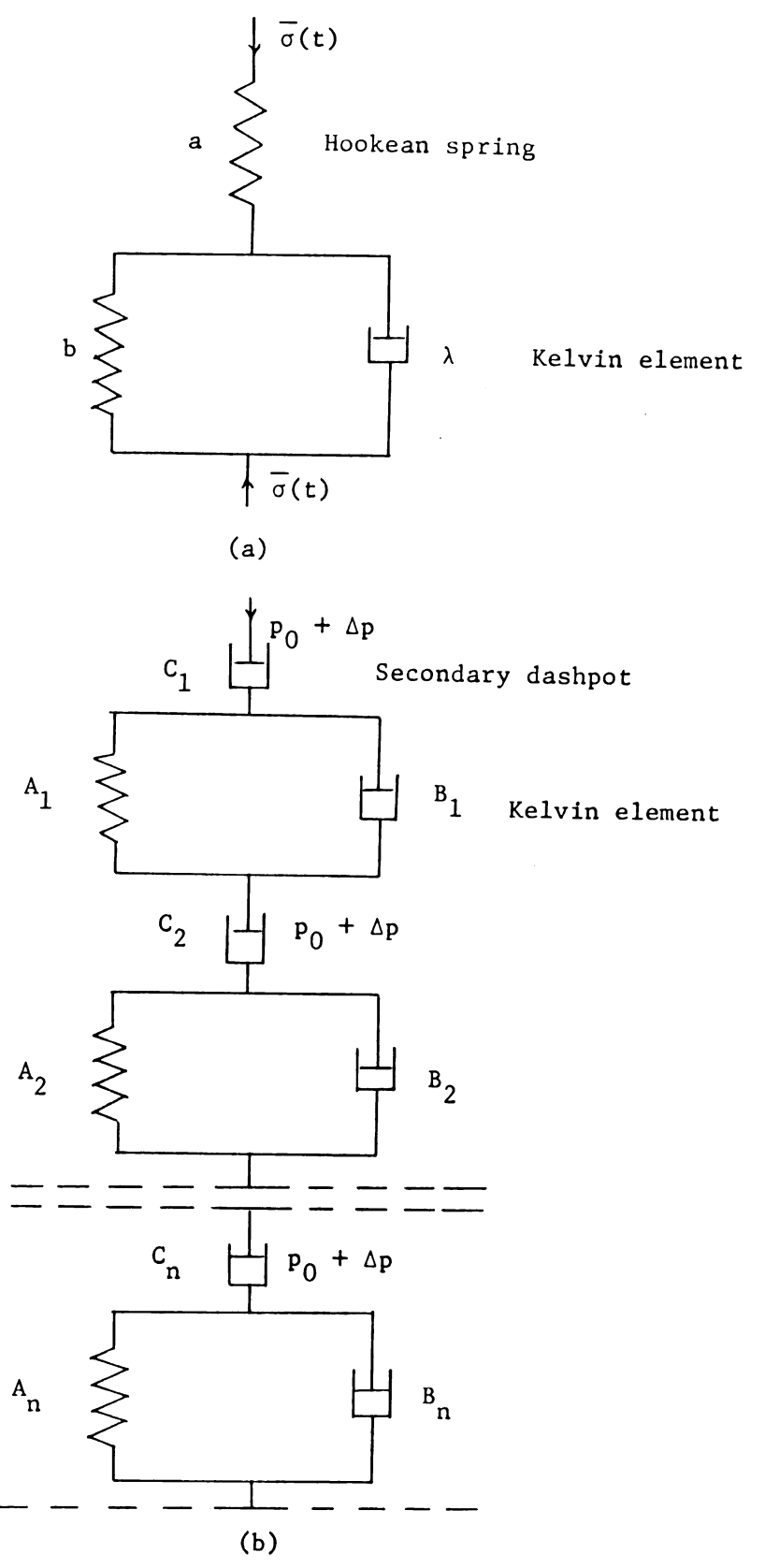


Figure 2.2. Models for the consolidation process. (a) Gibson and Lo (1961). (b) Wahls (1962).

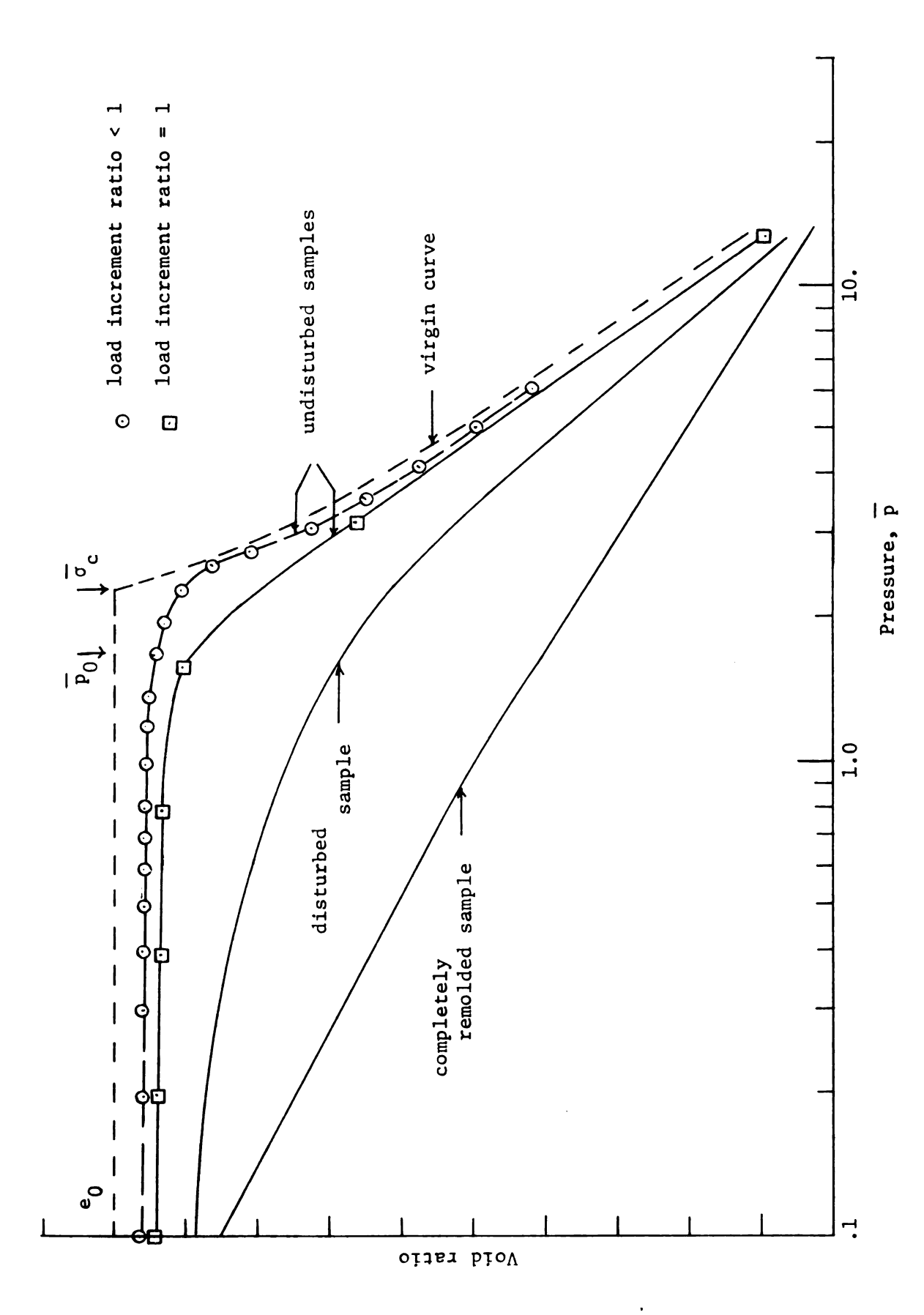


Figure 2.3. Void ratio -- effective stress relationships for a normally consolidated clay, (Leonards, 1962).

#### CHAPTER III

## EVALUATION OF SLUDGE ENGINEERING CHARACTERISTICS

The physical properties and stress-deformation behavior of the papermill sludge are needed for making predictions for comparison with observed field behavior of the experimental landfill. Methods used for the measurement of these engineering characteristics are described below. Reference is made to standard test procedures where possible.

# 3.1 Physical Properties

Physical properties of papermill sludge characterize, to some extent, the quality of the sludge relative to engineering purposes.

Those properties important to this project include water content, unit weight, specific gravity, ash (or organic) content, and consistency limits.

## 3.1.1 Water Content

The water content of a soil or sludge sample is defined as the ratio of the weight of water to the weight of dry soil or dry sludge and is usually expressed as a percentage. Drying temperatures for sludges are the same as used for mineral soils (105 - 110°C). In order to obtain consistent dry sludge weights, careful control of the oven temperature is required. Care must be exercised so as to obtain a representative sample that avoids local variations. A minimum

sample size of at least 10 gm of dry solids is recommended. Lambe (1951) gives additional information on the water content of soils.

Fresh papermill sludges contain large amounts of water, hence some prefer to use solids content by weight rather than water content by weight. The solids content is defined as the ratio of the weight of solids to the weight of the wet sample. A simple conversion from solids content to water content is

$$w = 100 \left[ \frac{100}{\% \text{ dry solids}} - 1 \right]$$
 (3.1)

where  $w = \frac{W_W}{W_S}$  (100) is the water content in percent based on the dry weight of solids,  $W_S$ , and the weight of water,  $W_W$ .

Water contents of sludge samples taken from the landfill are given in Table 5.2 and Figure 5.1. The lower layer had an average initial water content of 265 percent with a range from 213 to 308 percent. The upper layer had an average initial water content of 257 percent and a range from 212 to 290 percent. All water content samples were taken shortly after the sludge had been placed in its final location by the dragline. Variations present are due to: (1) changes in sludge output from the dewatering plant, (2) localized surface wetting and drying as a result of weather changes, and (3) different times of sludge exposure before sampling. It should be noted that after the construction of a sludge layer the water contents toward the bottom were less than those at the top because leachate drained from the sludge into the bottom sand blanket during construction. Application of the surcharge reduced the water content throughout both sludge layers as the leachate was expelled. The water contents

resulting from this are shown in Figure 5.1 and are discussed in Chapter V.

## 3.1.2 Unit Weight

The unit weight of sludge is defined as the weight of the aggregate (sludge plus water) per unit volume. It depends on the solids content, unit weight of the solid constituents, and the degree of saturation of the sludge. The natural unit weight can be determined by careful volume and weight measurements. The unit weight of fluid sludges may approach that of water (62.4 lb/cu ft) whereas the unit weight of dewatered sludges cannot exceed that for the solid constituents. The dry unit weight,  $\gamma_d$ , may be computed as

$$\gamma_{\rm d} = \frac{G_{\rm S}}{1 + e} \gamma_{\rm w} \tag{3.2}$$

where  $G_s$  is the specific gravity of the solids,  $e = \frac{V_v}{V_s}$  is the void ratio expressed in terms of the volume of voids,  $V_v$ , the volume of solids,  $V_s$ , and  $\gamma_w$  is the unit weight of water.

Two procedures were used to determine the total unit weight of the papermill sludge as placed in the landfill. In the first procedure, a truck carrying sludge was weighed both when full and when empty to determine the total weight of the sludge being carried. The volume of the truck box was then determined and divided into the sludge weight to determine the unit weight. This procedure gave a total sludge unit weight of 69.7 lb/cu ft. The second procedure involved packing the sludge by hand into a bucket of known volume (1/10 cu ft), and then weighing to determine the quantity of sludge in

the bucket. The sludge was placed into the bucket in 5 lifts, and care was exercised to be sure that no air pockets were present. The total unit weight determined from this procedure was 69.0 lb/cu ft. The second procedure is similar to the method used for determination of the unit weight of fresh concrete.

## 3.1.3 Specific Gravity

The specific gravity of papermill sludge is the ratio of the weight in air of a given volume of sludge particles to the weight in air of an equal volume of distilled water at a temperature of 4°C. The lower limit for sludge will approximate the specific gravity of the organic material. The upper limit will correspond to the specific gravity of the mineral matter, generally greater than 2. Accurate determination of the specific gravity requires special care because of the presence of small gas bubbles in the sludge sample. This was overcome by the application of a vacuum to the pycnometer containing the water and sludge. Details of the test to determine the specific gravity of the sludge solids are given under ASTM designation D 854-58. Oven dry test samples were used for the papermill sludge.

## 3.1.4 Ash Content, Organic Content

The organic material of sludge, primarily cellulose fibers, is combustible carbonaceous matter, whereas the mineral constituents are incombustible and ash forming. In the manufacture of paper, kaolinite is used in filler and coating operations. In waste paper reclamation this clay is removed from the fiber and becomes a part of the paper sludge. The sludge also contains small amounts of aluminum hydrate, titanium oxide, lime and iron (Gillespie, Gellman, and

Janes, 1970).

The ash content of papermill sludge is determined by firing an oven dried sample in a muffle furnace at a temperature of 925  $\pm$  25  $^{\circ}$ C (ASTM test method D 586-63). The ash content A is determined from the equation

$$A_c$$
 (%) =  $\frac{\text{weight of ash or residue}}{\text{dry weight of sample}}$  x 100. (3.3)

MacFarlane (1969) states that for peat it is standard engineering practice to determine the ash content as described above and then to consider the organic content equal to  $(100 - A_c)$ . Comparative results (Andersland and Laza, 1971; Andersland and Paloorthekkathil, 1972) between the ash content determined from the above method and the organic content determined by the method given in Agronomy No. 9, Sec. 92-3.3 (Black, 1965) support the use of  $(100 - A_c)$  for estimating the organic content of papermill sludges. Although the kaolinite also loses its OH lattice water when fired to  $925^{\circ}$ C, this dehydration would amount to only a small portion of the total combustible material.

The ash content of the sludge in the landfill will remain essentially constant with time (Gillespie, Mazzola, and Gellman, 1970). This has been attributed to the presence of lignin and clay and the absence of sufficient nitrogen in the sludge, inhibiting the biological breakdown of cellulose.

## 3.1.5 Consistency Limits

The consistency, or Atterberg, limits indicate the range of water contents in which a soil or sludge may be considered as a fluid,

plastic, or solid. The liquid limit is the water content at which the soil or sludge has such a small shear strength that it will flow and close a groove of standard width when jarred in a specified manner. The plastic limit is the water content at which the soil or sludge begins to crumble when rolled into threads of a specified size. The amount of water which must be added to change a soil or sludge from its plastic limit to its liquid limit is an indication of the plasticity of the material. The plasticity is measured by the plasticity index, which is equal to the liquid limit minus the plastic limit. Detailed procedures for the consistency limits are given by Lambe (1951). Values for the sludge can be found in Table 5.1.

Papermill sludges containing fibers do not readily lend themselves to the standard consistency tests. The fibers interfere with the test procedures and probably alter the shear strength of the material adjacent to the standard groove in the liquid limit test.

Andersland and Laza (1971) show that both the liquid and plastic limits decrease with a decrease in organic content.

## 3.2 Stress Deformation Characteristics

The stress-deformation behavior of papermill sludge will determine its volume change and settlement and will control the stability of sludge landfills. The methods used for evaluating the consolidation behavior and the undrained shear strength of the sludge are given below.

# 3.2.1 Consolidation Behavior

The process of leachate flow from sludge, involving volume change as a function of time, is called consolidation. When volume change occurs only in the vertical direction, as in a horizontal sludge

layer (Figure 2.1a), changes in the surface elevation are labeled settlement. Two forms of volume change in papermill sludges include primary and secondary compression (Figure 3.1). Primary compression involves a transference of load from the pore water to the sludge structure and is accompanied by a change in volume equal to the volume of water drained from the sludge. The rate at which primary compression occurs in sludge is directly related to the sludge permeability (the speed at which pore water can escape). Pore water pressure measurements taken during the settlement study provide information on this rate of consolidation. When the excess hydrostatic pressure associated with primary compression has been dissipated, the change in void ratio generally continues at a reduced rate. This phenomenon is referred to as secondary compression and is often expressed by the slope,  $C_{\alpha}$ , of the final portion of the time-compression curve plotted on semi-log paper (Figure 3.1b).

Laboratory consolidation tests (Lambe, 1951) were used to provide quantitative information on the sludge compressibility. The Wykeham Farrance consolidation test machine shown in Figure 3.2, designed by Professor A. W. Bishop, provided consistent laboratory consolidation test results. The first step required in running a test on fresh sludge (sludge as placed in the landfill) was to carefully place the sludge, in small amounts, into a 2-1/2 in. diameter by 3/4 in. high consolidation ring and to then knead the mass by hand to obtain a continuous sample free of large air pockets. The top and bottom of the sample were carefully smoothed off and trimmed to conform to the right height. The sample was then placed in the cell chamber (with

perspex wall) shown in Figure 3.2b and the clamp ring and top pressure pad were situated in their proper location. The cell was then placed in the consolidation machine (Figure 3.2a) and the load increment applied. Drainage from the sample took place through two bauxilite discs, one located on the bottom of the cell and one attached to the top pressure pad. Deformation of the sample was obtained from a displacement transducer attached to the frame of the consolidation machine and connected to a Sargent recorder. Recorder output was verified at the start of testing by comparison to deformations measured with a dial gauge. In a standard, multiple increment test, stresses of 0.1, 0.2, 0.4, 0.8, 1.6, and 3.2 kg/cm<sup>2</sup> were applied for a period of 24 hours to the sample. Special single increment tests were also carried out, usually involving a 24 hour time period.

Undisturbed block samples of sludge were obtained from the landfill when one of the confining dikes was removed for a stability study. Consolidation tests were run on sludge samples trimmed from these blocks. After a block was cut from the exposed sludge slope, it was wrapped in aluminum foil and plastic wrap and placed into a one cubic foot wooden box. Wax was then poured around the sample and the box was sealed shut. Three block samples were taken from each sludge layer at different elevations and transported back to the soil mechanics laboratory for testing.

Two blocks were chosen to provide samples for laboratory consolidation tests. Block B was located at the mid-point of the upper sludge layer, 4.0 ft. below the upper sand blanket, and block F at the approximate mid-point of the lower sludge layer, 4.0 ft. below the

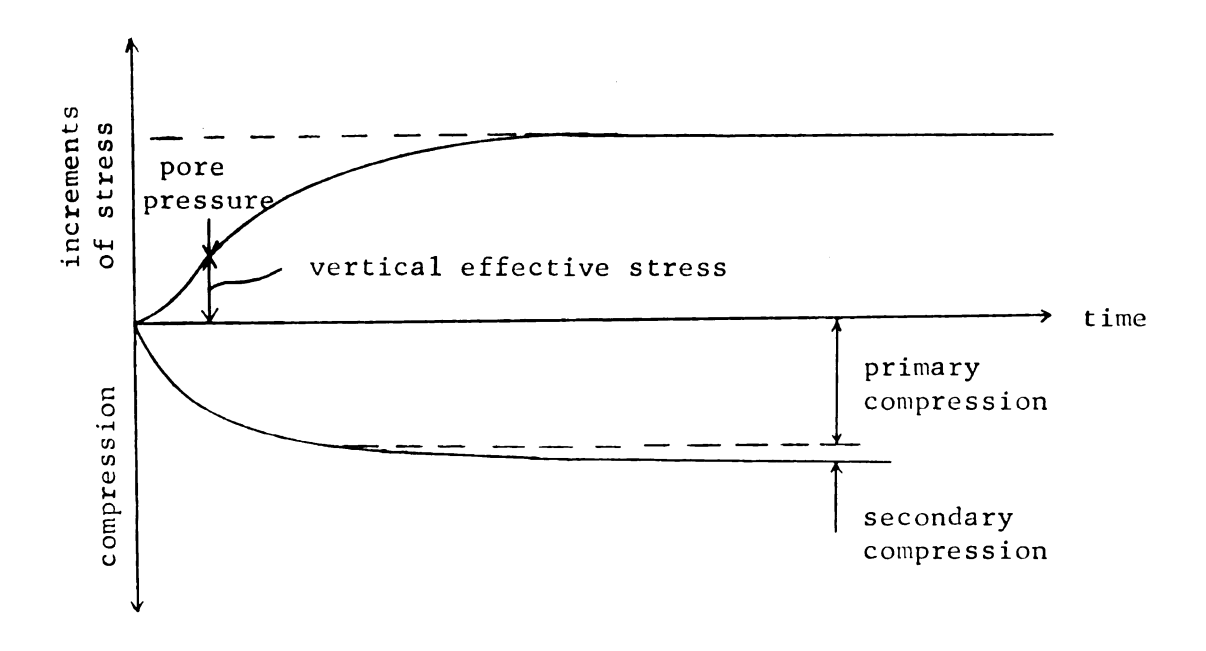
middle sand blanket. A total of four consolidation tests were run on samples obtained from each block. Two of the tests were run with rapidly applied load increments of 15 min. duration, and two with load increments of 12 hr. duration. The rapid loading tests were used to obtain a definitive e vs. log p curve and had load increment ratios less than one. The 12 hr. tests were run with a load increment ratio of one.

Because of the fibrous nature of the sludge, standard wire saws and trimming devices could not be used to trim sludge samples from a block. A regular hand saw was first used to cut a 6" X 6" X 4" chunk of sludge from a block, and then a small (1 lb) rotary electric hobby tool with a rapidly rotating (24000 rpm) 3/4 in. diameter circular saw tooth blade was used to trim the sludge to the consolidation ring dimensions (3 in. diameter, 3/4 in. high). Once inside the ring, the sludge surface was wetted slightly and smoothed to conform to the ring height. Although this procedure resulted in considerable disturbance, both through handling and vibration from the saw, the low sensitivity of the sludge allowed fair results to be obtained. Consolidation characteristics of the undisturbed samples are summarized in Table 5.3 and Figures 5.5 and 5.6.

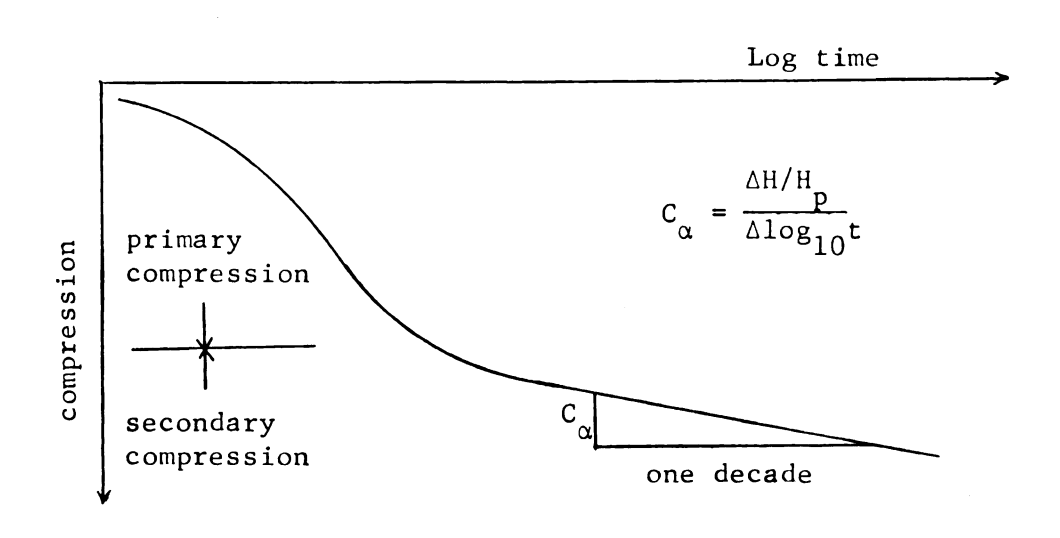
## 3.2.2 Undrained Shear Strength

The undrained shearing resistance of papermill sludge may be determined using a cylindrical compression test (Bishop and Henkel, 1962) or a vane shear test (Terzaghi and Peck, 1967). The vane shear test was used to measure the increase in undrained shearing resistance, with consolidation, at various levels in the experimental sludge landfill. The vane shear apparatus consists of a four-bladed vane

attached to the bottom of a vertical rod, as shown in Figure 3.3. The vane and rod can be forced into the soft sludge without appreciable disturbance. The assembly can then be rotated and the shearing resistance computed by using the dimensions of the vane and the observed torque. The sludge fails along a cylindrical surface passing through the outer edges of the vane, as well as along the conical surfaces at the top and bottom of the blades. When the vane is rotated rapidly through several revolutions, the sludge becomes remolded and the shear strength in this state can be determined. The ratio of the undisturbed shear strength to the remolded value gives the sensitivity of the sludge. Details on the apparatus and procedures for the vane shear test as used on the project are given in Chapter IV.



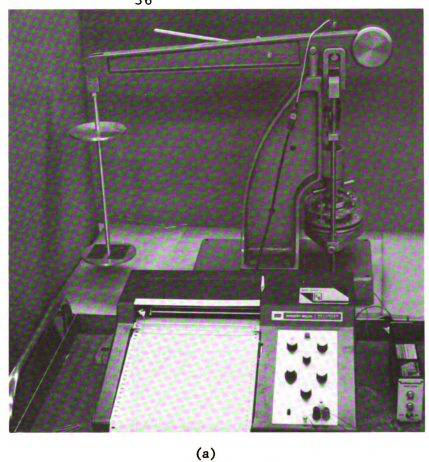
a) Primary and secondary compression.



Definitions.

b)

Figure 3.1. Time-compression curves.



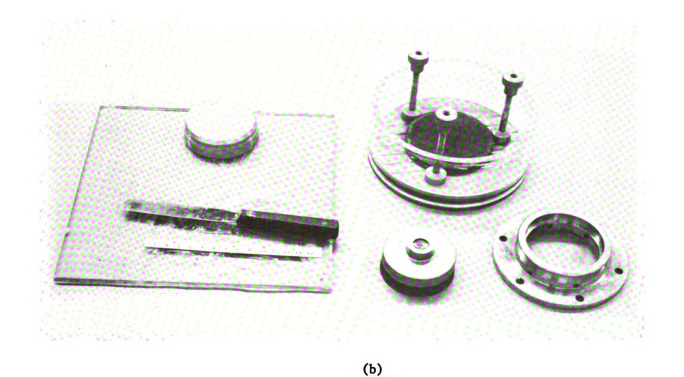


Figure 3.2. (a) Consolidation machine and recorder. (b) Fixed ring consolidation unit and sludge sample.

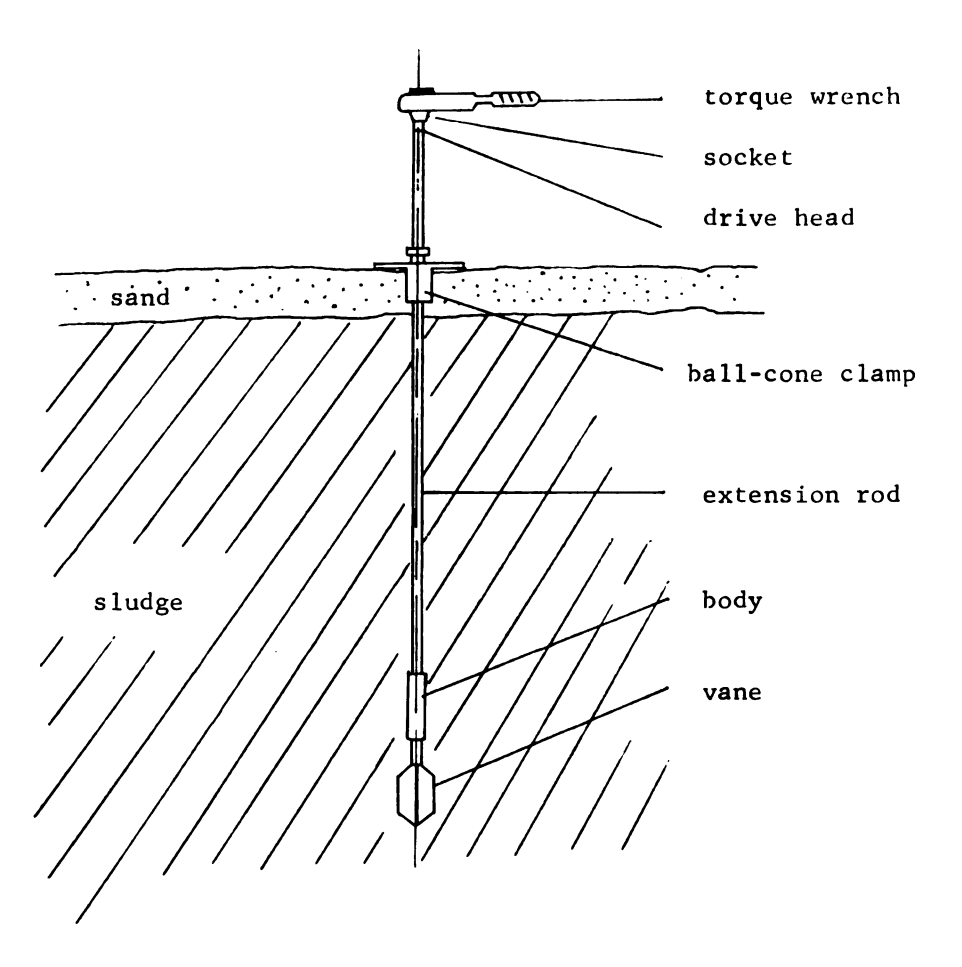


Figure 3.3. Vane shear apparatus.

#### CHAPTER IV

#### CONSTRUCTION, INSTRUMENTATION AND MONITORING

# 4.1 Construction of the Experimental Landfill

Construction methods employed at the site are summarized here for later reference. They are described in terms of the site preparation and dike construction, sludge placement, drainage blanket placement, and earth surcharge placement. The B. G. Danis Company, Inc., Dayton, Ohio, provided equipment and operators. Coordination of construction operations was handled by the author through Mr. Tom Danis, Sr. Field work on the papermill sludge landfill commenced on August 23, 1971.

## 4.1.1 Site Preparation and Dike Construction

A section of an old gravel pit located close to West Carrolton, Ohio, and within hauling distance of the papermill was selected for the experimental sludge landfill site. A pre-construction map of the immediate gravel pit area and the dike layout is shown in Figure 4.1. Other areas of this gravel pit already contained large amounts of dewatered papermill sludge from previous fill operations. A small pond in the gravel pit, about 400 ft. north of the existing slope, provided a reference as to the groundwater elevation. This information indicated that the groundwater level would not be encountered during dike construction. The pond also served as an outlet for the drainage pipe installed in the lower sand blanket. Several bench marks were

established and a stadia survey was completed of the immediate gravel pit area, as shown in Figure 4.1. From the stadia survey it was apparent that a maximum dike grade elevation of 95.5 ft. would allow the entire west dike and part of the south dike to be shaped from the natural ground. Excavated soil would provide material for the remaining dike areas. The bottom grade elevation of 77.0 ft. was about 7 ft. above the groundwater level.

Prior to excavation for the dikes, an 8 in. diameter pipe was installed to the pond to provide drainage for the sand drainage blankets. The upper end extended under the north dike and into a gravel pocket in the lower sand blanket (invert elevation 77.0 ft) as shown in Figures 4.2 and 4.3. The lower end (invert elevation 73.6 ft) drained into the pond. The gravel drain surrounding the pipe entrance was continued up the inner dike wall to provide drainage for the middle sand blanket (Figure 4.3). Observations at the pipe outlet both during and after construction indicated that it was functioning properly. The pipe joints were not sealed, hence some seepage to and from adjacent soil could occur.

The top inside corners of the dikes and the required grades were established using results from the stadia survey (Figure 4.1). A one cubic yard 35-ton Link Belt power shovel did the bulk of the excavation work, while a D-6 caterpillar dozer moved the excavated earth and shaped the dikes. Excavation began near corner 1 (Figure 4.1), with the power shovel digging into the existing bank and side casting to the dike area. The dozer would spread the soil toward corner 2, gradually building up the south dike. As grade was

approached, the dozer spread the soil toward corner 3, building up the east dike. The excavated material was a well graded till consisting of particles ranging in size from clay to gravel. It was easy to handle and during placement some compaction was achieved from the dozer, thus permitting construction of a fairly steep inner dike slope. This slope helped minimize the volume of material required and reduced construction time.

After the power shovel had completed the excavation near the top, it was moved to the bottom area and proceeded to excavate down about 6 ft. to the final grade at elevation 77.0 ft. The excavated material was used to complete the north and east dikes. Corner 3 was left low until sand for the lower drainage blanket had been dumped inside the dike area. When the bottom of the landfill area reached grade, the power shovel was converted into a dragline unit, and soil for completing the dikes was obtained outside the fill area. The dozer spread this soil, and also leveled the sand dumped for the lower drainage blanket. The gravel surrounding the upper end of the drainage pipe and extending up the slope (Figure 4.3) was placed near the end of the dike construction period. Shaping of this 10 ft. wide gravel chimney drain was handled by the dozer.

# 4.1.2 Sludge Placement

After the spreading of the sand for the lower sand blanket and the shaping of the gravel chimney drain, sludge was dumped by truck over the west and south dikes as shown in Figure 4.4b. The sludge exhibited a plastic behavior and would not support the usual construction equipment. The dragline (Figure 4.4a) proved ideal for

moving the sludge to other locations in the landfill. A lightweight dozer with extra track width arrived at the site too late for use in spreading the sludge. Current use of this lightweight dozer by the contractor indicates that it is quite effective in moving sludge and that it should be considered for future operations.

Some initial difficulty was encountered when unmonitored sludge dumping was permitted over a weekend. Unusually high sludge production (about 300 cu yd/day) caused more area to be used at the bottom of the landfill than was anticipated, and a sludge flow towards the center of the site occurred. Two settlement plates with vertical rods were shoved out of position and required replacement. Leachate draining from about ten feet of sludge stacked along the west dike saturated the sand blanket. Temporary channels were dug in the sand blanket to the drainage pipe to remove the leachate. After the re-leveling of the sand surface and a more uniform re-placement of the sludge with the dragline, dumping was continued with daily monitoring. Shortly thereafter, sludge production dropped to about one-half its normal rate, delaying the landfill construction. The dragline was used for the placement of both sludge layers.

# 4.1.3 Drainage Blanket Placement

Placement of the lower sand blanket was described in the preceding sections. When the lower sludge layer reached grade it was roughly leveled with the dragline bucket, and then two telephone poles cabled together were dragged over the surface. This reduced variations in the sludge surface to about ± 3 inches. Sand was then dumped along one dike edge and distributed by dragline over the sludge layer. Again

the two telephone poles were dragged over the surface to give a reasonably level sand blanket. The use of a lightweight dozer for the spreading of the sand was not attempted because of the possibility of its sinking into the sludge and because the surface of the lower sludge layer was 11 ft. below the top of the dike, as shown in Figure 4.5. The steep inner dike slopes at this time would have made an attempt to use a dozer quite dangerous. Sludge placement was resumed upon completion of the middle sand blanket.

When the upper sludge layer reached grade, the surface was roughly leveled off with the dragline bucket and then brought to final elevation by dragging the pole rig over the surface. Sand was dumped at the dike edge and a lightweight dozer pushed the sand out over the sludge surface. Because the sand acted as a supporting mat, the small dozer was readily able to travel over the landfill while spreading the sand. Placement of the sand with the dozer was considerably faster than with the dragline.

#### 4.1.4 Earth Surcharge Placement

The earth surcharge was constructed of the same soil used to build the dikes. It was obtained outside the dike area by the dragline and dumped onto the landfill surface near instrument group 7. Both the D-6 and lightweight dozers were then used to spread the soil over the required area. Some compaction occurred as the dozers operated over the surcharge. Placement required only 1-1/2 days, hence for analysis purposes the surcharge was placed instantaneously. The lateral dimensions of the surcharge were selected (Figures 4.2 and 4.3) so that one-dimensional consolidation would be approximated at all instrument

group locations. Field density determinations using the sand-cone method established a soil unit weight equal to 130.4 pcf for the surcharge material. Preliminary consolidation data indicated that the 3 ft. thick soil layer would give time-settlement curves suitable for the project research objectives.

## 4.2 Instrumentation and Monitoring

The instrumentation and monitoring of the experimental sludge landfill provided information, both during and after construction, on vertical movements, pore water pressures, lateral earth pressures, temperatures, and undrained shear strengths. Instrument placement and monitoring commenced on September 10, 1971, with the installation of settlement plates in the lower sand blanket. Instrumentation of the landfill continued as construction progressed. Monitoring began with each instrument installation and was continued throughout the year. The frequency of readings was based on the relative change in the observed phenomena, with the most frequent readings (2 per week) required during the first few weeks after construction. The following sections describe the settlement plates, piezometers, total pressure cells, temperature sensors, and vane shear tests used to obtain the field data.

## 4.2.1 Settlement Plates

A settlement plate consisted of a 2 ft. by 2 ft. by 1/8 in. thick aluminum plate with a 3/8 in. diameter steel rod of known length attached to the center, as shown in Figure 4.6a. Additional rods of known length were added at each location as sludge placement progressed.

To minimize the adhesion of the sludge on the steel rod, a 1-1/2 in.

O. D. aluminum tube was placed around each rod when it was installed.

Radiator hose (1-1/2 in. I. D.) provided a flexible connection for the aluminum tubing. Elevations taken with a surveyor's level (or transit) on the top of each steel rod were referenced to a bench mark outside the fill area.

Installation of the plates in a sand blanket and in the sludge is shown in Figure 4.6. A hole 3 ft. square by 4 to 6 in. deep was first excavated in the sand or sludge, the bottom was tamped lightly to densify the material, and using the plate as a guide, the bottom of the hole was carefully leveled. Then the settlement plate, attached rod, and aluminum tube were installed in the hole, an initial elevation reading taken on the plate, and the hole backfilled. Because the aluminum plates were light, there was no danger of their sinking into the sludge. The sludge consistency was such that a man could walk on its surface.

A total of 32 settlement plates were installed at various levels in 8 instrument groups. The distribution of settlement plates in each group is shown in Figure 4.7. The lower plate was placed at the center of the group, with each higher plate offset 1-1/2 ft. from the center so that no interference could occur between rods and higher plates. Duplicate locations served as insurance in the event that certain groups should be accidentally destroyed during construction, and the additional data served as a check on adjacent groups. Location of each instrument group is shown in Figure 4.2.

### 4.2.2 Piezometers

Piezometers measure the static pressure or head (elevation to which water will rise in an open standpipe) of the fluid in the pore space between the solid sludge particles. The pneumatic type piezometer (Slope Indicator Company model 51401) used on this project did not require in-place calibration and was not subject to changes in sensitivity. The sensitivity of the transducer approaches 0.5 in. of water. Because the sludge has a high degree of saturation, the standard Norton Casagrande type filter with large pore size and low air entry pressure was used. The transducer (Figure 4.8a) converts the in situ water pressure into a pneumatic pressure that is relayed to the surface reading station by means of twin nylon tubing. Pore pressure readings were taken with the model 51421 (Slope Indicator Company) portable pore pressure indicator.

Installation of the pore pressure transducers first required excavation of a small hole in the sludge, as shown in Figure 4.8b. At least 3 inches of sand and water were then placed in the hole, followed by the transducer, and ample slack was allowed for in the twin nylon tubing. Next, the piezometer was covered with a minimum of 3 inches more of saturated sand followed by a layer of wet sludge. The sand pocket was used because it was unknown how sludge decomposition might influence piezometer readings. The twin nylon tubes were connected to a terminal unit housed in a waterproofed wooden box located at the edge of the landfill. The pore pressure measuring system appeared to function well, with no pinched or disconnected lines occurring during construction operations. The observed pore water pressure—time curves

indicate that the readings are consistent and that they are in agreement with duplicate piezometers.

A total of 16 piezometers were installed as part of instrument groups 5, 6, and 7. Their group identification and relative elevation is shown in Figure 4.7, with group locations given in Figure 4.2. Piezometers located at the same level as a settlement plate were offset about 6 to 12 inches from the plate.

## 4.2.3 Total Pressure Cells

Total pressure cells assist in determining the state of stress in the sludge mass. The model T-9010 (Terra Tec) cell consists of two 9 in. diameter steel plates welded together at the circumference with a void between them that is filled with an incompressible oil. The oil transmits the external pressure to a sensing unit consisting of a double bellow assembly. Air pressure from the control unit (Terra Tec model C 1000) is applied through a closed loop system to the inside of the bellows to balance the external cell pressure. This air pressure is relayed from the surface reading station to the total pressure cell by means of twin nylon tubing. Calibration charts based on a hydraulic and a sand loading give the limits of possible pressures that can act on the cell by the sludge.

Three total pressure cells were installed in the lower sludge layer near group 7, as shown in Figure 4.7. Two of the cells were installed in the vertical position to measure horizontal stresses, and the remaining unit was installed in the horizontal position to measure total vertical stresses. The horizontal cell was installed by digging a hole 1 ft. square by 4 in. deep and placing the cell so that it was

firmly imbedded in the bottom. An elevation reading was then taken on the cell surface and the hole backfilled. The vertical cells were pushed part way into the bottom of a similar hole, and then loose sludge was placed around the cell and tamped until the cell became firmly imbedded. An elevation reading was taken on the top edge of the cell before backfilling was completed.

## 4.2.4 Temperature Sensors

The temperature sensors are small YSI precision thermistors which are made of a material whose electrical resistance varies sharply in a known manner with temperature. Given the resistance reading, the thermistor temperature is obtained from a calibration chart. Ten YSI precision thermistors (part #44033) were mounted at 2 ft. intervals on a 1 in. square wooden pole. The thermistors and wooden pole were installed via a 4 in. I. D. hollow core auger using a truck mounted drill rig. Since the augered hole was not expected to remain open without casing, the wooden pole was lowered through the hollow core of the auger, and then the auger was carefully pulled up around it. The elevation of the top thermistor equals 95.43 ft., with the additional thermistors being located below this at 2 ft. intervals. Thermistor lead wires followed the pole to the surface and then across the fill to the readout box. Resistance readings were obtained with a model 300 digital passive scalor from Western Electronics, Inc. Data indicated that 9 of the 10 thermistors were functioning properly.

## 4.2.5 Vane Shear Tests

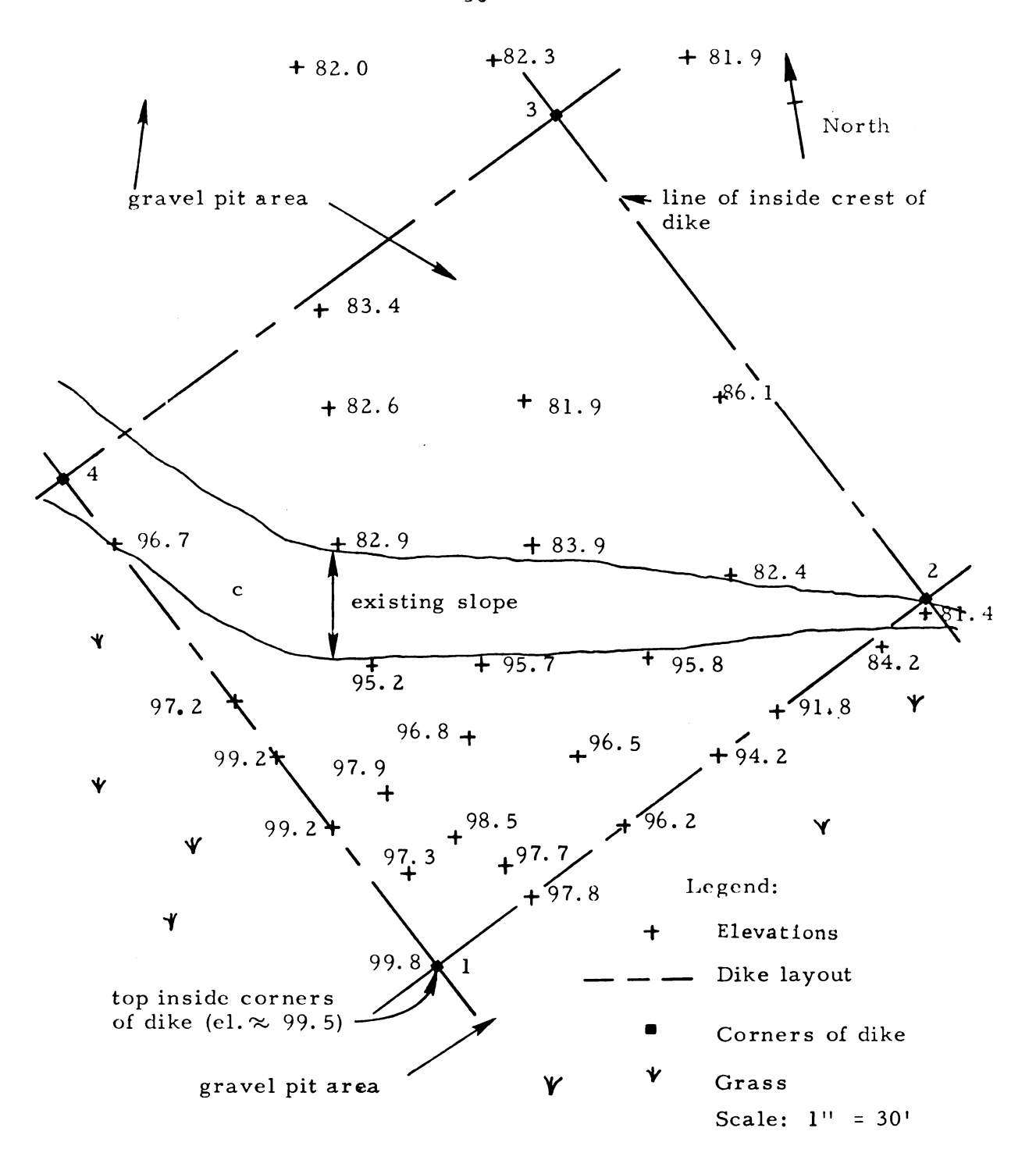
All but one set of vane shear tests were carried out using a Geonor H-70 heavy field inspection vane borer. It is a hand operated

unit that comes equipped with a torque wrench, 3 different size vanes, extension rods, and various accessories. The basic unit, as it would be set up in the field, is illustrated in Figure 3.3. Undrained shear strengths up to 12 tons/sq m can be measured with the small vane (55.9 x 111.8 mm). One final set of vane strengths was taken using a 2 in. O. D. Acker vane that was pushed into the bottom of a hole augered to within 6 in. of the test depth. This prevented the capacity of the torque wrench from being exceeded.

The test procedure for all but the last set first involved driving, with a sledge, the vane and claw coupling (lower part) into the sludge to the desired depth. The measurement of shear strength was then carried out in four stages for each depth. The extension-rod friction was first measured by turning the torque wrench slowly clockwise through an arc a little less than 180 degrees. The rods were then rotated still further in a clockwise direction until the dogcoupling in the lower vane borer engaged. The measurement of shear strength was then taken by slowly turning the extension rods clockwise until the maximum shear reading was obtained. The difference between the maximum reading and the rod friction reading, with the proper conversion, equaled the undrained shear strength of the sludge. The vane was then turned 20 times clockwise in order to remold the sludge adjacent to the vane and rod. The rod was then rotated 1/2 of a revolution counterclockwise before measuring the rod friction and shear strength of the remolded sludge using the same procedure as before.

Shear strengths were obtained at 3 elevations in the upper sludge layer and at two elevations in the lower sludge layer for all but the final set. Because of augering through the surcharge and upper

sand blanket with a hand auger, the upper layer rod friction was low and difficult to read on the torque wrench. Shear strengths were relatively easy to obtain. In the lower sludge layer much greater driving resistance was encountered and rod friction became high. Thus the vane shear strengths were obtained only at the two higher elevations in the lower sludge layer. At the lower elevation the capacity of the torque wrench would have been exceeded using the small vane. The final set of vane shear strengths, taken using a truck mounted drill rig to pre-auger to the desired depth, had the strengths recorded at one foot intervals throughout both layers.



Assumed elevation datum top of gas line marker = 100.00 ft.

Figure 4.1. Pre-construction map of existing gravel pit area including dike layout.

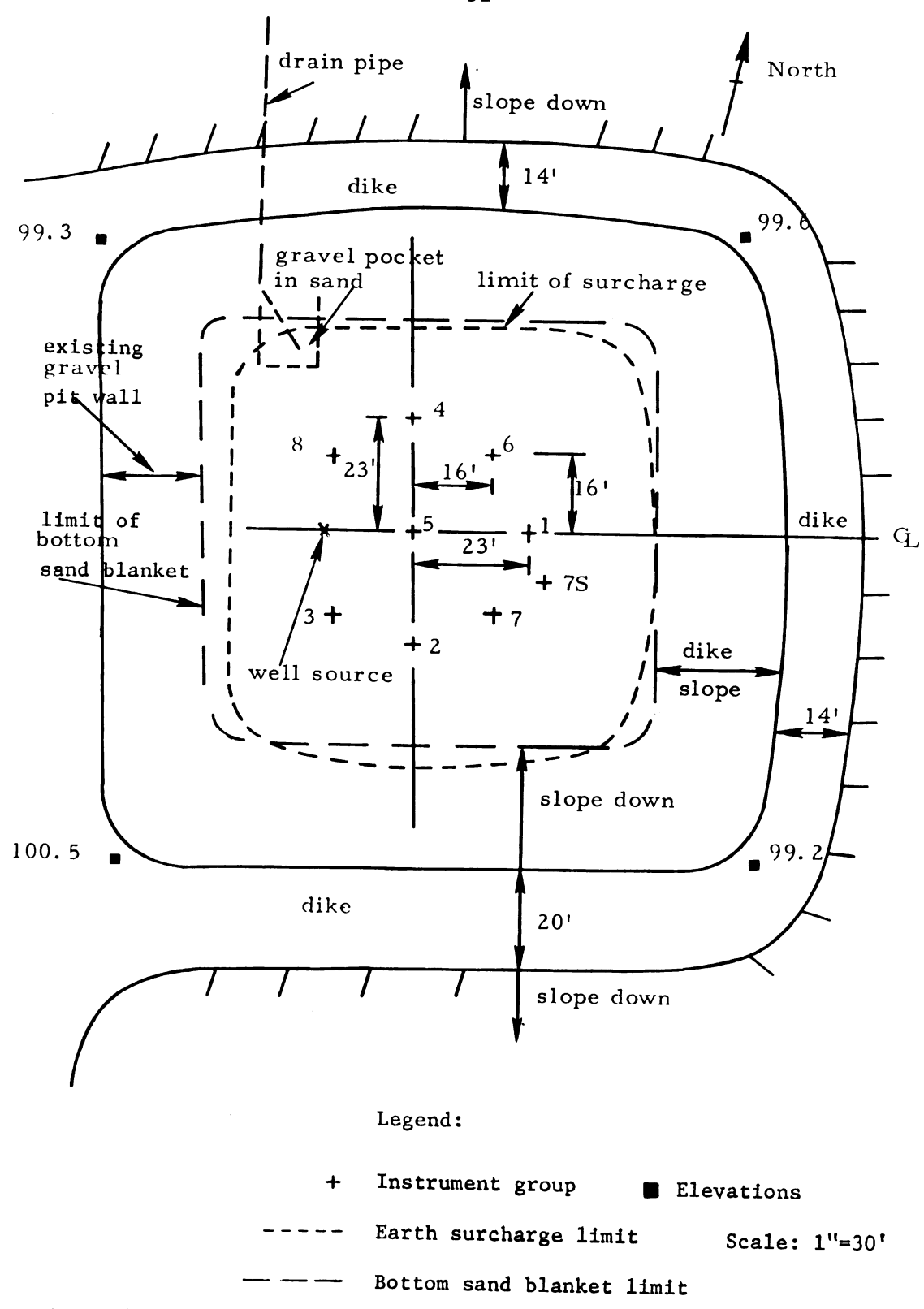
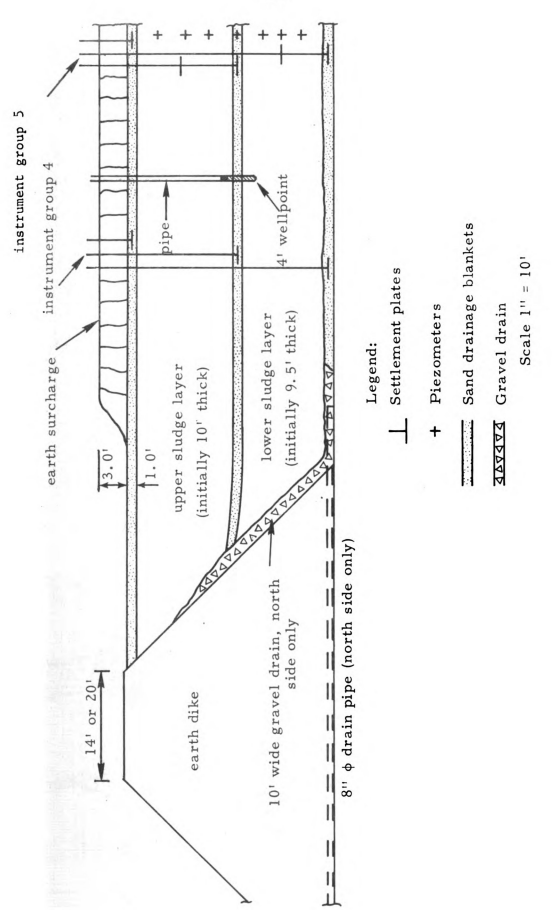


Figure 4.2. Experimental landfill and instrument group locations, plan view.



Section of landfill (typical), north dike at end of construction. Figure 4.3.



(a) Dragline operation.

(b) Dumping over the dike sides.

Figure 4.4. Sludge placement.

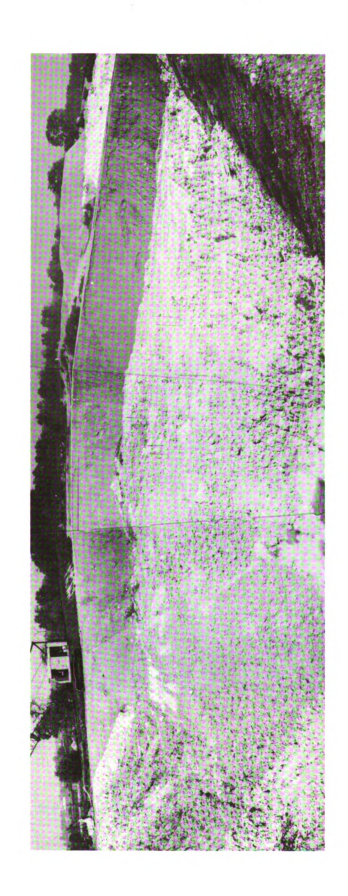
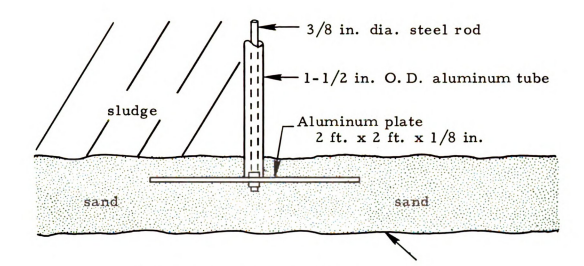


Figure 4.5. Experimental sludge landfill during placement of the lower sludge layer.

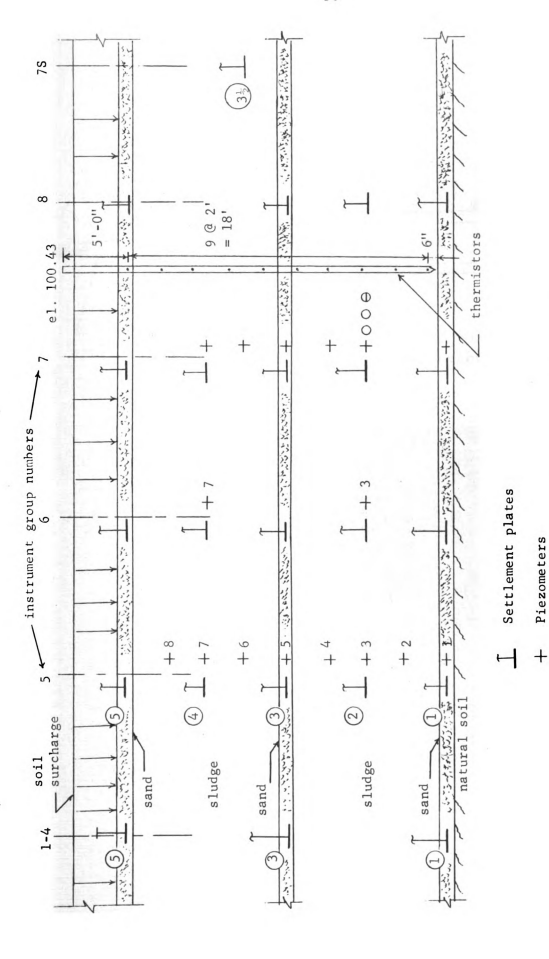


(a) Installation in a sand blanket.



(b) Placement in the sludge, carpenters level shown on the plate.

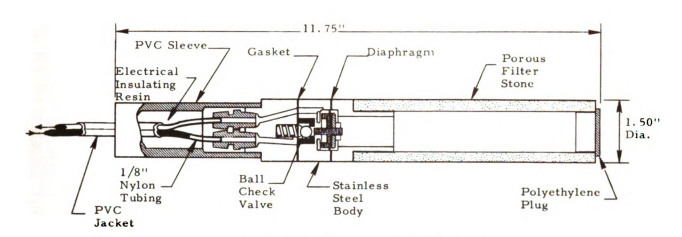
Figure 4.6. Settlement plate.



Distribution of settlement plates, piezometers, and total pressure cells in the instrument groups. Figure 4.7.

Total pressure cells (0 - vertical, 0 - horizontal)

0



(a) Pore pressure transducer.



(b) Installation in a small sand pocket in the sludge.

Figure 4.8. Piezometer.

#### CHAPTER V

#### EXPERIMENTAL RESULTS

The experimental results are presented under three headings: physical properties of the papermill sludge, stress-deformation behavior of the sludge, and field monitoring. Each section may include both laboratory test data and field observations.

## 5.1 Physical Properties of the Papermill Sludge

Physical properties of the papermill sludge used in the experimental landfill are summarized in Table 5.1. Properties given include the liquid and plastic limits, ash content, solids content, and specific gravity. Of the eight samples listed, data shown for samples L-1 and L-2 each represent the average of three different locations at the given elevation. Data shown for samples U-1 through U-5 represent the average of three tests on each sludge sample obtained from one given location. The sludge variability within the landfill is apparent for samples U-1 through U-5, although the average ash content (41.8 percent) is close to that for samples 2 and 3. The initial solids contents shown in Table 5.1 range from 26.9 to 34.4 percent by weight. Using equation 3.1, the equivalent water contents range from 190.7 to 271.7 percent. Additional water content samples taken at several instrument group locations and elevations are summarized in Table 5.2. These water contents appear to fall in the vicinity of the liquid limit. The bulk

unit weight of the papermill sludge was 69.7 lb/cu ft based on the weight and volume of a truck box full of sludge. Using a standard 1/10 cu ft bucket and careful hand placement, the observed bulk unit weight was 69.0 lb/cu ft. For the soil surcharge material, the sand cone method gave a bulk unit weight of 130.4 lb/cu ft.

Water contents of the sludge in the landfill after completion of consolidation are shown in Figure 5.1. These values were obtained from the undisturbed block samples and from grab samples taken from the exposed slope face. Despite the somewhat wide range of water contents obtained, the average for the upper layer dropped to 189 percent and the lower layer to 164 percent. Ash contents from samples obtained from the undisturbed sample blocks in each layer were fairly close to the average ash contents reported in Table 5.1. Block sample B for the upper layer had an average ash content, based on three tests, of 38.6 percent. Sample F for the lower layer had an average of 39.3 percent. This indicates that these block samples can be considered as representative for each sludge layer for consolidation testing.

### 5.2 Stress-Deformation Behavior of the Sludge

Laboratory consolidation tests were run on fresh sludge samples and undisturbed samples taken from the landfill at the end of consolidation to determine parameters needed for estimating and analyzing the settlement of the landfill. In-place vane shear tests provided data on the undrained shear strength of the sludge at various stages of consolidation.

## 5.2.1 Laboratory Consolidation

Results from one-dimensional consolidation tests on fresh

sludge samples from four different locations are summarized in Table 5.3 in terms of the coefficient of consolidation c., primary compression ratio r, coefficient of secondary compression  $C_{\alpha}$ , and the compression index C. Based on the average placement water contents (Table 5.2), sludge samples U-3 and L-2 (Table 5.1) appear to be reasonably representative of the sludge in the landfill. Data for several single increment tests, such as those recommended by MacFarlane (1969) for peat, are included. The earlier tests, including U-4-1, U-3-1 through U-3-9, and L-2-1 were run using the fixed ring container and the loading methods illustrated in Figures IX-5a and IX-4 in SOIL TESTING FOR ENGINEERS by T. W. Lambe (1951). All remaining tests were run on the Bishop consolidation machine. The latter tests were less subject to equipment errors and inconsistencies. Data from test U-3-10 are used in Figure 5.2 to show the consolidation characteristics of fresh sludge and include the void ratio, coefficient of consolidation, and primary compression ratio plotted against the logarithm of total effective stress. The high compression index,  $C_c$ , equal to 1.70 represents a highly compressible material. Coefficient of consolidation values from both the logarithm of time and square root of time fitting methods are included for comparison. The primary compression ratio shows a sharp drop after the first load increment followed by an increase with subsequent load increments. This initial drop in r for loads of 0.1 to 0.2  $kg/cm^2$  appears to be characteristic of the fresh sludge. Two typical compression dial reading-logarithm of time curves are shown in Figure 5.3. The coefficient of secondary compression, C, shown in Figure 5.4a, increases slightly over the

total effective pressure range of 0.1 to 3.2 kg/cm<sup>2</sup>. Since stress appears to be a factor in determining the magnitude of secondary compression (MacFarlane 1969; Leonards and Girault, 1961), the ratio of  $C_{\alpha}$  to the load increment,  $\Delta p$ , is presented in Figure 5.4b. The ratio  $C_{\alpha}/\Delta p$  decreases rapidly with an increase in the load increment.

Figures 5.5 and 5.6 show typical consolidation test results for the undisturbed sludge samples taken from the landfill, and Table 5.4 summarizes the consolidation characteristics for each undisturbed sample test. In Figure 5.5, two e vs. log p curves are shown for each undisturbed block sample location along with a representative curve for a sample of fresh sludge. The curves obtained from the rapid increment tests are at higher equilibrium void ratios than those obtained from the slow tests because of the absence of secondary compression. The data indicate that the sample obtained from the lower layer has a lower compression index, lower initial void ratio, and a higher back-computed overburden pressure than the sample for the upper layer. The coefficient of consolidation, primary compression ratio, and coefficient of secondary compression have been plotted against the logarithm of effective pressure in Figure 5.6. The coefficients of consolidation were obtained by the square root of time method and vary widely with pressure for both samples. Substantially higher values occur at pressures below the effective overburden stress. The primary compression ratio and coefficient of secondary compression both increase with an increase in the load increment and effective pressure.

## 5.2.2 In-Place Vane Shear Tests

Test procedures for measurement of the in-place vane shear

strength of the sludge were given in Chapter IV. Vane shear strengths taken after completion of each sludge layer and after partial and total primary consolidation are summarized in Figures 5.7a and 5.7b. Some consolidation occurred during placement of each sludge layer, hence an increase in strength with depth was observed before placement of the second sludge layer and before placement of the surcharge load. The degree of sensitivity, defined as the ratio of the undisturbed to the remolded shear strength is small, ranging from about 1.5 to 2.5. This is very similar to that of many clays (Terzaghi and Peck, 1967). Both layers increased substantially in strength during consolidation, as shown by data taken on March 20, 1972 (Figure 5.7a) and on Sept. 7, 1972, immediately prior to slope excavation (Figure 5.7b).

# 5.3 Field Monitoring

Field monitoring involved making observations of elevations from the settlement plates, pore water pressures from the piezometers, temperatures from the thermistors, and both horizontal and vertical pressures from the total pressure cells. Figures and graphs are used to summarize the tabulated data, which are given in Appendices A through D. The results are presented under the headings of settlement, pore water pressures, temperatures, and lateral sludge pressures.

## 5.3.1 Settlement

Time-settlement curves for each instrument group are shown in Figures 5.8a through 5.8h for both the upper and lower sludge layers.

The upper part of the figure shows the landfill surface elevation, both during construction and during consolidation, as a function of time.

Also shown at different times are the vertical locations of the settlement plates and the relative thickness of each portion of the sludge landfill. Notation on Figure 5.8, such as 5 - 3, indicates that the settlement of plate 3 has been subtracted from the total settlement of plate 5, in this case giving the time-settlement curve for the upper sludge layer.

Upon completion of the upper sludge layer, the rapid placement of the top sand drainage blanket (2-1/2 days) and surcharge load (1-1/2 days) gave an approximation to instantaneous loading. The settlement versus square root of time curves for the top sludge layer are presented in Figures 5.9a and 5.9b for each instrument group. The initial point is not at zero since some compression of the layer occurred during placement of the sand blanket and surcharge load. The data plotted represent obervations taken after completion of the surcharge placement and give square root of time plots similar to those observed in the conventional consolidation test. Values for the coefficient of consolidation, c<sub>V</sub>, backfigured from these plots, are fairly large and vary some for the different instrument group locations. Settlement-logarithm curves for the upper and lower sludge layers are shown in Figures 5.10 and 5.11 for each instrument group.

# 5.3.2 Pore Water Pressures

Piezometers used for the measurement of pore water pressures gave the data summarized in Figures 5.12a through 5.12g. Pore pressures are plotted against time in the lower half of Figure 5.12, with the location of the piezometer in the landfill given in the upper half.

Observed pore pressures in both layers showed a consistent increase with

time during placement of the sludge. An abrupt increase in pore pressure occurs during the rapid placement of the surcharge load and is followed by dissipation to some residual value, perhaps related to a threshold hydraulic gradient required for flow. In the upper sludge layer the observed pore pressure increase at the center of the layer is close in magnitude to the applied pressure resulting from the placement of the top sand blanket and earth surcharge load. During the later stages of consolidation some fluctuations occurred with time for plezometers in the upper sludge layer and middle sand blanket. High rainfall, involving seepage into the drainage blankets, appears to be responsible for this pore pressure fluctuation. The pore pressure in the middle sand blanket (Figure 5.12g) is the result of a dish effect produced by the greater consolidation of the central area of the sludge landfill. Field data are given in Appendix B.

## 5.3.3 Temperature

Thermistors used for temperature measurement gave the data summarized in Figure 5.13. An increase in temperature caused by biological activity is observed, with the higher values occurring in the lower sludge layer about 50 days after completion of the landfill. Subsequent temperatures show a pattern indicating that the sludge was responding to atmospheric and ground temperatures. Inconsistent temperatures for thermistor 2 indicate a malfunction or damaged unit. Field data are given in Appendix D.

### 5.3.4 Lateral Sludge Pressures

Total pressure cells installed in the lower sludge layer gave the data summarized in Figure 5.14 for both total lateral and vertical

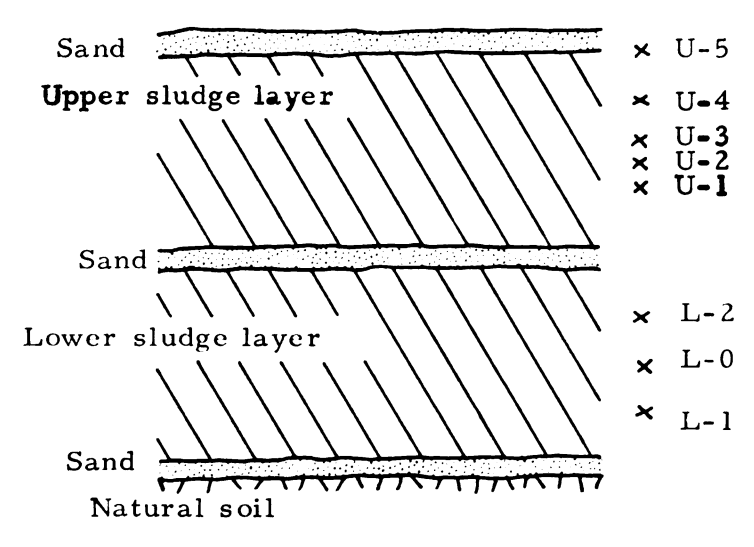
pressures. Pore water pressure data from an adjacent piezometer are included on Figure 5.14 to permit the computation of effective lateral and vertical pressures. The measured total pressures increased gradually during placement of the upper sludge layer and increased sharply upon placement of the earth surcharge load. Subsequently it required about 2 months for the lateral pressures to stabilize at a lower value. The total observed vertical pressure shows an unexplained increase occurring after the initial increase from application of the surcharge. This is opposite to what would be expected as leachate drained from the sludge landfill. Data for pressure cell G7-2 have been omitted from Figure 5.14 because instrument readings indicated that there was a malfunction. Field data are given in Appendix C.

TABLE 5.1 PHYSICAL PROPERTIES OF THE PAPERMILL SLUDGE

Sludg	e sample	Consister	ncy limits <sup>1</sup>	Ash <sup>2</sup>	Solids <sup>3</sup>	Specific 4
No.	Elevation in layer, ft.	L w	P w	content	content % by wt.	gravity
L-0	8 5	325.4	141.6	35.7	28.5	2.01
L-1*	2.5	257.3	102.7	42.2	27. 2	2.05
L-2*	7.5	247.7	105.6	43.3	28.2	2.07
U-1 <sup>+</sup>	2.5	184.5	86.0	59.4	34.4	2.24
U-2 <sup>+</sup>	4	218.5	101.6	46.5	31.9	2.07
U-3 <sup>+</sup>	5	297.5	133.0	36.5	26.9	1.91
U-4 <sup>+</sup>	7.5	287.4	122.1	34.2	29.0	1.87
U-5+	10	302.8	138.6	32.2	28.4	1.92

<sup>\*</sup>Average of three samples. +Average of 3 tests per sample location.

Laboratory test sample locations.



<sup>&</sup>lt;sup>1</sup>L<sub>w</sub>--liquid limit. P<sub>w</sub>--plastic limit. ASTM test methods D 423-66 and D 424-59.

<sup>&</sup>lt;sup>2</sup>ASTM test method D 586-63.

<sup>&</sup>lt;sup>3</sup>Solids content of fresh sludge. Water content by dry weight given by the equation  $w\% = 100 \left[ \frac{100}{\% \text{ solids by wt.}} - 1 \right].$ 

<sup>&</sup>lt;sup>4</sup>ASTM test method D 854-48.

TABLE 5.2 SLUDGE PLACEMENT WATER CONTENTS

Elevation			Group N					
in layer (ft)	1	2	3	4	5	6	7	8
		Lower	Sludge	Layer				
2.5	-	-	-	-	242 277	292	-	-
3.0	-	282	-	284	230 245	-	283	-
4.0	-	-	308	270	-	-	276	298
5.0	-	-	-	-	261	269	262	213
					283	240	265	244
					264	271	262	219
						226		<b>2</b> 53
7.5	-	-	-	279	267	-	-	-
				267	266			
					252			
					265			
					253			
					257		_	
8.0	-	-	274	274	273	-	271	-
			291		264		246	
							258	
							256	
9.0	-	-	278 294	275	-	-	-	-
10.0	-	-	-	-	280	-	-	-
					267			
					276			
	<del></del>				255	<del></del>		
		Upper	Sludge	Layer				
2.5	.262	-	-	-	268	-	270	-
	260				248		270	
	262						270	
	26 <b>2</b>						<b>2</b> 90	
3.0	-	-	-	-	251	-	-	-
					262	_		
6.0	-	-	-	-	251	279	244	_
					284	264	262	
					264	278	271	
7 5	_	_	_	_	276	277	261	_
7.5	-	-	-	_	235	254	232	
					256	237	234	
					257	234	224	
					232	269	212	

Oven temperature 105°C.

Average initial water and solids contents:

Lower sludge layer 265.%, 27.4% Upper sludge layer 257.%, 28.0%

TABLE 5.3 SUMMARY OF CONSOLIDATION CHARACTERISTICS, FRESH SLUDGE

Sample	Test	Load increment	c <sub>v</sub> (in <sup>2</sup> ,/min.)	min.)	Ħ	O	U t	<b>.</b>
No.	No.	$(kg/cn^2)$	log t	$\sqrt{t}$			or remarks	)
U-4	1*	子-0	0.033	0.035		0.00737	1.73	4.67
		w. •	0.028	0.030	0.79	0.0112		
		} <b>-</b> 1	0.024	0.019		0.0136		
		1 - 2	0.0067	0.0067		0.0128		
		2 - 4	0.00826	0.0095		0.0144		
		8 - 7	0.00462	0.00538		0.0167		
		8 - 16	0.00162	0.00463	0.95	0.0102		
U-3	*	0 - 0.1	0.0133	0.0134	0.86	0.00791	1.38	5, 42
		0.1 - 0.2	.017	0.0228	0.76	0.00945	) ) •	
		0.2 - 0.4	0.0211	0.0207	0.80	0.00768		
		0.4 - 0.8	0.0221	0.0180	0.84	0.00584		
			;	:	:	!		
		.3	0.0164	0.0175	0.83	0.00932		
u-3	* m	0 - 0.1	0.0162	0.0160	0.74	0.00907	1.24	5.21
		0.1 - 0.2	0.0161	0.0174	0.71	0.00943		
			0.0216	0.0216	0.63	:		
		0	0.0348	0.0312	0.70	0.00572		
		- i.	•	•	•	0.00500		
		1.6 - 3.2	0.0183	0.0167	0.83	0.00947		
U-3	* 7	0 - 0.239	0.0154	0.0185	:	0.00567	1 increment, 24-hr.	5.64
U-3	*^	0 - 0.239	0.0245	0.0187	1	0.00720	1 increment, 24-hr.	7.40
U-3	*9	0 - 0.239	0.0264	0.0215	1	0.0103	1 increment, 24-hr.	5.48
u-3	*_	0	0.0101	0.00985	08.0	0.00905	1.13	5.67
		0.1 - 0.2	0.0124	0.0166	0.82	0.00604		
		•	0.0121	0.0105	98.0	0.00361		
		0.4 - 0.8	0.0145	0.0128				
			•	0.0304	ا:ر	0.003/5		

TABLE 5.3.--continued

Sludge	lge	Load	4;) 0	c (in <sup>2</sup> /min)	ч	ິວ	ິ່ງ	<b>a</b>
Sample	Test	increment	ντ ) Δ	, , ,,,,,,,		•		o
No.	No.	(kg/cm <sup>2</sup> )	log t	۸ţ			remarks	
L-2	+ <sub>2</sub>	0 - 0.1	0.00985	0.00853	0.86	0.00984	1.67	5.52
		0.1 - 0.2	0.00904	0.00894	0.62	0.0135		
		0.2 - 0.4	0.00622	0.00882	0.72	0.0162		
		0.4 - 0.8	0.00555	90600.0	0.75	0.0168		
		0.8 - 1.6	0.00495	0.00991	0.77	0.0161		
		1.6 - 3.2	0.00378	09900.0	0.78	0.0167		
L-2	+ <sub>m</sub>	0 - 0.1	0.0120	0.0115	0.86	0.00923	1.64	5.43
		0.1 - 0.2	0.0108	0.0141	0.61	0.0122		
		0.2 - 0.4	0.00788	0.0115	0.73	0.0143		
		0.4 - 0.8	0.00647	0.00920	0.77	0.0136		
		0.8 - 1.6	0.00482	0.00728	0.74	0.0158		
		1.6 - 3.2	0.00390	0.00583	0.74	0.0191		
U-4	5 <sup>+</sup>	0 - 0.1	0.0178	0.0173	0.80	0.0103	1.62	4.74
		0.1 - 0.2	0.0135	0.0180	0.61	0.0125		
		0.2 - 0.4	0.00973	0.0150	0.68	0.0166		
		0.4 - 0.8	0.00726	0.0127	92.0	0.0170		
		0.8 - 1.6	0.00510	0.00786	0.72	0.0190		
n-4	+6	0 0.24	0.0161	0.0154	0.82	0.0151	l increment, 24-hr.	4.43
L-2	++	0 - 0.63	0.0118	0.0103	06.0	0.0145	l increment, 24-hr.	5.46
U-2	+	0 - 0.24	0.0170	0.0162	0.87	0.0106	lincrement 24-hr	4.38
						1		

<sup>+</sup>Bishop type consolidation machine, Figure 3.2.  $c_{
m v}$  - coefficient of consolidation, t - time, r - primary compression ratio, \*Load frame similar to Figure IX-4, Lambe, 1951.

C<sub>a</sub> - coefficient of secondary compression, C<sub>c</sub> - compression index, e<sub>o</sub> - initial void ratio.

TABLE 5.4 SUMMARY OF CONSOLIDATION CHARACTERISTICS, UNDISTURBED SAMPLES

									,
Sludge	lge	Load	c, (in <sup>2</sup> /min)	2/min)	ы	ပႛ	υ <sup>°</sup>	o <sup>°</sup>	po kg/cm²
Sample No.	Test No.	(kg/cm <sup>2</sup> )	log t	€		3	o O		Casagrande construction
* <sub>¤</sub>	+,-	rapid load increments (every 25 min) See Figure 5.5	$rac{\Delta p}{p} < 1$ , not computed	computed		1	1.92	4.65	.31
<b>*</b> ¤	<b>5</b> +	rapid load increments (every 15 min)	$\frac{\Delta p}{p} < 1$ , not	not computed	ł	l	1.86	4.65	.30
* <u> </u>	† <sub>m</sub>	0.00 - 0.05 0.05 - 0.10 0.10 - 0.20 0.20 - 0.40 0.40 - 0.80	.0956 .0525 .0386 .0273 .0150	.0620 .0497 .0464 .0341 .0168	54.5 56.2 62.2 63.8 73.4	.00216 .00427 .00687 .0130 .0184	1.84	4.48	. 28
* ¤	+4	1.60 - 3.20 0.00 - 0.05 0.05 - 0.10	.00542 .0378 .0224	.00875	77.0 62.4 57.8	.0187 .00264 .00427	1.61	3.81	1
		0.10 - 0.20 0.20 - 0.40 0.40 - 0.80 0.80 - 1.60 1.60 - 3.20	.0215 Bad Incr. .00677 .00400	.0400 Increment .00990 .00697	79.2 80.5 80.8 78.7	.00311  .0190 .0215			

# * *	+	rapid load increments (every 15 min) See Figure 5.5	Δ <u>p</u> < 1, n	$\frac{\Delta p}{p} < 1$ , not computed	1	I	1.51	3.50	.77
т. * *	+2	<pre>rapid load increments (every 15 min)</pre>		$\frac{\Delta p}{p}$ < 1, not computed	1	I	1.51	3.52	.77
* *	+6	0.00 - 0.05 0.05 - 0.10 0.10 - 0.20 0.20 - 0.40 0.40 - 0.80 0.80 - 1.60 1.60 - 3.20	.0537 .0447 .0360 .0282 .0146 .00712	.0521 .0400 .0364 .0339 .0233 .00932	60.6 50.0 50.6 60.8 73.2 74.0	.00121 .00218 .00498 .00674 .00932 .01740	1,55	3,50	. 64
* *	+4	0.00 - 0.05 0.05 - 0.10 0.10 - 0.20 0.20 - 0.40 0.40 - 0.80 0.80 - 1.60 1.60 - 3.20	.0351 .0447 .0291 .0176 .0113 .00622	.0395 .0308 .0318 .0229 .0183 .00898	61.0 46.7 49.6 61.5 68.9 71.6	.00108 .00204 .00344 .00508 .00944 .01520	1.51	3,38	.72

<sup>+</sup>Bishop type consolidation machine, Figure 3.2 \*\*Undisturbed sample 4.0 ft. below the upper sand blanket Undisturbed sample 4.0 ft. below the middle sand blanket

 $c_{
m V}$  - coefficient of consolidation, t - time, r - primary compression ratio,

e - initial void ratio  $_{\alpha}$  - coefficient of secondary compression,  $_{c}$  - compression index,

 $\frac{-}{p}$  - back-computed in-situ vertical effective stress

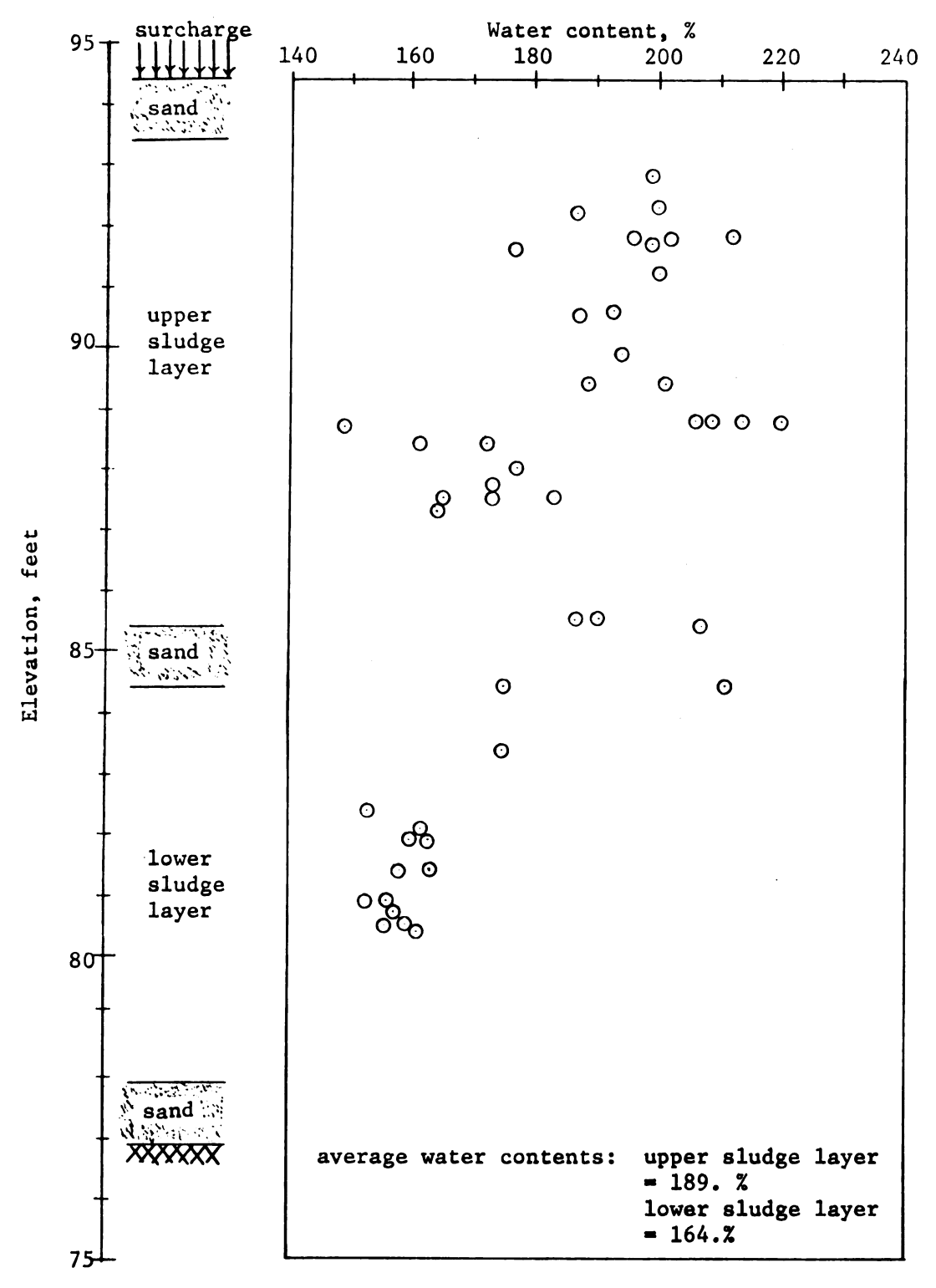


Figure 5.1. Water contents of the sludge in the landfill at the end of consolidation.

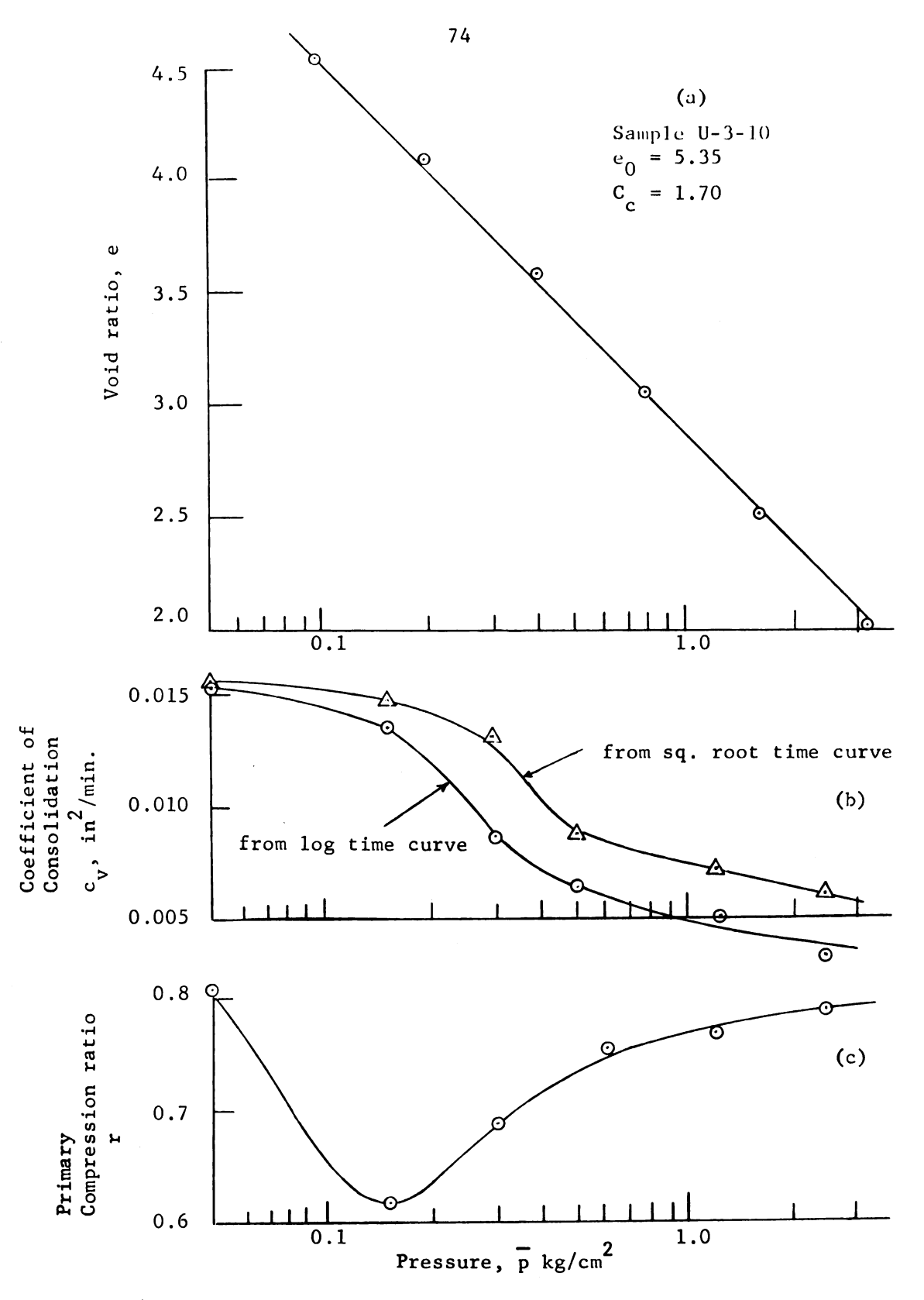
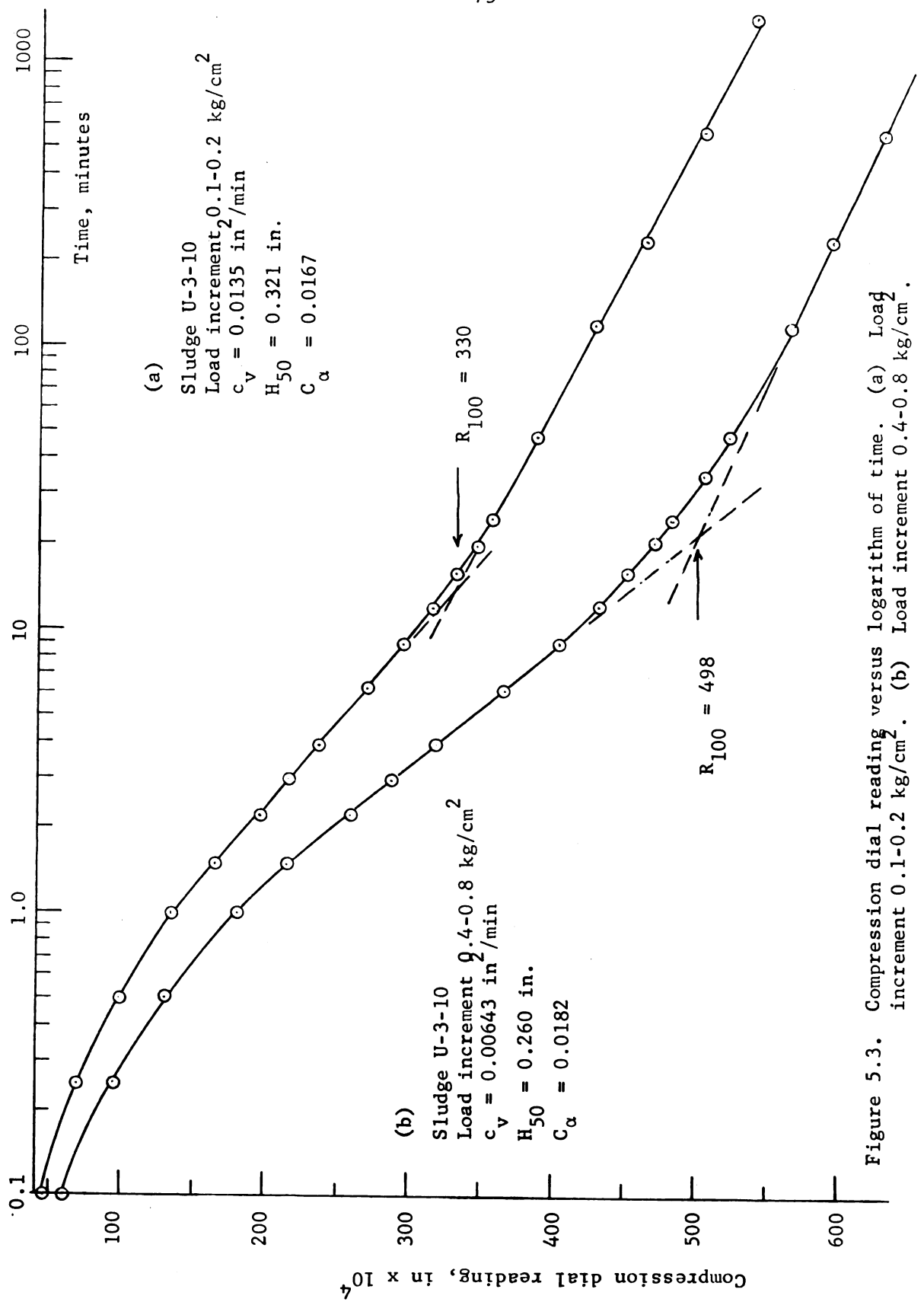


Figure 5.2. Consolidation characteristics for sludge sample U-3.

(a) Void ratio, e. (b) Coefficient of consolidation, c
(c) Primary compression ratio, r.



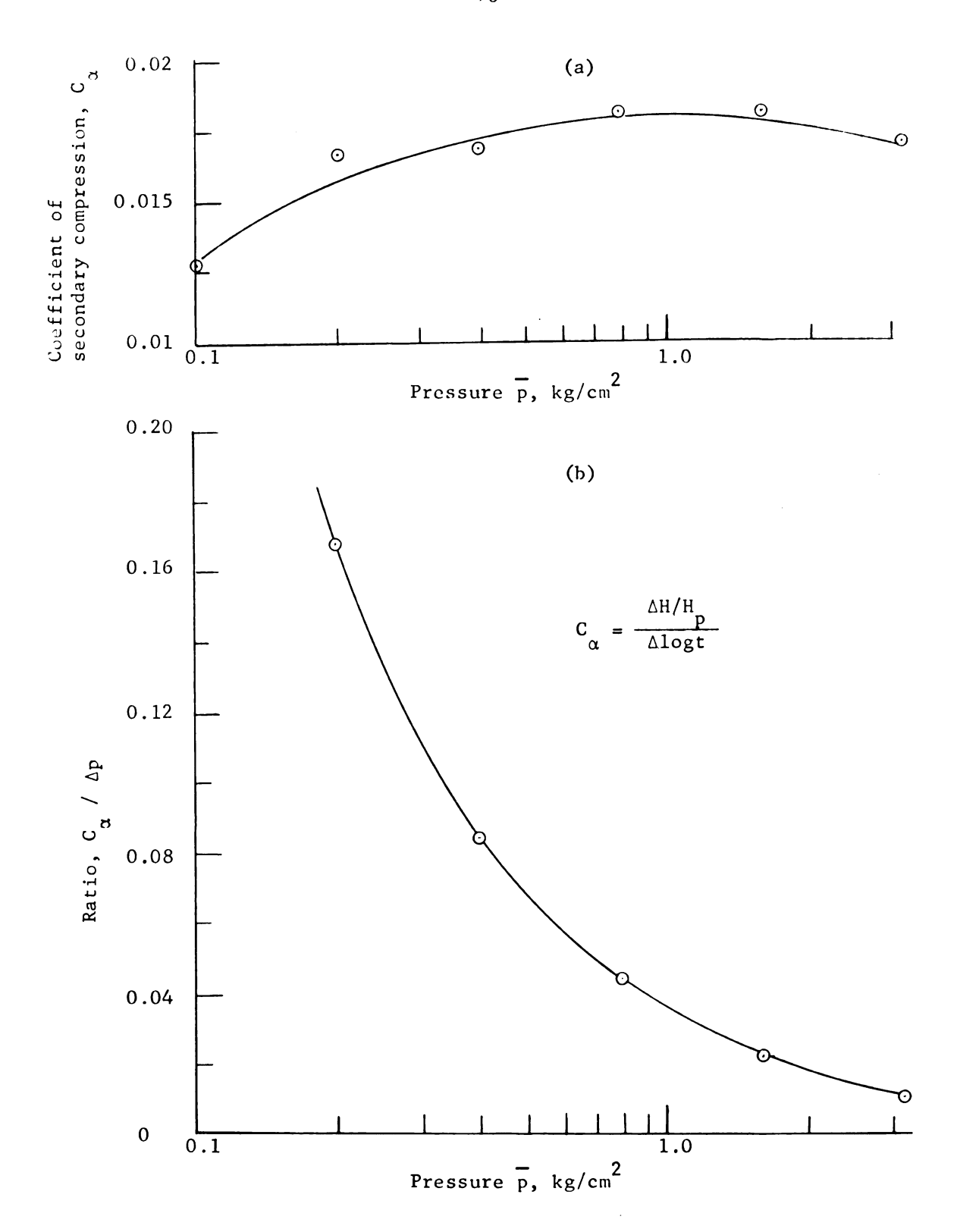


Figure 5.4. Coefficient of secondary compression C  $_{\alpha}$  (a) C  $_{\alpha}$  versus log  $\overline{p}$ .

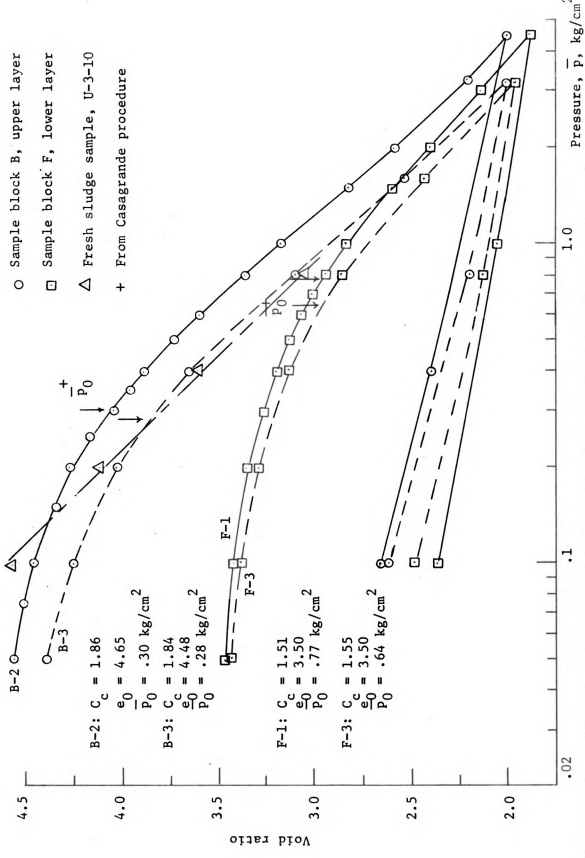
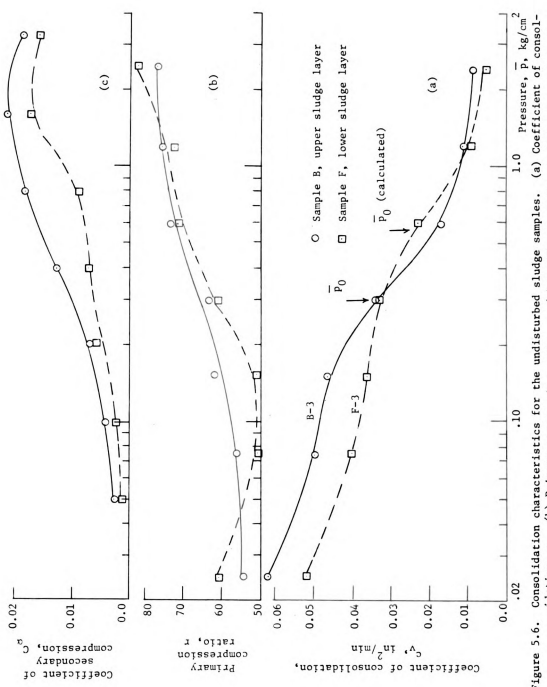
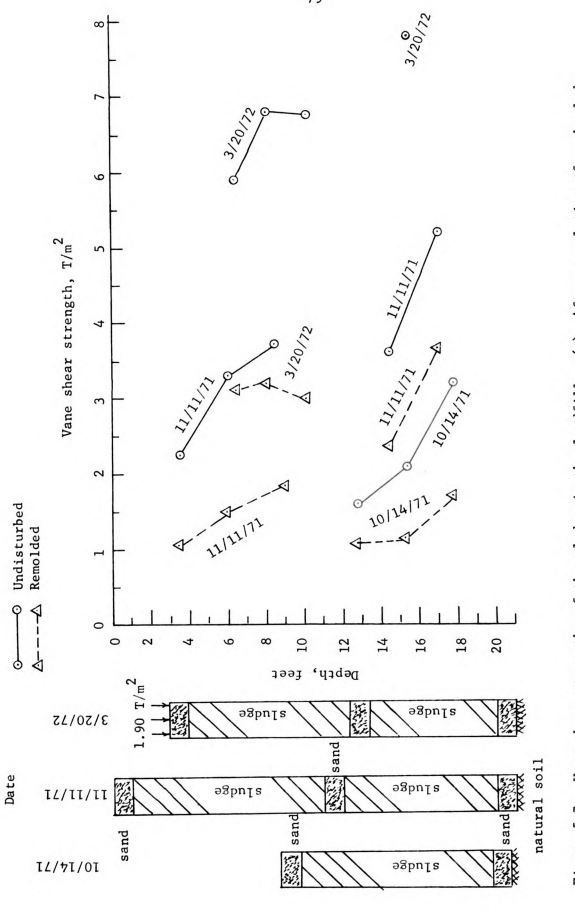


Figure 5.5. Void ratio -- effective stress relationships, undisturbed sludge samples.



Consolidation characteristics for the undisturbed sludge samples. (a) Coefficient of consolidation,  $c_{\rm u}$ , (b) Primary compression ratio, r. (c) Coefficient of secondary compression,  $c_{\rm u}$ Figure 5.6.



Vane shear strengths of the sludge in the landfill. (a) After completion of each sludge layer and after primary consolidation, hand driven vane tests. Figure 5.7.

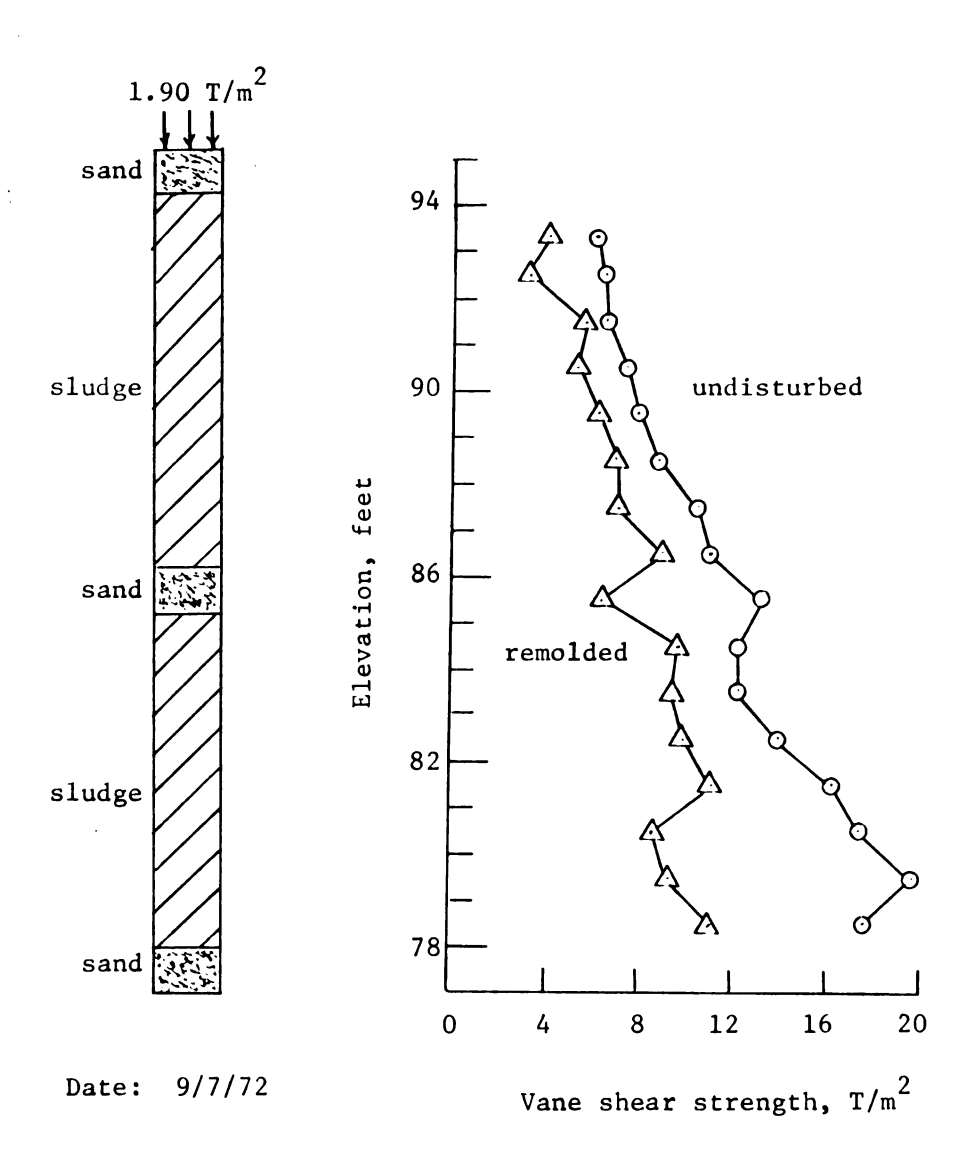
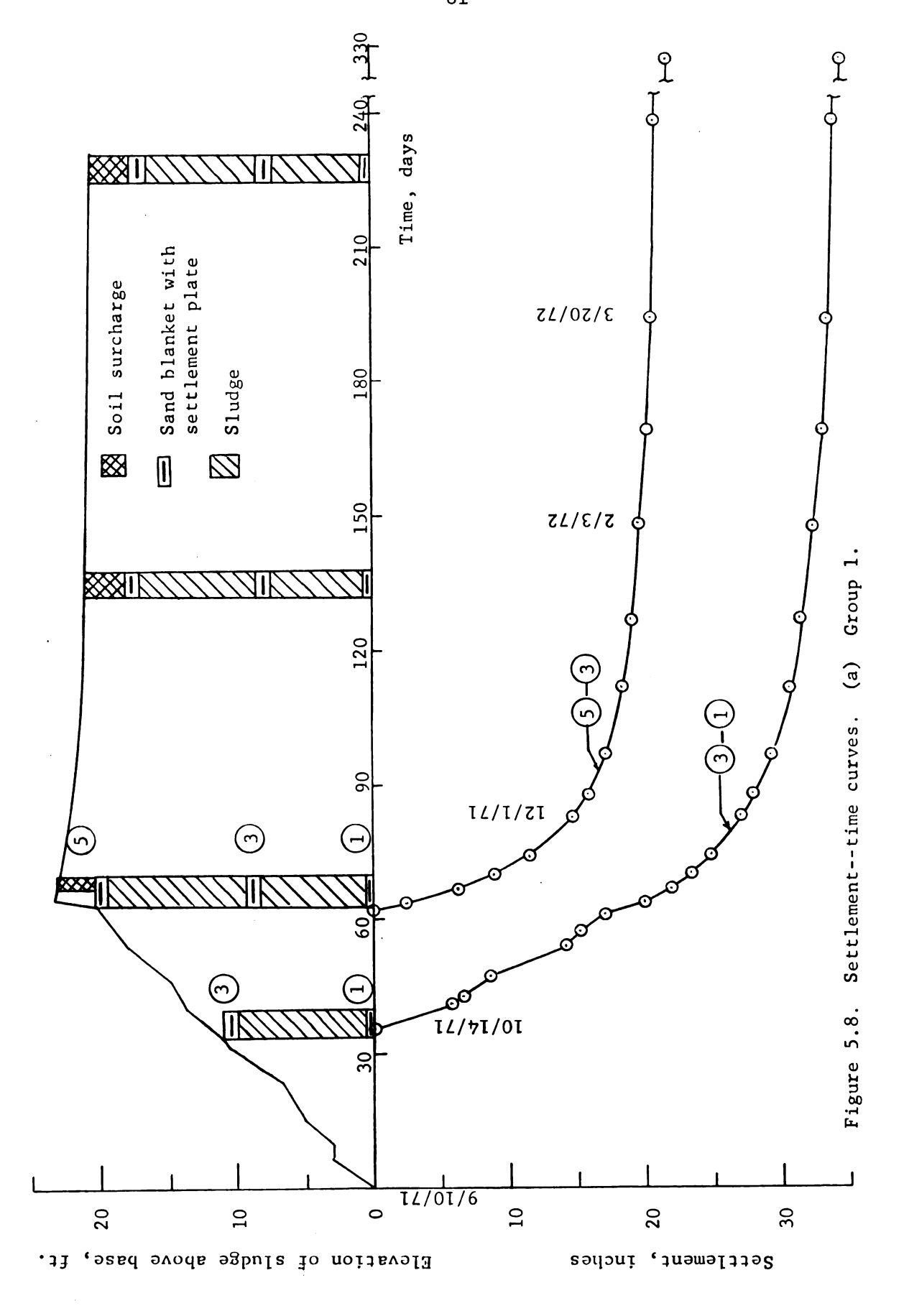
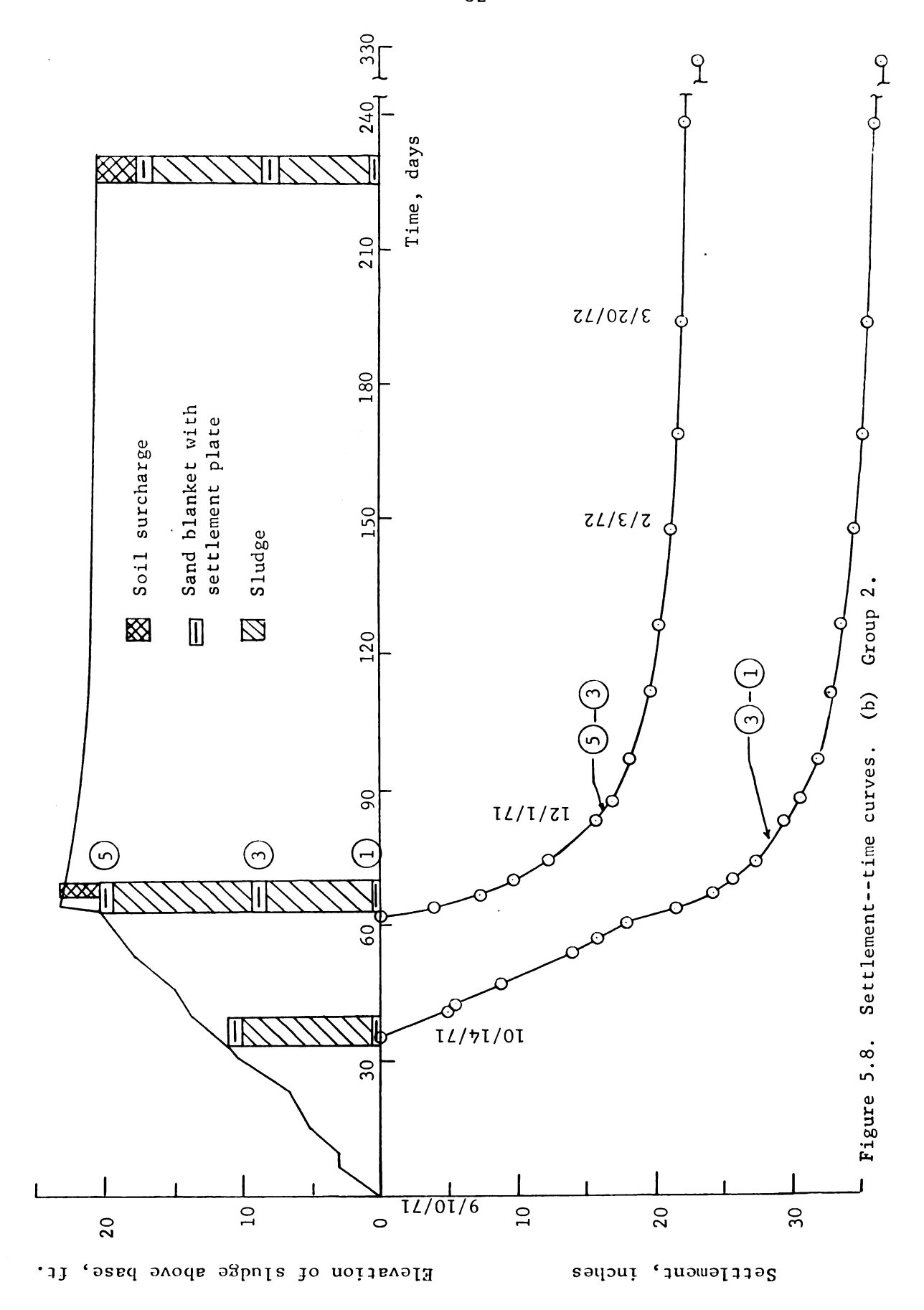


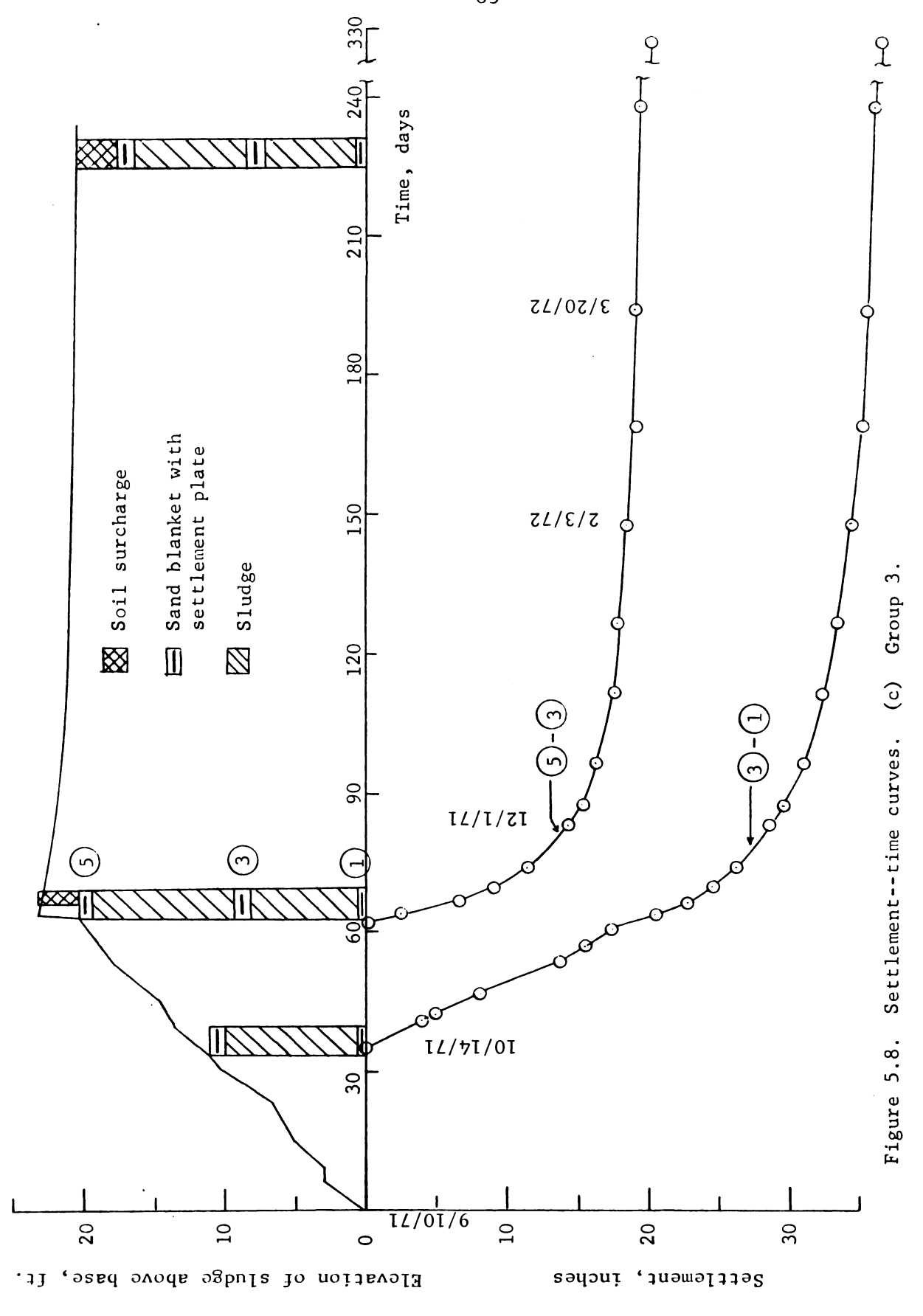
Figure 5.7. Vane shear strengths of the sludge in the landfill.

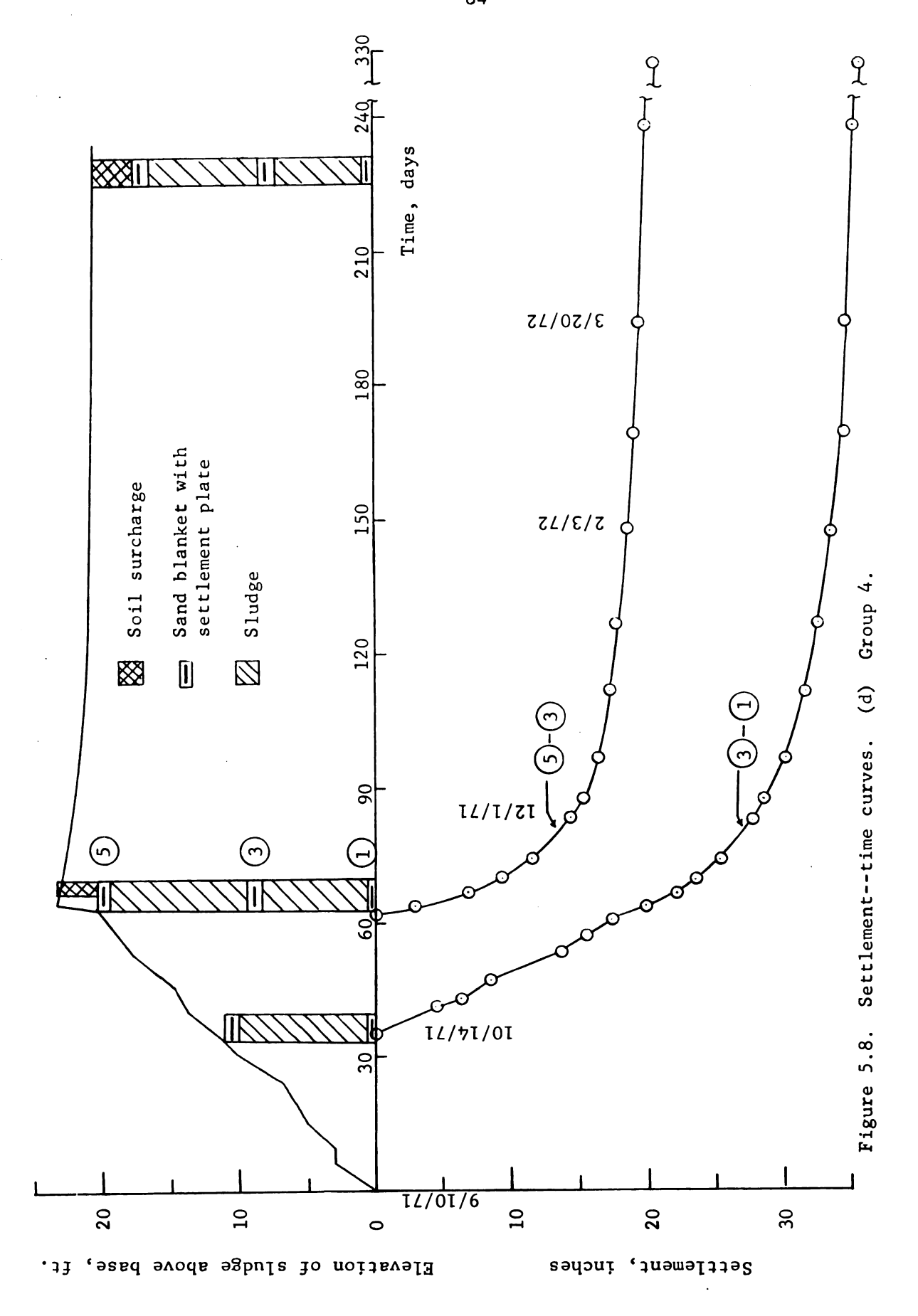
(b) Immediately prior to slope excavation, vane test run with a pre-augered hole.

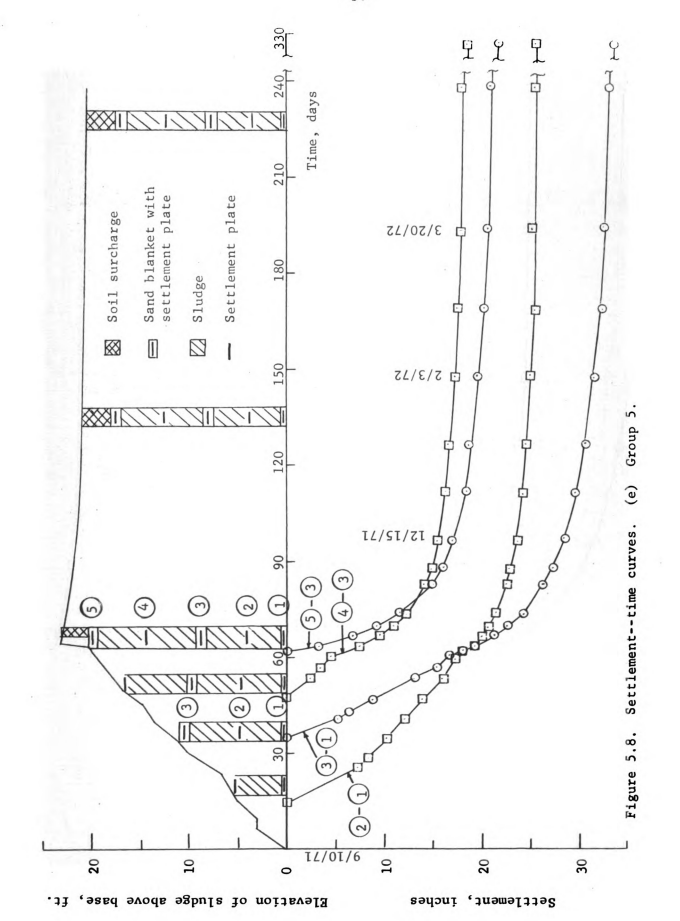


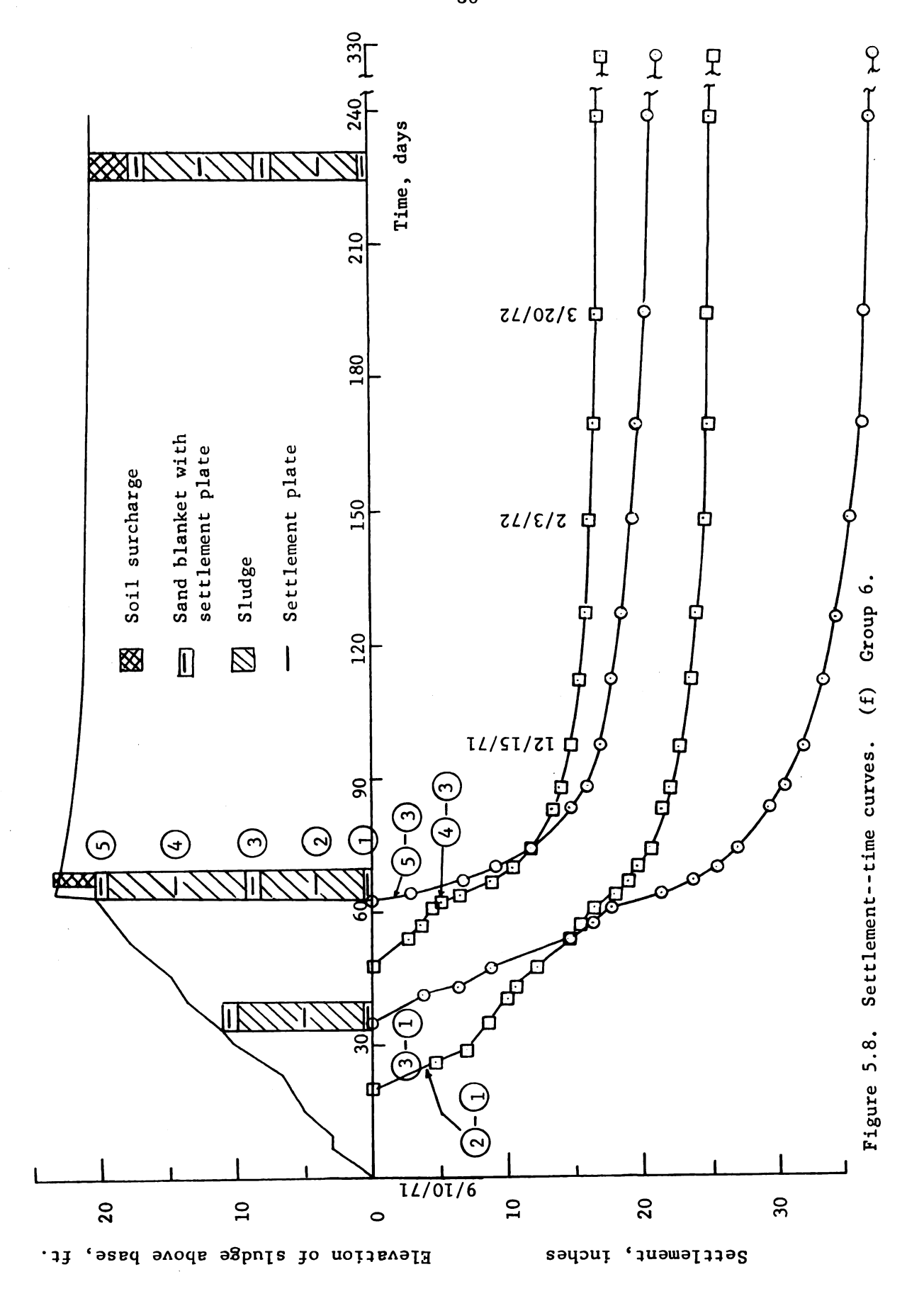


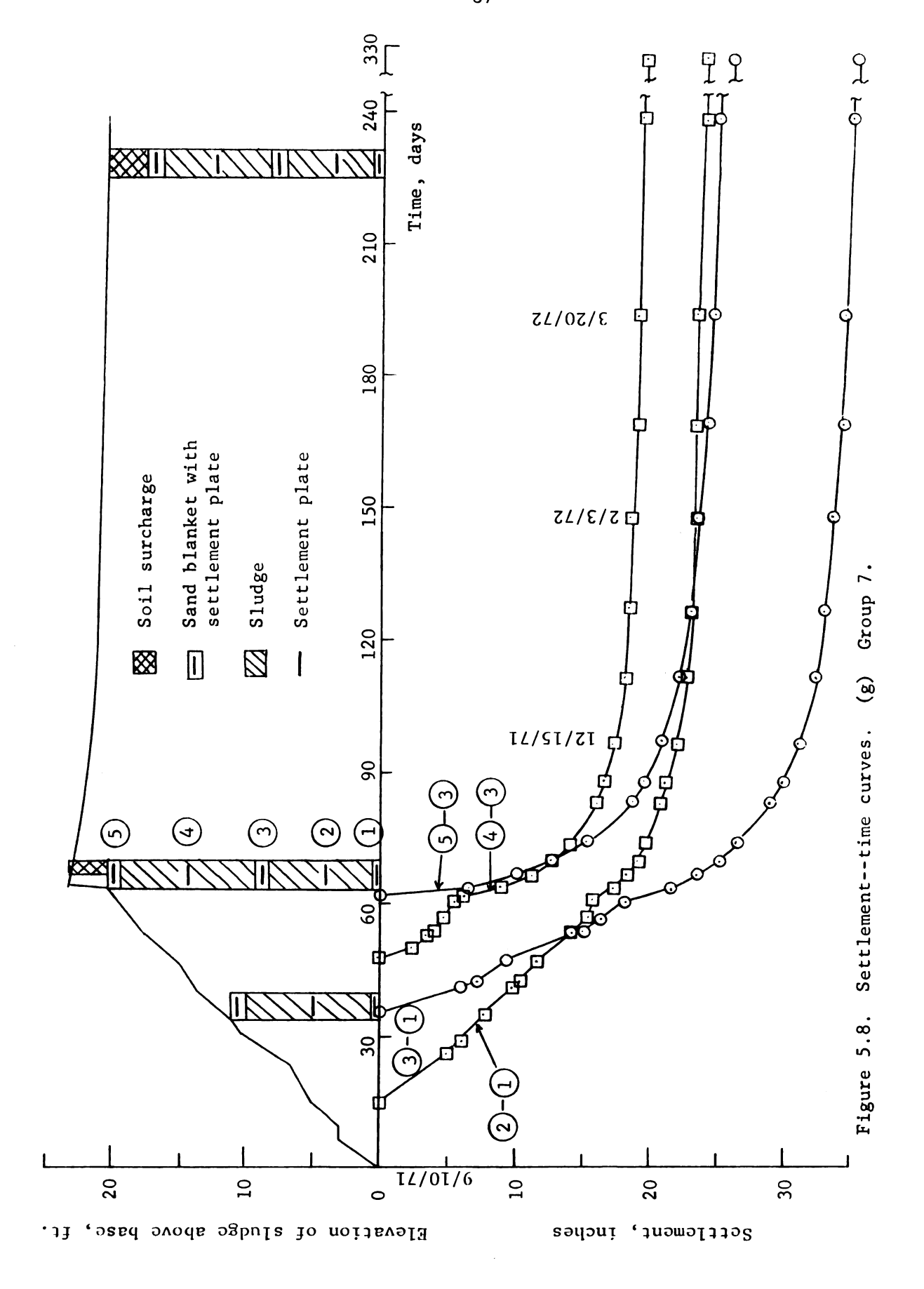


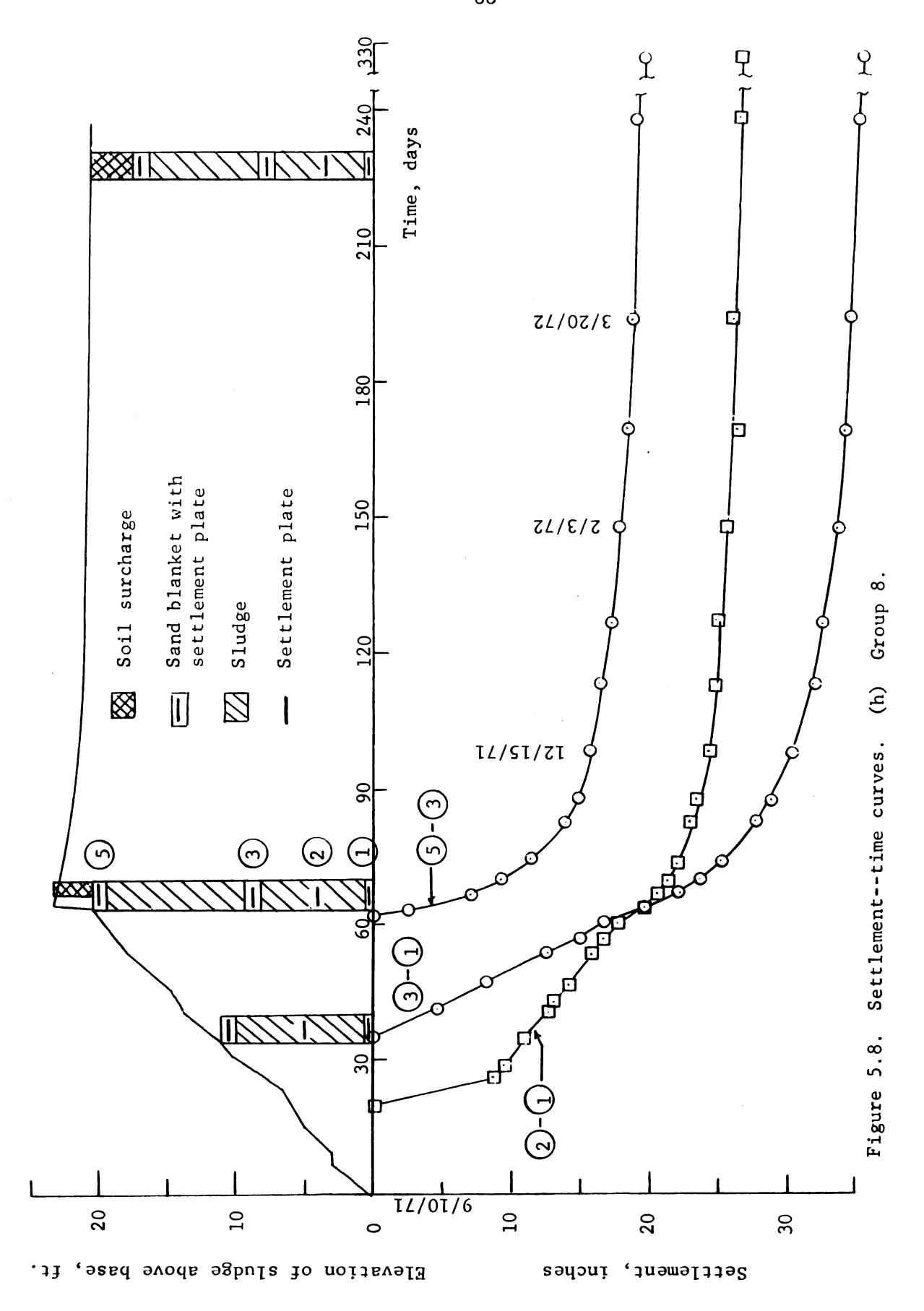


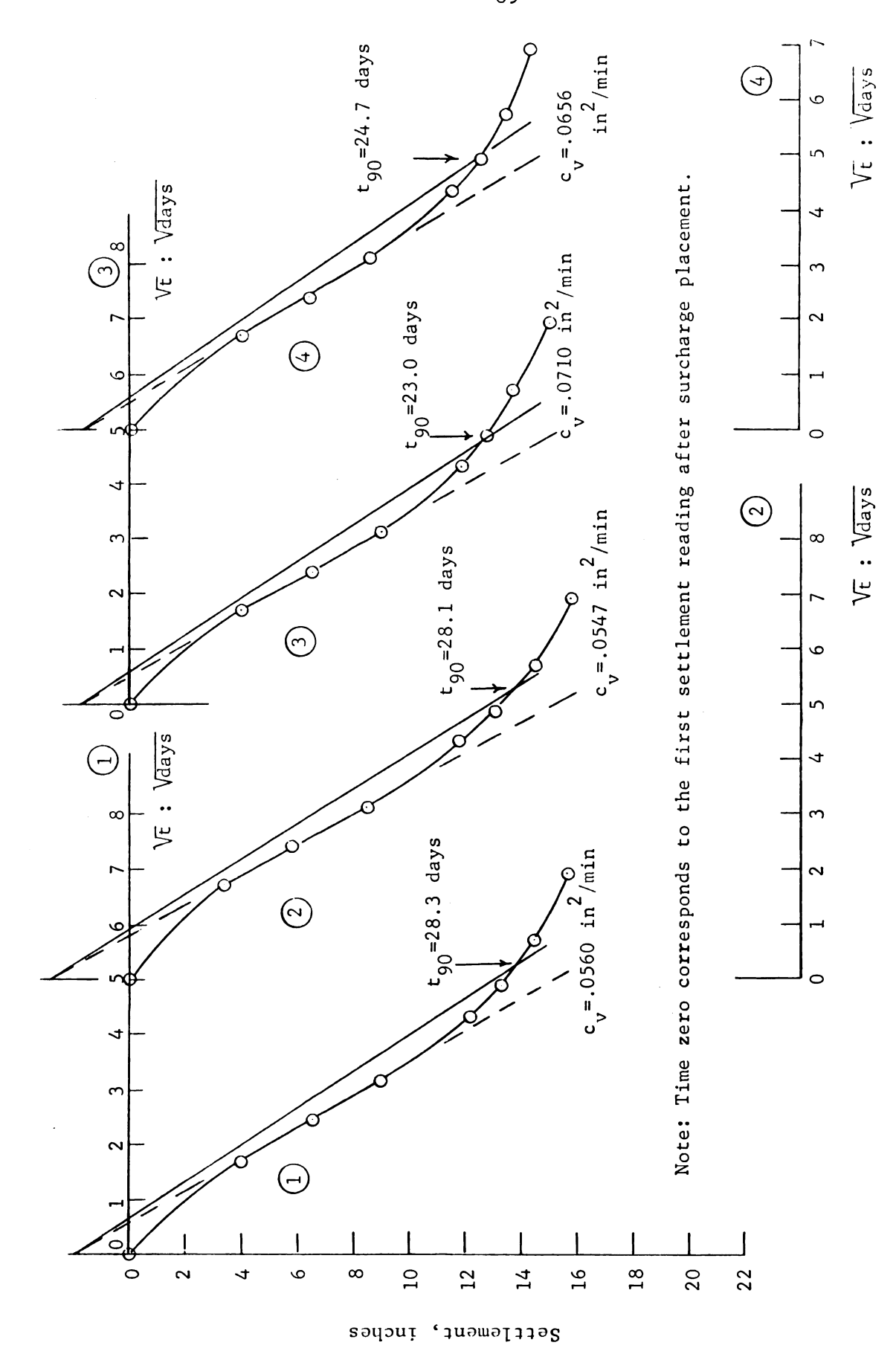




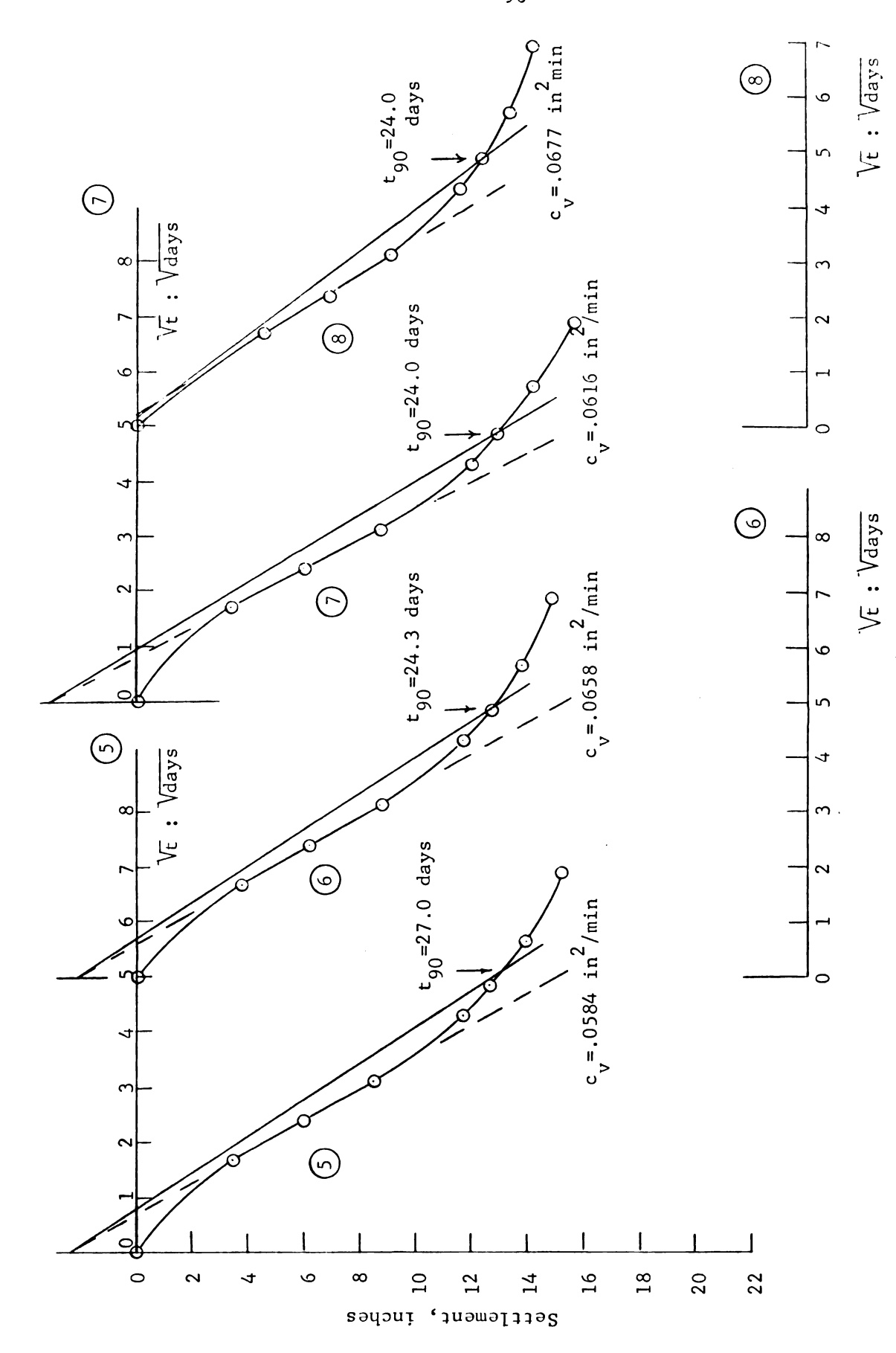








Groups 1-4. (a) Settlement versus square root of time curves, upper sludge layer. Figure 5.9.



(b) Groups 5-8. Settlement versus square root of time curves, upper sludge layer. Figure 5.9.

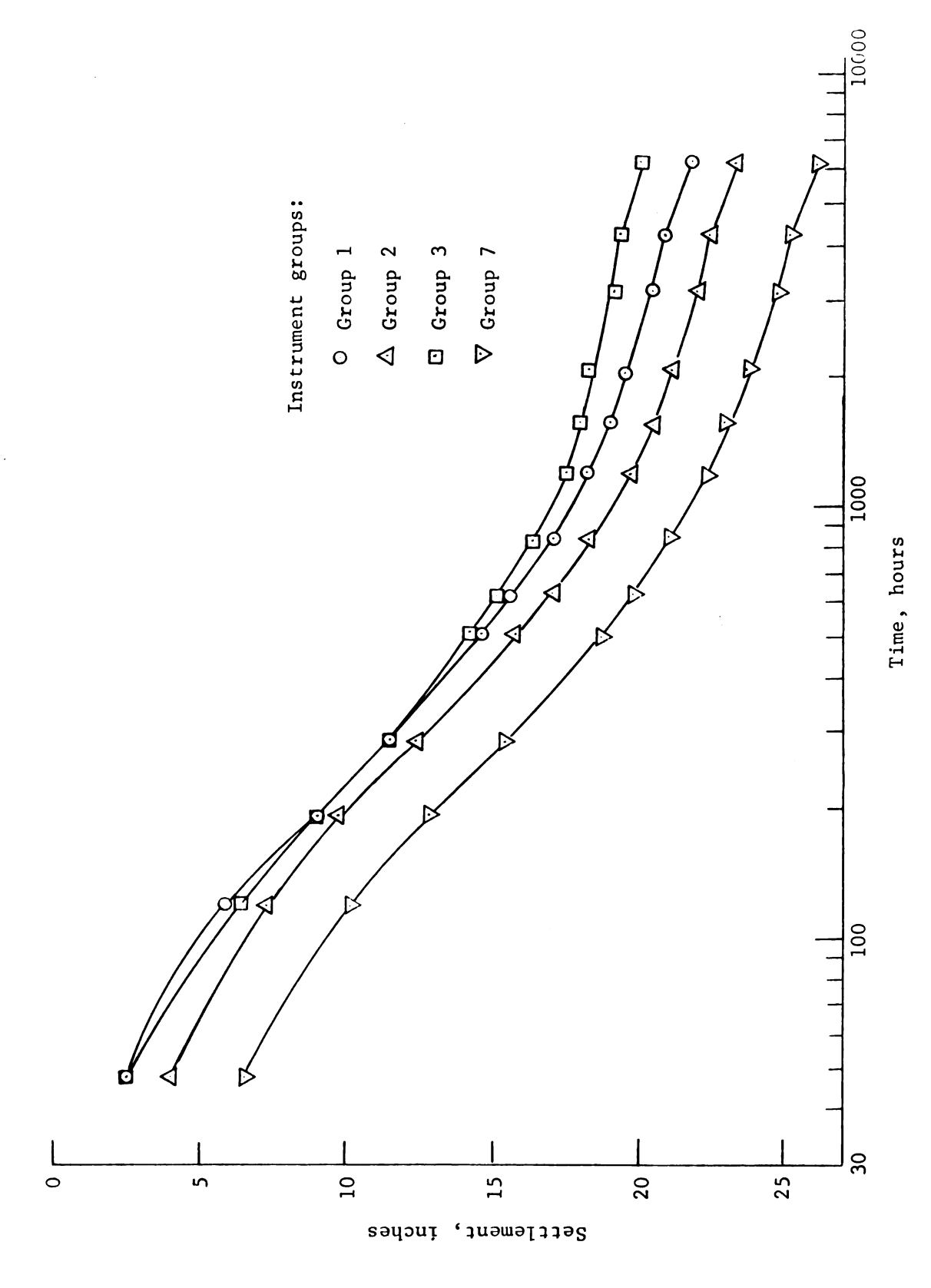
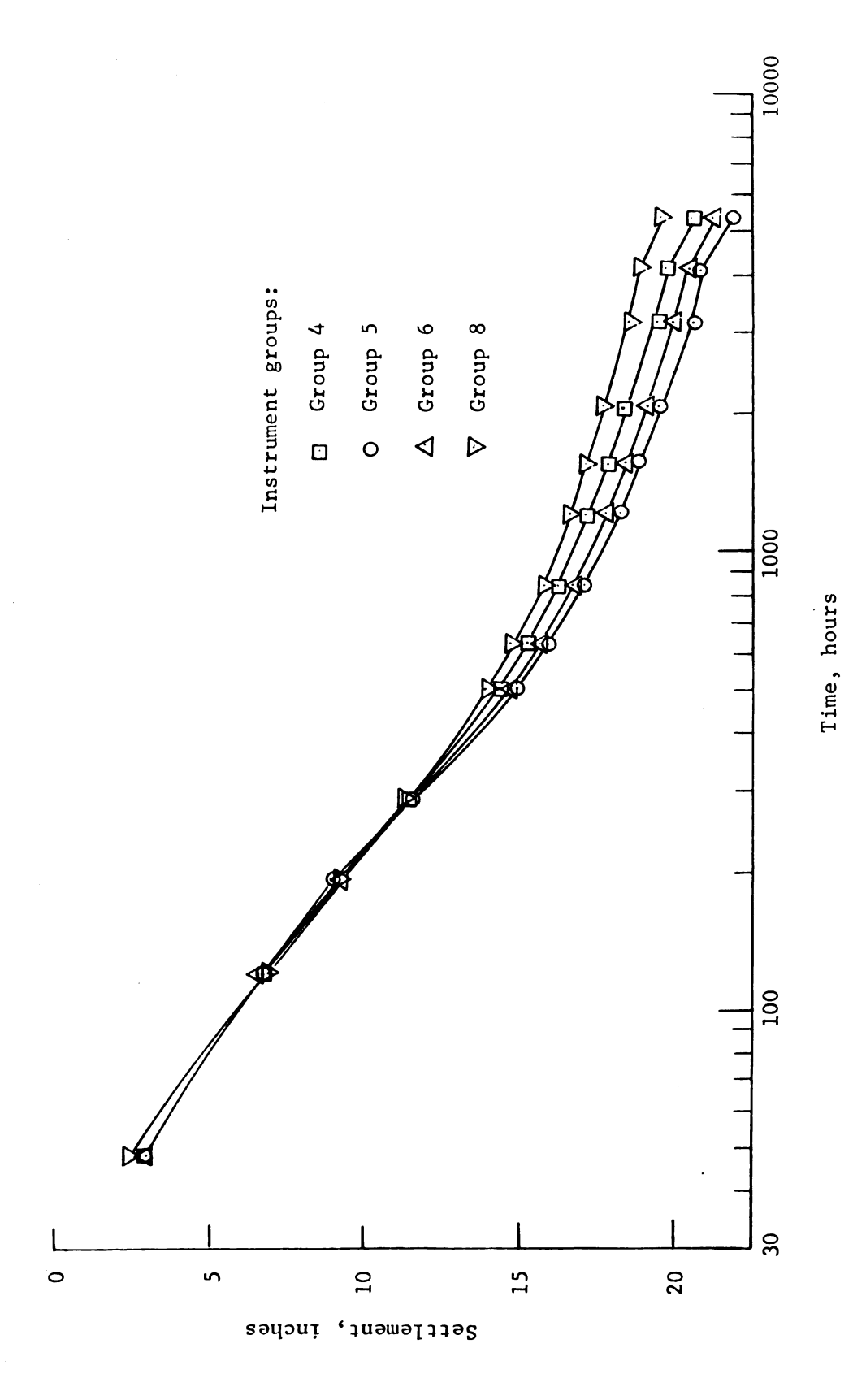
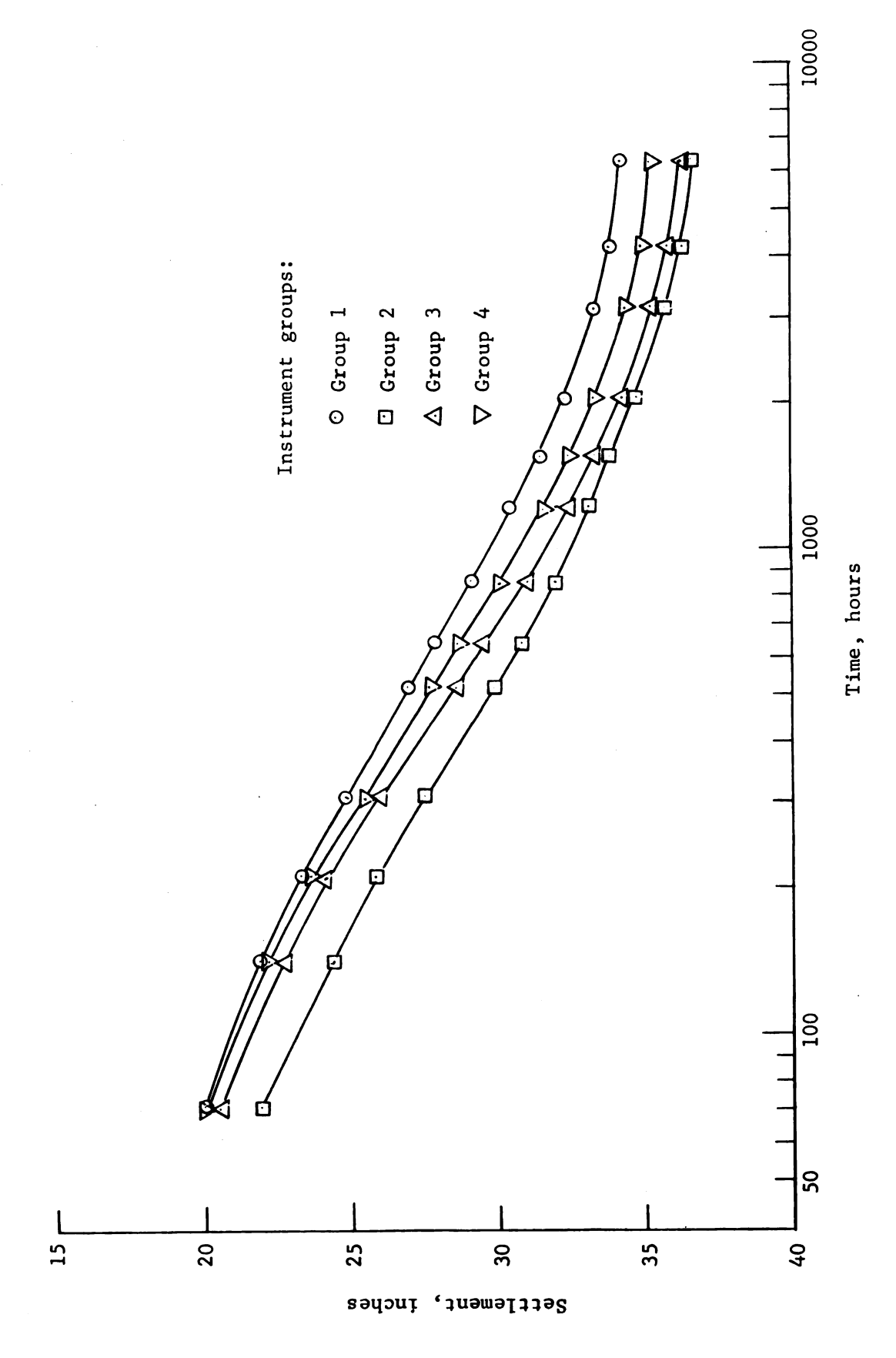


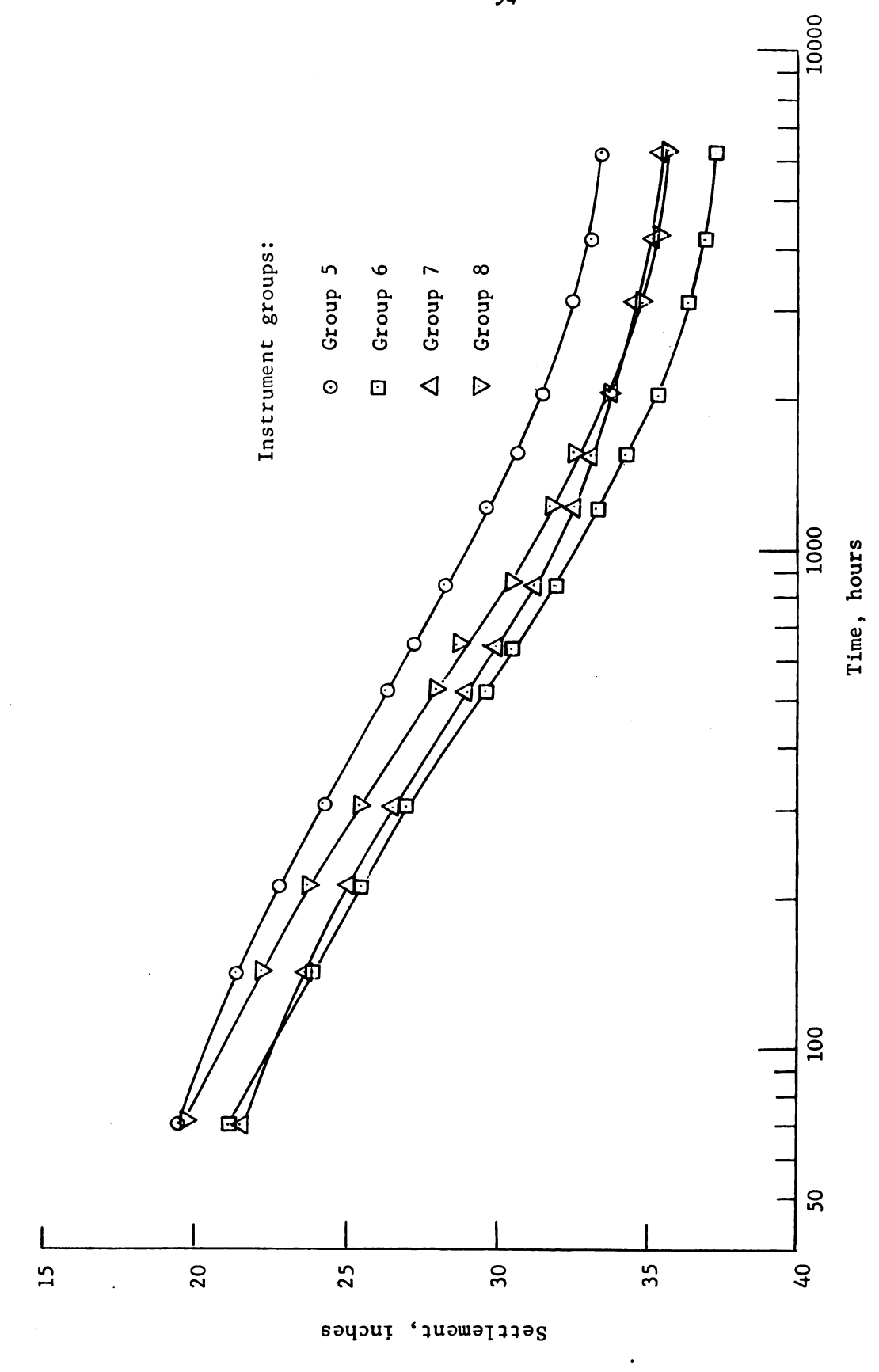
Figure 5.10. Settlement--logarithm of time curves, upper sludge layer. (a) Groups 1,2,3, and 7.



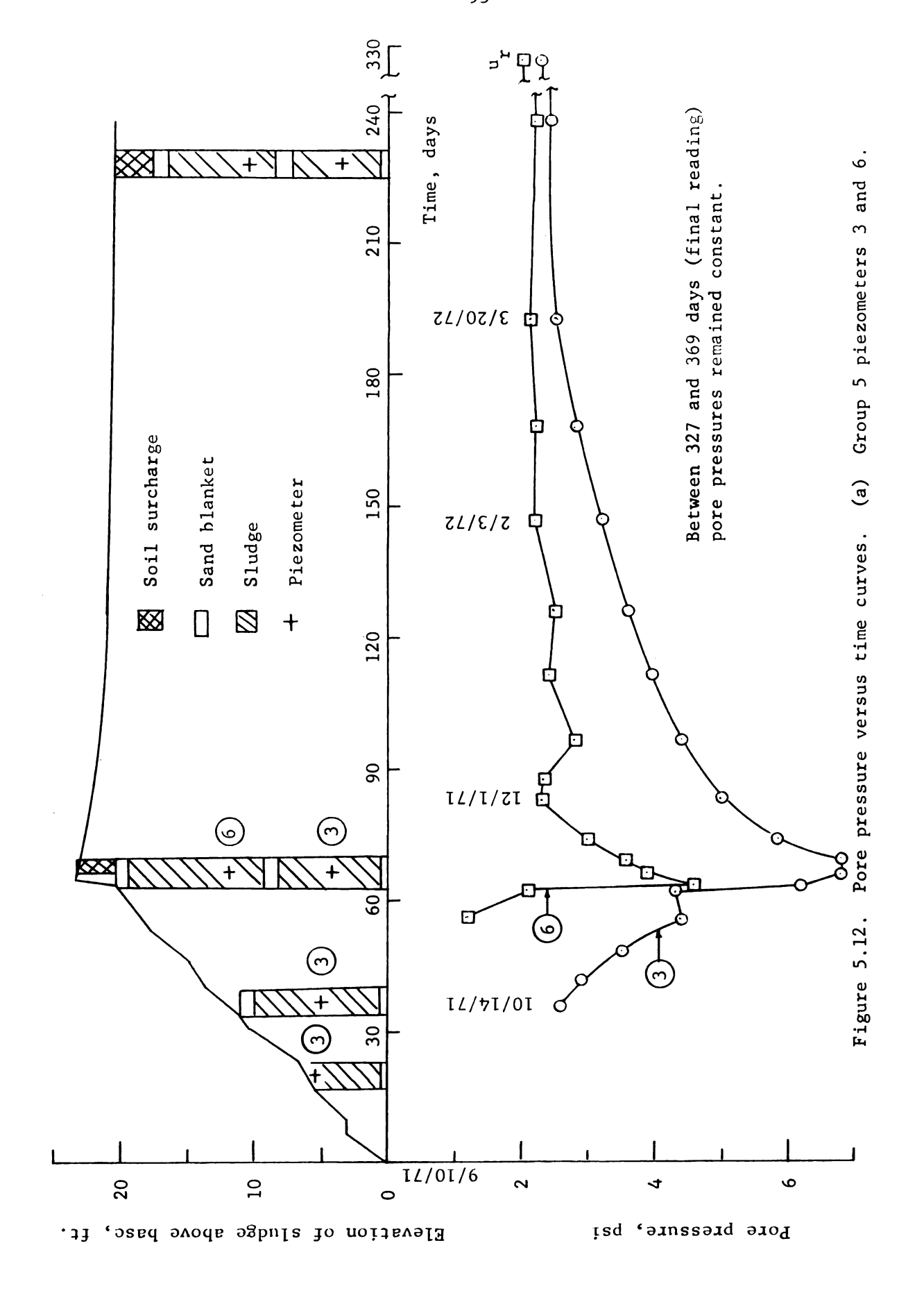
Groups 4,5,6, and 8. (<del>b</del>) Settlement--logarithm of time curves, upper sludge layer. Figure 5.10.

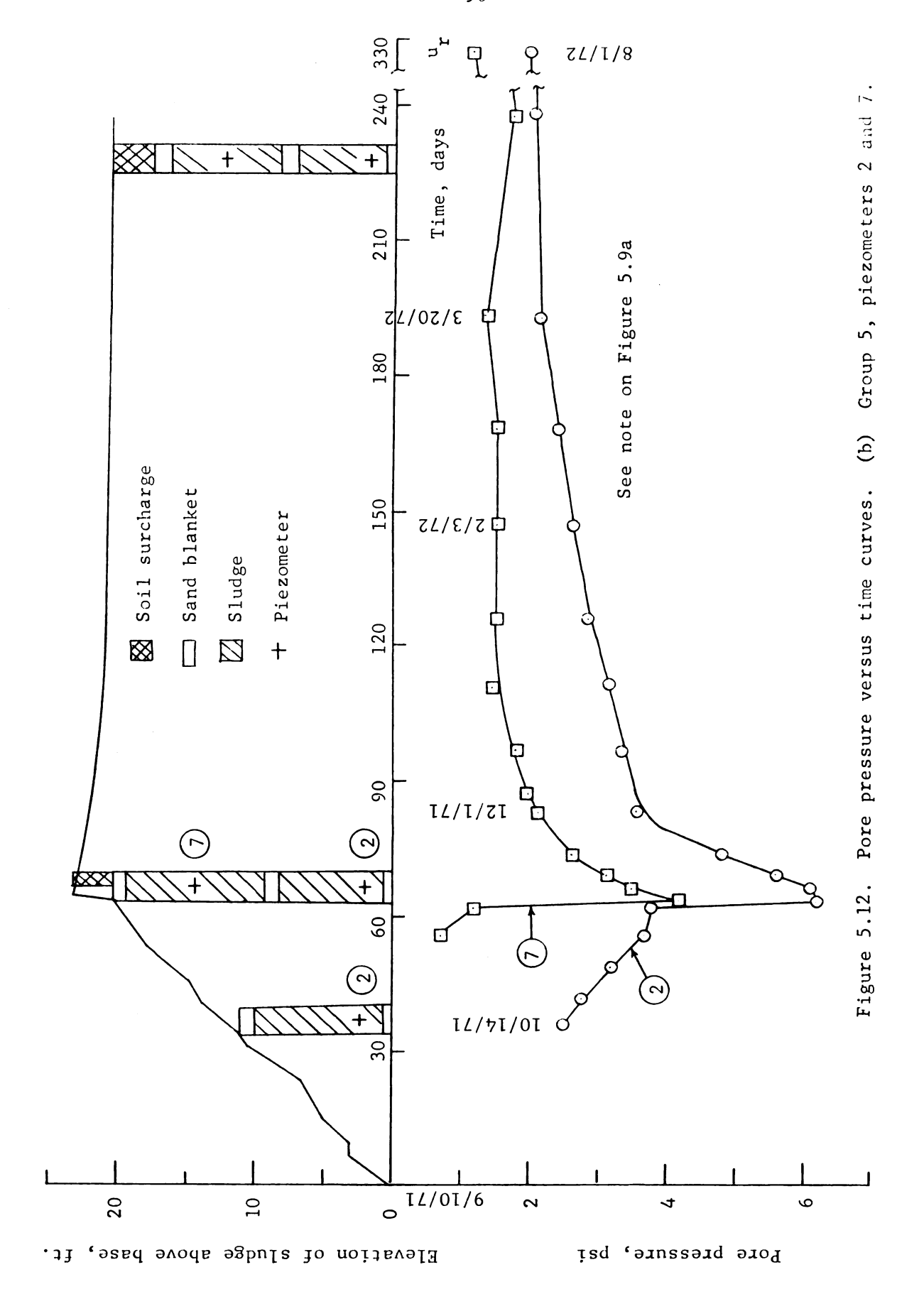


Settlement--logarithm of time curves, lower sludge layer after surcharge placement. (a) Groups 1,2,3, and 4. Figure 5.11.

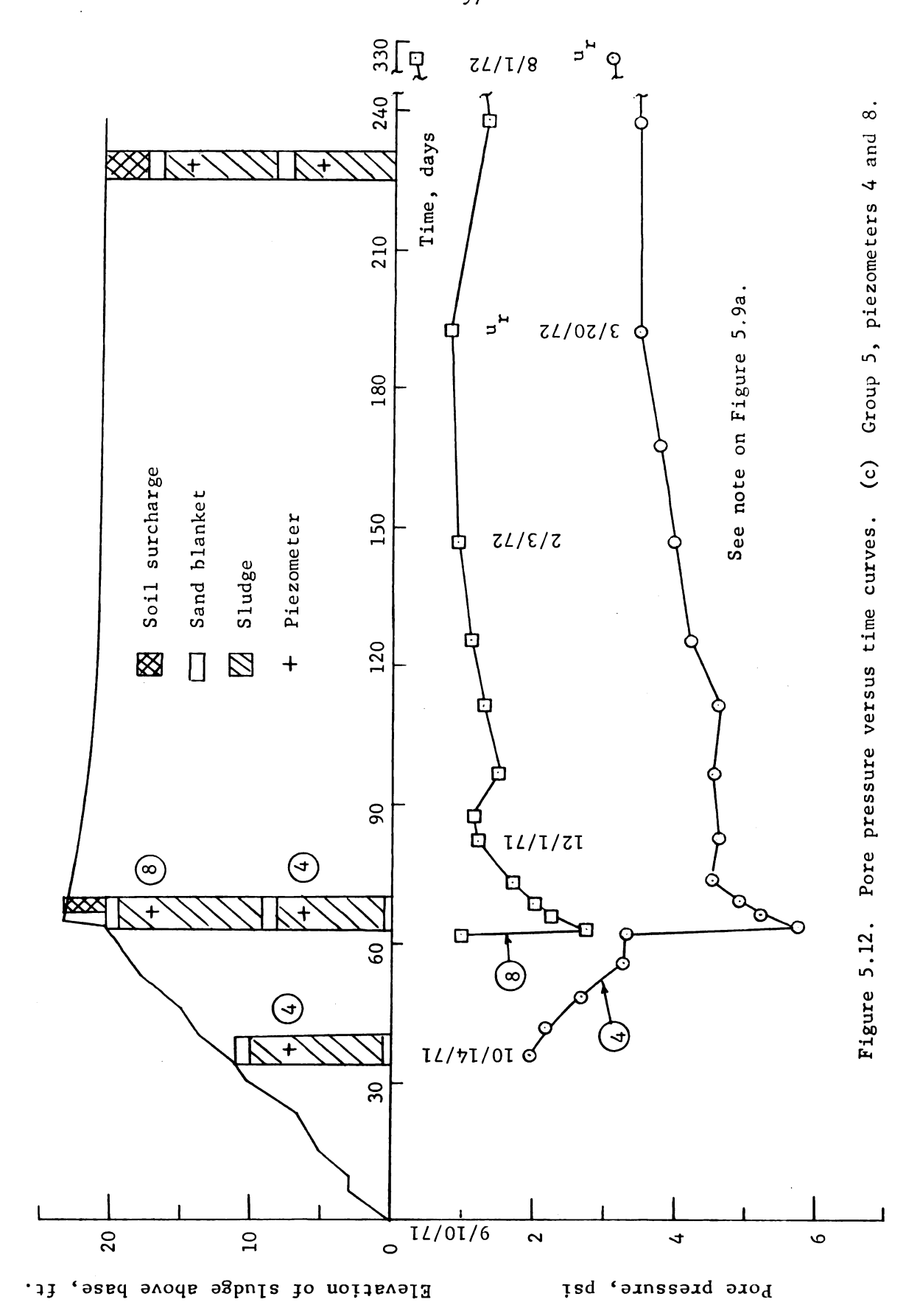


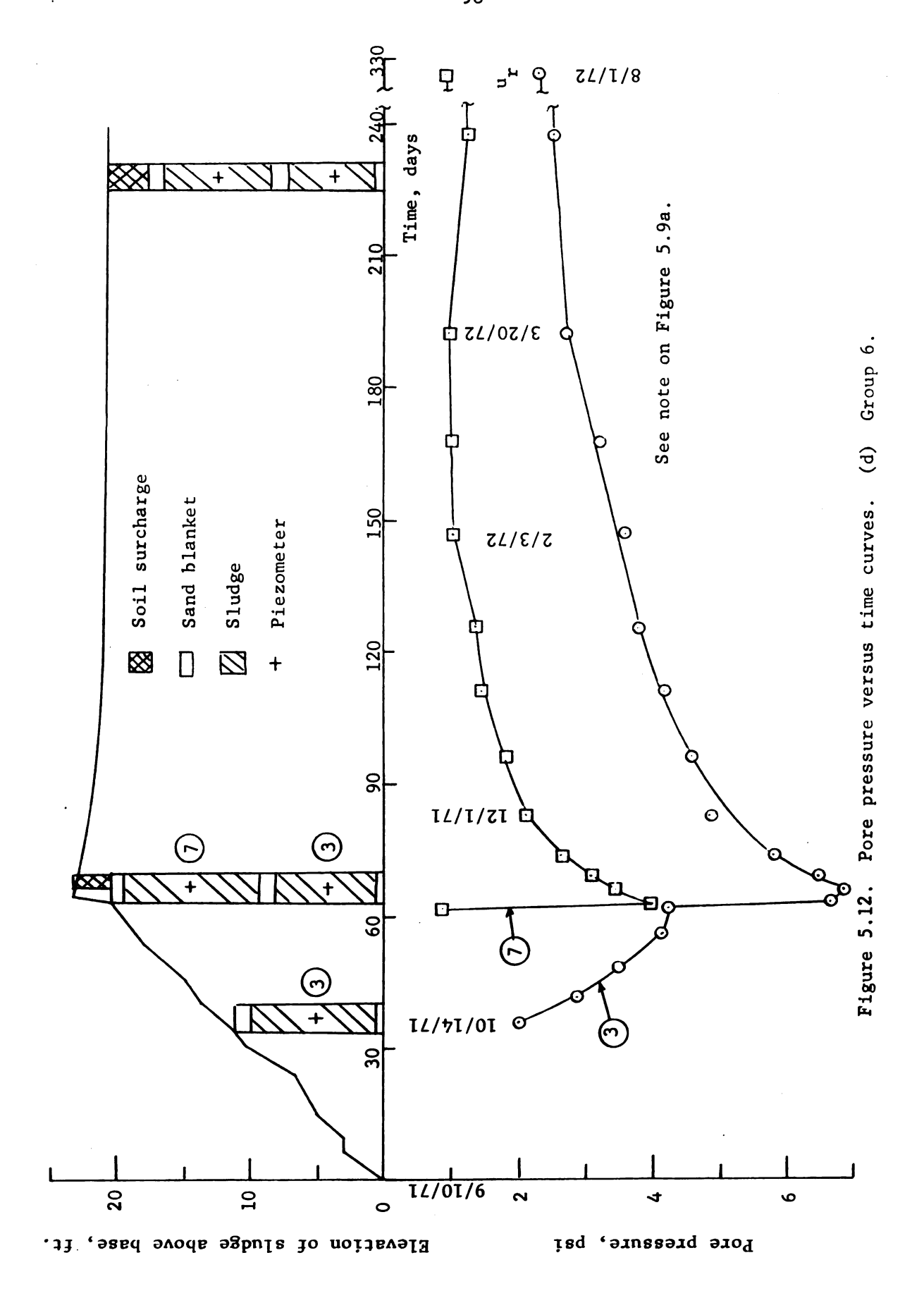
Settlement--logarithm of time curves, lower sludge layer after surcharge placement. (b) Groups 5,6,7, and 8. Figure 5.11.

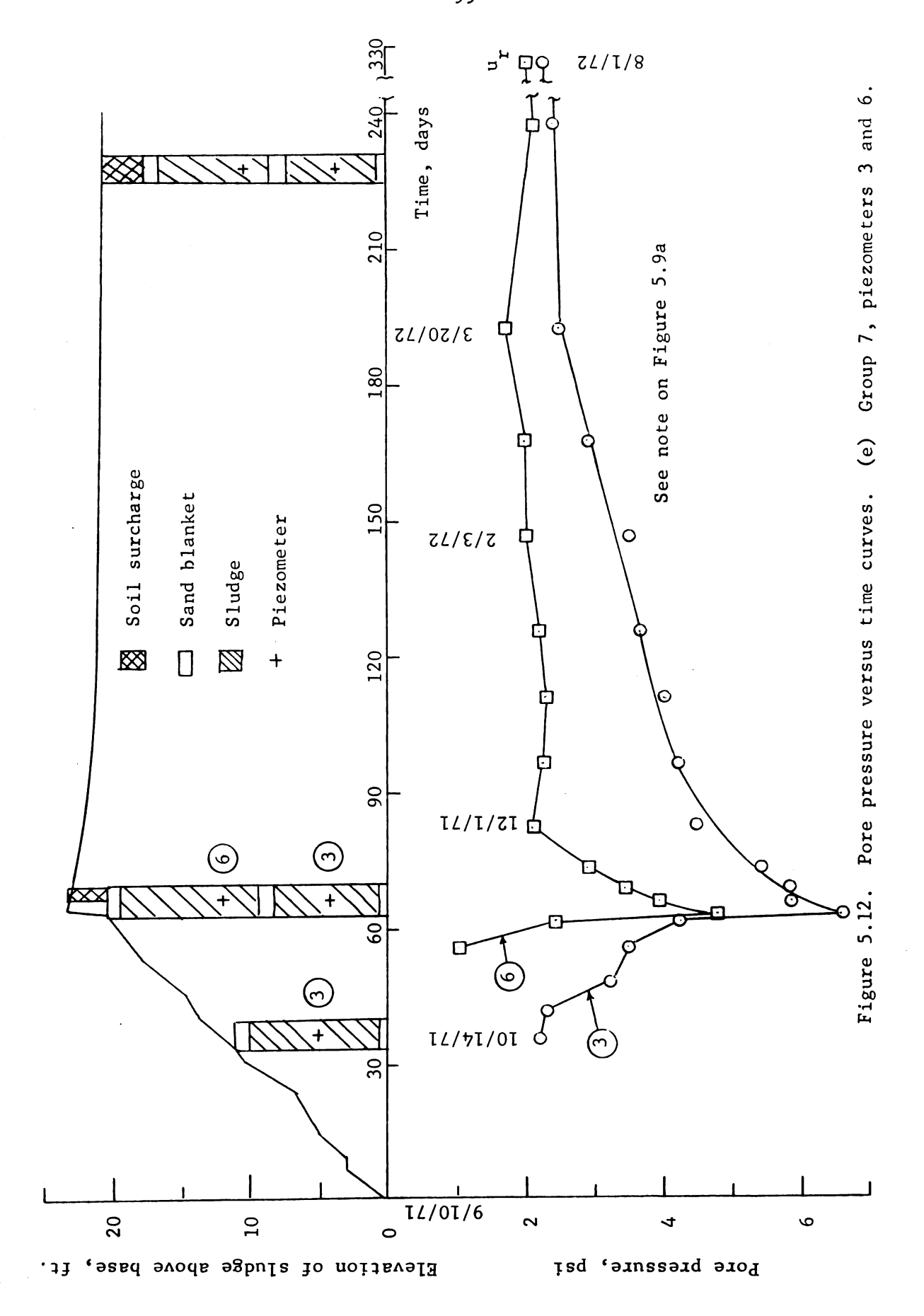


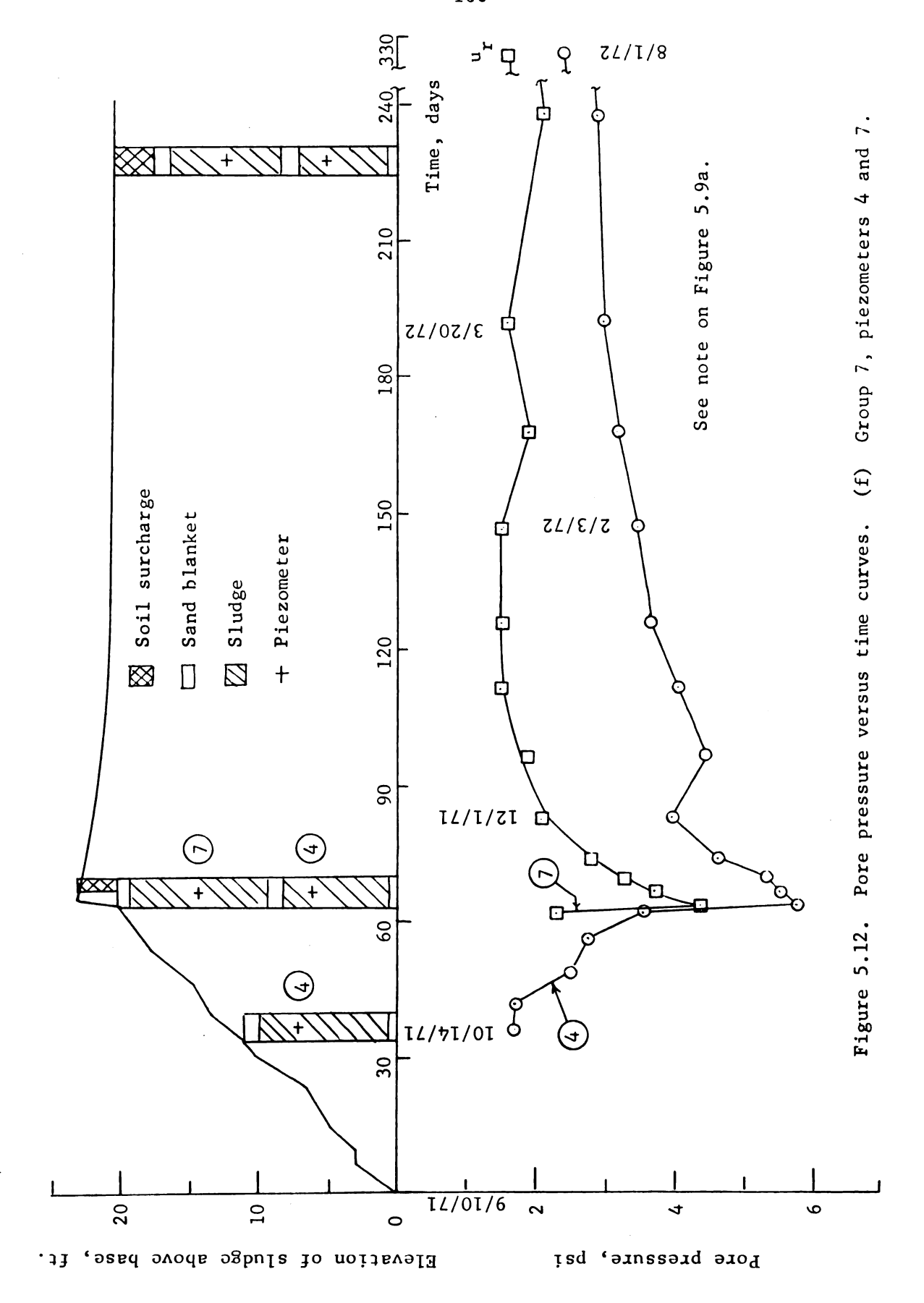


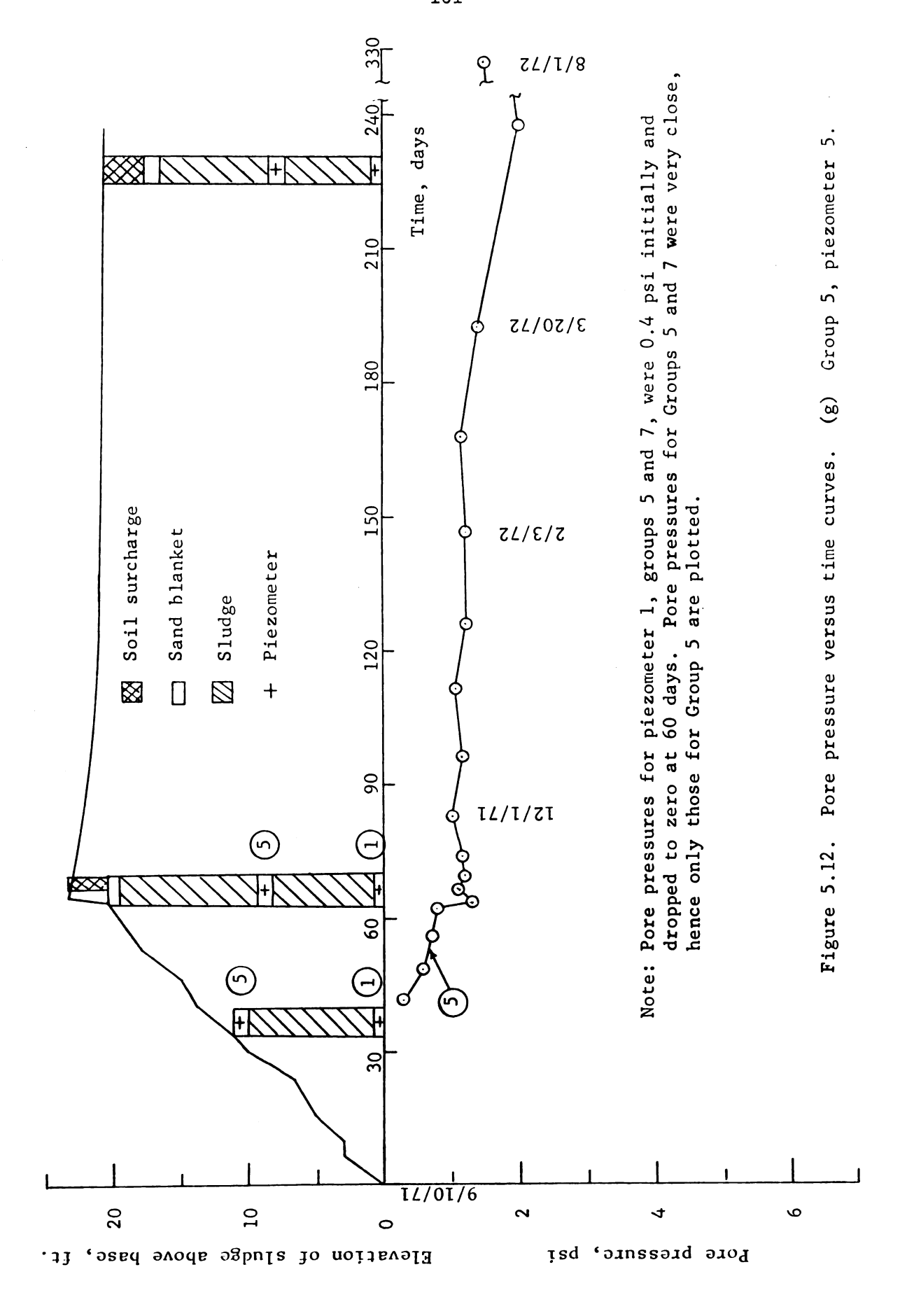


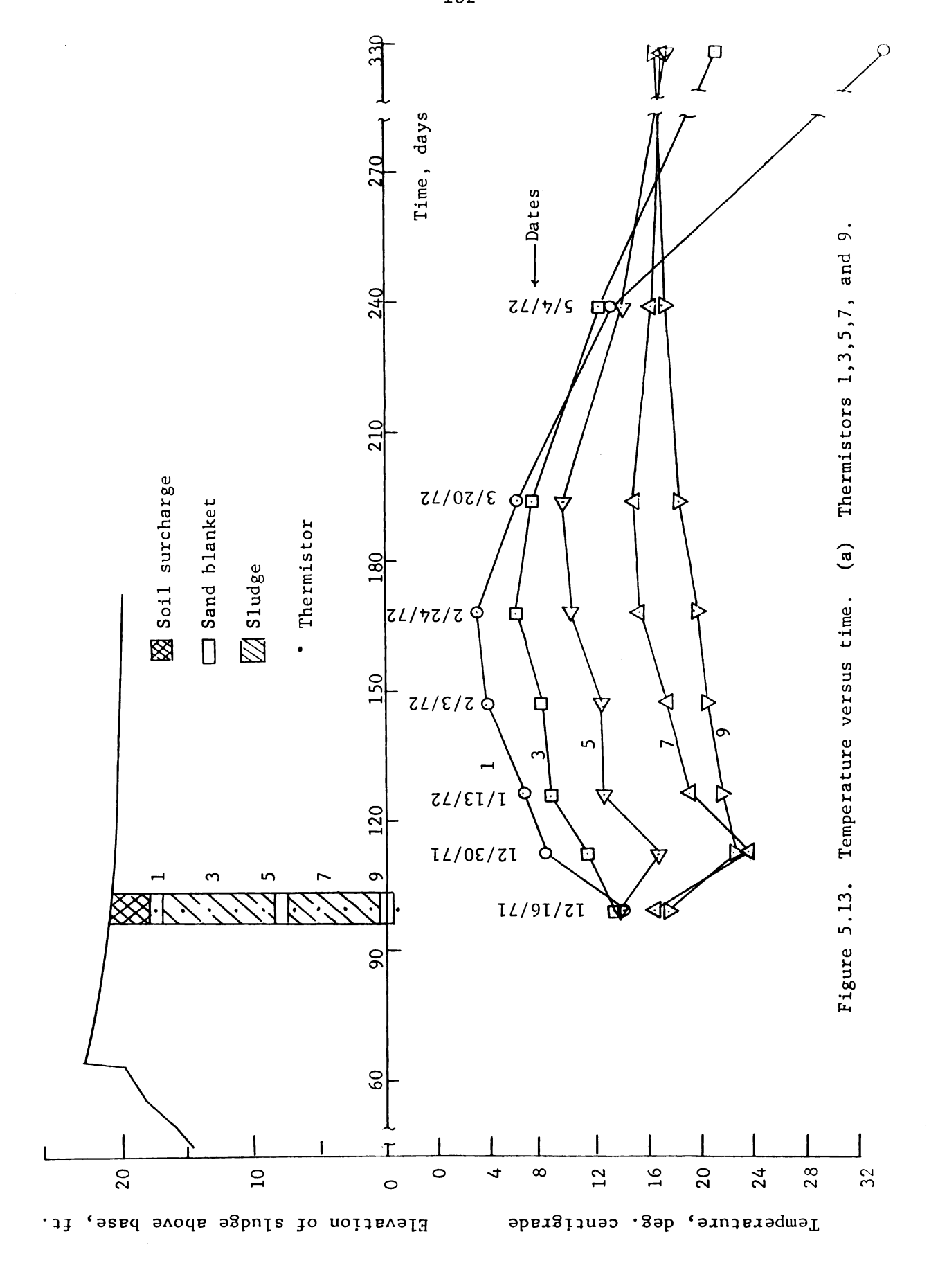


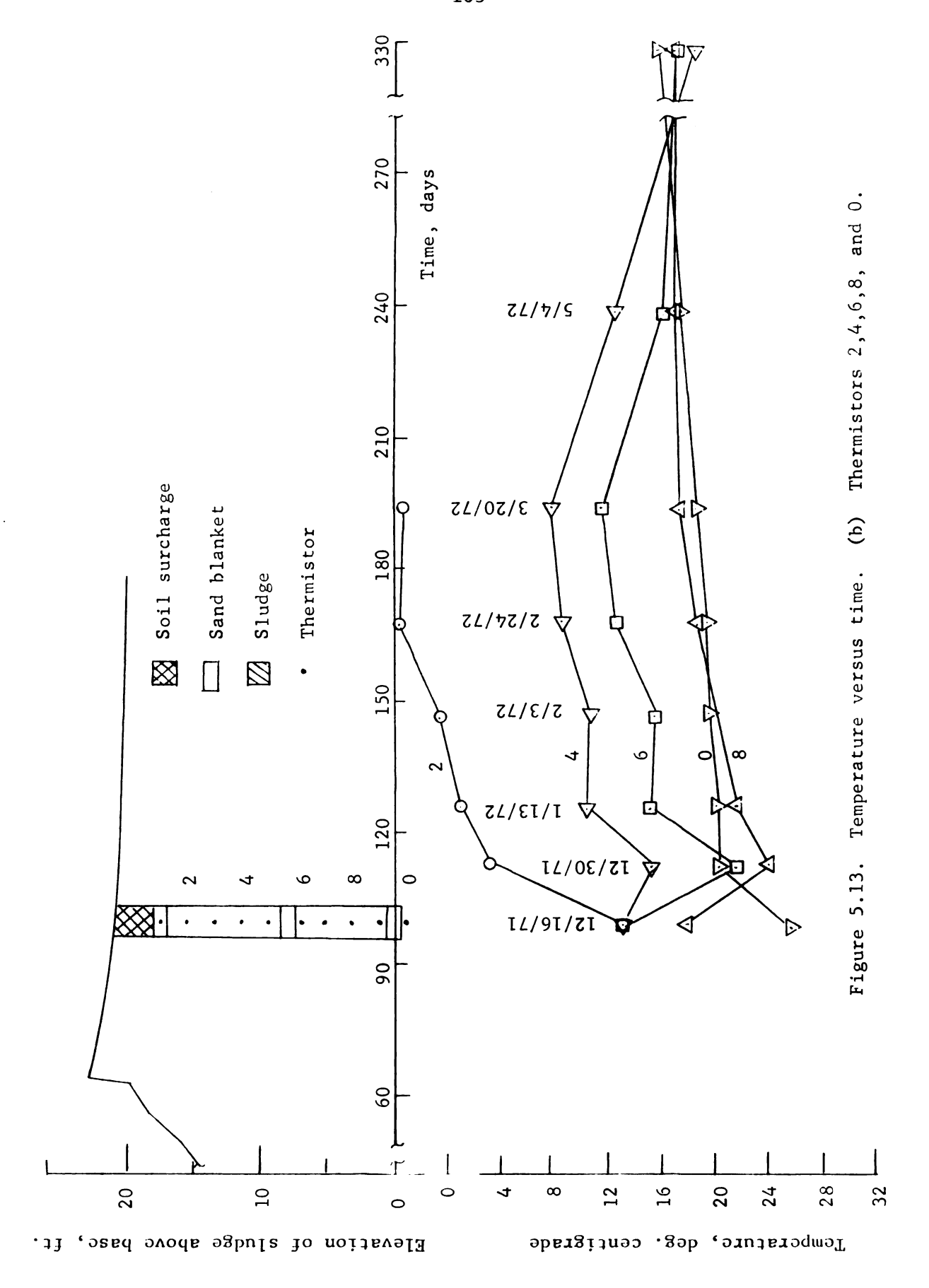












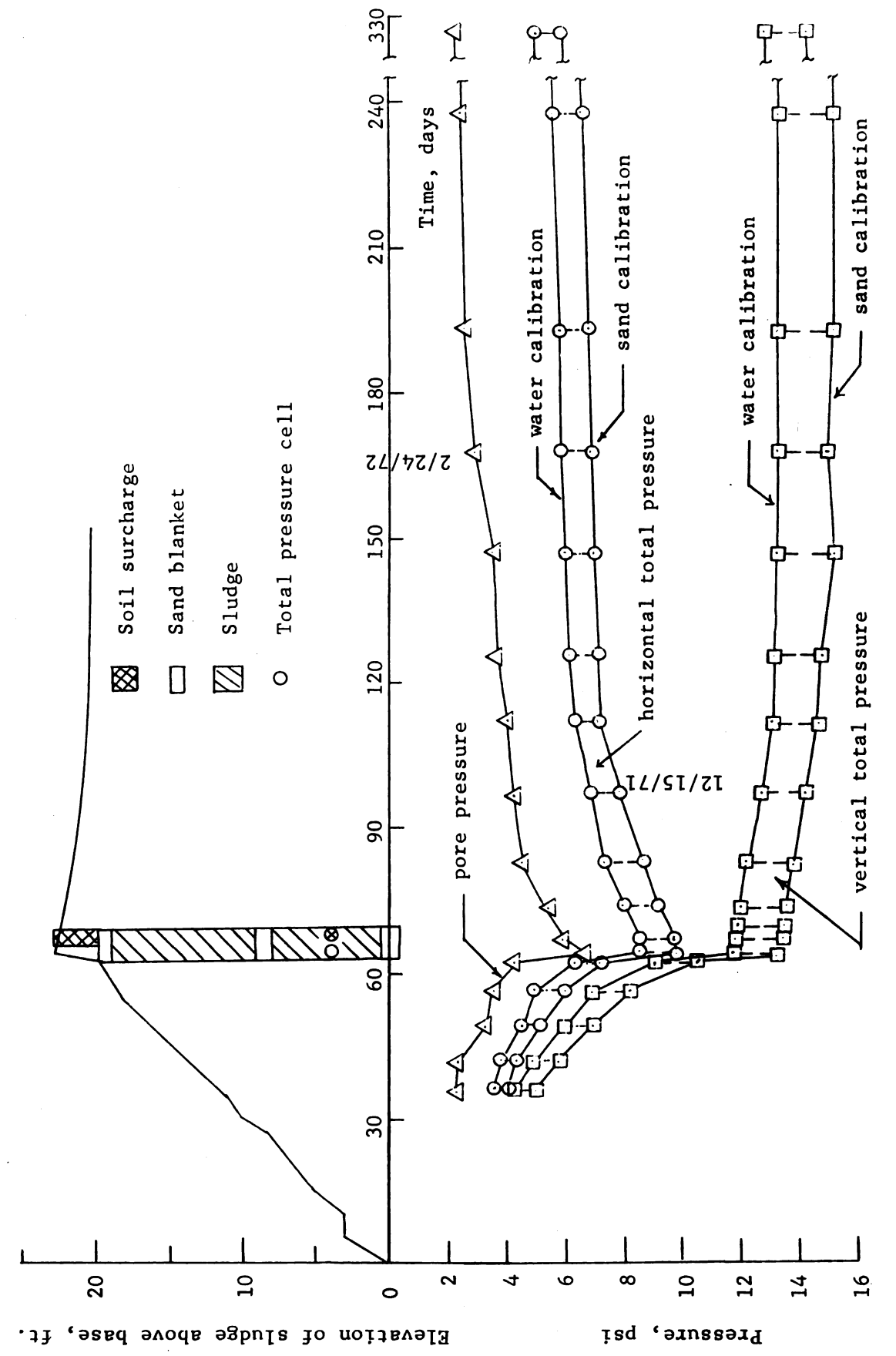


Figure 5.14. Horizontal and vertical total stresses, lower sludge layer.

#### CHAPTER VI

#### INTERPRETATION OF RESULTS

The discussion and interpretation of results includes both laboratory and field data. The material is presented in three sections, including: (1) sludge placement, (2) engineering characteristics of the papermill sludge, and (3) settlement behavior of the landfill.

# 6.1 Sludge Placement

A wide variety of equipment is available for papermill sludge landfill operations. Equipment selected for the project was based primarily on the contractor's experience with the sludge. The two main factors considered in the selection included the cost of the equipment and its ability to meet the project needs. For example, the placement of the sludge in 10 ft. layers with reasonable uniformity required the use of a dragline that could reach to the central area of the landfill. The dragline was ideally suited to handle the loose bulk sludge where casting and placement were important, and the skill of the operator helped to minimize hand shovel work adjacent to instrumentation. There was no problem with operating space requirements, and a firm support for the dragline was provided by the earth dikes surrounding the landfill. Sludge was delivered to the site from the dewatering facility by a large truck and was dumped either over the dike edge or adjacent to the site. Drainage blankets were placed by dumping sand at the site

and then distributing it with the dragline and/or dozer. For the top blanket, adequate support was obtained for the dozer from the sand pushed ahead of it. For the middle sand blanket, use of the dozer was avoided because of the possibility of its sinking into the soft sludge and because of the high dike walls at the time of placement shown in Figure 4.5. The sand in this case was placed using the dragline and was leveled by pulling a makeshift drag (two telephone poles tied together) over the surface. Some hand shovel work was required next to instrumentation.

### 6.2 Engineering Characteristics of the Papermill Sludge

The engineering characteristics of the papermill sludge are discussed under headings which include (1) physical properties,

(2) consolidation behavior, (3) undrained shear strength, (4) stress state in the sludge, and (5) temperature.

#### 6.2.1 Physical Properties

The water content of the dewatered sludge is unusually high in comparison to inorganic soils normally encountered in engineering practice. The average water content for the upper sludge layer was equal to 257 percent and for the lower layer was equal to 265 percent for the data summarized in Table 5.2. Both the liquid and plastic limits shown in Table 5.1 tend to decrease for sludge samples with higher ash contents. This correlates with the decrease in water retention when organic content is reduced (Andersland and Laza, 1971). The presence of fibers in the sludge interfered with the mechanical test procedures used to determine the liquid and plastic limits, so that some error may have been introduced in the consistency limits.

The volume change and settlement discussed in later sections involves a reduction in water content due to the weight of overlying sludge and surcharge loads. This reduction is reflected in the reduced average water content for each layer shown in Figure 5.1. The scatter of the points shown in this figure can be attributed to sampling from an exposed slope face and to the initial variability of the sludge in the landfill.

Specific gravities of the sludge are directly related to the ash content, with the lower values shown in Table 5.1 corresponding to samples containing more organic material. Data in Table 5.1 show that the sludge composition will vary from day to day, with this variation being dependent on operations at the papermill. The average specific gravity for the lower sludge layer, equal to 2.04, is not greatly different from the average for the upper layer, equal to 2.00. This small difference in average specific gravities, together with average water contents which are close for both sludge layers, indicates that initial unit weights should be about the same. The more accurate determination of the sludge unit weight using the weight and volume of a truck load of sludge gave a value equal to 69.7 1b/cu ft. The total unit weight of the sludge at the completion of consolidation, as determined from the undisturbed sample consolidation tests assuming 100 percent saturation, was approximately 72.6 lb/cu ft for the upper layer and 76.5 lb/cu ft for the lower layer. The change from the initial state was small despite the large amount of consolidation that occurred. The greatly increased shear strength of the sludge at the completion of consolidation in combination with this low density

suggests that the sludge could be used effectively as a lightweight fill material.

### 6.2.2 Consolidation Behavior

The highly compressible nature of the papermill sludge is shown in Figure 5.2a, where the linear void ratio-logarithm of pressure curve gives a compression index,  $C_{\rm c}$ , of 1.70. This high value for  $C_{\rm c}$  is a result of the high organic and high water contents which are characteristic of fresh papermill sludge. Andersland and Paloorthekkathil (1972) have shown the dependence of  $C_{\rm c}$  on these factors. The nonorganic fraction, primarily kaolinite clay, has a compression index close to 0.25 and also contributes to the compressibility of the sludge.

The variation in the coefficient of consolidation,  $c_v$ , with each load increment is illustrated in Figure 5.2b. The square root of time fitting method gives higher values for  $c_v$  than the logarithm of time fitting method. The change in  $c_v$  during compression depends on the change in both the permeability and compressibility of the sludge, since  $c_v$  equals  $\frac{k}{m_V \gamma_w}$ . Here, k is the coefficient of permeability;  $\gamma_w$  is the unit weight of water; and  $m_v$  is the coefficient of compressibility of the soil skeleton, equal to  $-\frac{1}{1+e}\frac{\partial e}{\partial \overline{\sigma}}$ , where e is the void ratio, and  $\overline{\sigma}$  is the effective stress. It is apparent from Figure 5.2b that the coefficient of permeability for the sludge has decreased more rapidly than the compressibility. This has reduced  $c_v$  for increasing values of effective stress, as shown in Figure 5.2b.

The variation in primary compression ratio, r, with pressure is shown in Figure 5.2c. Compression can be separated into three parts

such that  $\frac{d_i}{n} + \frac{d_p}{n} + \frac{d_s}{n}$  equals unity, where D is the total compression experienced over the load increment and  $d_i$ ,  $d_p$ , and  $d_s$  are the initial, primary, and secondary compression, respectively. In this case, r equals  $\frac{d}{n}$  and is a measure of the amount of compression that occurs only as a result of pore water expulsion. The variation in r shown in Figure 5.2c is difficult to explain. For larger loads, Andersland and Paloorthekkathil (1972) obtain a fairly constant r with pressure, although there is considerable scatter in their results. The curve in Figure 5.2c shows results typical for all tests run with the Bishop consolidation machine at smaller loads. The drop in r with the second load increment could be due to a reduced hydrodynamic effect associated with the small amount of pressure added after the first increment (0.1 kg/cm<sup>2</sup>). Since secondary compression is a function of stress level, its effect may increase slightly over the load increment. However, the load increment is so small that hydrodynamic compression due to pore water expulsion may exhibit a reduced effect and secondary compression may become more prominent in the total compression over the load increment. This is shown by the flatter dial reading versus logarithm of time curve shown in Figure 5.3a. As the load increments increase in size, the hydrodynamic effect becomes more dominant and r increases. The high value of r for the first increment (0 to 0.1  $kg/cm^2$ ) may be due to the large amount of deformation occurring over the increment (e changes from 5.35 to 4.51). Figure 5.3b illustrates the curved shape of the logarithm of time curves associated with larger load increments.

Figure 5.4a shows the variation in the coefficient of secondary

compression,  $C_{\alpha}$ , with effective pressure. There is a slight increase in  $C_{\alpha}$  with pressure, as might be expected because of the greater deviatoric stresses occurring at higher pressures. However, this is somewhat compensated for by the increased density and reduced compressibility of the sludge resulting from compression. Andersland and Paloorthekkathil (1972) show a fairly constant  $C_{\alpha}$  with effective pressure. Figure 5.4b illustrates the reduction in the ratio  $C_{\alpha}/\Delta p$  with increasing load increment.

The results of the consolidation tests on the undisturbed samples of sludge are somewhat different from the results of the tests on the fresh samples of sludge. The e vs. log p curves are typical of those that might be obtained from a moderately disturbed normally consolidated soil sample. Theoretical values of  $\overline{p}$  have been back-computed from the curves using the Casagrande procedure and are shown in Figure 5.5. Using a sludge unit weight of 72.0 lb/ft and an average residual pore pressure of 1.2 psi, the calculated in situ vertical effective stress for the upper layer sample is .301 kg/cm<sup>2</sup>, which agrees closely with the back-computed values shown. However the lower layer calculated effective stress is .55 kg/cm<sup>2</sup>, which is less than the values shown for the lower layer in Figure 5.5 (.65 - .77 kg/cm $^2$ ). This discrepancy could be the result of using the Casagrande procedure to back-compute  $\overline{p}_{o}$ . Disturbance effects relative to this are discussed below. pressures computed by the two methods for the lower layer lie close together on the log scale even though the difference in their magnitudes is fairly high.

The vertical effective stress calculated in the lower layer from the total pressure cell and piezometer data of Figure 5.14 is

.77 kg/cm<sup>2</sup> (water calibration), which agrees closely with the back-computed value from the e vs.  $\log p$  curve. However it is the author's opinion that this pressure is too high, primarily because of the increase in measured total pressure exhibited by the pressure cell after surcharge application. If the value of total pressure measured at the completion of surcharge application is used to compute the in situ stress, a value of .65 kg/cm<sup>2</sup> is obtained. This discrepancy is discussed further in a following section on the stress state in the sludge.

Since the sample obtained from the lower layer was under a greater in situ effective stress than the upper layer, it would be expected that the lower layer would have a lower initial void ratio and higher back-computed  $\overline{p}_0$ . The difference in  $C_c$  between the two sample locations is likely a result of the non-homogeneity of the sludge in the landfill. Somewhat higher ash contents were present in the lower sludge layer, which would help to account for this difference.

The high values of c<sub>v</sub> at stresses below the effective overburden pressure shown in Figure 5.6a are related to the sample disturbance and are difficult to physically interpret. As Terzaghi and Peck (1967) point out, a perfectly undisturbed sample recovered from the ground would be subjected to an all around capillary pressure with an intensity of approximately 0.7 to 0.9 times the effective overburden pressure. If this sample were to be loaded in an oedometer to a stress level less than this, it would theoretically have to swell to reach equilibrium under the lower effective stress. The addition of load at this lower stress level would then cause the sample to follow a reload

curve until the initial in situ conditions  $(e_o, \overline{p}_o)$  were again reached. Since there is always some degree of disturbance that occurs in sampling, however, a good undisturbed sample will usually result in a flat curve below  $\overline{p}_o$ , similar to that shown in Figure 2.3. The relatively high degree of disturbance of the sludge samples caused a breakdown in the capillary pressures and, as a result, the samples were consolidated when subjected to stresses below the effective overburden pressure. The resulting compression occurred rapidly until equilibrium was reached, yielding high values of  $c_v$ . The e vs.  $\log \overline{p}$  curve does not represent a reload curve in the usual sense, as no swelling occurred, and its shape would change depending on the degree of sample disturbance. Thus the observed compression below  $\overline{p}_o$  can be quite variable, and the resulting values of  $c_v$ ,  $C_\alpha$ , and r can be affected.

The low primary compression ratios below  $\overline{p}_0$  in Figure 5.6b indicate that creep of the soil skeleton is a significant portion of the measured deformation in this stress region. The reduced hydrodynamic effect associated with this can be related to the capillary and disturbance effects discussed above. The values of the coefficient of secondary compression shown in Figure 5.6c are also smaller at low stresses, indicating that the field consolidation has increased the resistance of the soil skeleton to creep deformation. The magnitude of  $C_{\alpha}$  increases steadily over the entire stress range and approaches that of fresh sludge at the higher pressures. The sample from the lower layer has values of  $C_{\alpha}$  which are somewhat less than the upper layer, again indicating reduced compressibility of the soil skeleton due to the higher consolidation pressure.

### 6.2.3 Undrained Shear Strength

The undrained vane shear strengths summarized in Figure 5.7 show a large dependence on the degree of consolidation. The slightly greater initial strength in the upper layer (11/11/71) as compared to the lower sludge layer (10/14/71) can be explained by the lower average initial water content (footnote, Table 5.2) in the upper layer. The increase in strength with depth shows up with only partial consolidation. Laboratory data (Andersland and Laza, 1971) show a linear relationship between undrained strength and consolidation pressure. Sensitivity of the sludge in terms of the ratio of the undisturbed to remolded strength is small, ranging from about 1.5 to 2.5. This is comparable to that for many inorganic clays (Terzaghi and Peck, 1967). Very significant increases in strength have occurred in 3-1/2 months, as shown by data obtained on 3/20/72. Most of this improvement in strength presumably occurred during primary consolidation. There was also a strength increase after this period, as shown by the data in Figure 5.7b. Secondary compression could be responsible for a large portion of this increase.

According to recent data presented by Bjerrum (1972), the vane shear strengths summarized in Figure 5.7 do not represent the actual field undrained shear strengths needed in a slope stability analysis. Bjerrum (1972) recommends that the vane shear strengths be adjusted according to the relation

$$(s_{ij})_{field} = (s_{ij})_{vane} \cdot \mu \tag{6.1}$$

where  $\boldsymbol{s}_{\boldsymbol{u}}$  is the undrained shear strength and  $\boldsymbol{\mu}$  a parameter which is

dependent on the plasticity index. For the sludge plasticity index of about 150, Bjerrum's (1972) chart gives a value of  $\mu$  = 0.6. A comparison of  $(s_u)_{vane}$  ·  $\mu$  values with preliminary laboratory undrained triaxial data gives reasonable agreement.

## 6.2.4 Stress State in the Sludge

Both the vertical and the lateral total stresses recorded on the total pressure cells (Terra Tec model T-9010) located near the middle of the lower sludge layer are summarized in Figure 5.14 for the period covering sludge placement, surcharge loading, and consolidation. Values determined from the water calibration curve are probably on the low side, with the real pressures falling between the water and sand calibration curves. As consolidation proceeded after completion of the landfill, the horizontal pressures decreased while the vertical pressures increased. This increase is contrary to what would be expected because as water drains from the sludge and leaves the area, the total vertical pressure should decrease. It is presumed that this peculiar behavior is due to certain limitations of the total pressure cell.

Subtraction of the pore pressures (piezometer G7-3) from the total pressures gives the effective stresses. Taking the ratio of the effective horizontal to vertical stress gives an estimate of the coefficient of lateral earth pressure, K<sub>o</sub>. After completion of the lower layer, measured values of K<sub>o</sub> were .63 (water cal.) and .68 (sand cal.). Immediately after surcharge application these values were reduced to 0.38 and 0.48, respectively. For the final stages of consolidation the values for K<sub>o</sub> dropped to 0.30 (water calibration) and 0.34 (sand

calibration). These final values of K should approximate normal consolidation of the papermill sludge.

Since the stress-strain relation shown in Figure 6.1 for papermill sludge does not exhibit a peak, the determination of a friction angle,  $\overline{\phi}$ , requires that a somewhat arbitrary failure strain (thus stress difference) be assumed. Andersland and Laza (1971) assumed 20 percent strain as failure and calculated a friction angle of approximately  $57^{\circ}$  for the sludge. This would correspond to a K value of .16 using the empirical relation,  $K_0 = 1-\sin \overline{\phi}$ , for normally consolidated inorganic clays (Lambe and Whitman, 1969). Although this does not agree with the field value of  $K_0$ , a smaller assumed failure strain would result in a K value that would be more consistent with field observations. Since the stress-strain curve has a break in it at approximately 3 percent strain, anything above this value could conceivably represent "failure." Thus it is possible to compute, from the field value of  $K_0$ , a friction angle for the sludge equal to 43° that could be argued to be theoretically correct. These results indicate the limitations involved in estimating the in situ lateral effective stresses in papermill sludge.

## 6.2.5 Temperature

Temperatures at various levels in the sludge landfill, with corresponding dates, are summarized in Figure 5.13. Difficulties with the installation of the thermistors delayed the initial temperature readings until about 1 month after placement of the surcharge load. The temperature rise due to increased biological activity appears to have peaked about 50 days after completion of the landfill. The maximum

temperature rise of about 7°C occurred in the upper half of the lower sludge layer. Subsequent winter weather reduced the sludge temperatures at all levels until spring and summer, when the seasonal warming effects prevailed. During January and February, when average monthly air temperatures were close to zero degrees centigrade, sludge temperatures ranged from about 3°C near the surface to 20°C in the bottom sand blanket.

Warmer spring air temperatures decreased this range in temperatures, and in the early part of August the colder temperatures were near the bottom of the landfill. The warmer summer temperature, plus a period of low rainfall, appears to have influenced the pore pressure readings shown in Figure 5.12 for the upper portion of the top sludge layer. This will be discussed in a later section on pore pressure dissipation.

Although it has been shown that temperature can alter the equilibrium void ratio, coefficient of consolidation, coefficient of secondary compression, and primary compression ratio (Andersland and Paloorthekkathil, 1972), its effect has not been incorporated into any practical consolidation theory and thus it can be included in an analysis only qualitatively. The variation in the parameters mentioned above was found to be small for a temperature range of 6°C to 38°C, so any temperature changes occurring in the landfill (assuming no dessication) would have only a slight effect on its behavior. Temperatures were not measured in the landfill during construction or for the first month after surcharge placement, so data covering the period of primary compression are absent.

### 6.3 Settlement Behavior of the Landfill

The settlement behavior of the landfill is discussed under two

headings: the upper sludge layer and the lower sludge layer. Both sections include information on (1) loading and general field observations, (2) ultimate settlement, (3) time-rate of settlement, and (4) pore pressure dissipation.

### 6.3.1 Upper Sludge Layer

6.3.1.1 Loading and Field Observations. -- The upper sand blanket and earth surcharge provided a total applied load of about 490 psf on the surface of the upper sludge layer. This load was applied in a period of about 4 days (Figure 5.8), with most of the surcharge placement occurring on the last day. This loading rate approximates an instantaneous loading condition. Because of the landfill area involved, the resulting settlement is due to drainage and compression in the vertical direction only. The similarity of time-settlement curves (Figure 5.8) between instrument groups supports this fact. Any difference in the ultimate settlement between groups can be attributed to small differences in load application (maximum ± 3 inches in surcharge thickness) and nonhomogenity of the sludge, with respect to water content, occurring during placement (Table 5.2). The major difference involved instrument group 7, where excess settlement occurred because soil for the surcharge was piled there prior to spreading with a dozer.

The square root of time and logarithm of time versus settlement curves (Figures 5.9 and 5.10) for the upper sludge layer provide information on the amount of primary and secondary compression, the coefficient of consolidation, c,, and the coefficient of secondary

compression, C. The square root of time curves in Figure 5.9 were prepared on the assumption that the initial point (commencement of compression) occurred at the completion of surcharge placement. bend in the upper portion of the curve results from the fact that about 3 inches of settlement occurred at most instrument groups during surcharge load placement. However, the assumed initial point gives an average c,, equal to 0.0626 in 2/min for 90 percent consolidation, that is in agreement with the logarithm of time curves (Figure 5.10) and the pore pressure dissipation curves (Figure 5.12). The logarithm of time curve fitting method shows that primary settlement was complete after about 750 hours, and was then followed by secondary compression. Primary compression is rate controlling and determines the shape of the curve only during the initial stages of settlement because it occurs more rapidly than secondary compression. Using the time-settlement curves for instrument group 6 (Figure 5.8f) as representative of the sludge landfill, primary compression is computed to be 16.7 inches and secondary compression, 4.1 inches (for a total t = 238 days). The pore pressure dissipation curves (Figure 5.11d) confirmed that primary compression was essentially complete at about 34 days.

The decreasing secondary compression rate, shown in Figure 5.10, is not in full agreement with the laboratory curves shown in Figure 5.3. The laboratory curves showed a linear relation between settlement and logarithm of time after a relatively short transition curve.

The settlement experienced over the last time interval shown on the settlement versus logarithm of time curves for the upper layer

(Figure 5.10) was larger than expected. This was due to a drying of the upper half of the layer as a result of high summer temperatures and low rainfall. As shown in Figure 5.12c, piezometer G5-8 exhibited a large reduction in pore pressure over this time interval. Calculations showed that approximately 65 percent of the total settlement over this interval occurred in the upper half of the layer. Thermistors 1 and 3 (Figure 5.13a) showed increased temperatures in the upper half of the upper sludge layer at the time of the last reading (t = 327 days).

To illustrate the correlation between landfill settlement and leachate drainage, a comparison has been made, in Figure 6.2, between the measured leachate flow rate,  $\mathbf{Q}_{\mathrm{m}}$ , at the drainage pipe outlet shown in Figures 4.1 and 4.3 and the calculated flow rate,  $Q_c$ , based on the slope of the time-settlement curves (Figure 5.8). All but one of the points shown give  $Q_c$  greater than  $Q_m$ . This would be expected because the drainage system was not constructed to be leakproof and leachate was undoubtedly lost into the dike and the material surrounding the pipe. The point shown for 11/12/71 was calculated from the slope of the time-settlement curve for the lower layer only, since the upper layer was not yet completed. Because leachate was draining from the upper layer also, the point should be displaced to the right to be more accurately located. It was assumed that for the upper layer one half of the flow went to the top of the layer and the other half to the drainage pipe. Despite the uncertainties involved in the flow rate measurements, the correlation to the settlements is fairly good. Heavy rain after December 1, 1971, caused infiltration of rainwater into the pipe and flow rates measured at the pipe outlet increased considerably. 6.3.1.2 Ultimate Settlement.—For plastic clays and organic soils (including papermill sludge) the ultimate settlement estimate must include both primary and secondary compression. When data are not available from previous experience, the parameters needed for a settlement analysis are obtained from laboratory tests and extrapolated to field behavior. The following discussion reviews several procedures for estimating ultimate settlement and applies them to the experimental sludge landfill.

A common method for estimating ultimate primary settlement uses the stress-strain relation

$$\varepsilon = \frac{{}^{C}_{\bullet c}}{1 + e_{o}} \log_{10} \frac{\overline{\sigma}_{f}}{\overline{\sigma}_{o}}$$
 (6.2)

where  $\varepsilon=\frac{ds}{dz}$  is the vertical strain at a point,  $C_c$  the compression index,  $e_o$  the initial void ratio,  $\overline{\sigma}_o$  the initial effective normal vertical stress, and  $\overline{\sigma}_f$  the final effective normal vertical stress. Equation 6.2 is an extension of equation 2.1. The total or ultimate primary settlement,  $\Delta H$ , for a sludge layer of initial thickness, H, can be found by integration.

$$S = \Delta H = \int_0^H \frac{C_c}{1 + e_o} \log_{10} \frac{\overline{\sigma}_f}{\overline{\sigma}_o} dz$$
 (6.3)

Application of this equation to in situ soil layers is straightforward since the soil is in static equilibrium with a fixed groundwater table, which readily permits the computation of changes in effective vertical stresses. However, in the sludge landfill the presence of excess pore

pressures both before loading, due to the weight of overlying sludge, and after completion of primary compression, a residual pore pressure assumed due to an insufficient gradient for flow, complicate computation of the effective stresses. The procedure followed in the application of equation 6.2 is illustrated in Figure 6.3. The initial effective stresses in the sludge after placement of the upper sand blanket are given in Figure 6.3a. Pore pressures represent field data from instrument group 7 just prior to surcharge loading. The sand blanket was not yet placed at other instrument groups when these data were obtained. Total vertical stresses were computed using a constant sludge unit weight equal to 70 pcf. Initial void ratios were taken from a laboratory e -  $\log \overline{p}$  curve at the effective stresses,  $\overline{\sigma}_0$ , shown. Final effective vertical stresses are given in Figure 6.3b. That portion of the final stresses due to the overburden weight of sludge and sand is actually different from those shown by an amount dependent on the decrease in the sludge water content. This effect would be to reduce the overburden pressure. For this analysis it was assumed that this reduction in overburden pressure would not greatly alter the results. Subtracting the residual pore pressure in Figure 6.5 from the total stresses in Figure 6.3b gave the final effective normal stresses. Substitution of the stresses from Figures 6.3a and 6.3b into equation 6.3 gave the strain values shown in Figure 6.3c. Integration of this strain over the thickness of the upper sludge layer provided an estimate of the ultimate primary settlement equal to 18.1 inches. Since this value is close to the observed primary settlement of 16.7 inches, use of equation 6.2 appears to be justified. For design purposes the use of equation 6.2 will be somewhat limited, since no methods are available for predicting

residual pore pressures. Initial pore pressures generated during sludge placement can be estimated by the procedure discussed in the next section.

The accuracy of the analysis shown in Figures 6.3 and 6.12 can be seen from Table 6.1. Here the settlements calculated from the assumed strain distribution are compared to the actual settlement of the upper and lower halves of the two sludge layers. The end of primary compression for the field calculations was taken from the pore pressure dissipation curves (Figure 5.12), and the total primary settlement at this time was found from the settlement-time curves (Figure 5.8). Any settlement of the plates located at the mid-point of each layer that occurred prior to completion of the sludge layer had to be subtracted from the total primary settlement because the strain analyses of Figures 6.3 and 6.12 have initial conditions that occur after completion of the layer. The analyses appeared to underestimate the settlement of the lower half of each layer and overestimate the settlement of the upper half, with the actual settlement corresponding to a nearly constant strain condition.

MacFarlane (1969) has proposed that the ultimate primary settlement in peat be computed on the basis of the equation

$$\Delta H_{f} = \frac{H_{o}}{H_{o}} \times \Delta H_{L}$$
 (6.4)

where  $\Delta H_f$  is the total primary settlement of a peat layer in the field,  $H_c$  the initial thickness of the peat layer in the field,  $\Delta H_c$  the initial compression of the laboratory sample, and  $H_c$  the initial

thickness of the laboratory sample. This method required that a representative laboratory sample be tested in an oedometer under an increment of load equal to the load applied in the field. The average unit strain in the laboratory specimen is then equated to the average unit strain in the field peat layer to obtain the settlement. An average primary settlement of 19.4 inches was obtained using average data from 5 laboratory tests with an applied load equal to 3.4 psi (weight of sand blanket plus soil surcharge). This method overestimates the actual primary settlement by about 2.7 inches. The validity of equation 6.4 is dependent on several factors including (1) the selection of a fully representative laboratory sample, (2) the preparation of the laboratory sample at a representative average initial void ratio for the layer, and (3) the different strain rates for the laboratory sample as compared to the field.

Secondary compression may be estimated on the basis of the equation (MacFarlane, 1969)

$$\Delta H_{s} = H_{p}C_{\alpha} \log_{10} \frac{t}{t_{p}}$$
 (6.5)

where  $\Delta H_s$  is the settlement due to secondary compression,  $C_{\alpha}$  the coefficient of secondary compression equal to the strain (relative to  $H_p$ ) occurring over one cycle of the secondary portion of the settlement-logarithm of time curve, t the field time considered,  $t_p$  the estimated field time for primary compression, and  $H_p$  the thickness of the sludge layer at time  $t_p$ . Using a laboratory value of  $c_v$  equal to 0.017 in  $^2$ /min to calculate  $t_p$  equal to 103 days, and using a laboratory value of  $C_{\alpha}$  equal to 0.0150 gives an estimate of  $\Delta H_s$  equal to 0.4 inch

for a t equal to 176 days (total t = 238 days). When a more realistic value of t equal to 34 days is used, the secondary compression becomes 1.0 inch. Since the actual secondary compression is close to 4.1 inches, the laboratory value of  $C_{\alpha}$  appears to be too low.

Gibson and Lo's (1961) theory can be used to estimate the ultimate settlement of the upper sludge layer by the use of equation 2.9. Substituting the parameters shown in Figure 6.4 into this equation, with  $q_o$  equal to 3.4 psi and H equal to 120 inches, gives an estimate of ultimate settlement equal to 22.4 inches for the upper sludge layer. Primary compression, represented by (a ·  $q_o$  · H), equals 20.3 inches and secondary compression, represented by (b ·  $q_o$  · h), equals 2.1 inches. Although the primary compression has been overestimated and the secondary compression underestimated, the total compression estimate appears reasonable. This method is subject to the same uncertainties in extending laboratory test data to the field prediction of settlements as was discussed earlier.

6.3.1.3 Time-Rate of Settlement.--Time-rate of settlement predictions involving primary consolidation are generally based on the Terzaghi (1943) consolidation theory. This theory involves the solution of the differential equation

$$\frac{\partial \mathbf{u}}{\partial \mathbf{t}} = \mathbf{c}_{\mathbf{v}} \frac{\partial^2 \mathbf{u}}{\partial \mathbf{z}^2} \tag{6.6}$$

where u is the excess pore water pressure, t the time after application of load, z the distance from the mid-point of a doubly drained stratum, and  $c_v$  the coefficient of consolidation. The solution of equation 6.6 for various boundary conditions is given by Terzaghi (1943), Leonards

(1962) and others. The degree of consolidation, U, for a given time, t, is commonly expressed as some function of the time factor,  $T_v$ , equal to  $^{4c}v^t/_{H^2}$ . The use of this theory in estimating the time settlement relation for the upper sludge layer is illustrated in Figure 6.6. Since this theory cannot model secondary compression, it has been used in combination with equation 6.5. Here t<sub>p</sub> was taken as the time at which 92 percent consolidation was theoretically reached ( $T_v = 1.00$ ).

Using MacFarlane's (1969) method, the total primary compression was taken equal to 19.4 in. and the secondary compression equal to 0.4 This procedure relies on laboratory data and can be considered representative of a design estimate. Curve (1) in Figure 6.6a shows the observed time-settlement relation for instrument group 6 in the landfill, and curve (2) gives the time-settlement relation using Terzaghi's theory and parameters based on the field data. Curve (2)considers primary compression equal to 16.7 in. and secondary compression equal to 4.1 in. ( $C_{\alpha} = 0.0556$ ). The laboratory parameters give an underestimate of the time-rate of settlement. Part of the discrepancy between actual and calculated curves results from the assumption that the theoretical curves start after completion of surcharge placement whereas the field curve begins earlier. A plot of settlement versus logarithm of time for curves (1) and (2)in Figure 6.6b. This figure illustrates how the secondary portion of the field curve is concave upwards, as compared to the linear secondary portion of the theoretical curve. This would indicate that the field compression curve exhibits Type I (Lo, 1961) secondary compression. However, as mentioned earlier, the laboratory curves, even with one

3.4 psi load increment recorded for a week, did not indicate this behavior. The lower layer also exhibits this upward curvature in the secondary range. However, the field pore pressures indicate that slow pore pressure dissipation is still occurring in this layer, and so this curvature may be part of the transition zone between the primary and secondary compression regions.

Gibson and Lo's (1961) theory has been used to obtain the theoretical time-settlement curves shown in Figure 6.6c. Curves for three different values of  $c_{_{\mathbf{N}}}$  have been plotted, none of which closely follow the actual field settlement curve over the entire range of time. Part of the difference results from the predicted ultimate settlement being slightly larger than the actual settlement. At times up to approximately 300 hours, the theoretical curves for the two higher values of c, are closely parallel to the field curve, but between 300 and 1000 hours the settlement predicted from theory increases at a faster rate than the actual settlement. For the given parameters, Gibson and Lo's (1961) theory predicts that the ultimate settlement is reached very rapidly, without the development of a linear (with log time) secondary compression curve. The theoretical type of secondary compression that develops from this theory is dependent on the value of a parameter, N, equal to  $H^2/\frac{1}{\lambda} \cdot b \cdot c_y$ . Values of this parameter for the sludge landfill are large (700 for  $c_v = .063 \text{ in}^2/\text{min}$ ) and result in the theoretical curves shown in Figure 6.6c. For N values of approximately .04, secondary compression occurs for a much longer period of time. The low value of the viscosity measured in the laboratory  $(6.95 \times 10^4 \text{ lb/in}^2/\text{min})$  appears to be the soil property largely responsible for the theoretical results obtained, being on the

order of  $10^2$  to  $10^3$  times smaller than values obtained from clays tested by Gibson and Lo (1961). The dependence of the development of secondary compression on layer thickness is apparent from N, which helps to explain the difference between the lab and field secondary compression behavior.

Wahls's (1962) theory has been used to obtain the two theoretical curves shown in Figure 6.6d. As discussed in Chapter II,  $\Delta H_p$  in equation 2.18 represents primary settlement only, and since Wahls's theory assumes that secondary compression can occur simultaneously with primary compression, it is necessary to establish a value of  $\Delta H_p$  from the parameters given. This was done by assuming an initial value of primary settlement equal to 16.7 in., obtained from field settlement and pore pressure data, and subtracting from this the theoretical amount of secondary compression that occurred during the time necessary to reach this amount of settlement (assuming  $T_V=1.0$  for the end of primary compression). This can be computed as  $\Delta H_p=16.7-(.0147)\cdot(103)\cdot(.8684)=15.4$  in. Here  $0.0147=assumed\ C_{\alpha}$ ,  $103=H_p$ , and  $0.8684=h(T_V)$ . Thus the time settlement relation is given by

$$\Delta H(t) = 15.4 f(T_v) + (103)(.0147) h(T_v)$$
 (6.7)

The results obtained from Wahls's theory are similar to those that were obtained using Terzaghi's theory. The back computed field value of  $c_v$  (.0626 in  $^2$ /min) accurately models the settlement up to the end of primary compression, and the laboratory determined value of  $C_{\alpha}$  (.0147 in  $^2$ /min) appears to be too low. A larger value of  $C_{\alpha}$  would accurately model the settlement for only a limited time because Wahls's theory

assumes a secondary compression rate that is linear with log time while the field secondary compression rate is decreasing with log time. Since Wahls's theory includes secondary compression in its mathematical formulation, it results in a smoother curve in the transition region than the method that was used to model secondary compression with Terzaghi's theory.

Assumptions in Terzaghi's theory which may cause deviation from the field results have been discussed in Chapter II. In addition to these, Terzaghi's theory also assumes that the soil is fully saturated. Any gas present in the sludge prior to surcharge application would be compressed on application of the load, giving an immediate settlement. This may be responsible for part of the 3 in. of settlement which occurred during surcharge placement. Pore pressures generated upon loading (Figure 6.7) are less than the applied load, indicating that there was partial dissipation during this loading period.

estimating total primary settlement requires information on initial pore pressures. The pore pressures shown in Figure 6.3a resulted from stresses induced by the sand blanket and weight of the sludge. Pore pressures resulting from the placement of the sand blanket were assumed equal to its load (100 psf) throughout the layer. Initial pore pressures resulting from the sludge layer increasing in thickness with time were estimated using Gibson's (1958) theory. Pore pressures from this theory are presented in Figure 6.8 for both laboratory and field values of c<sub>v</sub>, along with the measured pore pressures. The observed pore pressures fall between the predicted values, with the exception

of the 30 in. depth. No duplicate piezometer readings are available for this depth, hence a recording error or malfunction is possible. The 115 psf pore pressure in the middle sand blanket may have influenced the value at the 90 in. depth. Except for these factors Gibson's (1958) theory appears to accurately predict pore pressures generated during sludge placement.

Pore pressure dissipation during placement of the sand and surcharge load appeared to be responsible for  $\Delta u/\Delta p$  values less than unity, as shown in Figure 6.7. The pore pressure increase at the center of the layer ranged from 94 to 99 percent of the applied load, whereas at the 1/4 point pore pressures were about 85 percent of the applied load. The  $\Delta$  data point for group 7 in Figure 6.7b represents only the surcharge load, whereas for the other groups the pore pressures include application of the sand plus surcharge load. Adding a 100 psf load due to the sand layer for group 7 gives a point very close to  $\Delta u/\Delta p$  equal to unity, as shown by the second point.

Residual pore pressures summarized in Figure 6.5 represent data from the pore pressure versus time curves in Figure 5.12. The data in Figure 6.5 represent average values of u obtained from these curves. Piezometer 8 in group 5 appears to have a reduced pore pressure at 327 days due to drying of the earth surcharge and the upper portion of the upper sludge layer during a relatively dry summer. The fluctuation in pore pressures after 90 days appears to be due to measurement deviations and environmental effects, such as seasonal wetting and drying. Pore pressures in the middle sand blanket are the result of the sand forming a bowl shape because of less settlement along the periphery of the landfill, thus holding water up to a certain elevation.

The field pore pressure dissipation curve at the mid-point of the upper sludge layer in instrument group 6 is compared, in Figure 6.9a, to computed curves based on Terzaghi's (1943) theory. The initial excess pore pressure used for computation was assumed equal to the difference between the maximum and residual pore pressures. The laboratory value of  $c_{\rm V}$  (0.0170 in  $^2$ /min) gives pore pressures substantially higher than the observed pore pressures during the consolidation period. Using the  $c_{\rm V}$  (0.0626 in  $^2$ /min) value based on field data, Terzaghi's (1943) theory slightly overestimates the pore pressures (curve 3) up to about 70 percent dissipation and thereafter gives an underestimate. The slower dissipation rate occuring after about 70 percent dissipation was also observed in the laboratory by Andersland and Paloorthekkathil (1972). The pore pressures predicted from the theory of Gibson and Lo (1961) are in close agreement with those of Terzaghi, as shown in Figure 6.9b.

The decrease in pore pressure dissipation rate after 70 percent dissipation may be the result of non-Darcy flow in the sludge. Mitchell and Younger (1967) discussed this effect in detail and concluded that there are indications that deviations from Darcy's law exist in many fine-grained soils subjected to low hydraulic gradients but that not much direct field evidence is available concerning seepage or consolidation to corroborate this effect. The recorded field dissipation curves (Figures 5.12 and 6.9) indicate that non-Darcy flow does exist in the sludge landfill and that this flow precedes the formation of residual pore pressures in both sludge layers. These residual pore pressures imply the existence of a threshold gradient in the sludge below which no flow occurs. For a threshold gradient, i, drainage will occur

only when

$$i > i_0 = \frac{1}{\gamma_w} \frac{du_r}{dz}$$
 (6.8)

where i is the existing hydraulic gradient,  $u_r$  the residual pore pressure at depth z, and  $\gamma_w$  the unit weight of water. If this gradient can be considered a constant property, then integration of equation 6.8 will give a theoretical distribution of the residual pore pressures shown in Figure 6.10. The observed residual pore pressure distribution summarized in Figure 6.5 is influenced by the pore pressures in the middle sand blanket. If the pore pressure in the sand blanket was reduced to zero, as it would be if complete drainage were possible, and if the value at the lower one-quarter point was reduced, the resulting distribution would likely agree with theory. Assuming that the theory represents the field conditions, using the maximum residual pore pressure at the center of the layer gives a value for  $i_0$  equal to 0.885. Below this gradient primary consolidation will cease, with no additional dissipation of pore pressures.

Reasons quoted by Mitchell and Younger (1967) for the development of non-Darcy flow and a threshold gradient include:

(1) resistance to flow caused by cations in the electrical double layer surrounding the clay particles, (2) particle movements leading to reversible void plugging and unplugging, and (3) the existence of a quasi-crystalline adsorbed water (leachate) structure. If any of these reasons apply to papermill sludge, the author believes that (3) would best help explain the development of a threshold gradient. Since the existence of such a gradient implies a no-flow condition it would seem

necessary for the water (or leachate) to develop a quasi-crystalline structure that could be considered as solid below the threshold gradient. Grim (1968) also favors this quasi-crystalline concept to explain the clay-water system. It should be noted that the chemical makeup of the leachate and the presence of large amounts of organic material in the sludge could have a marked effect on the leachate flow properties at low gradients. Andersland and Laza (1972) observed that a threshold gradient was required to initiate flow in the sludge only in the case of low backpressures, and that when the undissolved gas in the pore fluid was reduced to zero this gradient was not necessary. Such a result would indicate that gas generation in the sludge contributes to the reduced leachate flow rate and residual pore pressure formation observed in the landfill. In addition, there might also be chemical interactions between organic compounds in the leachate and the clay particles, such as the adsorption of polar organic molecules onto the surface of the clay. Chemical reactions such as this might also lead to the development of a threshold gradient.

The pore pressure dissipation and time-settlement curves predicted from Terzaghi's (1943) theory are based on the assumption of a uniform initial excess pore pressure. Because deviations from this assumption can cause changes in the dissipation-settlement relations, its validity is examined in Figure 6.11. From this figure it can be seen that the increase in pore pressures from their initial values to the maximum values generated under the applied loads is fairly uniform. Since the residual pore pressures are relatively close in magnitude to the initial pore pressures, the assumption of a uniform initial excess pore pressure in Terzaghi's theory appears to be valid. If the

residual pressures were much different from the initial pressures, then the condition of one-dimensional consolidation would best be analyzed with water flow controlled by  $v = k(i - i_0)$ , where v is the velocity of flow and k is the coefficient of permeability. This condition is described by Mitchell and Younger (1967) and the inclusion of a threshold gradient in the consolidation process is covered by Janbu (1965).

## 6.3.2 Lower Sludge Layer

6.3.2.1 Loading and Field Observations.—The lower sludge layer supported an applied load of about 1290 psf from the weight of the middle and upper sand blankets, the upper sludge layer, and the earth surcharge. The upper sludge layer was placed at a fairly constant rate over a period of about 30 days. The settlement and pore pressure changes observed in the lower sludge layer are summarized in Figures 5.8 and 5.11. Pore pressures were generated in the lower sludge layer during placement of the upper sludge layer, however, some dissipation and settlement also occurred concurrently with this sludge placement. The surcharge placement induced an immediate increase in pore pressures throughout the lower sludge layer, followed by their dissipation and the resulting curved time-settlement relation.

The logarithm of time and square root of time curve fitting methods used in a settlement analysis assume an instantaneous application of load. In the case where loads are increased at some rate, such as for the lower sludge layer, these curves are of limited value. The logarithm of time versus settlement curves for the lower sludge layer in Figure 5.11 provide information on the secondary compression

behavior of the sludge. The curve appears to show a decreasing secondary compression rate rather than a constant rate. The characteristic S-shape for the entire curve has been flattened due to the gradually increased load resulting from sludge placement of the upper layer. Separation of the settlement into primary and secondary portions is more difficult for the lower sludge layer. The square root of time fitting method cannot be used.

6.3.2.2 Ultimate Settlement.—The ultimate primary settlement of the lower sludge layer is computed to be 32.8 inches in Figure 6.12, using equation 6.2. The procedure is the same as described for the upper layer, with Figure 6.12a giving the stresses in the sludge after placement of the middle sand blanket and Figure 6.12b the stresses after application of the surcharge. Since the lower sludge layer has been subjected to larger effective stresses for a longer period of time than the upper layer, the amount of secondary compression should be greater. If 7 inches is assumed for secondary compression, based on the same primary compression ratio as for the upper layer, this leaves about 29 inches for primary compression. This means that equation 6.2 overestimates the primary settlement, but considering all the assumptions involved, this estimate appears reasonable.

A check on the total stresses calculated at the mid-point of the lower layer in Figure 6.12b can be made using the total pressure cell data from Figure 5.14. The calculated total vertical stress at the mid-point is 1740 psf (12.1 psi) whereas that shown in Figure 5.14 varies from 11.8 to 13.2 psi (water calibration). Since the slow increase in total vertical stress measured by the pressure cell cannot

be explained, it is assumed that the actual stress falls between 11.8 and 13.2 psi, giving support to the calculated value of 12.1 psi.

A consolidation test using a single load increment equal to 1290 psf (0.63 kg/cm<sup>2</sup>) was carried out on a sludge sample from the lower layer to provide a basis for estimating the ultimate primary settlement by MacFarlane's (1969) method. Using data from test No. L-2-4 in equation 6.4 gives a value for primary settlement equal to 35.3 inches. This value is closer to the actual field settlement of 36 inches, which includes both primary and secondary settlement. It is possible that the high initial void ratio of the laboratory sample, greater than the average initial in situ void ratio of the field layer, permitted greater volume change than is representative for the sludge layer.

It is difficult to determine from the field data the exact amount of secondary compression in the lower sludge layer. For analysis purposes a value of  $C_{\alpha}$  equal to 0.0556 and a  $t_{p}$  equal to 26 days (total t=60 days) were used in equation 6.5. For H equal to 94 inches a value of 4.7 inches was obtained for the secondary compression for t=204 days (total t=238 days). The use of a value of  $C_{\alpha}$  backfigured from the upper layer along with a  $t_{p}$  equal to 26 days, appeared realistic in light of the high amount of primary consolidation that occurred throughout most of the loading period. The value of 4.7 inches of secondary compression appears low based on results from the upper sludge layer.

6.3.2.3 Time-Rate of Settlement.--A theoretical estimate of the time-settlement relation for the lower sludge layer requires that the loading be represented by the numerical procedure shown in

Figure 6.13. The placement of the upper sludge layer and upper sand blanket has been modeled as an applied stress linearly increasing with time, and the surcharge has been represented as an instantaneously applied stress. Equation 6.6 is placed in finite difference form (Harr, 1966) with  $\frac{\partial u}{\partial t}$  and  $\frac{\partial^2 u}{\partial z^2}$  becoming

$$\frac{\partial \mathbf{u}}{\partial t} = \lim_{\Delta t \to 0} \frac{\mathbf{u}(\mathbf{z}_{\mathbf{i}}, \mathbf{t}_{\mathbf{j}+1}) - \mathbf{u}(\mathbf{z}_{\mathbf{i}}, \mathbf{t}_{\mathbf{j}})}{\Delta t} = \frac{\mathbf{u}_{\mathbf{i},\mathbf{j}+1} - \mathbf{u}_{\mathbf{i},\mathbf{j}}}{\Delta t}$$
(6.9)

and

$$\frac{\partial^{2} u}{\partial z^{2}} = \frac{u_{i+1,j} - 2u_{i,j} + u_{i-1,j}}{(\Delta z)^{2}}$$
 (6.10)

Substituting these expressions in equation 6.6 gives

$$u_{i,j+1} = u_{i,j}(1-2\alpha) + (u_{i+1,j} + u_{i-1,j})\alpha$$
 (6.11)

where  $\alpha$  is  $\frac{c_v^{\Delta t}}{(\Delta z)^2}$  and is assumed equal to 1/6 (Scott, 1963),  $\Delta t$  is the time increment,  $\Delta z$  equals H/8 (H is the thickness of the layer), and  $c_v$  is the coefficient of consolidation. Using the time factor  $T_v$  equal to  $v^t/(H/2)^2$ , and  $\alpha$  equal to 1/6, results in a value for  $\Delta T_v$  equal to 1/96. To model the linear stress, a unit initial pore pressure (stress) is first applied throughout the layer. This is allowed to dissipate over the interval  $\Delta T_v$  equal to 1/96, at which time another unit of pore pressure is added to obtain a new pore pressure distribution. This process is repreated over the required number of increments (n) as shown in Figure 6.13, where n is defined as  $v^t/\Delta t$  equal to  $v^t/\Delta t$  equal to  $v^t/\Delta t$  is the time at which the surcharge is applied. Since  $\Delta t$  is fixed, the number of increments n is dependent on the values

of  $c_v$  and  $t_s$ . For the sludge landfill with  $c_v = 0.063 \text{ in}^2/\text{min}$ , n was equal to 113. The percent consolidation, defined as

$$U(t) = 1 - \frac{1}{H} \int_{0}^{H} \frac{u(t)}{u_{o}} dz$$
 (6.14)

where u(t) is the excess pore pressure at any time t and u is the initial excess pore pressure, has been evaluated numerically, using the trapezoidal rule, for the finite difference formulation described.

For the linearly increasing load,  $u_0$  at any time t is equal to the total number of increments of pore pressure applied up to time t ( $u_0$  = n at t =  $t_s$ ). To obtain the settlement at time t it is necessary to determine the load acting on the lower layer at that time. The settlement of the lower layer then equals the ultimate settlement for that load multiplied by the percent consolidation based on the above consolidation theory. Estimates of the ultimate settlement of the lower sludge layer for three different elevations of the upper sludge layer (different loads) are given in Figure 6.14 for use in obtaining the theoretical time-settlement curve.

In the lower sludge layer it was assumed that the pore pressures measured in the field after application of the middle sand blanket acted as "static" pore pressures for analysis purposes. This means that they have been considered as both the initial and the residual pressures, and they must be added to the excess pressures calculated from the above theory to obtain the actual pore pressures. Since the actual residual pore pressures are slightly different from the above assumed values, the consolidation percentages calculated by

the theory contain a small error. Gibson's (1958) theory would provide accurate values of pore pressures generated in the sludge due to its own weight if estimates of initial pore pressures were needed for design purposes.

Using a computer program written for the above analysis (Appendix G), two theoretical time-settlement relations for the lower sludge layer have been determined and are shown in Figure 6.15a, along with the actual field settlement curve for group 3. The two theoretical curves occur after surcharge placement, one being calculated using c. equal to 0.063  $in^2/min$  and the other with c equal to 0.015  $in^2/min$ . A  $c_{\rm w}$  equal to 0.063 in  $^2/{\rm min}$  was assumed during the linear loading range and was chosen based on the analysis of the upper sludge layer. Values of  $t_n$  equal to 26 days and  $C_n$  equal to 0.0556 (from the upper layer analysis) were used in calculating the secondary compression. The ultimate primary settlements used in the analysis are those shown in Figures 6.12 and 6.14. The three analyses shown in Figure 6.14 were used during linear loading and the 32.6 inches in Figure 6.12 was used after surcharge application. The computer program assumes an average thickness for the sludge layer for the computations during linear loading and adjusts the thickness after each settlement computation after surcharge application.

The theoretical procedure above appears to give an adequate time-settlement relation for the lower layer. Although the occurrence of secondary compression has been poorly modeled, the governing factor affecting the time-settlement relation still appears to be the selection of a representative value of  $c_v$ . The fact that the actual settlement curve falls above the curve for  $c_v$  equal to 0.063 in  $^2$ /min would indicate

that  $c_v$  has decreased during the settlement process. This would be in accordance with the laboratory data, which show a drop in  $c_v$  with an increase in deformation and effective stress (Figure 5.2).

Leonards (1962) describes a simple procedure, suggested by Terzaghi, for obtaining the time-settlement relation of a clay layer subjected to a constant rate of loading. Using this procedure, the theoretical curve shown in Figure 6.15b has been drawn and is seen to agree very well with the field curve and the previous theoretical solution of Figure 6.15a. The solution was obtained by using the Terzaghi procedure in the linear loading range and then combining it with the solution for an instantaneous loading after the application of the surcharge.

6.3.2.4 Pore Pressure Dissipation.—A comparison between the predicted and measured pore pressures at the mid-point of the lower sludge layer is shown in Figure 6.16. The initial pore pressure was assumed equal to the residual value of 2.3 psi and was added to the excess pore pressures generated during loading. Pore pressures generated during the linear loading period were estimated using a value of  $c_v$  equal to 0.063 in  $^2$ /min. This estimation appears to give a reasonable approximation to the measured pore pressures. Two predicted curves are shown after surcharge application, one representing a  $c_v$  equal to 0.063 in  $^2$ /min and the other a  $c_v$  equal to 0.015 in  $^2$ /min. The larger  $c_v$  value predicts pore pressure dissipation more rapidly than it occurs. This again suggests that  $c_v$  has decreased for the lower layer as a result of its consolidation under the linearly increasing load. The measured pore pressures fall between the two theoretical curves for

a period of 30 days after surcharge placement, after which they dissipate more slowly. This would correlate with the decrease in the rate of pore pressure dissipation which occurred after 70 percent dissipation in the upper sludge layer (Figure 6.9).

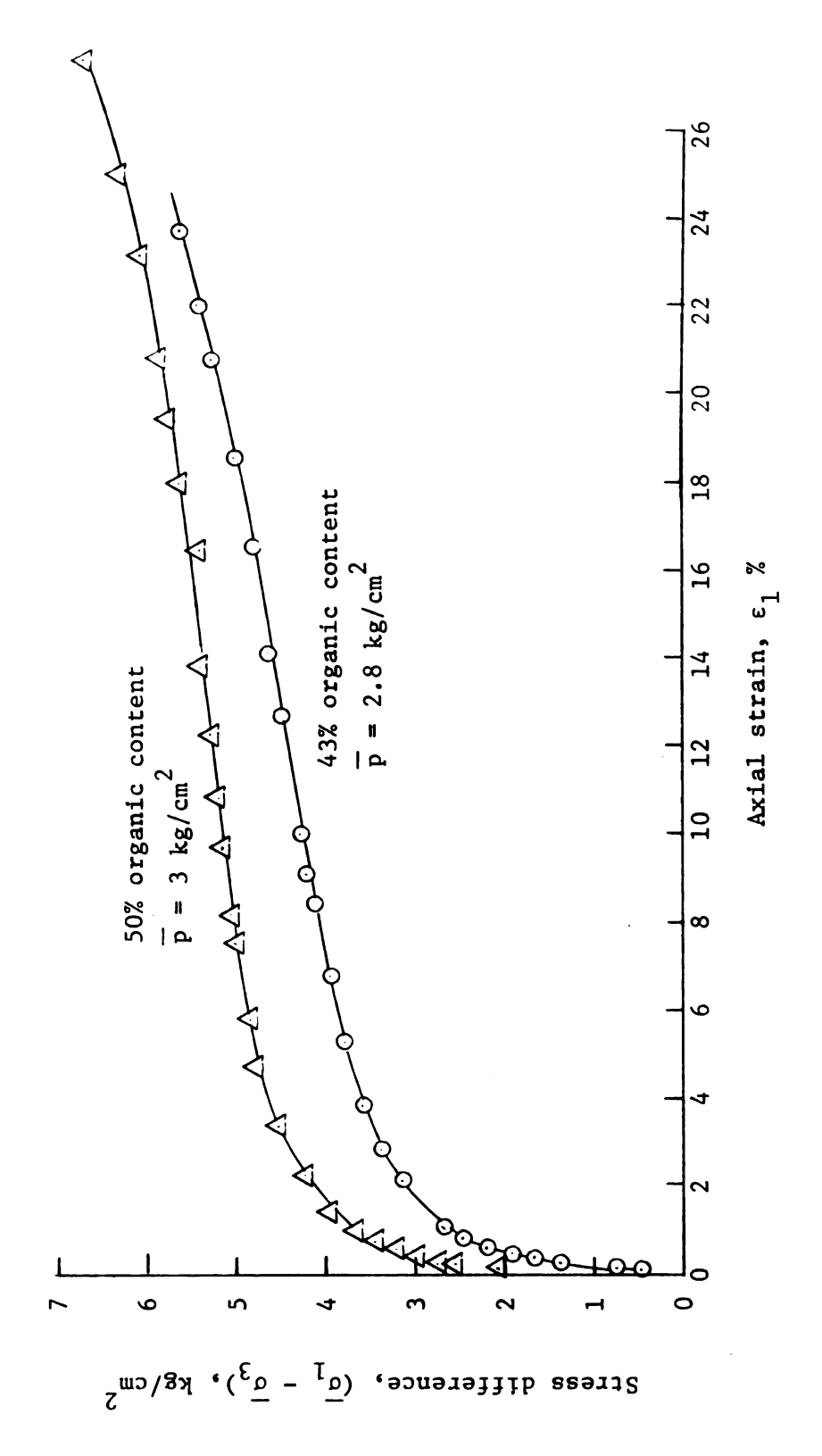
Initial pore pressures generated in the lower sludge layer due to its own weight are shown in Figure 6.17, and residual pore pressures remaining after consolidation are shown in Figure 6.5. The initial pore pressures were obtained by subtracting 100 psf (stress due to the middle sand blanket) from the pore pressure readings taken immediately after placement of the middle sand blanket. These pore pressures agree fairly well with those that would be predicted using Gibson's (1958) theory. Residual pore pressures shown in Figure 6.5 were obtained in a manner similar to the upper sludge layer. After 327 days (Figure 5.12) the pore pressures had stabilized sufficiently so that they could be labeled "residual" for analysis purposes. The values are somewhat higher than those measured in the upper sludge layer, indicating that a higher threshold gradient exists in the lower layer. The higher sludge density of the lower sludge layer in combination with any gas formation due to sludge decomposition may have contributed to the formation of the higher residual pore pressures. Using the maximum observed residual pore pressure at the mid-point of the lower layer gives a value of i equal to 1.63.

The  $\Delta u/\Delta p$  ratios shown in Figure 6.7 are somewhat less for the lower sludge layer as compared to the upper layer. The lower ratios may be the result of partial drainage having occurred during placement of the upper sand blanket and surcharge. A shorter length of drainage

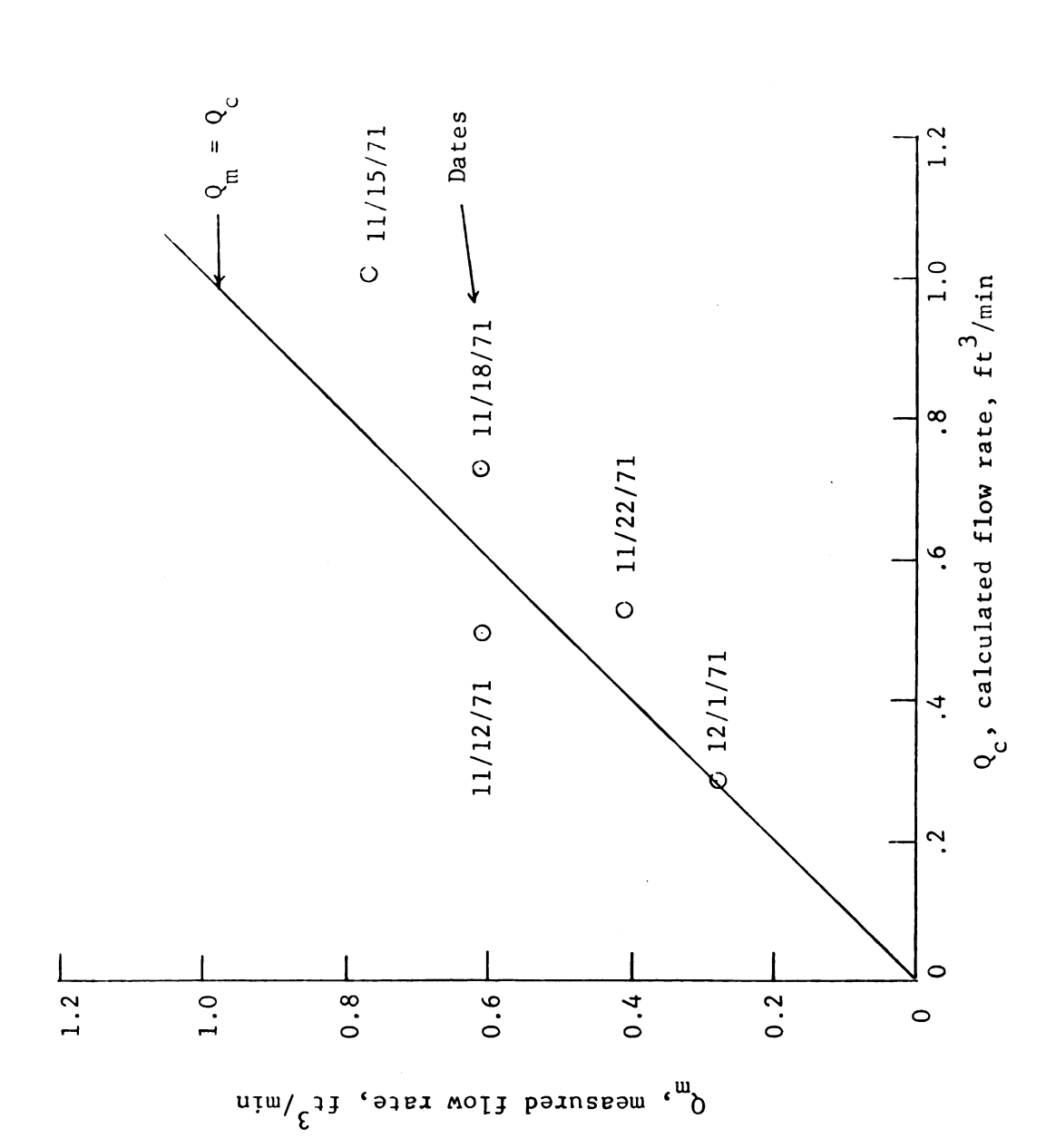
path existed in the lower layer than the upper layer at the time of surcharge application. The theoretical pore pressure increase shown in Figure 6.16 is consistent with the field measurements and would support this explanation. Because the surcharge covers a fairly large area it would appear that the reduction in the  $\Delta u/\Delta p$  ratio is not due to reduced stresses in the lower sludge layer.

Table 6.1 COMPARISON OF ACTUAL AND CALCULATED PRIMARY SETTLEMENTS.

Location	Computed settlement from Figure 6.3 or 6.12	Actu <b>a</b> l field settlement
Upper sludge layer		
Upper half	10.8 in	9.0 in
Lower half	7.3 in	8.0 in
Lower sludge layer		
Upper half	19.6 in	14.7 in
Lower half	13.2 in	14.3 in



Typical stress--strain curves for papermill sludge with 43% and 50% organic contents (Andersland and Laza, 1971). Figure 6.1.



Comparison between the measured leachate flow rate and the flow rate calculated from the time--settlement curves. Figure 6.2.

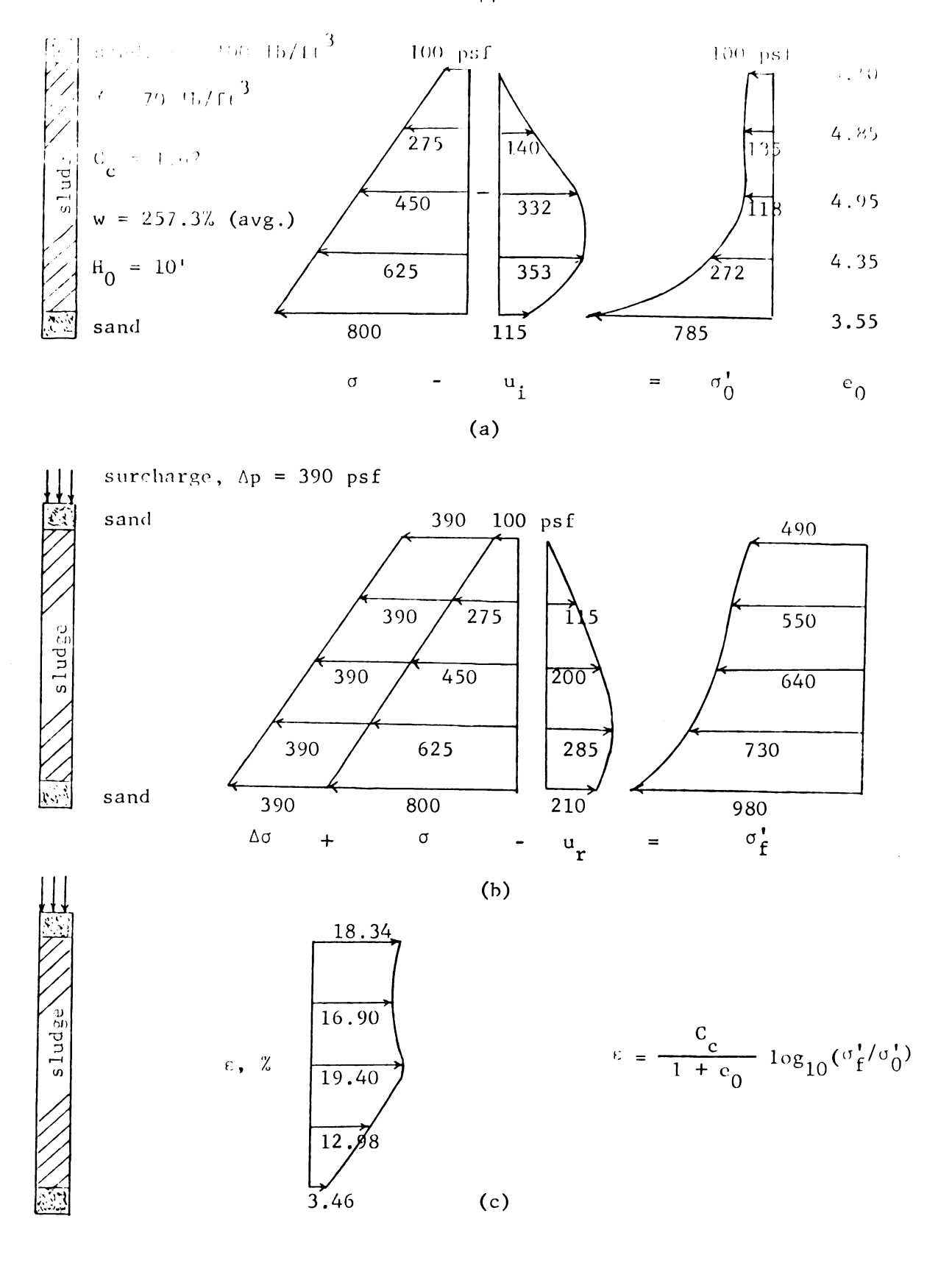


Figure 6.3. Estimated effective stress changes and strain distribution in the upper sludge layer. (a) Initial stresses. (b) Final stresses. (c) Strain distribution.

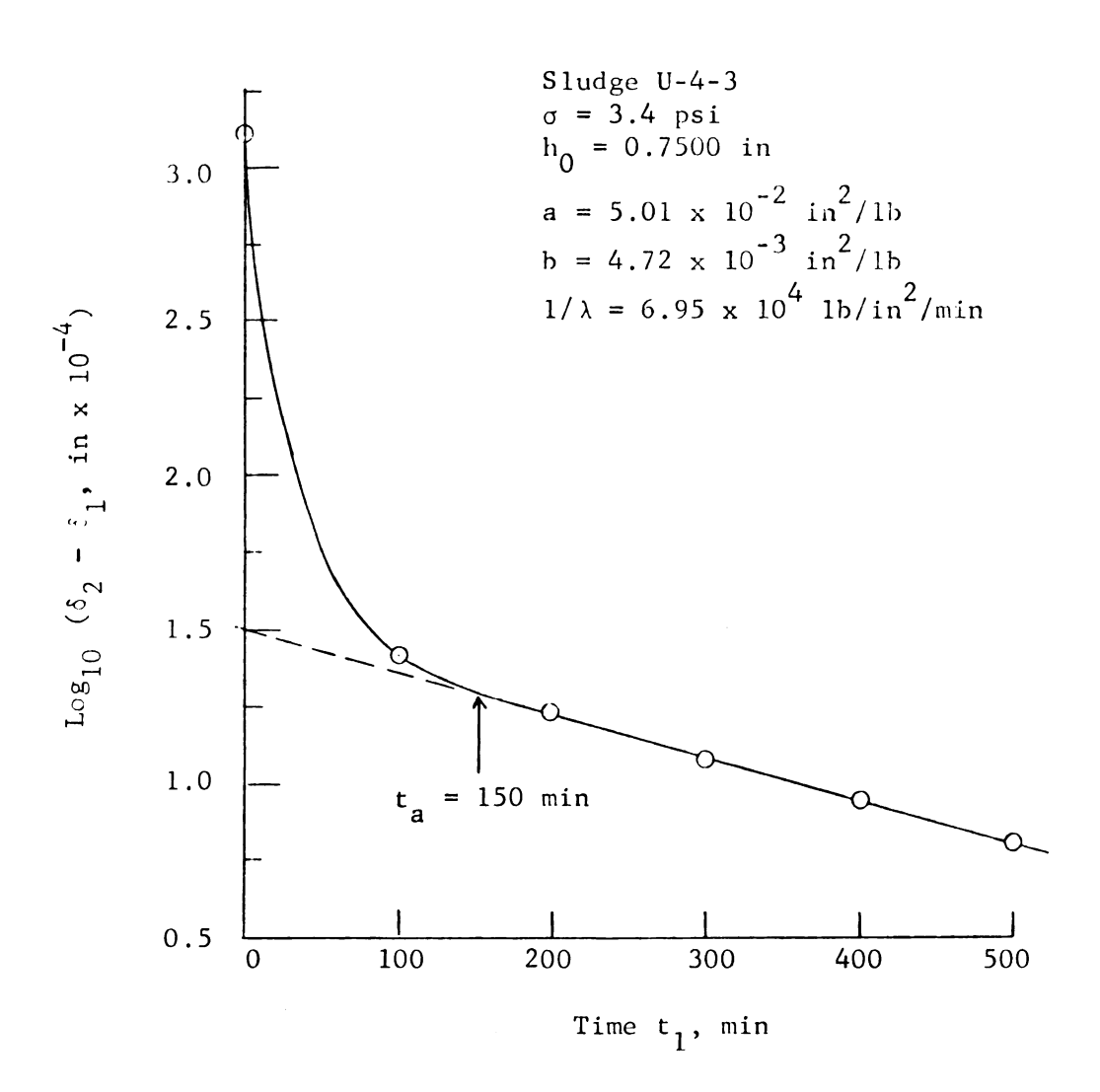


Figure 6.4. Parameter determination for the method of Gibson and Lo.

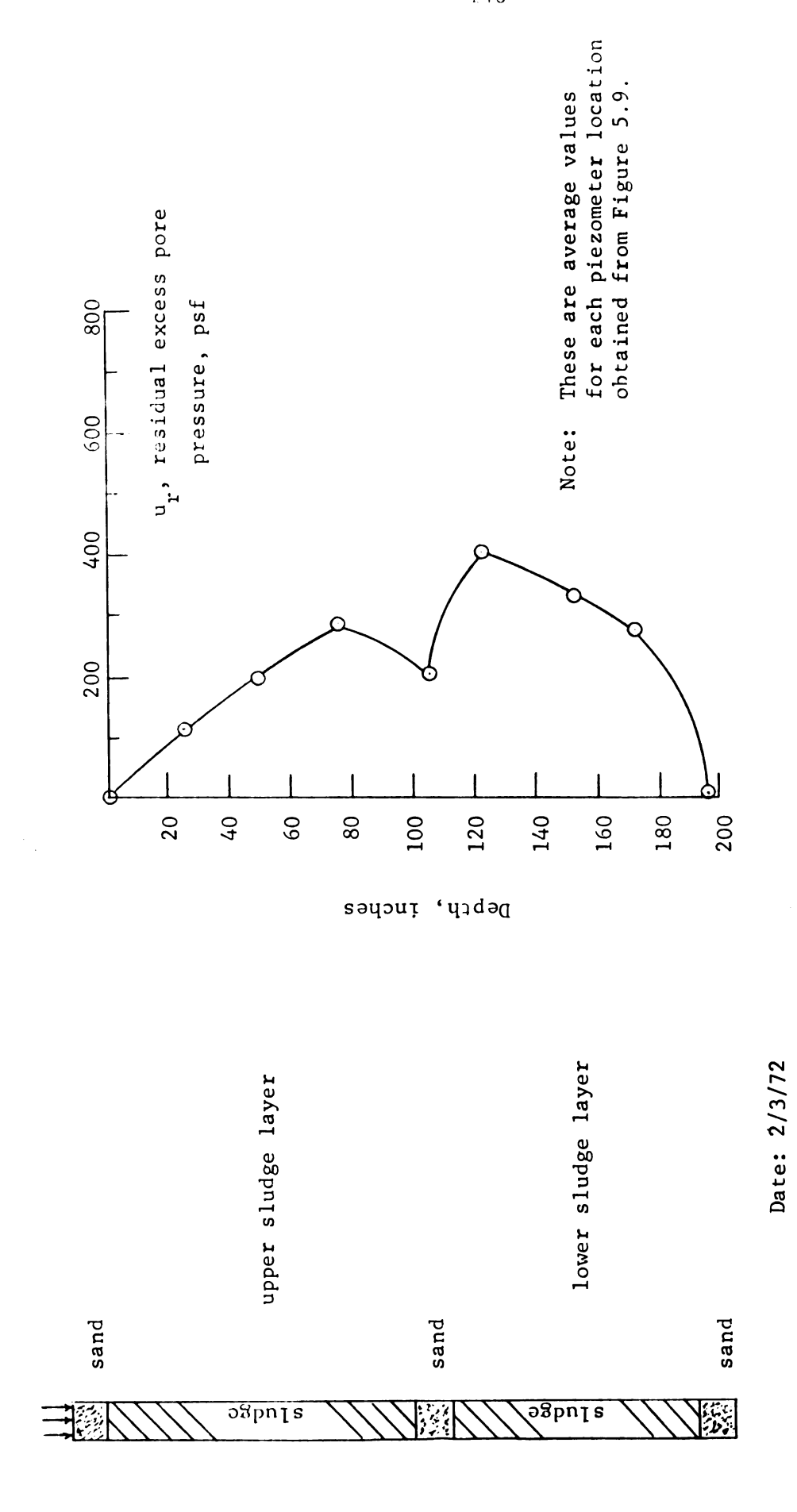
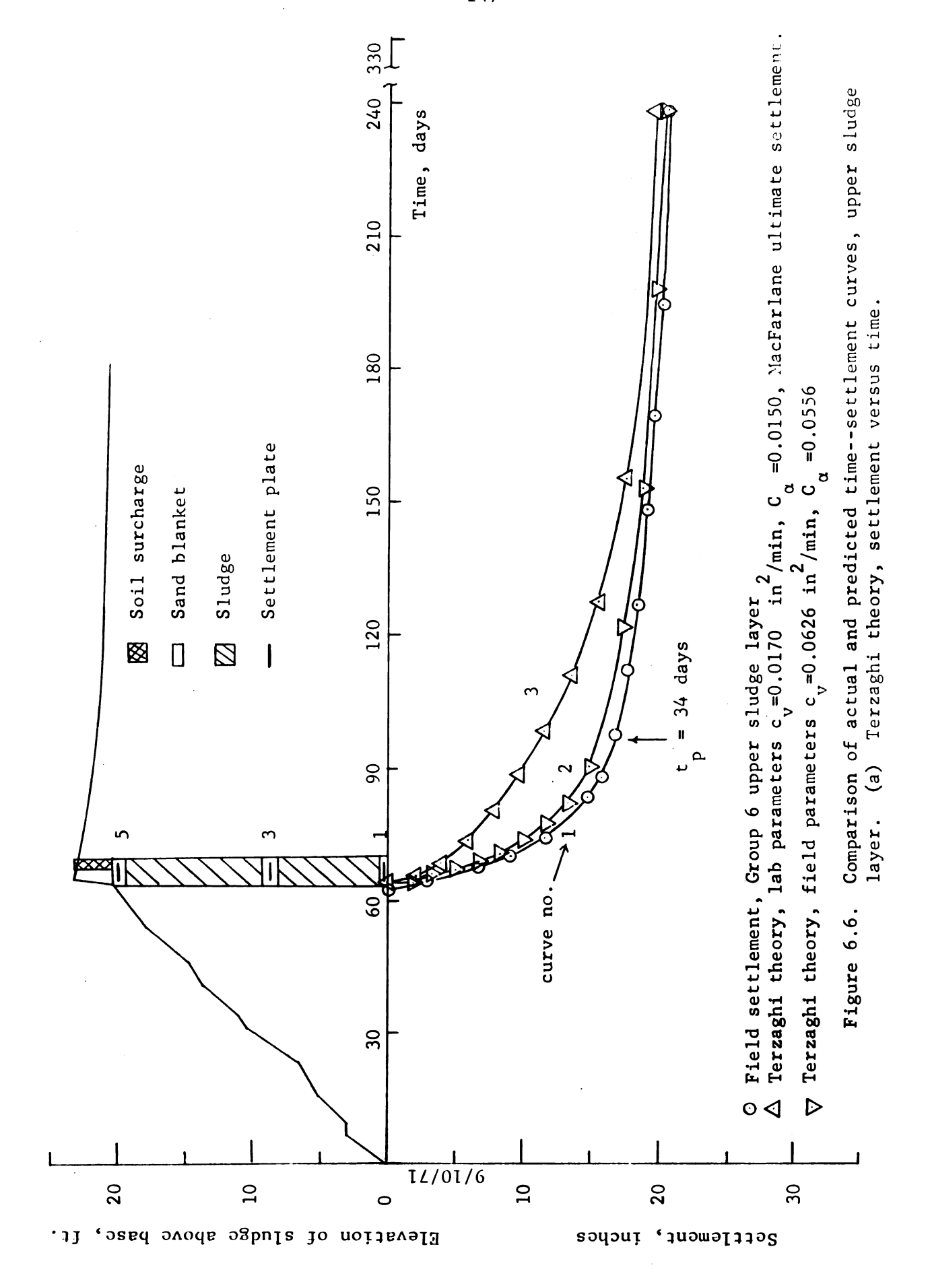
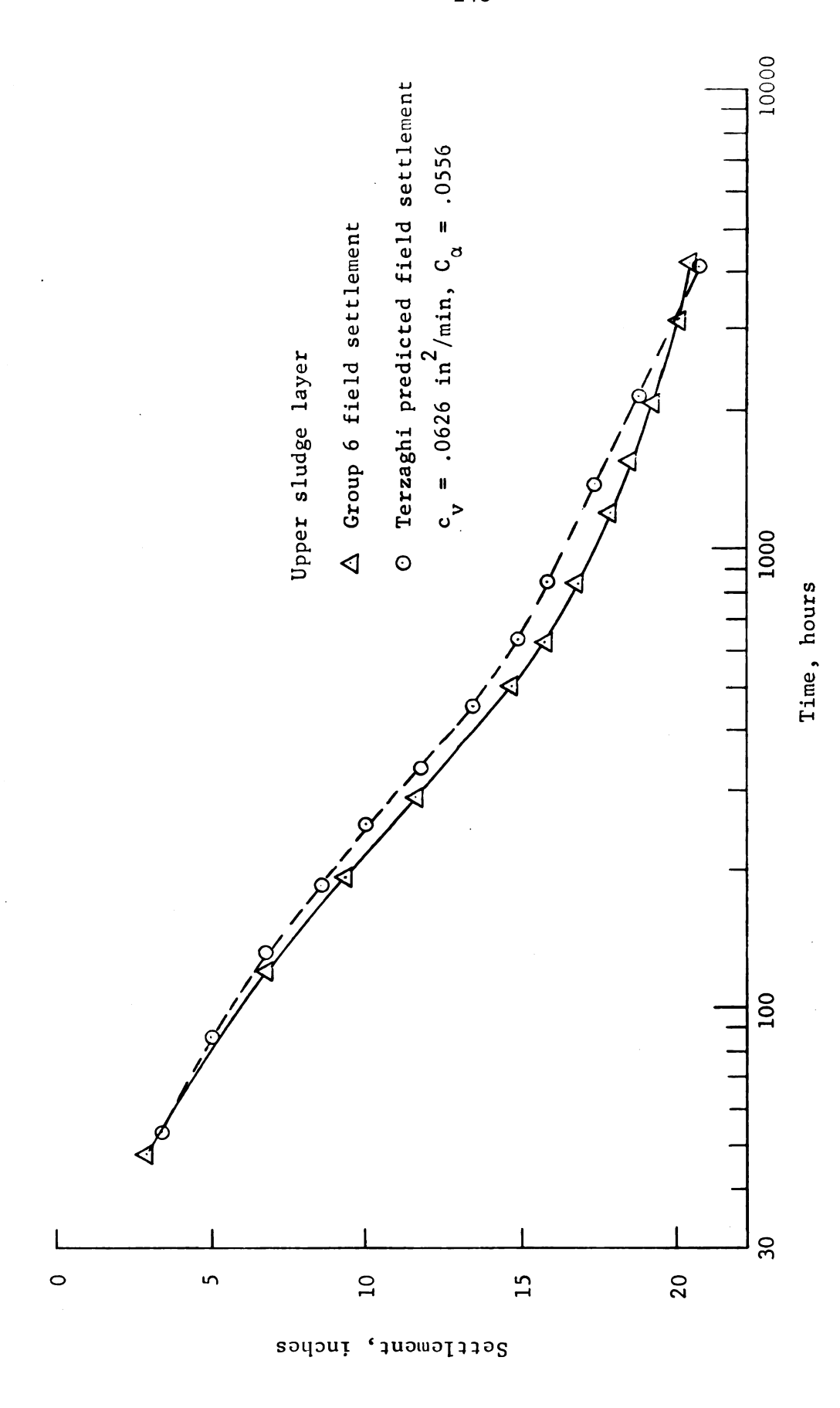
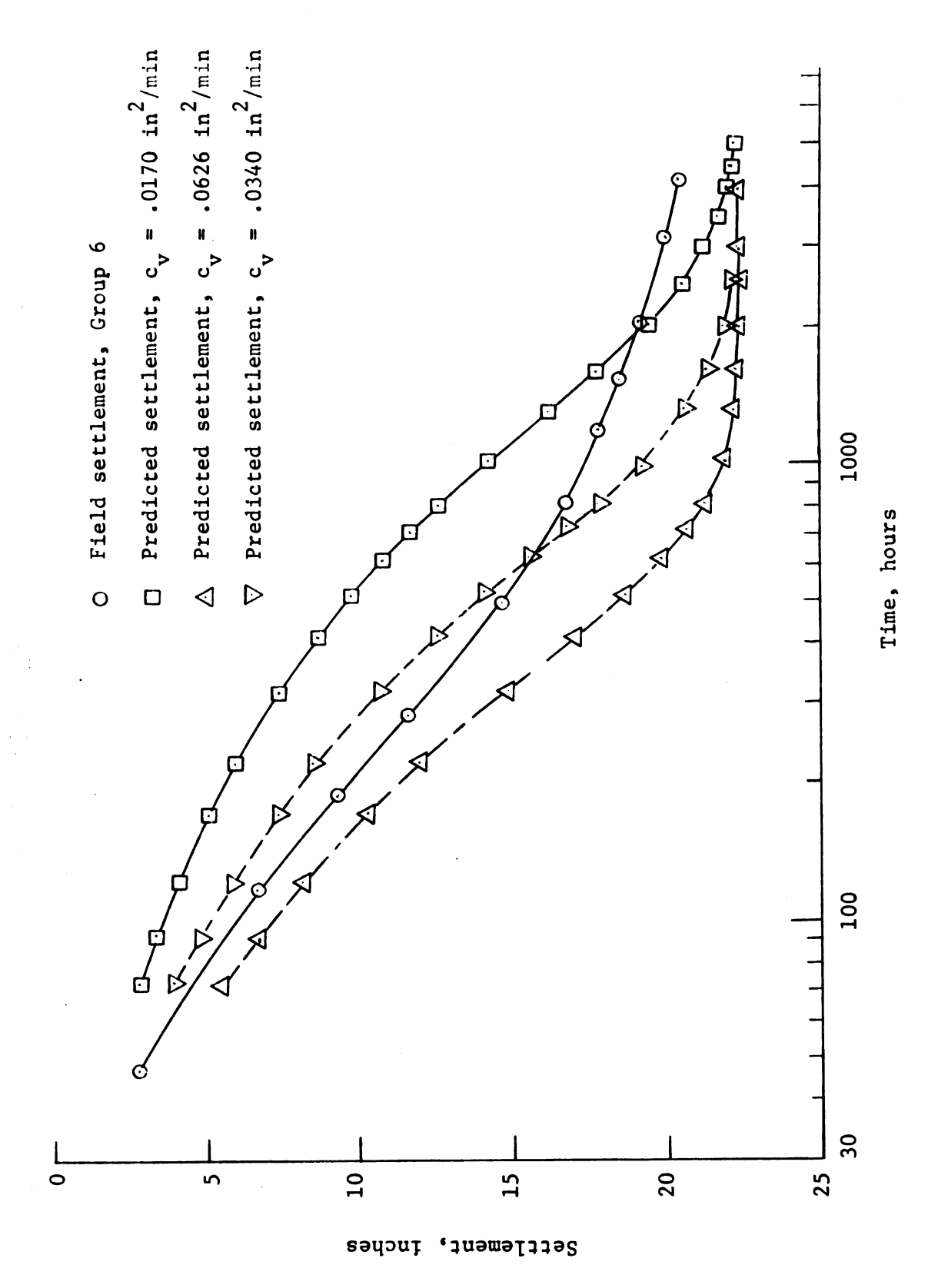


Figure 6.5. Measured residual excess pore pressure versus depth.

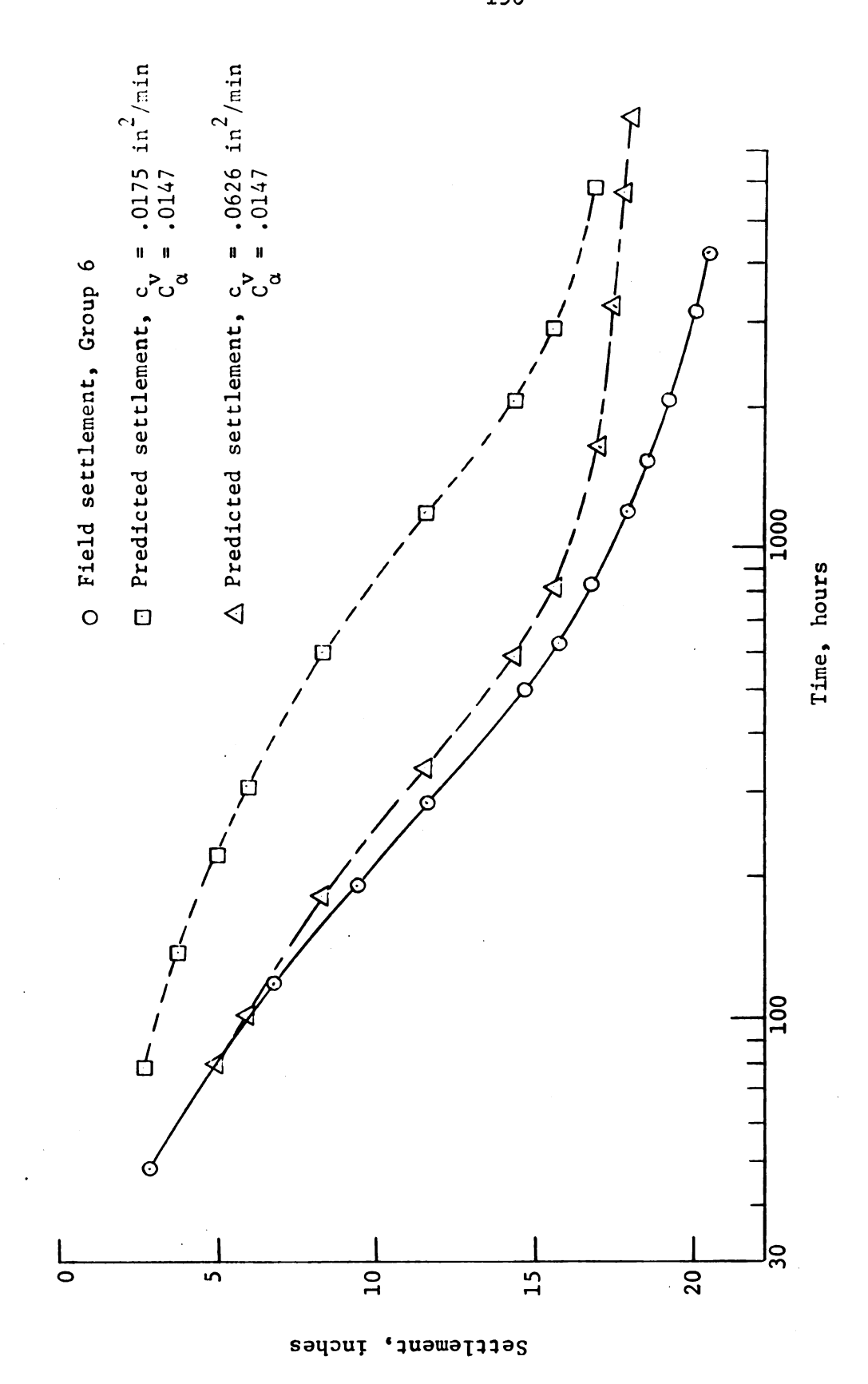




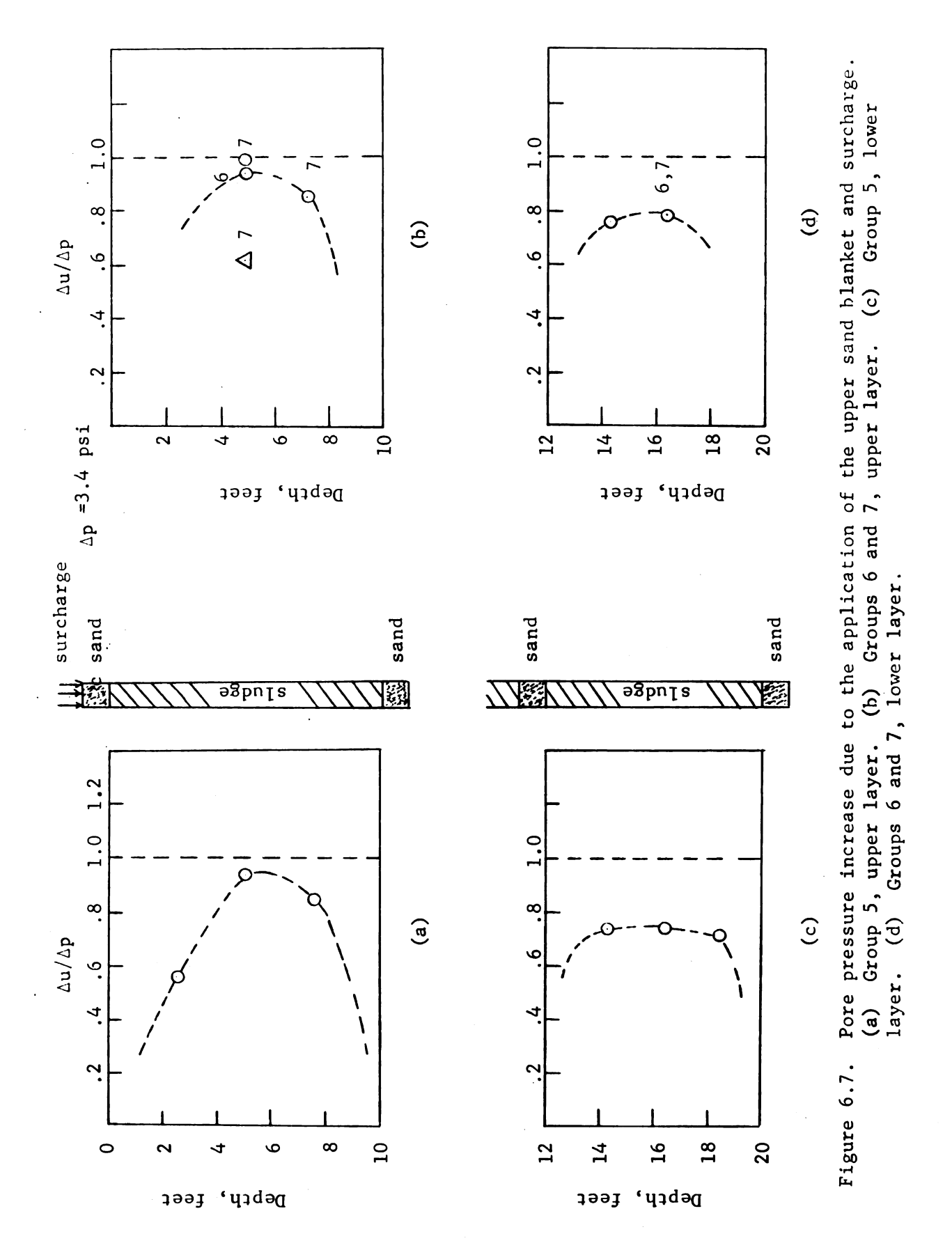
Comparison of actual and predicted time--settlement curves, upper sludge layer. (b) Terzaghi theory, settlement versus logarithm of time. Figure 6.6.

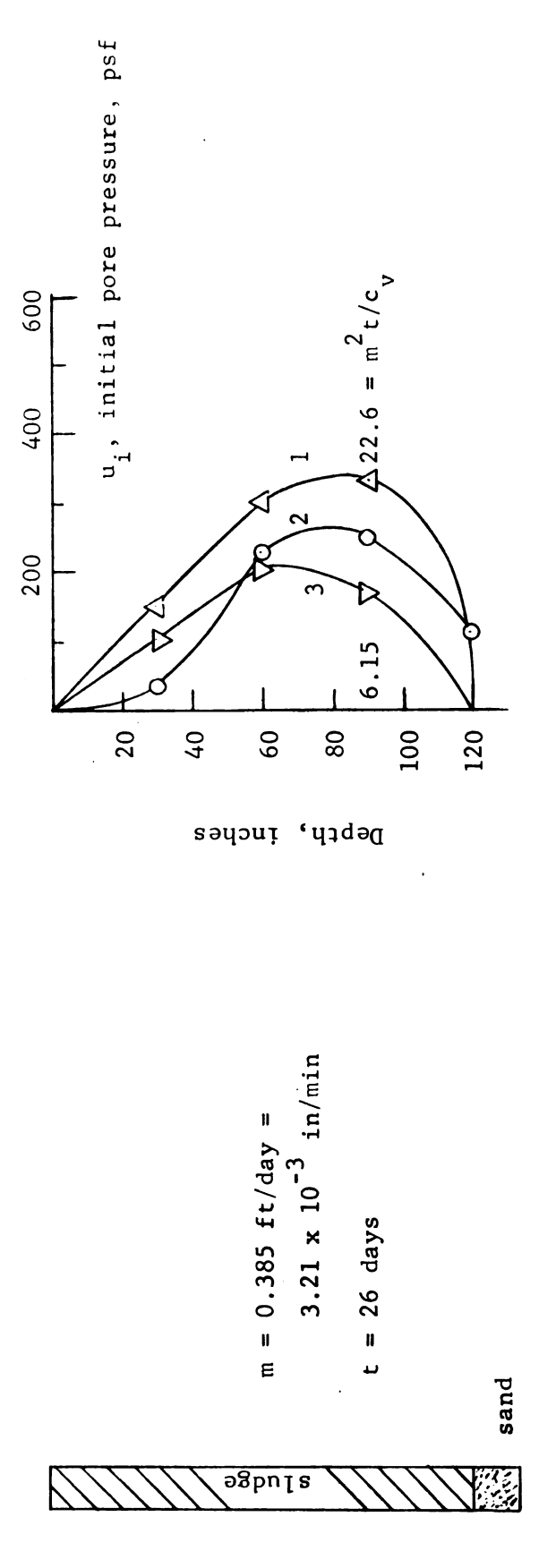


Comparison of actual and predicted time--settlement curves, upper sludge layer. (c) Theory of Gibson and Lo, settlement vs. logarithm of time. Figure 6.6.



Comparison of actual and predicted time--settlement curves, upper sludge layer. (d) Wahls's theory, settlement vs. logarithm of time. Figure 6.6.



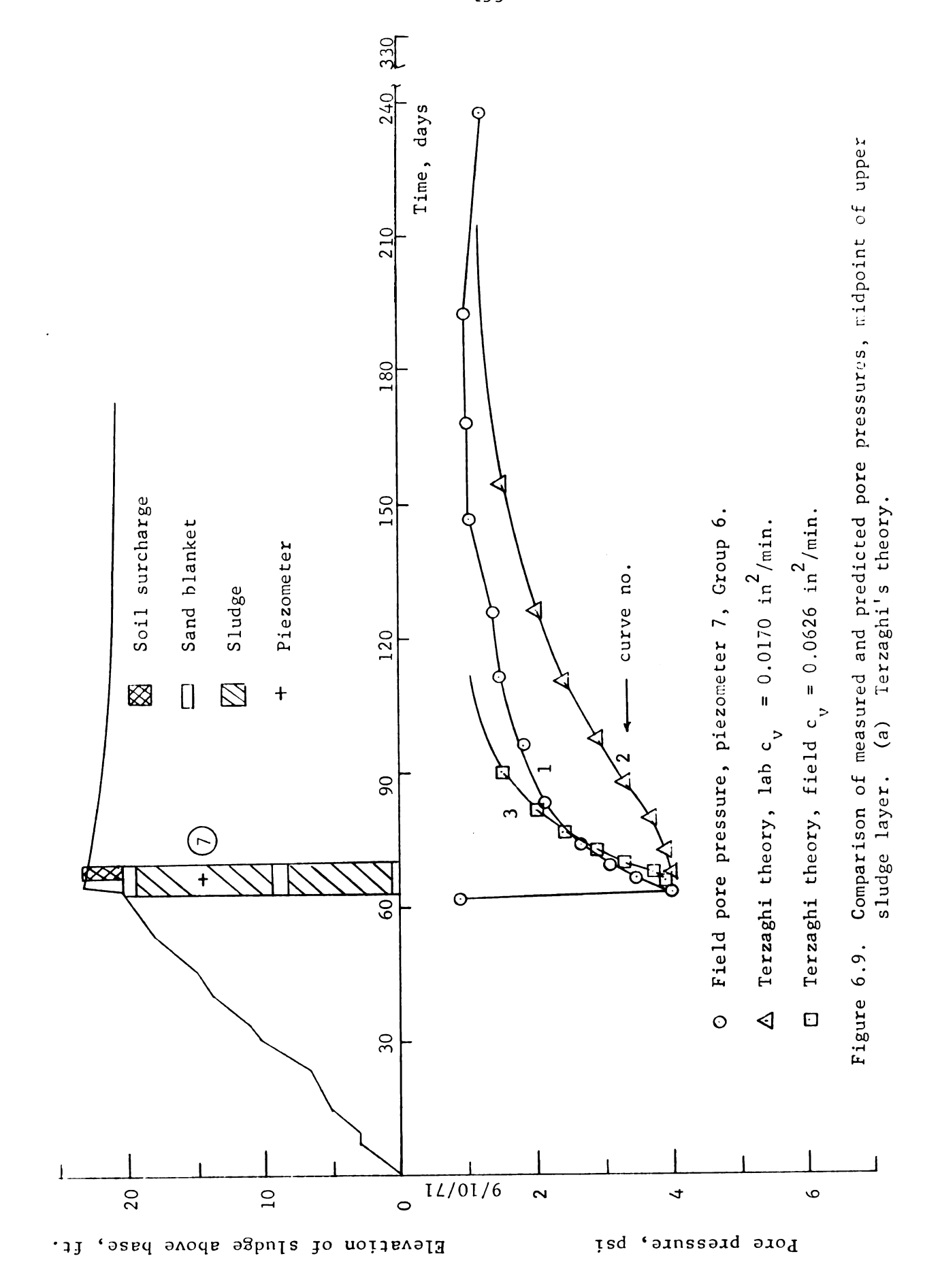


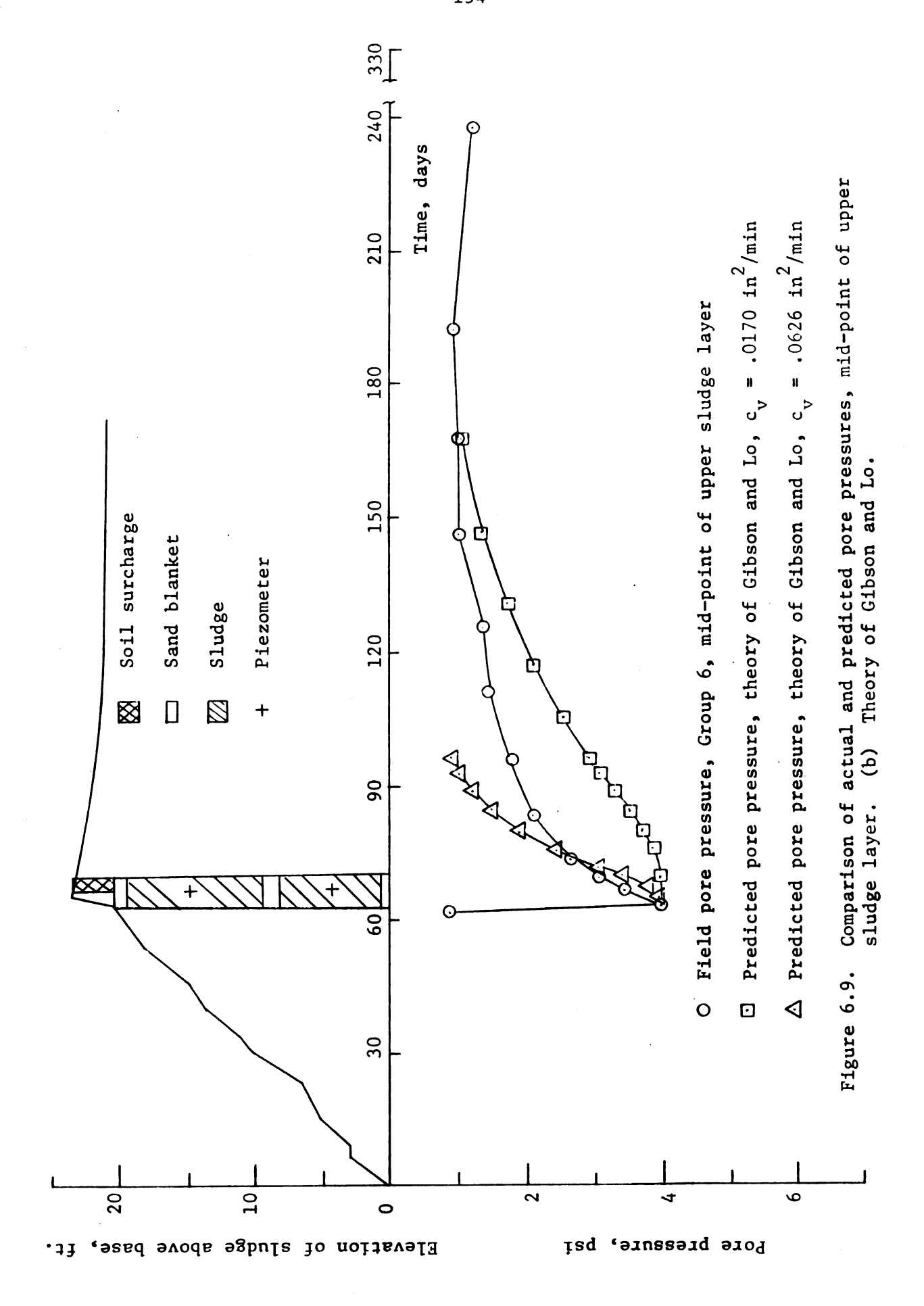
O Average value of initial measured pore pressure Gibson's theory, field  $c_v = 0.0626 \text{ in}^2/\text{min}$ 

 $\Delta$  Gibson's theory, lab  $c_{_{\rm U}}=0.0170~{\rm in}^2/{\rm min}$ 

D

Comparison of measured and predicted initial pore pressures, upper sludge layer. Figure 6.8.





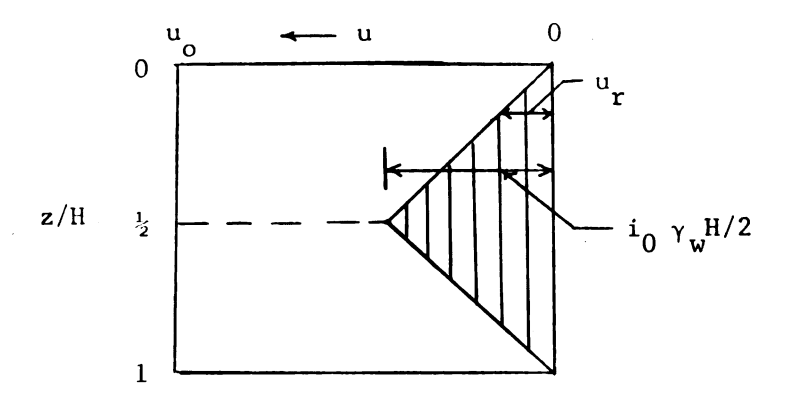


Figure 6.10. Theoretical final pore pressure distribution at the end of consolidation if a threshold gradient exists.

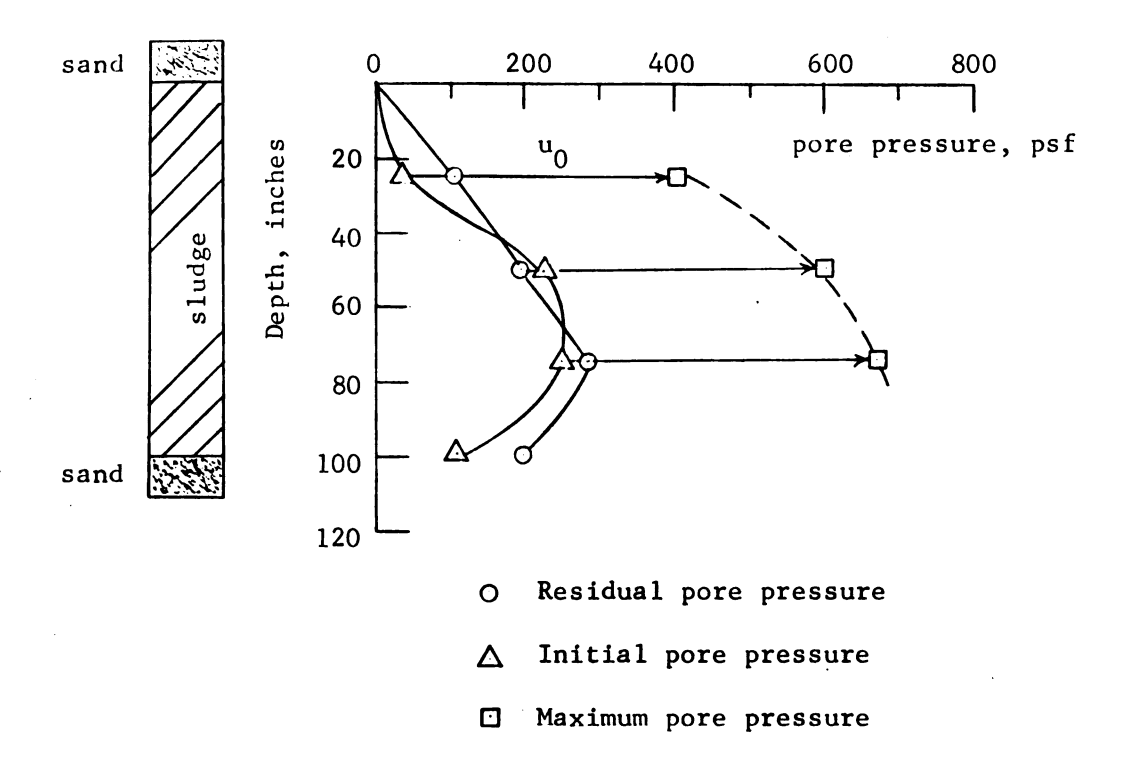


Figure 6.11. Comparison of initial, maximum, and residual pore pressures for the upper sludge layer.

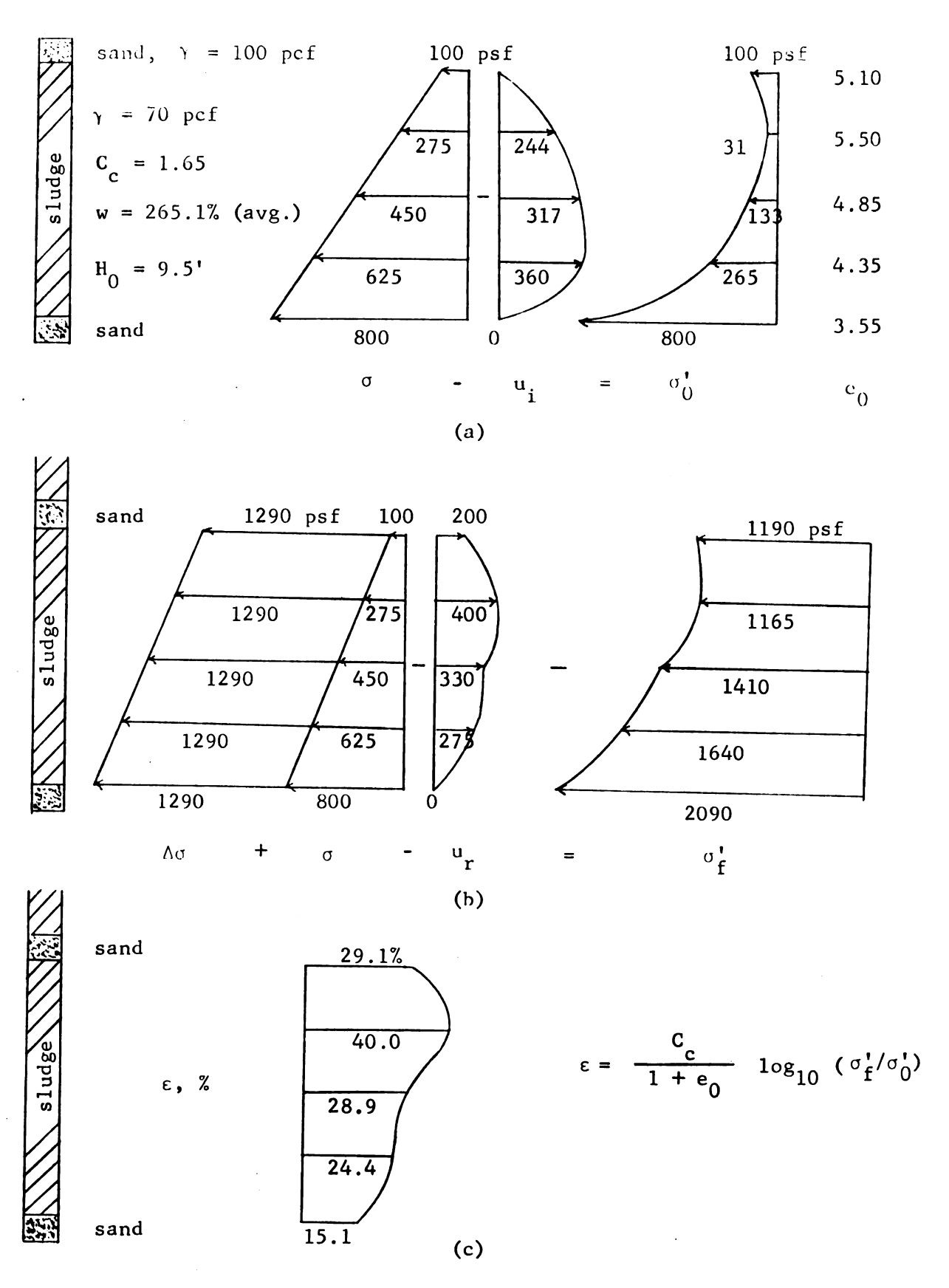


Figure 6.12. Estimated effective stress changes and strain distribution in the lower sludge layer. (a) Initial stresses. (b) Final stresses. (c) Strain distribution.

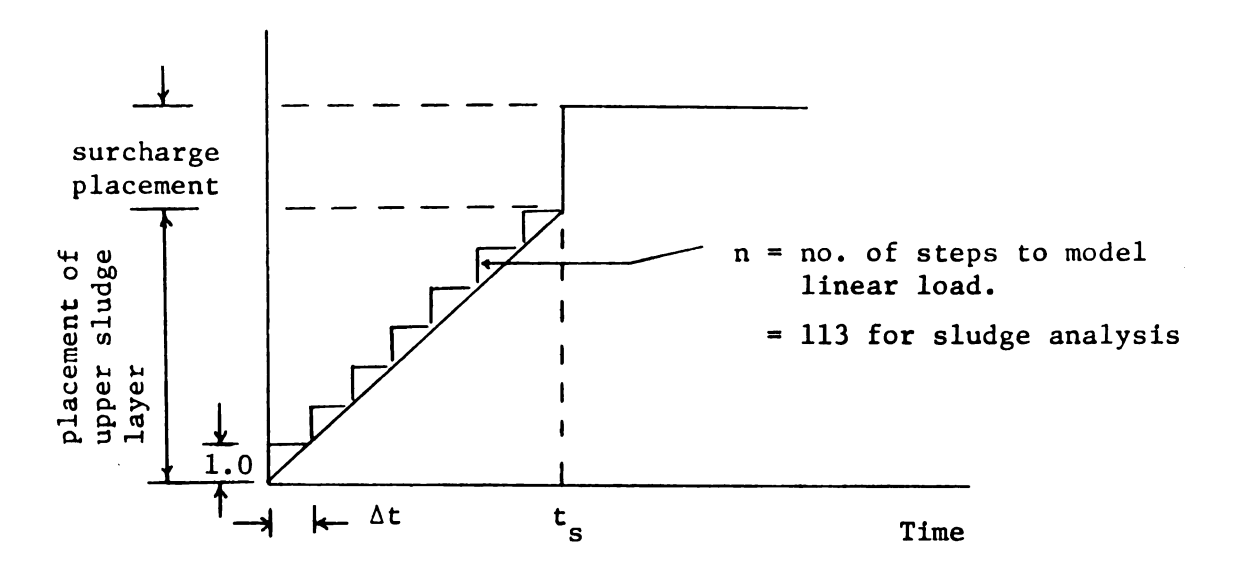
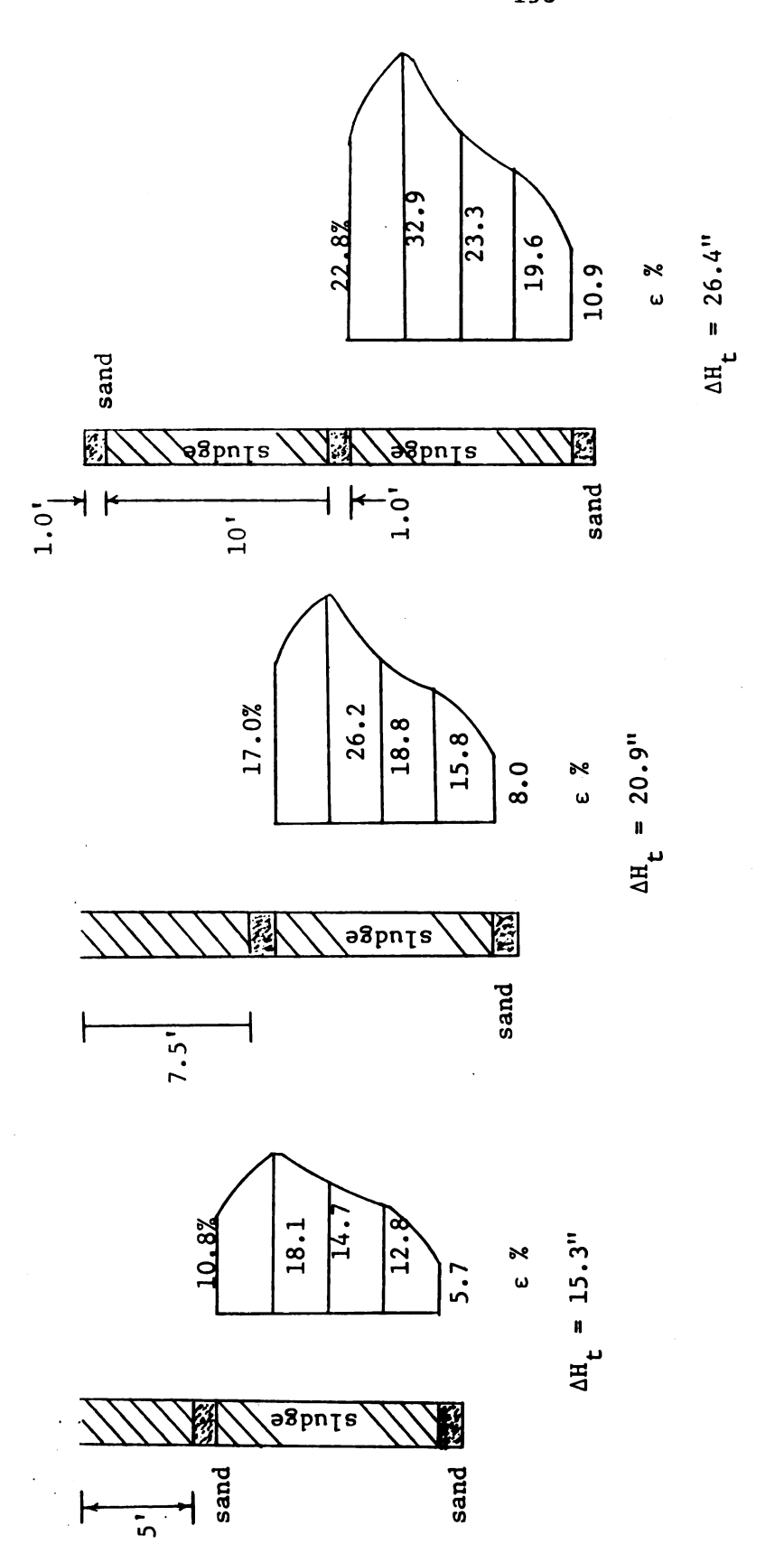
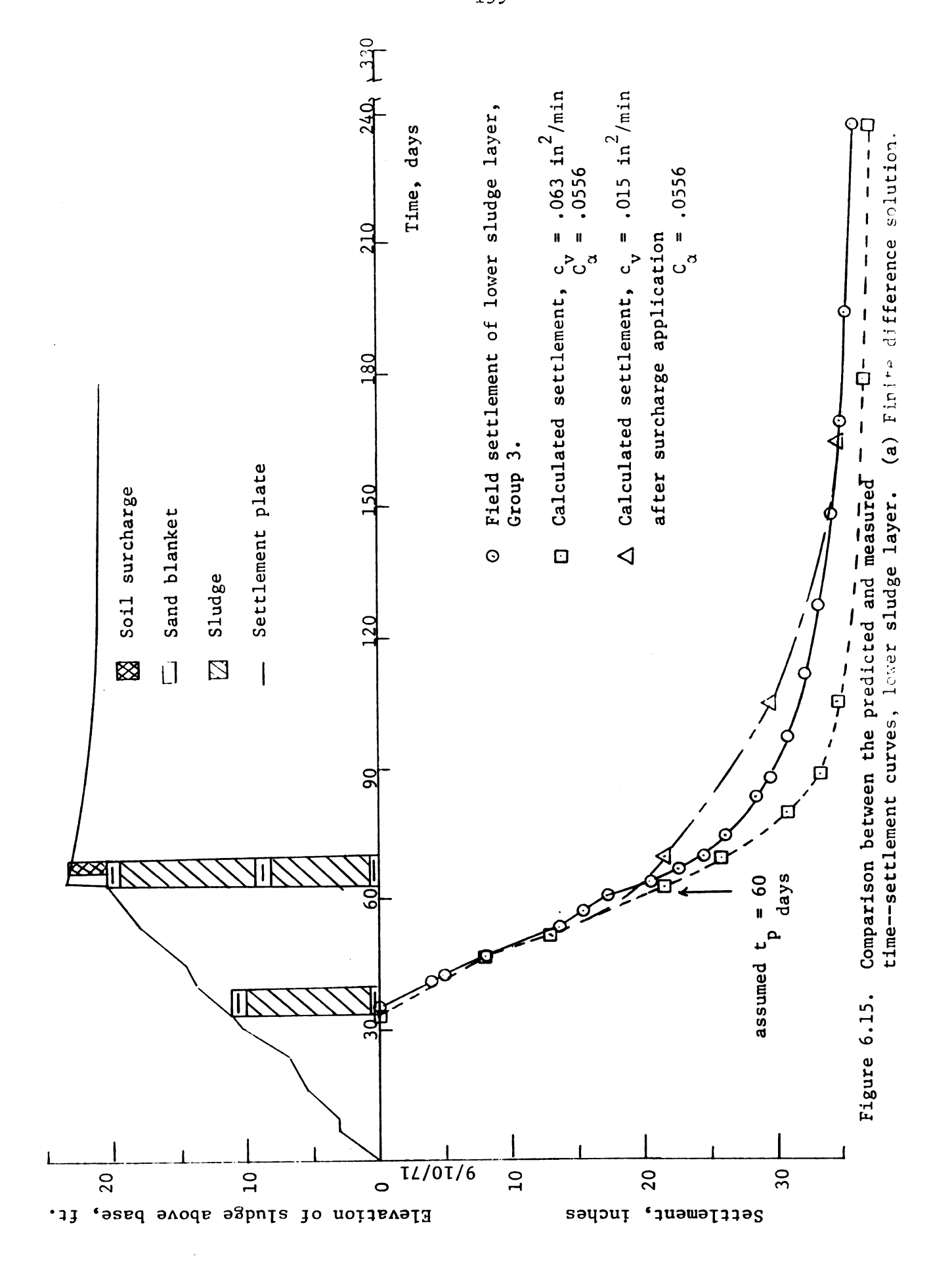


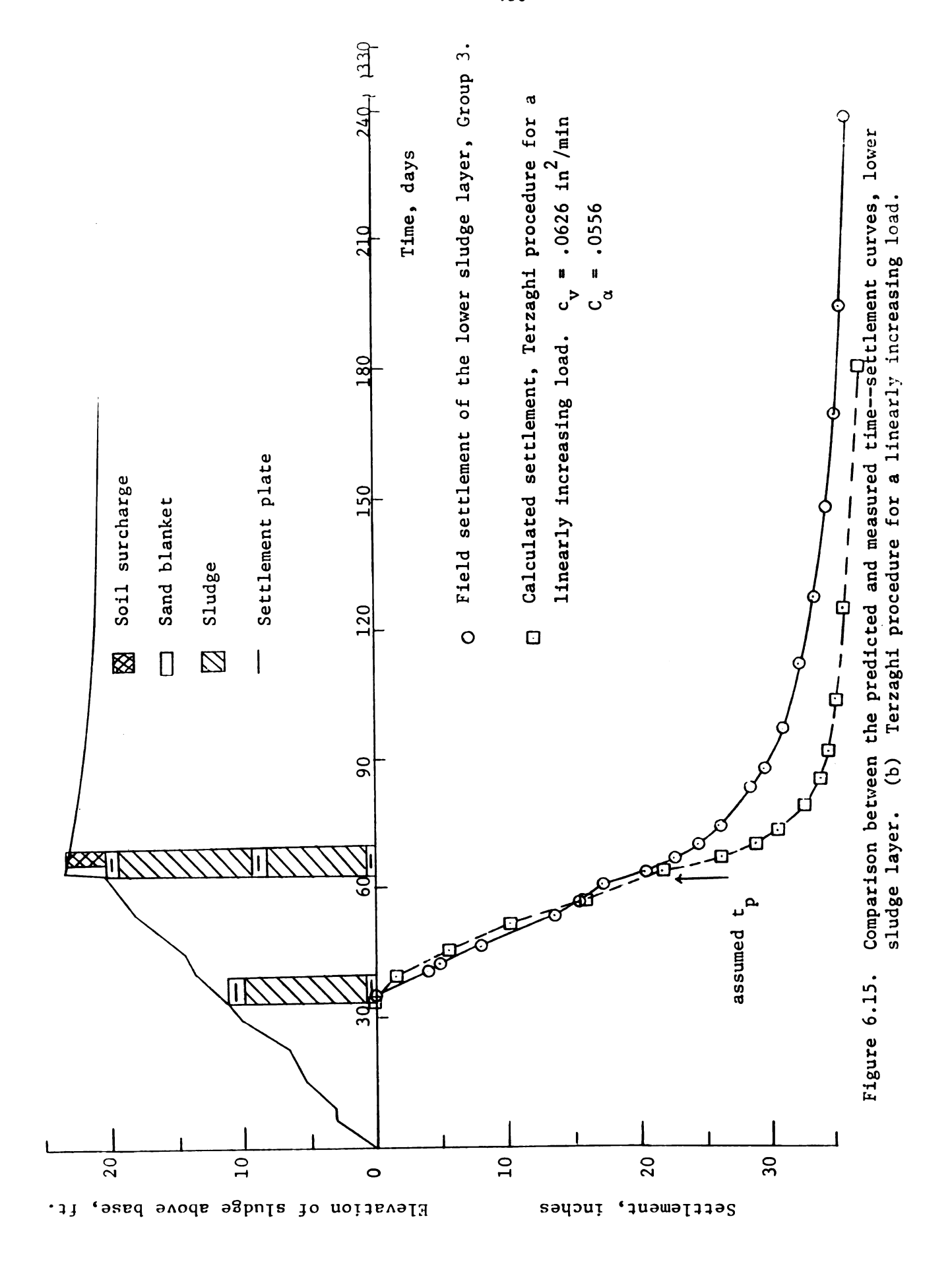
Figure 6.13. Load increasing linearly with time followed by an instantaneous surcharge application.

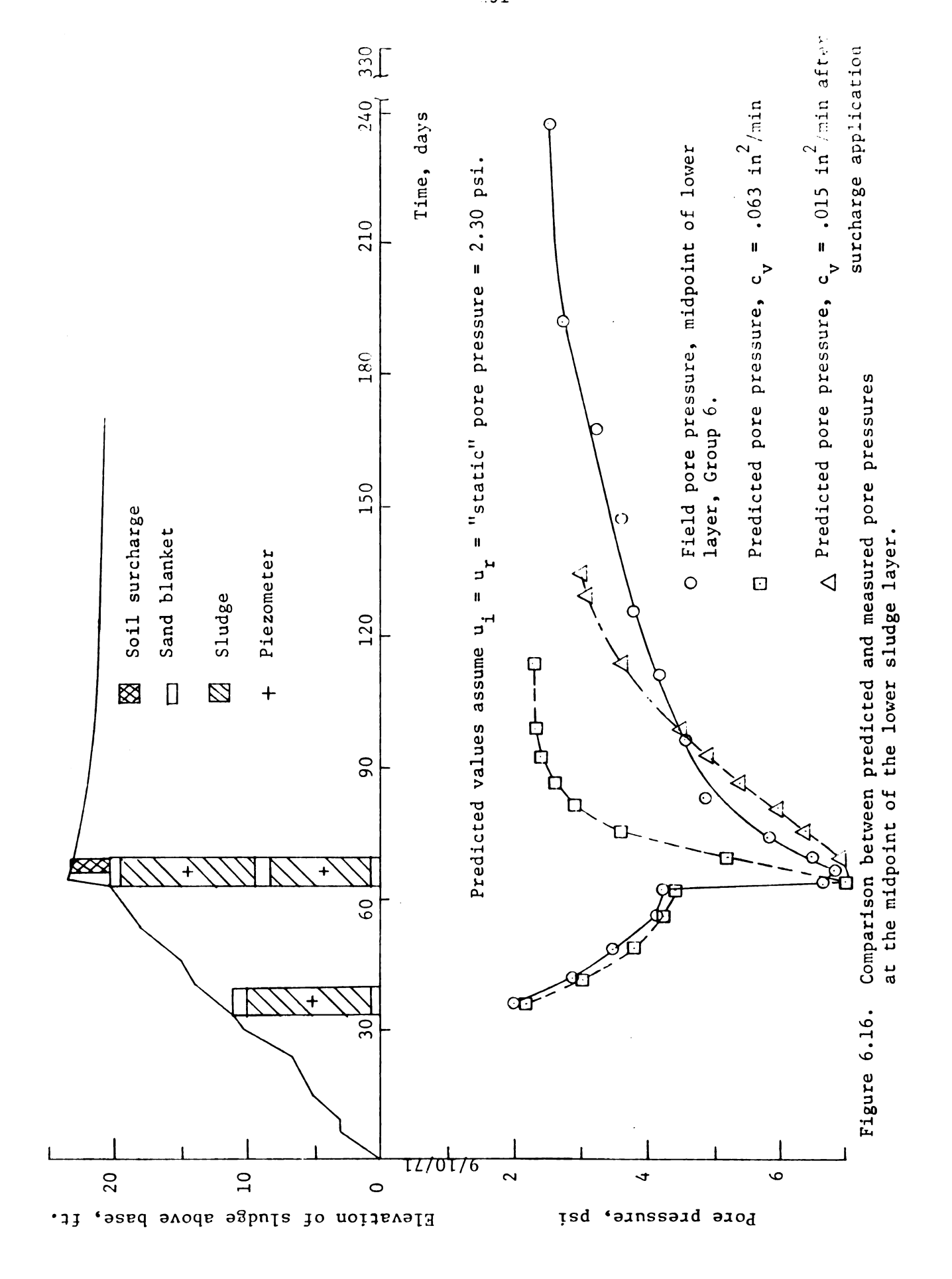


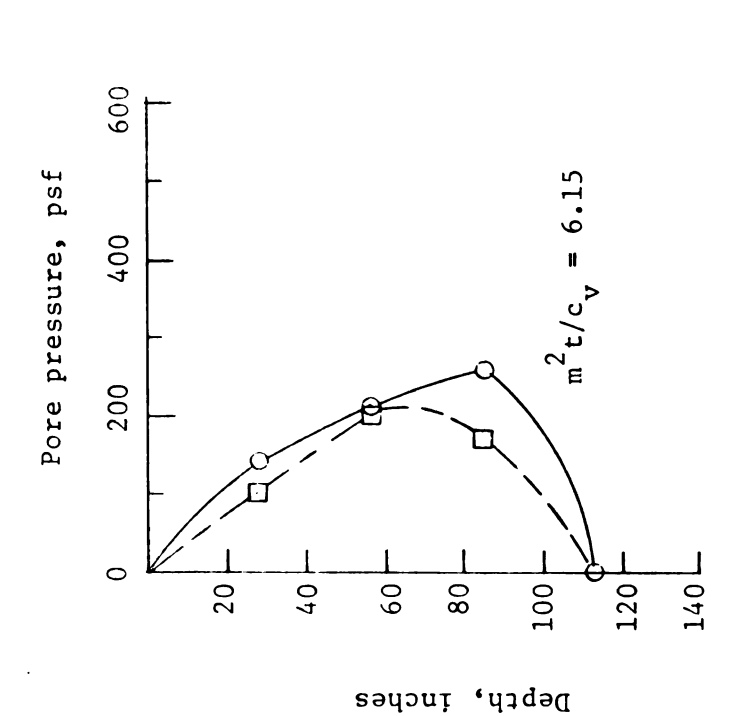
The analyses shown here follow the same procedure as shown in Figure 6.12 except that Δσ is different for each case. Note:

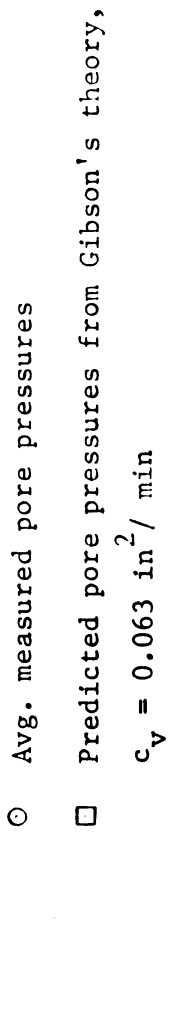
Estimates of ultimate settlement of the lower sludge layer for different elevations of the upper sludge layer. Figure 6.14.











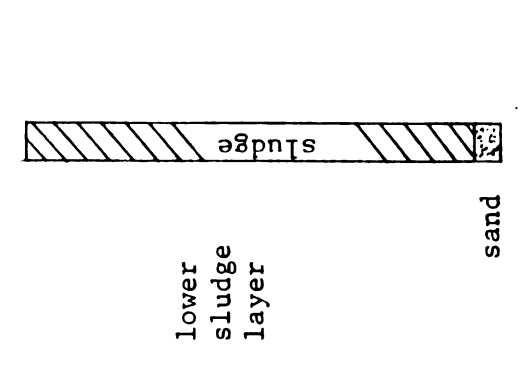


Figure 6.17. Measured and estimated initial excess pore pressures in the lower sludge layer.

#### CHAPTER VII

### SUMMARY AND CONCLUSIONS

## 7.1 Field Consolidation

An experimental papermill sludge landfill was constructed and monitored to obtain engineering information essential to developing guidelines and recommendations for the design and operation of solid papermill waste landfills. The landfill consisted of 2 sludge layers, initially 10 ft. thick, with sand drainage blankets at the top, middle, and bottom. An earth dike provided lateral confinement for the soft sludge during and after construction, and 3 ft. of natural soil provided the surface load. The landfill was instrumented with 32 settlement plates, 16 piezometers, 3 total pressure cells, and 10 thermistors. Field data were obtained, during the year, on settlement, pore water pressures, vertical and lateral earth pressures, temperature, sludge unit weights, specific gravity, and water contents. Laboratory work included consistency limits, ash contents, and consolidation tests on both fresh and undisturbed samples of sludge. Comparisons have been made between field settlement behavior and predicted behavior using laboratory test parameters, backfigured field parameters, and soil mechanics theories, including those on consolidation and pore pressure dissipation. Conclusions are given under the following headings: (1) settlement, (2) pore pressures, and (3) stress and temperature conditions.

### 7.1.1 Settlement

- 1. Reasonable estimates of ultimate primary settlement for the sludge can be obtained using equation 6.2, provided that both the initial and residual pore pressures are used in computing effective stresses. A laboratory value for the compression index  $\mathbf{C}_{\mathbf{C}}$  appears to be appropriate, and the initial void ratio  $\mathbf{e}_{\mathbf{0}}$  for the field sludge layer may be taken from a laboratory void ratio-logarithm of pressure curve at the appropriate stress level.
- 2. MacFarlane's (1969) method, using data from a single increment laboratory consolidation test, overestimates primary settlement. Results for this method gave estimates of primary settlement that were closer to the actual total settlement of each sludge layer. This may be due to the high initial void ratio of the laboratory samples.
- 3. Gibson and Lo's (1961) theory provides an accurate estimate of total settlement and time-rate of settlement under instantaneous loading conditions. The time-settlement relation is dependent on the assumed value of  $c_{_{\rm V}}$  and predicts that the ultimate settlement is reached without the development of a linear (with log time) secondary compression curve. Careful laboratory tests were required to determine the parameters a, b, and  $\lambda$  used in this theory.
- 4. The field settlement versus logarithm of time curves shown in Figures 5.10 and 5.11 exhibit a decreasing secondary compression rate with log time. This behavior was observed for both the upper and lower sludge layers although it was not experienced with any of the samples tested in the laboratory.

- 5. Estimates of secondary compression, based on equation 6.5 and Wahls's (1962) theory, are too low for laboratory values of the coefficient of secondary compression,  $C_{\alpha}$ . Backfigured field parameters yielded appropriate estimates for the upper sludge layer, while a somewhat arbitrary value of  $t_p$  had to be assumed for the lower sludge layer.
- 6. Terzaghi's (1943) theory and Wahls's (1962) theory appear to adequately predict the hydrodynamic portion of the time-settlement relation for the sludge, provided that an appropriate value for the coefficient of consolidation, c<sub>v</sub>, is used in each theory. Satisfactory results were obtained for both the upper and lower sludge layers for the different conditions of loading. The coefficient of consolidation appears to decrease with an increase in field consolidation similar to the decrease shown by laboratory tests. Environmental factors (surface drying, etc.) influenced the time-settlement relation for the upper sludge layer in the landfill.
- 7. Settlement rates for the landfill gave a good estimate of the flow rate for leachate draining from the papermill sludge.
- 8. Undisturbed samples taken from the landfill yielded valuable information concerning the sludge's laboratory e vs.  $\log p$  relationship and the variation, with effective stress, in the coefficient of consolidation,  $c_v$ , primary compression ratio, r, and the coefficient of secondary compression,  $C_\alpha$ , that occurred with field consolidation followed by sampling and laboratory testing.

## 7.1.2 Pore Pressures

1. Gibson's (1958) theory gives estimates of pore pressures

generated during sludge placement that are in accordance with field observations. Pore pressures in the sludge were influenced by excess pore pressures that built up in the middle sand drainage blanket. These were the result of incomplete drainage and were caused by greater settlement occurring in the central portion of the landfill.

- 2. Terzaghi's (1943) theory and Gibson and Lo's (1961) theory accurately predicted pore pressures in the upper sludge layer up to about 70 percent dissipation, provided that an appropriate value for the coefficient of consolidation was used. It was also possible to predict pore pressures for the lower sludge layer, which experienced different conditions of loading. After 70 percent dissipation, the pore pressures decreased at a slower rate and eventually appeared to stabilize at some residual value. This indicates that a threshold gradient exists for the sludge in the landfill, below which little or no flow of pore water can occur. Pore pressures may also be influenced by environmental factors, as demonstrated by the pore pressure fluctuations of the upper sludge layer with time.
- 3. The assumption of a uniform initial excess pore pressure for use with Terzaghi's theory appears to be reasonable because of the closeness in magnitude between the initial pore pressures generated during sludge placement and the residual pore pressures.

# 7.1.3 Stress and Temperature Conditions

1. The undrained shear strength of the sludge increased considerably during consolidation and is greatest at points in the landfill that are under the highest effective stresses. A linear relationship between undrained strength and consolidation pressure

was indicated by the data shown in Figure 5.7. Sensitivity of the sludge in terms of the ratio of undisturbed to remolded vane strength was less than two.

- 2. The vertical stress measured close to the mid-depth of the lower sludge layer by the total pressure cells was in fair agreement with the stress calculated on the basis of material unit weights, indicating that the measured lateral stresses should be equally accurate.
- 3. The coefficient of lateral stress,  $K_0$ , based on total stress and pore pressure data, decreased from about 0.65 immediately after sludge placement to about 0.32 for the final stage of consolidation.
- 4. Temperature increase due to increased biological activity peaked about 50 days after completion of the landfill giving a maximum temperature rise close to 7°C in the upper half of the lower sludge layer. Thereafter sludge temperatures were determined by ground and seasonal air temperatures.

REFERENCES

#### REFERENCES

American Society for Testing and Materials, <u>Book of ASTM Standards</u>, Parts 11 and 15, Philadelphia, Pennsylvania.

Andersland, O. B., and Laza, Robert W., "Permeability of High Ash Papermill Sludge," <u>Journal of the Sanitary Engineering Division</u>, Proc. ASCE, Vol. 98, No. SA 6, December, 1972.

Andersland, O. B., and Laza, Robert W., "Shear Strength and Permeability of High Ash Pulp and Papermill Sludges," Tech. Rpt. 1 for the National Council of the Paper Industry for Air and Stream Improvement, Inc., Div. of Engineering Research, Mich. State Univ., E. Lansing, Mich., 1971.

Andersland, O. B., and Paloorthekkathil, John M., "Consolidation Behavior of High Ash Pulp and Papermill Sludges," Tech. Rpt. 2 for the National Council of the Paper Industry for Air and Stream Improvement, Inc., Div. of Engineering Research, Mich. State Univ., E. Lansing, Mich., 1972.

Bishop, Alan W., and Henkel, D. J., <u>The Measurement of Soil Properties</u> in the Triaxial Test, Edward Arnold (Publishers) Ltd., London, 1962.

Bjerrum, Laurits, "Engineering Geology of Norwegian Normally-Consolidated Marine Clays as Related to Settlements of Buildings," Geotechnique, London, 17:81-118, 1967.

Bjerrum, Laurits, "Embankments on Soft Ground," Proc., Specialty Conf. on Performance of Earth and Earth-supported Structures, Am. Soc. of Civil Engrs., II:1-54, June, 1972.

Black, C. S., ed., Methods of Soil Analysis, No. 9 in the series Agronomy, Am. Soc. Agronomy, Inc.. Part 2, 1965.

Casagrande, A., "The Determination of the Preconsolidation Load and Its Practical Significance," Proceedings, 1st International Conference on Soil Mechanics and Foundation Engineering, Cambridge, 3:60, 1936.

Davis, E. H., and Raymond, G. P., "A Non-linear Theory of Consolidation," Geotechnique, London, 15:161-173, 1965.

Follett, Robert, and Gehm, Harry W., "Manual of Practice for Sludge Handling in the Pulp and Paper Industry," National Council of the Paper Industry for Air and Stream Improvement, Inc., Tech. Bull. No. 190, June, 1966.

- Garlanger, John E., "The Consolidation of Soils Exhibiting Creep Under Constant Effective Stress, "Geotechnique, London, 22:71-78, 1972.
- Gibson, R. E., "The Progress of Consolidation in a Clay Layer Increasing in Thickness with Time," <u>Geotechnique</u>, London, 8:171-182, 1958.
- Gibson, R. E., and Lo, K. Y., "A Theory of Consolidation for Soils Exhibiting Secondary Compression," Norwegian Geotechnical Institute, Publication 41, Oslo, Norway, 1961.
- Gibson, R. E., England, G. L., and Hussey, M. J. L., "The Theory of One-dimensional Consolidation of Saturated Clays," <u>Geotechnique</u>, London, 17:261-273, 1967.
- Gillespie, W. J., "Summary Report--Questionnaire Survey--Sludge Cake Disposal on Land," National Council of the Paper Industry for Air and Stream Improvement, Inc., Unpublished, September 1969.
- Gillespie, W. J., Gellman, I., Janes, R. L., "Utilization of High Ash Papermill Waste Solids," Proc. 2nd Mineral Waste Utilization Symposium, IITRI, Chicago, Ill., 1970.
- Gillespie, W. J., Mazzola, C. A., and Gellman, I., "Landfill Disposal of Papermill Waste Solids," presented at the 7th TAPPI Air and Water Conference., Minneapolis, Minn., June 7-10, 1970.
- Grim, R. E., <u>Clay Mineralogy</u>, McGraw-Hill Book Co., Inc., New York, 1968.
- Grim, R. E., Applied Clay Mineralogy, McGraw-Hill Book Co., Inc., New York, 1962.
- Harr, M. E., Foundations of Theoretical Soil Mechanics, McGraw-Hill Book Co., In., New York, 1966.
- Janbu, N., "Consolidation of Clay Layers Based on Non-linear Stress-strain," Proc. 6th Internat. Conf. on Soil Mech. and Found. Eng., II:83-87, 1965.
- Lambe, T. William, Soil Testing for Engineers, John Wiley and Sons, Inc., New York, 1951.
- Lambe, T. William, and Whitman, Robert V., Soil Mechanics, John Wiley and Sons, Inc., New York, 1969.
- Leonards, G. A., Foundation Engineering, McGraw-Hill Book Co., Inc., New York, 1962.
- Leonards, G. A., and Ramiah, R. K., "Time Effects in the Consolidation of Clay," STP No. 254, ASTM, 116-130, (1959).

Leonards, G. A., and Girault, P., "A Study of the One-dimensional Consolidation Test," Proc. 5th International Conf. on Soil Mech., and Found. Engr., Dunod, Paris, I:213-218, 1961.

Lo, K. Y., "Secondary Compression of Clays," Journal of the Soil Mech. and Found. Div., ASCE, 87:SM4:61-87, 1961.

MacFarlane, Ivan E., ed., Muskeg Engineering Handbook, Univ. of Toronto Press, 1969.

Mitchell, J. K., and Younger, J. S., "Abnormalities in Hydraulic Flow Through Fine-grained soils," STP No. 417, ASTM, pp. 106-139, 1966.

Scott, R. F., <u>Principles of Soil Mechanics</u>, Addison-Wesley Publ. Co., Inc., Reading, Mass., 1963.

Terzaghi, Karl, Theoretical Soil Mechanics, John Wiley and Sons, Inc., New York, 1943.

Terzaghi, Karl, and Peck, Ralph B., Soil Mechanics in Engineering Practice, 2nd ed., John Wiley and Sons, Inc., New York, 1967.

Wahls, Harvey E., "Analysis of Primary and Secondary Consolidation," Journ. of the Soil Mech. and Found. Div., ASCE, 88:SM6:207-231, 1962.

APPENDICES

TABLE A-1

SETTLEMENT PLATE ELEVATIONS AT THE BOTTOM SAND BLANKET

			ELEVATION,	F	T.			
PLATE	G1-1	G2-1*	G3-1	G4-1	G5-1	G6-1	G7-1	G8-1
Date								
9/10/71	_	78.30						
10/5/71	_	78.09						
· 🔊	_	78.08						
7	_	78.09						
10/20/11		78.10						
27	_	78.10						
26	_	78.11						
$\sim$		78.07						
	_	78.07						
6	_	78.08						
$\tilde{\mathbf{z}}$	_	78.07						
75	_	78.03						
$\mathbb{Z}$	_	78.04						
11/18/81	_	78.03						
/27	_	78.03						
$\vec{<}$		78.04						
9		78.04						
7		78.04						
`	_	78.05						
1/14/72		78.05						
7		78.03						
2/24/72	_	78.01						
/50/		78.04						
/4/7		78.02						
`	78.27	78.05	77.71	77.43	77.65	77.92	78.26	77.72
9/11/72	_	78.04						

\*Note: G2-1 refers to group no. 2 settlement plate no. 1, etc.

TABLE A-2
SETTLEMENT PLATE ELEVATIONS AT THE MID-POINTS
OF THE LOWER AND UPPER SLUDGE LAYERS

111	2. 29 2. 18 3. 03. 01. 01
-----	---------------------------------

SETTLEMENT PLATE ELEVATIONS AT THE MIDDLE SAND BLANKET TABLE A-3

			ELEVATION,	TION, FT	· .			
PLATE	G1-3	G2-3	G3-3	G4-3	G5-3	G6-3	G7-3	G8-3
Date								
10/14/7	1 88.47			œ		88.82		
	1 87.98	88.52	88.25	88.25	88.03	88.51	88.15	88.10
. ` `	1 87.93			<b>∞</b>		88.29		
7	1 87.75			7		88.08		_
. ` `	87.29			2		87.63		
11/5/71	87.19			7		87.47		
.``	87.			7		87.35		
11/10/7	86.			7		87.73		_
11/12/7	86.			9		87.04		
11/15/7	86.			9		86.83		
/18	86.			6.		86.69		_
/22	86.			9		86.56		
7	86.			9		86.36		
9	86.			•		86.28		
/15	86.			9		86.16		
7	85.			9		86.04		
/14/	85.			5.		85.97		
/3/1	85.77			5.		85.87		
2/24/72	85.70			5.		85.80		
/50/	85.69			5.		85.79		
74/7	85.64			5		85.74		
/1/7	85.61			5.		85.71		
/11/	85.60			5.		85.69		

TABLE A-4

SETT	SETTLEMENT	T PLATE		ELEVATIONS AT	THE TOP	SAND	BLANKET	[ <del>-</del>
			ELEVATION,	H	T.			
PLATE	G1-5	G2-5	G3-5	G4-5	G5-5	G6-5	G7-5	G8-5
Date								
11/10/71	98.		98.23	98.01		_		
11/12/71	97.		97.88	97.59		_		
11/15/71	97.		97.33	97.07		_		
11/18/71	97.		96.99	96.74		_		
11/22/71	96		96.65	96.42		_		
12/1/71	96		96.20	95.99				
12/6/71	96		96.04	95.83		_		
12/15/71	95.		95.84	95.63		_		
12/30/71	95.		95.63	95.43		_		
1/14/72	95.		95.52	95.31		_		
2/3/72	95.		95.38	95.16		_		
2/24/72	95.		95.27	95.05		_		
3/20/72	95.		95.23	95.00				
5/4/72	95.17	95.05	95.16	94.93	95.04	94.95	94.90	94.81
8/1/72	95.		92.06	94.83		_		
9/11/72	94.		94.99	94.72		_		

TABLE B-1
PORE WATER PRESSURES FOR THE BOTTOM SAND BLANKET
AND LOWER SLUDGE LAYER

PORE PRESSURE, PSI G7-3 G7-4 PIEZOMETER G5-1 G7-1 G5-2 G5-3 G6-3 G5-4 INITIAL EL.FT 78.0 78.5 81.0 83.5 83.6 83.9 83.0 86.4 Date 10/15/71 .30 2.50 2.65 2.00 2.15 1.95 1.65 .10 10/21/71 .05 . 45 2.80 2.90 2.90 2.30 2.15 1.70 10/28/71 0.0 . 30 3.20 3.50 3.50 3.25 2.70 2.50 11/4/71 .10 . 25 3.70 4.40 4.15 3.50 3.30 2.75 11/10/71 0.0 . 20 3.80 4.30 4.25 4.20 3.35 3.55 11/12/71 0.0 5.80 . 50 6.20 6.20 6.70 6.65 5.90 11/15/71 .10 5.25 5.55 . 30 6.10 6.60 6.90 5.90 11/18/71 0.0 .30 5.60 6.60 6.50 5.85 4.90 5.35 11/22/71 0.0 . 20 4.80 4.55 4.65 5.85 5.85 5.45 12/1/71 3.55 4.50 4.65 4.00 0.0 0.0 5.00 4.90 . 10 12/15/71 0.0 3.35 4.60 4.55 4.50 4.45 4.25 12/30/71 0.0 . 20 3.15 3.95 4.20 4.05 4.65 4.10 1/13/72 0.0 3.70 4.25 3.70 0.0 2.85 3.60 3.80 2/3/72 0.0 2.60 3.50 4.00 3.50 .10 3.20 3.60 2/24/72 .30 0.0 2.40 2.80 3.20 2.90 3.80 3.20 3/20/72 2.10 2.70 2.50 3.50 3.00 .30 0.0 2.50 5/4/72 . 10 2.00 2.50 3.50 2.90 .20 2.40 2.40 8/1/72 . 30 1.90 2.25 2.30 2.25 3.10 2.40 .30 9/6/72 . 40 2.00 2.25 3.25 2.60 .25 2.25 2.25 9/11/72 .35 2.00 2.30 2.45 2.35 2.65 .50 2.15

TABLE B-2

PORE WATER PRESSURES FOR THE MIDDLE SAND BLANKET

AND UPPER SLUDGE LAYER

		PORI	E PRES	SURE,	PSI			
PIEZOMETER	G5-5	G7-5	G5-6	G7-6	G5-7	G6-7	G7-7	G5-8
INITIAL EL. F	T 88. 1	88.3	91.3	91.4	93.9	93.8	94.0	95.5
Date								
10/21/71	.30	. 20						
10/28/71	.60	. 50						
11/4/71	. 70	. 75	1.20	1.00				
11/10/71	.80	1.05	2.10	2.45	1.20	. 85	2.35	. 95
11/12/71	1.30	1.35	4.60	4.80	4.20	4.00	4.40	2.80
11/15/71	1.10	1.20	3.90	3.95	3.50	3.50	3.75	2.25
11/18/71	1.20	1.25	3.55	3.45	3.10	3.10	3.30	2.00
11/22/71	1.15	1.25	3.00	2.90	2.65	2.65	2.80	1.70
12/1/71	1.00	1.10	2.30	2.10	2.10	2.10	2.10	1.20
12/6/71			2.30	2.20	1.95	1.95	2.00	1.15
12/15/71	1.15	1.15	2.80	2.25	1.80	1.80	1.80	1.50
12/30/71	1.05	1.10	2.41	2.30	1.45	1.45	1.50	1.30
1/13/72	1.20	1.10	2.50	2.20	1.50	1.35	1.50	1.10
2/3/72	1.20	1.10	2.20	2.00	1.50	1.00	1.50	. 90
2/24/72	1.30	1.00	2.20	2.00	1.50	1.00	1.90	
3/20/72	1.40	1.30	2.10	1.70	1.30	1.00	1.60	. 80
5/4/72	2.00	1.40	2.20	2.10	1.70	1.20	2.10	1.30
8/1/72	1.50	1.10	2.00	2.00	1.10	. 90	1.60	. 25
9/6/72	2.00	1.60	2.10	1.95	1.85*	. 90	1.60	.05
9/11/72	1.90	1.50	1.80	2.00	1.25	1.00	1.70	. 05

\*Drilling rig near here at time of reading.

TABLE C-1 TOTAL PRESSURE CELL DATA

TOTAL									<del></del>
PRESSURE CE INITIAL ELEV			loriz. .60	. G	7-2 V∈ 83.7			-3 Ver 33.48	·t.
Date	I*	W+	s#	Ī	W	S	I	W	S
10/15/71	9.0	4.3	5.0	7.7	3.0	3.5	8.1	3.5	4.1
10/21/71	9.5	4.9	5.7	8.2	3.6	4.1	8.3	3.7	4.2
10/28/71	10.8	6.0	6.9	10.1	5.2	6.1	9.2	4.5	5.2
11/4/71	11.8	7.0	8.1	10.2	5.2	6.1	9.8	5.0	6.0
11/10/71	13.9	9.1	10.5	12.8	8.2	9.3	11.1	6.3	7.2
11/12/71	16.3	11.7	13.2				13.3	8.6	9.8
11/15/71	16.5	11.9	13.4	13.1	8.5	9.7	13.1	8.5	9. 7
11/18/71	16.5	11.9	13.4	12.8	8.2	9.3	12.8	8.2	9.3
11/22/71	16.6	12.0	13.5	12.2	7.7	8.8	12.5	8.0	9. 1
12/1/71	16.9	12.2	13.7	12.7	8.1	9.2	12.0	7.3	8.6
12/15/71	17.2	12.7	14.2	13.9	9.1	10.5	11.4	6.9	7.9
12/30/71	17.7	13.0	14.6				11.1	6.3	7.2
1/13/72	17.8	13.1	14.7	15.0	10.2	11.8	10.7	6.1	7.1
2/3/72	18.0	13.2	15.1	15.8	Discor	tinued	10.5	6.0	7.0
2/24/72	17.9	13.2	14.9	15.9			10.3	5.8	6.8
3/20/72	18.0	13.2	15.1	16.3			10.3	5.8	6.8
5/4/72	18.0	13.2	15.1	16.6			10.2	5.5	6.5
8/1/72	17.3	12.7	14.2				9.5	4.9	5.8
9/6/72	17.3	12.7	14.2				9.7	5.1	6.0

NOTE: CELL G7-2 GAVE ERRATIC DATA (MALFUNCTIONED) AND THESE VALUES ARE AN AVERAGE OF FOUR DIFFERENT READINGS.

<sup>\*</sup> I - INSTRUMENT READING

<sup>+</sup> W - TOTAL PRESSURE, WATER CALIBRATION, Psi

<sup>#</sup> S - TOTAL PRESSURE, SAND CALIBRATION, Psi

TEMPERATURE DATA FOR PAPERMILL SLUDGE LANDFILL TABLE D-1

Thermistor no.	no.	-		2		3			u ,	
Elevation,	ft. 95.	5, 43	93.	. 43	91	91.43	89.43	.43	87.	. 43
Date	*		I	T	н	H	н	H	H	H
12/16/71	3.69	14.1	3.90	12.9	3.84	13.2	3.84	13.2	3.80	13.5
12/30/71	4.87		6.30	3.0	4.20	11.3	3.53	15.1	3.25	16.8
1/13/72	5.30		7.04	6.	4.75	& &	4.43	10.2	3.95	12.6
2/3/72	6.05		7.62	7	4.95	8.0	4.34	10.7	4.00	12.4
2/24/72	6.30		9.07	-4.0	5.44	6.0	4.85	8.4	4.43	10.2
3/20/72	5.45		8.78	-3.5	5.16	7.1	5.00	7.7	4.60	9.4
5/4/72	3.81		;	!	4.04	12.2	3.99	12.5	3.71	14.0
8/1/72	1.99		!	;	2.65	21.3	3.04	18.2	3.15	17.5
21/9/6	2.16		:	!	2.36	23.9	2.72	20,7	2.90	19.3

Thermistor no.	, no. 6			2		8		6		
Elevation,	ft. 85.4	33	83	83.43	81	81.43	79.	79.43	77	. 43
Date										
12/16/71	84			16.4	3.11	17.7		17.8	2.26	24.9
12/30/71	63			23.4	2.37	23.9		22, 7		20.3
1/13/72	53			19.0	2.67	21.2		21.6		20.0
2/3/72	50			17.4	2.84	19.7		20.4		19.5
2/24/72	3.95 1	12.6	3.47	15.4	3.05	18.5	2.88	19.7		19.1
3/20/72	31			14.9	3.20	17.2		18.3		18.5
5/4/72	38			16.5	3.23	17.0		17.3		17.4
8/1/72	21			17.3	3.20	17.2		16.9		15.8
8/6/72	10			17,8	3.19	17.2		16.7		15.4

\*I INSTRUMENT READING (K-OHMS)

+T TEMPERATURE (DEGREES CENTIGRADE)

TABLE E-1 UNDISTURBED VANE SHEAR STRENGTHS

					Ü	PPER :	SLUD	GE LA	YER	
Elev. below sludge top	N .	-2-1/	2 ft.		-5 ft	•		- 7	-1/2 ft.	Vane Size
Date	R*	M <sup>+</sup>	S#	R	M	S	R	M	S	
10/14/71	0	245	1.23	0	2 <b>4</b> 0	1.70	0	570	2.85	LARGE
10/14/71	0	300	1.50	0	485	2.43	0	620	3.10	LARGE
10/14/71	0	175	1.75	0	230	2.30	0	330	3.30	INTER.
10/14/71	0	190	1.90	0	200	2.00	0	360	3.60	INTER.
11/11/71	0	255	2.55	20	320	3.00	62	3 95	3.33	INTER.
11/11/71	0	100	2.00	20	150	3.00	60	265	4.60	SMALL
Elevation		-25 ir	1.		- 50	in.		-	-75 in.	
3/20/72	35	330	5.90	60	400	6.80	130	465	6.70	SMALL
3/20/72	45	320	5.50	140	380	4.80	185	480	5.90	SMALL

<sup>\*</sup>R ROD FRICTION READING

<sup>#</sup>S SHEAR STRENGTH, T/M<sup>2</sup>

	<del></del>					LOWER	SLUDGE LAYER	
Elev. belo		-2-1/	2 ft.		-5 ft	:•	-7-1/2 ft	•
11/11/71 11/11/71	170 155	480 360	3.10 4.10		670 545	4.50 5.90	TORQUE WREN CAPACITY EXCEEDED OFF SCALE	CH SMALL SMALL
Elevation		-2	5 in.		- 4	0 in.		
3/20/72	340	720	7.60	370	850	9.60		SMALL
3/20/72	560	~950	7.80	CAP	ACITY	EXCE	EDED	SMALL

<sup>&</sup>lt;sup>+</sup>M MAX. READING

TABLE E-2 REMOLDED VANE SHEAR STRENGTHS

				UF	PPER S	LUDG:	E LA	YER		
Elev. below sludge top	′ -2	-1/2 f	t.		<b>-</b> 5 ft	t.	- 7	-1/2 ft	•	Vane Size
Date	R*	M <sup>+</sup>	S#	R	M	S	R	M	S	
10/14/71	0	180	. 90	0	135	.68	0	340	1.70	LARGE
10/14/71	0	210	1.05	0	260	1.30	0	340	1.70	LARGE
10/14/71	0	110	1.10	0	130	1.30	0	190	1.90	INTER.
10/14/71	0	120	1.20	0	120	1.20	0	150	1.50	INTER.
11/11/71	0	135	1.35	20	160	1.40	62	240	1.78	INTER.
11/11/71	0	40	.80	20	70	1.00	55	150	1.90	SMALL
Elevation		-25 in			-50	in.		-75 ir	1.	
3/20/72	25	180	3.10	25	185	3.20	90	240	3.00	SMALL
3/20/72	30	155	2.50	80	230	3.00	130	280	3.00	SMALL

					LOW	ER SLU	DGE LAYER	
Elev. belo	_	2-1/2	ft.		-5 ft.		-7-1/2 ft.	
11/11/71	155	345	1.90	200	440	2.40	TORQUE WRENG CAPACITY	SMALL
11/11/71	140	280	2.80	205	330	2.50	EXCEEDED	SMALL
Elevation		-25 i	n.		-40 i	n.		
3/20/72	235	435	4.00					SMALL

<sup>\*</sup>R ROD FRICTION READING

<sup>&</sup>lt;sup>+</sup>M MAX. READING

<sup>#</sup>S SHEAR STRENGTH, T/M<sup>2</sup>

# 1 CONVENTIONAL CONSOLIDACION DATA

Studge -- 4 :, antial water content 250%, wt. dry specimen 26.5 gms. February 15, 1972

time	dial reading	time	dial reading	time	dial reading
nan.	$\frac{\text{in.} \times 10^4}{2}$	min.	in. $\times 10^4$	min.	in. x 10 <sup>4</sup>
load	kg/cm <sup>2</sup>	load l	kg/cm²	load 4	kg/cm <sup>2</sup>
0.00		0.00	0	0.00	0
0.25		0.10	120	0.10	115
0.50		0.25	185	0.25	180
1.00		0.50	250	0.50	255
2.25		1.00	340	1.00	355
4.00		2.25	475	2.25	525
6.25		4.00	5 75	4.00	660
9.00		6.25	640	6.25	760
12.25		9.00	6 75	9.00	845
16.00		12.25	705	12.25	873
20.25		16.00	720	16.00	903
25 <b>.00</b>		20.25	740	20.25	933
36.00		25.00	750	25.00	950
49.00		36.00	770	36.00	977
120.00		49.00	785	49.00	993
240.00		120.00	825	120.00	1043
580.00		240.00	856	240.00	1074
1440.00	1200	580.00	890	580.00	1103
		1440.00	930	1440.00	1137
load	kg/cm <sup>2</sup>	load 2	kg/cm <sup>2</sup>	load 8	kg/cm <sup>2</sup>
0.00	0	0.00	0	0.00	0
0.10	115	0.10	95	0.10	60
Ò.25	175	0.25	125	0.25	90
0.50	244	0.50	153	0.50	125
1.00	331	1.00	185	1.00	170
2.25	470	2.25	240	2.25	240
4.00	570	4.00	300	4.00	305
6.25	630	6.25	425	6.25	350
9.00	670	9.00	480	9.00	3 90
12.25	697	12.25	510	12.25	420
16.00	718	16.00	533	16.00	440
20.25	735	20.25	544	20.25	460
25.00	750	25.00	560	25.00	475
36.00	765	26.00	5 70	36.00	495
49.00	785	49.00	5 95	49.00	510
120.00	832	120.00	635	120.00	555
240.00	863	240.00	655	240.00	580
580.00	897	580.00	675	580.00	600
1440.00	937	1440.00	710	1440.00	640

Sludge U-3-1, initial water content 306%, wt. dry specimen 23.9 gms. February 28, 1972

time	dial reading	time	dial readin	ig time	dial reading	
min.	in. x 10		in. $\times 10^4$	min.	in. $\times 10^4$	
	1 kg/cm <sup>2</sup>		load .4 kg/cm <sup>2</sup>		load 1.6 kg/cm <sup>2</sup>	
0.00	0	0.00	0	0.00	0	
0.10	130	0.10	65	0.10	70	
0.25	175	0.25	105	0.25	110	
0.50	215	0.50	145	0.50	153	
1.00	<b>275</b>	1.00	210	1.00	210	
2.25	390	2.25	300	2.25	283	
4.00	505	4.00	373	4.00	337	
6.25	605	6.25	423	6.25	380	
9.00	690	9.00	460	9.00	409	
12.25	755	12.25	480	12.25	455	
16.00	805	16.00	495	16.00	483	
20.25	835	20.25	510	20.25	500	
25.00	855	25.00	515	25.00	512	
36.00	885	36.00	530	36.00	525	
49.00	905	49.00	540	49.00	537	
120.00	945	120.00	565	120.00	565	
240.00	965	240.00	590	240.00	583	
580.00	995	580.00	610	580.00	605	
1400.00	1025	1480.00	635	1450.00	635	
load .	2 kg/cm <sup>2</sup>	load .8	kg/cm <sup>2</sup>	load 3.	2 kg/cm <sup>2</sup>	
0.00	0	0.00	0	0.00	0	
0.10	50	0.10	70	0.10	95	
0.25	85	0.25	110	0.25	140	
0.50	120	0.50	155	0.50	192	
1.00	175	1.00	220	1.00	262	
2.25	260	2.25	320	2.25	360	
4.00	330	4.00	410	4.00	428	
6.25	380	6.25	465	6.25	475	
9.00	420	9.00	485	9.00	5 <b>07</b>	
12.00	450	12.25	495	12.25	325	
16.00	470	16.00	500	16.00	540	
20.25	490	20.25	5 <b>05</b>	20.25	550	
25.00	500	25.00	515	25.00	560	
36.00	520	36.00	520	36.00	570	
49.00	535	49.00	525	49.00	578	
120.00	575	120.00	545	120.00	603	
240.00	600	240.00	560	120.00	620	
580.00	630	580.00	570	580.00	640	
1460.00	665	1440.00	585	1410.00	660	

10ad .8 kg/cm<sup>2</sup>
720.00 190

TABLE F-3 CONVENTIONAL CONSOLIDATION DATA Sludge u-3-3, initial water content 271%, wt. dry specimen 24.7 gms.

March 11, 1972

time	dial reading	time	dial reading		dial reading
min.	in. x 10 <sup>4</sup>	min.	in. $\times 10^4$	min.	$\frac{10^4}{2}$
load	.l kg/cm²	load.	4 kg/cm <sup>2</sup>	load 1.6	kg/cm²
0.00	0	0.00	0	0.00	0
0.10	70	0.10	43	0.10	. 8 <b>7</b>
0.25	105	0.25	72	0.25	135
0.50	145	0.50	105	0.50	195
1.00	200	1.00	150	1.00	280
2.25	290	2.25	227	2.25	420
4.00	375	4.00	290	4.00	498
6.25	455	6.25	337	6.25	550
9.00	510	9.00	372	9.00	587
12.25		12.25	400	12.25	600
16.00		16.00	420	16.00	605
20.25		20.25	433	20.25	610
25.00		25.00	448	25.00	615
36.00		36.00	468	36.00	622
49.00		49.00		49.00	628
120.00		120.00		120.00	640
240.00		240.00		240.00	650
580.00		580.00		580.00	662
1580.00		1460.00		1480.00	682
load .	2 kg/cm <sup>2</sup>	load .	8 <b>k</b> g/cm <sup>2</sup>	load 3.2	kg/cm <sup>2</sup>
0.00	0	0.00		0.00	0
0.10	30	0.10		0.00	<b>7</b> 5
0.25	53	0.25	93	0.25	126
0.50	80	0.50	127	0.50	185
1.00	120	1.00	173	1.00	263
2.25	187	2.25	242	2.25	378
4.00	247	4.00	286	4.00	464
6.25	293	6.25	307	6.25	520
9.00	327	9.00	320	9.00	551
12.25	350	12.25	330	12.25	570
16.00	373	16.00	337	16.00	580 `
20.25		20.25		20.25	583
25.00		25.00	348	25.00	590
36.00	415	36.00	357	36.00	602
49.00	428	49.00	365	49.00	610
120.00	468	120.00	382	120.00	627
240.00		240.00		240.00	642
580.00		580.00		580.00	658
1470.00		1450.00		1430.00	683
				load .8 kg	$/cm^2$
			<del></del>	1044 00 10	
				1/1/1/1/1/1/1/1/1/1/1/1/1/1/1/1/1/1/1/	

1444.00 192

TABLE F-4 CONVENTIONAL CONSOLIDATION DATA
Sludge U-3-7, initial water content 299%, wt, dry specimen 23.0 gms.
March 27, 1972

time	dial reading	time	dial reading	time	dial reading
min.	in. x 10 <sup>4</sup>	min.	in. x 10 <sup>4</sup>	min.	in. x 10 <sup>4</sup>
load	.1 kg/cm <sup>2</sup>	load	$.4 \text{ kg/cm}^2$	load 1	.6 kg/cm <sup>2</sup>
0.00	0	0.00	0	0.00	0
0.10	125	0.10	40	0.10	90
0.25	5 170	0.25	63	0.25	145
0.50	220	0.50		0.50	213
1.00	300	1.00	133	1.00	292
2.25	5 440	2.25	200	2.25	410
4.00	585	4.00	262	4.00	475
6.25	730	6.25	340	6.25	516
9.00	850	9.00	383	9.00	547
12.29	945	12.25	401	12.25	575
16.00	0 1020	16.00	414	16.00	594
20.25	5 1075	20. 25	423	20.25	601
25.00	1110	25.00	430	25.00	610
36.00	1145.	36.00	440	36.00	622
49.00	)	49.00	448	49.00	
120.00	1215	120.00	460	120.00	637
240.00	1235	240.00	468	240.00	643
580.00	1270	580.00	478	580.00	655
1660.00	1310	1430.00	500	1450.00	660
load	.2 kg/cm <sup>2</sup>	load	.8 kg/cm <sup>2</sup>	load 3.	2 kg/cm <sup>2</sup>
0.00		0.00		0.00	0
0.10		0.10			
0.25		0.25		•	1
0.50		0.50			hit floor
1.00		1.00		incre	ment no good
2.25		2.25			
4.00		4.00			
6.25	5 283	6.25			
9.00	315	9.00			
12.25	335	12.25			
16.00		16.00			
20.25	368	20.25	351		
25.00		25.00			
36.00	400	36.00			
49.00	410	49.00			
120.00	440	120.00	389		
240.00	460	240.00	398		
580.00		580.00	406		
1460.00	498	1420.00	422	1530.00	600

TABLE F-5 CONVENTIONAL CONSOLIDATION DATA
Sludge U-3-8, initial water content 272%, wt. dry specimen 24.5 gms.
April 3, 1972

min.         in. x 104         min.         in. x 104         min.         in. x 104           load .1 kg/cm²         load 1.6 kg/cm²         load 1.6 kg/cm²           0.00         0         0.00         0         0.00         0           0.10         115         0.10         60         0.10         108           0.25         155         0.25         93         0.25         158           0.50         200         0.50         130         0.20         210           1.00         260         1.00         182         1.00         280           2.25         370         2.25         253         2.25         383           4.00         470         4.00         325         4.00         433           6.25         590         6.25         407         6.25         465           9.00         690         9.00         465         9.00         488           12.25         735         12.25         510         12.25         503           16.00         760         16.00         532         16.00         515           20.25         775         20.25         553         20.25         525	time	dial reading	time	dial reading	time	dial reading
load .1 kg/cm  2		in.x 104		in. x 10 <sup>-4</sup>	min.	in. $\times 10^4$
0.10 115 0.10 60 0.10 108 0.25 155 0.25 93 0.25 158 0.50 200 0.50 130 0.20 210 1.00 260 1.00 182 1.00 280 2.25 370 2.25 253 2.25 383 4.00 470 4.00 325 4.00 433 6.25 590 6.25 407 6.25 465 9.00 690 9.00 465 9.00 488 12.25 735 12.25 510 12.25 503 16.00 760 16.00 532 16.00 515 20.25 775 20.25 553 20.25 525 25.00 785 25.00 570 25.00 532 36.00 805 36.00 36.00 550 49.00 815 49.00 49.00 558 120.00 840 120.00 640 120.00 580 240.00 560 240.00 657 240.00 593 580.00 890 580.00 673 580.00 610 1465.00 925 1420.00 713 1440.00 630  10ad .2 kg/cm² load .8 kg/cm² load 3.2 kg/cm²  0.00 0 0 0.00 0 0.00 0 0.25 145 0.50 95 porous stone hung up 150.00 210 1.00 138 on ringreading of 1.00 295 2.25 290 9.00 315 9.00 673 20.25 570 9.00 315 9.00 600 12.25 333 12.25 570 9.00 345 12.25 570 9.00 345 12.25 570 9.00 345 12.25 570 9.00 345 12.25 570 9.00 368 25.00 673 12.25 125 125.00 637 20.25 570 9.00 315 9.00 673 580.00 610 12.25 250 5340 obtainednew 2.25 428 4.00 253 increment applied 4.00 515 6.25 290 9.00 315 9.00 600 12.25 358 20.25 648 25.00 368 25.00 677 49.00 397 49.00 678 120.00 480 120.00 705 240.00 453 5240.00 722 580.00 480 580.00 743	load	.1 $kg/cm^2$	load	$.4 \text{ kg/cm}^2$	load 1.	6 kg/cm <sup>2</sup>
0. 25	0.00	0 .	0.00	0	0.00	0
0.50 200 0.50 130 0.20 210 1.00 260 1.00 182 1.00 280 2.25 370 2.25 253 2.25 383 4.00 470 4.00 325 4.00 433 6.25 590 6.25 407 6.25 465 9.00 690 9.00 465 9.00 488 12.25 735 12.25 510 12.25 503 16.00 760 16.00 532 16.00 515 20.25 775 20.25 553 20.25 525 25.00 785 25.00 570 25.00 532 36.00 805 36.00 36.00 550 49.00 840 120.00 640 120.00 580 240.00 560 240.00 657 240.00 593 580.00 890 580.00 673 580.00 610 1465.00 925 1420.00 713 1440.00 630  10ad .2 kg/cm² load .8 kg/cm² load 3.2 kg/cm²  0.00 0 0 0.00 0 0.00 0 0.25 145 0.50 95 porous stone hung up 150.00 210 1.00 138 on ringreading of 1.00 295 2.25 290 340 obtainednew 2.25 428 4.00 253 increment applied 4.00 515 6.25 290 9.00 315 9.00 670 9.00 315 9.00 670 12.25 333 12.25 622 16.00 345 12.25 63 20.25 648 25.00 368 25.00 670 49.00 397 49.00 678 120.00 480 120.00 678 120.00 367 49.00 677 49.00 397 49.00 678 120.00 480 120.00 670 49.00 397 49.00 678 120.00 480 120.00 678 120.00 480 120.00 670 49.00 397 49.00 678 120.00 453 240.00 722 580.00 480 743	0.10	115	0.10	60	0.10	108
1.00 260 1.00 182 1.00 280 2.25 370 2.25 370 2.25 253 2.25 383 4.00 470 4.00 325 4.00 433 6.25 590 6.25 407 6.25 465 9.00 690 9.00 465 9.00 488 12.25 735 12.25 510 12.25 503 16.00 760 16.00 532 16.00 515 20.25 775 20.25 553 20.25 525 25.00 785 25.00 570 25.00 532 36.00 805 36.00 36.00 550 49.00 815 49.00 49.00 558 120.00 840 120.00 640 120.00 580 240.00 560 240.00 657 240.00 593 580.00 610 1465.00 925 1420.00 713 1440.00 630 1465.00 925 1420.00 713 1440.00 630 120.00 295 2.25 25 25 25 25 25 25 25 25 25 25 25 25 2	0.25	155	0.2	5 93	0.25	158
2. 25 370	0.50	200	0.50	130	0.20	210
4.00 470 4.00 325 4.00 433 6.25 590 6.25 407 6.25 465 9.00 690 9.00 465 9.00 488 12.25 735 12.25 510 12.25 503 16.00 760 16.00 532 16.00 515 20.25 775 20.25 553 20.25 525 25.00 785 25.00 570 25.00 532 36.00 805 36.00 36.00 550 49.00 815 49.00 49.00 558 120.00 840 120.00 640 120.00 580 240.00 560 240.00 657 240.00 593 580.00 890 580.00 673 580.00 610 1465.00 925 1420.00 713 1440.00 630  10ad .2 kg/cm² load .8 kg/cm² load 3.2 kg/cm²  0.00 0 0 0.00 0 0.00 0 0.00 0.10 40 0 0.10 43 0.25 63 0.25 145 0.50 95 porous stone hung up 150.00 210 1.00 138 on ringreading of 1.00 295 2.25 205 340 obtainednew 2.25 428 4.00 253 increment applied 4.00 515 6.25 290 6.25 570 9.00 315 9.00 600 12.25 333 12.25 622 16.00 345 16.00 670 49.00 397 49.00 678 120.00 430 120.00 775 240.00 678 120.00 430 120.00 775 240.00 453 250.00 772 580.00 480 580.00 773	1.00	260	1.00	182	1.00	280
6. 25 590 6. 25 407 6. 25 465 9. 00 690 9. 00 465 9. 00 488 12. 25 735 12. 25 510 12. 25 503 16. 00 760 16. 00 532 16. 00 515 20. 25 775 20. 25 553 20. 25 525 25. 00 785 25. 00 570 25. 00 532 36. 00 805 36. 00 36. 00 550 49. 00 815 49. 00 49. 00 815 49. 00 49. 00 580 240. 00 657 240. 00 593 580. 00 670 420. 00 670 49. 00 890 580. 00 673 580. 00 610 1465. 00 925 1420. 00 713 1440. 00 630 1440. 00 630 120. 00 630 120. 00 630 120. 00 600 120. 00 600 120. 00 600 120. 00 600 120. 00 600 120. 00 630 120. 00 630 120. 00 630 120. 00 630 150 140. 00 630 150 140. 00 630 150 140. 00 630 150 140. 00 630 150 140. 00 630 150 140. 00 630 150 150 150 150 150 150 150 150 150 15	2.25	370	2.2	5 253	2.25	383
9.00 690 9.00 465 9.00 488  12.25 735 12.25 510 12.25 503  16.00 760 16.00 532 16.00 515  20.25 775 20.25 553 20.25 525  25.00 785 25.00 570 25.00 532  36.00 805 36.00 36.00 550  49.00 815 49.00 49.00 558  120.00 840 120.00 640 120.00 580  240.00 560 240.00 657 240.00 593  580.00 890 580.00 673 580.00 610  1465.00 925 1420.00 713 1440.00 630     load .2 kg/cm  2	4.00	470	4.00	325	4.00	433
12. 25	6.25	5 90	6.2	5 407	6.25	465
16.00       760       16.00       532       16.00       515         20.25       775       20.25       553       20.25       525         25.00       785       25.00       570       25.00       532         36.00       805       36.00        36.00       550         49.00       815       49.00        49.00       558         120.00       840       120.00       640       120.00       580         240.00       560       240.00       657       240.00       593         580.00       890       580.00       673       580.00       610         1465.00       925       1420.00       713       1440.00       630         10ad .2 kg/cm²         0.00       0       0.00       0       0.00       0         0.10       40       0.10       43       0.25       145         0.50       95       porous stone hung up       150.00       210         1.00       138       on ringreading of       1.00       295         2.25       205       340 obtainednew       2.25       428         4.00       253	9.00	690	9.00	O 465	9.00	488
20. 25	12.25	735	12.2	5 510	12.25	503
25.00 785	16.00	760	16.00	532	16.00	515
36.00 805 36.00 36.00 550 49.00 815 49.00 49.00 558 120.00 840 120.00 640 120.00 580 240.00 560 240.00 657 240.00 593 580.00 890 580.00 673 580.00 610 1465.00 925 1420.00 713 1440.00 630     load .2 kg/cm²	. 20. 25	775	20. 2	5 553	20.25	525
49.00       815       49.00        49.00       558         120.00       840       120.00       640       120.00       580         240.00       560       240.00       657       240.00       593         580.00       890       580.00       673       580.00       610         1465.00       925       1420.00       713       1440.00       630         load .2 kg/cm²         0.00       0       0.00       0       0.00       0         0.10       40       0.10       43       0.25       145         0.50       95       porous stone hung up       150.00       210         1.00       138       on ringreading of       1.00       295         2.25       205       340 obtainednew       2.25       428         4.00       253       increment applied       4.00       515         6.25       290       6.25       570         9.00       315       9.00       600         12.25       333       12.25       622         16.00       345       16.00       637         20.25       358       25.00       6	25.00	785	25.00	570	25.00	532
120.00       840       120.00       640       120.00       580         240.00       560       240.00       657       240.00       593         580.00       890       580.00       673       580.00       610         1465.00       925       1420.00       713       1440.00       630         load .2 kg/cm²         0.00       0       0.00       0       0.00       0         0.10       40       0.10       43       0.25       145         0.50       95       porous stone hung up       150.00       210         1.00       138       on ringreading of       1.00       295         2.25       205       340 obtainednew       2.25       428         4.00       253       increment applied       4.00       515         6.25       290       6.25       570         9.00       315       9.00       600         12.25       622       16.00       637         20.25       358       20.25       648         25.00       368       25.00       657         36.00       325       36.00       670         49.	36.00	805	36.00	)	36.00	550
240.00 560 240.00 657 240.00 593 580.00 610 1465.00 925 1420.00 713 1440.00 630      load .2 kg/cm 2	49.00	815	49.00	)	49.00	558
240.00 560 240.00 657 240.00 593 580.00 610 1465.00 925 1420.00 713 1440.00 630      load .2 kg/cm 2						
580.00       890       580.00       673       580.00       610         1465.00       925       1420.00       713       1440.00       630         load .2 kg/cm²       load .8 kg/cm²       load 3.2 kg/cm²         0.00       0       0.00       0       0.00       0         0.10       40       0.10       43       43       43         0.25       63       0.25       145       0       25       145       0       25       145       0       25       145       0       25       145       0       25       145       0       25       145       0       25       145       0       25       145       0       25       145       0       20       25       145       0       295       20       25       145       0       295       225       225       226       25       2428       225       2428       225       2428       248       240       25       2428       240       25       570       9       9       9       00       600       25       570       9       9       00       600       25       570       9       9 <td>240.00</td> <td>560</td> <td></td> <td></td> <td></td> <td></td>	240.00	560				
1465.00       925       1420.00       713       1440.00       630         load .2 kg/cm²         0.00       0       0.00       0       0.00       0         0.10       40       0.10       43         0.25       63       0.25       145         0.50       95       porous stone hung up       150.00       210         1.00       138       on ringreading of       1.00       295         2.25       205       340 obtainednew       2.25       428         4.00       253       increment applied       4.00       515         6.25       290       6.25       570         9.00       315       9.00       600         12.25       333       12.25       622         16.00       345       16.00       637         20.25       358       20.25       648         25.00       368       25.00       657         36.00       325       36.00       670         49.00       49.00       678         120.00       705         240.00       453       240.00 <t< td=""><td>580.00</td><td>890</td><td>580.00</td><td></td><td>580.00</td><td></td></t<>	580.00	890	580.00		580.00	
0.00       0       0.00       0       0.00       0         0.10       40       0.10       43         0.25       63       0.25       145         0.50       95       porous stone hung up 150.00       210         1.00       138       on ringreading of 1.00       295         2.25       205       340 obtainednew 2.25       428         4.00       253       increment applied 4.00       515         6.25       290       6.25       570         9.00       315       9.00       600         12.25       333       12.25       622         16.00       345       16.00       637         20.25       358       20.25       648         25.00       368       25.00       657         36.00       325       36.00       670         49.00       397       49.00       678         120.00       430       120.00       705         240.00       453       240.00       722         580.00       480       580.00       743	1465.00	925				
0.00       0       0.00       0       0.00       0         0.10       40       0.10       43         0.25       63       0.25       145         0.50       95       porous stone hung up 150.00       210         1.00       138       on ringreading of 1.00       295         2.25       205       340 obtainednew 2.25       428         4.00       253       increment applied 4.00       515         6.25       290       6.25       570         9.00       315       9.00       600         12.25       333       12.25       622         16.00       345       16.00       637         20.25       358       20.25       648         25.00       368       25.00       657         36.00       325       36.00       670         49.00       397       49.00       678         120.00       430       120.00       705         240.00       453       240.00       722         580.00       480       580.00       743						
0.00       0       0.00       0       0.00       0         0.10       40       0.10       43         0.25       63       0.25       145         0.50       95       porous stone hung up 150.00       210         1.00       138       on ringreading of 1.00       295         2.25       205       340 obtainednew 2.25       428         4.00       253       increment applied 4.00       515         6.25       290       6.25       570         9.00       315       9.00       600         12.25       333       12.25       622         16.00       345       16.00       637         20.25       358       20.25       648         25.00       368       25.00       657         36.00       325       36.00       670         49.00       397       49.00       678         120.00       430       120.00       705         240.00       453       240.00       722         580.00       480       580.00       743	load	$.2 \text{ kg/cm}^2$	load	.8 kg/cm <sup>2</sup>	load 3.	$2 \text{ kg/cm}^2$
0.10       40         0.25       63         0.50       95         porous stone hung up       150.00         1.00       138         on ringreading of       1.00         2.25       205         340 obtainednew       2.25         4.00       253         increment applied       4.00         515         6.25       290         9.00       600         12.25       333         12.25       622         16.00       345         20.25       358         25.00       657         36.00       325         49.00       397         49.00       430         240.00       705         240.00       722         580.00       480					0.00	0
0. 25       63       0. 25       145         0. 50       95       porous stone hung up       150.00       210         1. 00       138       on ringreading of       1. 00       295         2. 25       205       340 obtainednew       2. 25       428         4. 00       253       increment applied       4. 00       515         6. 25       290       6. 25       570         9. 00       315       9. 00       600         12. 25       333       12. 25       622         16. 00       345       16. 00       637         20. 25       358       20. 25       648         25. 00       368       25. 00       657         36. 00       325       36. 00       670         49. 00       397       49. 00       678         120. 00       453       240. 00       722         580. 00       480       580. 00       743			·		0.10	43
0.50       95       porous stone hung up       150.00       210         1.00       138       on ringreading of       1.00       295         2.25       205       340 obtainednew       2.25       428         4.00       253       increment applied       4.00       515         6.25       290       6.25       570         9.00       315       9.00       600         12.25       333       12.25       622         16.00       345       16.00       637         20.25       358       20.25       648         25.00       368       25.00       657         36.00       325       36.00       670         49.00       397       49.00       678         120.00       430       120.00       705         240.00       453       240.00       722         580.00       480       580.00       743			•		0.25	145
1.00       138       on ringreading of       1.00       295         2.25       205       340 obtainednew       2.25       428         4.00       253       increment applied       4.00       515         6.25       290       6.25       570         9.00       315       9.00       600         12.25       333       12.25       622         16.00       345       16.00       637         20.25       358       20.25       648         25.00       36.00       657         36.00       325       36.00       670         49.00       397       49.00       678         120.00       430       120.00       705         240.00       453       240.00       722         580.00       480       580.00       743			poro	us stone hung up	150.00	210
2. 25       205       340 obtainednew       2. 25       428         4. 00       253       increment applied       4. 00       515         6. 25       290       6. 25       570         9. 00       315       9. 00       600         12. 25       333       12. 25       622         16. 00       345       16. 00       637         20. 25       358       20. 25       648         25. 00       368       25. 00       657         36. 00       325       36. 00       670         49. 00       397       49. 00       678         120. 00       430       120. 00       705         240. 00       453       240. 00       722         580. 00       480       580. 00       743					1.00	295
4.00       253       increment applied       4.00       515         6.25       290       6.25       570         9.00       315       9.00       600         12.25       333       12.25       622         16.00       345       16.00       637         20.25       358       20.25       648         25.00       368       25.00       657         36.00       325       36.00       670         49.00       397       49.00       678         120.00       430       120.00       705         240.00       453       240.00       722         580.00       480       580.00       743					2.25	428
6. 25       290       6. 25       570         9. 00       315       9. 00       600         12. 25       333       12. 25       622         16. 00       345       16. 00       637         20. 25       358       20. 25       648         25. 00       368       25. 00       657         36. 00       325       36. 00       670         49. 00       397       49. 00       678         120. 00       430       120. 00       705         240. 00       453       240. 00       722         580. 00       480       580. 00       743			incr	ement applied	4.00	515
9.00       315       9.00       600         12.25       333       12.25       622         16.00       345       16.00       637         20.25       358       20.25       648         25.00       368       25.00       657         36.00       325       36.00       670         49.00       397       49.00       678         120.00       430       120.00       705         240.00       453       240.00       722         580.00       480       580.00       743		290			6.25	570
12. 25       333       12. 25       622         16. 00       345       16. 00       637         20. 25       358       20. 25       648         25. 00       368       25. 00       657         36. 00       325       36. 00       670         49. 00       397       49. 00       678         120. 00       430       120. 00       705         240. 00       453       240. 00       722         580. 00       480       580. 00       743					9.00	600
16.00       345       16.00       637         20.25       358       20.25       648         25.00       368       25.00       657         36.00       325       36.00       670         49.00       397       49.00       678         120.00       430       120.00       705         240.00       453       240.00       722         580.00       480       580.00       743					12.25	622
20. 25       358       20. 25       648         25. 00       368       25. 00       657         36. 00       325       36. 00       670         49. 00       397       49. 00       678         120. 00       430       120. 00       705         240. 00       453       240. 00       722         580. 00       480       580. 00       743		345			16.00	637
36.00       325       36.00       670         49.00       397       49.00       678         120.00       430       120.00       705         240.00       453       240.00       722         580.00       480       580.00       743					20.25	648
49.00       397       49.00       678         120.00       430       120.00       705         240.00       453       240.00       722         580.00       480       580.00       743					25.00	657
49.00       397       49.00       678         120.00       430       120.00       705         240.00       453       240.00       722         580.00       480       580.00       743					36.00	670
120.00       430       120.00       705         240.00       453       240.00       722         580.00       480       580.00       743					49.00	678
240.00       453       240.00       722         580.00       480       580.00       743	120.00			•	120.00	<b>70</b> 5
580.00 480 580.00 743					240.00	722
1430.00 518 1425.00 770	580.00	480			580.00	743
	1430.00	518			1425.00	770

TABLE F-6 CONVENTIONAL CONSOLIDATION DATA
Sludge U-3-9, initial water content 313%, wt. dry specimen 22.0 gras.
April 9, 1972

time	dial reading	time	dial reading	time	dial reading
min.	in. x 10 <sup>4</sup>	min.	in. x 10 <sup>4</sup>	min.	in. x 10 <sup>4</sup>
load	$.1 \text{ kg/cm}^2$	load .	$4 \text{ kg/cm}^2$	load 1	$.6 \text{ kg/cm}^2$
0.00	0	0.00	0	0.00	0
0.10	90	0.10	53	0.10	115
0.25	130	0.25	77	0.25	158
0.50	1 75	0.50	108	0.50	208
1.00	240	1.00	150	1.00	275
2.25	355	2.25	215	2.25	378
4.00	505	4.00	270	4.00	465
6.25	660	6.25	320	6.25	512
9.00	795	9.00	405	9.00	532
12.25	925	12.25	472	12.25	550
16.00	1035	16.00	518	16.00	565
20.25	1125	20.25	550	20.25	580
25.00	1185	25.00	580	25.00	590
36.00	1255	36.00	610	36.00	602
49.00	1295	49.00	625	49.00	610
120.00	1365	120.00	655	120.00	632
240.00	1405	240.00	690	240.00	645
580.00	1435	580.00	715	580.00	660
1495.00	1495	1450.00	748	1430.00	682
load .	2 kg/cm <sup>2</sup>	load .8 kg/cm $^2$		load 3.	$2 \text{ kg/cm}^2$
0.00	0	0.00	0	0.00	0
0.10	30	0.10	62	0.10	85
0.25	50	0.25	90	0.25	130
0.50	73	0.50	115	0.50	182
1.00	110	1.00	148	1.00	260
2.25	175	2.25	180	2.25	390
4.00	230	4.00	200	4.00	505
6.25	280	6.25	215	6.25	590
9.00	315	9.00	225	9.00	635
12.25	350	12.25	237	12.25	662
16.00	380	16.00	243	16.00	682
20.25	400	20.25	252	20.25	695
25.00	415	25.00	258	25.00	705
36.00	440	36.00	270	36.00	720
49.00	460	49.00	275	49.00	730
120.00	495	120.00	292	120.00	755
240.00	520	240.00	305	240.00	770
580.00	550	580.00	315	580.00	782
1460.00	5 95	1440.00	333	1480.00	802

TABLE F-7 CONVENTIONAL CONSOLIDATION DATA

Sludge L-2-1 bag 1, initial water content 256%, wt. dry specimen 26.2

April 18, 1972 gms.

time	dial reading	time	dial reading	time	dial reading
min.	in. x 10 <sup>4</sup>	min.	in. x 10 <sup>4</sup>	min.	in. $\times 10^4$
load	.1 $kg/cm^2$	load .	$4 \text{ kg/cm}^2$	load 1.	6 kg/cm <sup>2</sup>
0.00	0	0.00	0	0.00	0
0.10	120	0.10	45	0.10	60
0.25	170	0.25	75	0.25	90
0.50	215	0.50	110	0.50	128
1.00	280	1.00	155	1.00	180
. 2.25	5 90	2.25	230	2.25	255
4.00	510	4.00	293	4.00	315
6.25	630	6.25	335	6.25	355
9.00	730	9.00	370	9.00	382
12.25	820	12.25	395	12.25	400
16.00	895	16.00	412	16.00	410
20.25	945	20.25	430	20.25	420
25.00	985	25.00	443	25.00	430
36.00	1030	36.00	465	36.00	445
49.00	1055	49.00	475	49.00	455
120.00	1105	120.00	515	120.00	480
240.00	1140	240.00	535	240.00	500
580.00	1170	580.00	557	580.00	518
1430.00	1210	1470.00	645	· 1480	540
load	$.2 \text{ kg/cm}^2$	load .	$8 \text{ kg/cm}^2$	load 3.	$2 \text{ kg/cm}^2$
0.00	0	0.00	0	0.00	0
0.10	43	0.10	60	0.10	75
0.25	70	0.25	93	0.25	115.
0.50	100	0.50	133	0.50	162
1.00	140	1.00	188	1.00	230
2.25	210	2.25	275	2.25	330
4.00	265	4.00	350	4.00	395
6.25	312	6.25	443	6.25	440
9.00	352	9.00	493	9.00	470
12.25	383	12.25	515	12.25	495
16.00	405	14.00	535	16.00	512
20.35	422	20.25	545	20.25	525
25.00	440	25.00	553	25.00	530
36.00	458	36.00	563	36.00	545
49.00	472	49.00		49.00	552
120.00	515	120.00	572	120.00	572
240.00	540	240.00	578	240.00	590
580.00	570	580.00		580.00	608
1450.00	5 95	1530.00	600	1445.00	620

TABLE F-8 BISHOP CONSOLIDATION DATA
Sludge U-3-10, initial water content 283%, wt. dry specimen 18.1 gms.
April 29, 1972

time min.	dial reading in. x 10 <sup>4</sup>	time min.	dial reading in. x 10 <sup>4</sup>	time min.	dial reading in. x 10 <sup>4</sup>
	.1 kg/cm <sup>2</sup>		$.4 \text{ kg/cm}^2$		1.6 kg/cm <sup>2</sup>
0.00	0	0.00	0	0.00	0
0.10	220	0.10	55	0.10	65
0.25	270	0.25	80	0.25	95
0.50	330	0.50	110	0.50	132
1.00	420	1.00	155	1.00	182
2.25	560	2.25	225	2.25	255
4.00	670	4.00	275	4.00	315
6.25	745	6.25	315	6.25	365
9.00	800	9.00	345	9.00	395
12.25	840	12.25	365	12.25	420
16.00	860	16.00	385	16.00	442
20.25	875	20.25	400	20. 25	458
25.00	885	25.00	410	25.00	470
36.00	905	36.00	435	36.00	490
49.00	920	49.00	450	49.00	505
120.00	9 <b>50</b>	120.00	495	120.00	545
240.00	975	240.00	525	240.00	570
580.00	1010	580.00	565	580.00	600
1440.00	1045	1460.00	600	1420.00	630
load	. 2 kg/cm <sup>2</sup>	load	.8 kg/cm <sup>2</sup>	load	3.2 kg/cm <sup>2</sup>
0.00	0	0.00	0	0.00	0
0.10	45	0.10	60	0.10	55
0.25	70	0.25	95	0.25	85
0.50	100	0.50	130	0.50	120
1.00	135	1.00	180	1.00	165
2.25	195	2.25	258	2.25	232
4.00	235	4.00	318	4.00	288
6.25	270	6.25	365	6.25	332
9.00	295	9.00	402	9.00	362
12.25	315	12.25	430	12.25	388
16.00	330	16.00	450	16.00	405
20.25	345	20.25	468	20.25	420
25.00	355	25.00	480	25.00	430
36.00	370	36.00	502	36.00	450
49.00	385	49.00	520	49.00	465
120.00	425	120.00	560	120.00	505
242.00	460	240.00	590	240.00	528
580.00	500	580.00	625	580.00	548
1415.00	535	1450.00	660	1440.00	575

TABLE F-9 BISHOP CONSOLIDATION DATA
Sludge U-3-12, initial water content 278%, wt. dry specimen 18.7 gms.
May 16, 1972

time	dial reading	time	dial reading	time	dial reading
min.	in. x 10 <sup>4</sup>	min.	in. $\times 10^4$	min.	in. x 10 <sup>4</sup>
lo	$pad.1 kg/cm^2$	load	$.4 \text{ kg/cm}^2$	load 1.	6 kg/cm <sup>2</sup>
0.0	0 0	0.00	0	0.00	0
0.1	0 130	0.10	40	0.10	62
0.2	5 190	0.25	62	0.25	93
0.5	0 262	0.50	90	0.50	130
1.0	0 365	1.00	130	1.00	178
2.2	5 540	2.25	193	2.25	252
4.0	0 675	4.00	240	4.00	312
6.2	5 775	6.25	275	6.25	355
9.0	0 835	9.00	298	9.00	390
12.2	5 870	12.25	320	12.25	412
16.0	0 890	16.00	338	16.00	433
20.2	5 910	20.25	355	20.25	450
25.0	0 920	25.00	36 <b>2</b>	25.00	462
36.0	0 945	36.00	385	36.00	483
49.0		49.00	405	49.00	495
120.0	0 980	120.00	440	120.00	535
240.0	0 1005	240.00	472	240.00	562
580.0	0 1040	580.00	515	580.00	590
1440.0	0 1070	1470.00	560	1490.00	622
10	pad . $2 \text{ kg/cm}^2$	load	$.8 \text{ kg/cm}^2$	load 3	$.2 \text{ kg/cm}^2$
0.0		0.00	0	0.00	0
0.1	0 35	0.10	555	0.10	55
0.2	5 55	0.25	90	0.25	85
0.5	0 78	0.50	123	0.50	115
1.0	0 110	1.00	175	1.00	162
2.2		2. 25		2.25	230
4.0		4.00		4.00	280
6.2	5 225	6.25	<b>35</b> 5	6.25	328
9.0		9.00		9.00	355
12.2	5 262	12.25	412	12.25	380
16.0	0 275	16.00	532	16.00	400
20.2	5 285	20.25	448	20.25	412
25.0	0 295	25.00	<b>4</b> 6 2	25.00	428
36.0	0 313	36.00	482	36.00	448
49.0	0 325	49.00	495	49.00	458
120.0	0 358	120.00	540	120.00	493
240.0		240.00	572	240.00	518
580.0	0 412	580.00	608	580.00	540
1440.0	0 450	1440.00	640	1480.00	570

TABLE F-10 BISHOP CONSOLIDATION DATA

Sludge L-2-2 bag 1, initial water content 274%, wt. dry specimen 19.0 may 24, 1972 gms.

time	dial reading	time	dial reading	time	dial reading
min.	in. x 10 <sup>4</sup>	min.	in. x 10 <sup>4</sup>	min.	in. $\times 10^4$
load	.1 kg/cm <sup>2</sup>	load	$.4 \text{ kg/cm}^2$	load 1	.6 kg/cm <sup>2</sup>
0.00	0	0.00	0	0.00	0
0.10	1 95	0.10	38	0.10	60
0.25	265	0.25	62	0.25	90
0.50	340	0.50	88	0.50	125
1.00	445	1.00	125	1.00	175
2.25	625	2.25	187	2.25	243
4.00	800	4.00	235	4.00	300
6.25	945	6.25	272	6.25	338
9.00	1050	9.00		9.00	370
12.25	1110	12.25	320	12.25	395
16.00	1150	16.00	340	16.00	405
20.25	1175	20.25		20.25	421
25.00	1190	25.00		25.00	432
36.00	1210	36.00	385	36.00	458
49.00	1220	49.00	400	49.00	468
120.00	1255	120.00	940	120.00	505
240.00	1270	240.00	470	240.00	528
580.00	1290	580.00		58 <b>0.00</b>	550
1440.00		1440.00	535	1530.00	580
load .	$2 \text{ kg/cm}^2$	load	$.8 \text{ kg/cm}^2$	load 3.	$2 \text{ kg/cm}^2$
0.00	0	0.00		0.00	0
0.10	25	0.10	62	0.10	60
0.25	45	0.25	90	0.25	90
0.50	63	0.50	123	0.50	122
1.00	90	1.00	170	1.00	167
2.25	135	2. 25	240	2.25	234
4.00	175	4.00	298	4.00	285
6.25	205	6.25	342	6.25	327
9.00	225	9.00	372	9.00	353
12.25	242	12.25		12.25	373
16.00	255	16.00	418	16.00	390
20.25	263	20.25	432	20.25	400
25.00	273	25.00	448	25.00	412
36.00	285	36.00	470	36.00	435
49.00	300	49.00	485	49.00	450
120.00	330	120.00	522	120.00	478
240.00	355	240.00	550	240.00	498
580.00	383	580.00		580.00	520
1440.00	420	1440.00	610	1510.00	545

TABLE F-11 BISHOP CONSOLIDATION DATA

Sludge L-2-3 bag 1, initial water content 263%, wt. dry speciment19.4 June 5, 1972 gms.

time min.	dial reading in. x 10 <sup>4</sup>	time min.	dial reading in. x 10 <sup>4</sup>	time min.	dial reading in. x 10 <sup>4</sup>
	.1 kg/cm <sup>2</sup>		4 kg/cm <sup>2</sup>		kg/cm <sup>2</sup>
0.00	0	0.00	0	0.00	0
0.10	140	0.10	45	0.10	64
0.25	203	0.25	70	0.25	92
0.50	232	0.50	98	0.50	123
1.00	372	1.00	136	1.00	170
2.25	545	2.25	198	2.25	238
4.00	6 95	4.00	244	4.00	292
6.25	818	6.25	280	6.25	337
9.00	8 90	9.00		9.00	363
12.25	940	12.25		12.25	390
16.00	970	16.00		16.00	406
20.25	990	20.25		20.25	420
25.00	1042	25.00		25.00	430
36.00	1020	36.00	385	36.00	453
49.00	1032	49.00		49.00	480
120.00	1058	120.00	433	120.00	503
240.00	1075	240.00	463	240.00	525
580.00	1095	580.00	492	580.00	548
1440.00	1125	1400.00	522	1490.00	580
load	.2 kg/cm <sup>2</sup>	load	$8 \text{ kg/cm}^2$	load 3.2	kg cm <sup>2</sup>
0.00	0	0.00	0	0.00	0
0.10	30	0.10		0.10	60
0.25	45	0.25		0.25	85
0.50	63	0.50		0.50	116
1.00	90	1.00		1.00	160
2.25	133	2. 25		2. 25	225
4.00	165	4.00		4.00	280
6.25	190	6. 25		6.25	320
9.00	208	9.00		9.00	348
12.25	222	12.25	400	12.25	370
16.00	233	16.00		16.00	391
20.25	243	20. 25		20. 25	405
25.00	251	25.00		25.00	4.8
36.00	270	36.00		36.00	435
49.00	278	49.00		49.00	468
120.00	308	120.00		120.00	485
240.00	328	240.00		240.00	507
580.00	358	580.00		580.00	534
1460.00	390	1570.00		1270.00	560

TABLE F-12 BISHOP CONSOLIDATION DATA
Sludge U-5-2, initial water content 263%, wt. dry specimen 19.6 gms.
June 19, 1972

time	dial reading	time	dial reading	time	dial reading
min.	in. x 10 <sup>4</sup>	min.	in. x 10 <sup>4</sup>	min.	in. x 10 '
load	.1 kg/cm <sup>2</sup>	load	$.4 \text{ kg/cm}^2$	load 1.6	kg/cm <sup>2</sup>
0.00	0	0.00	0	0.00	0
0.10	89	0.10	50	0.10	65
0.25	5 150	0.25	75	0.25	100
0.50	210	0.50	105	0.50	135
1.00	290	1.00	150	1.00	187
2.25	420	2.25		2.25	265
4.00	527	4.00	265	4.00	325
6.25	5 5 95	6.25	303	6.25	377
9.00	630	9.00	330	9.00	413
12.25	660	12.25	350	12.25	442
16.00	678	16.00	366	16.00	463
20.25	6 90	20.25	382	20.25	480
25.00	700	25.00	393	25.00	495
36.00	715	36.00	418	36.00	520
49.00	725	49.00	428	49.00	535
120.00	753	120.00	473	120.00	<b>57</b> 5
240.00	773	240.00	502	240.00	600
580.00	798	580.00	538	580.00	633
1440.00	830	1430.00	580	1470.00	670
	2		2		. , 2
	l .2 kg/cm <sup>2</sup>		.8 kg/cm <sup>2</sup>		kg/cm <sup>2</sup>
0.00		0.00		0.00	0
0.10		0.10		1095.00	67
0.25		0.25			
0.50		0.50			
1.00		1.00		load . 1 k	g/cm <sup>2</sup>
2.25		2. 25			<del></del>
4.00		4.00			•
6.25		6.25		0.00	0
9.00		9.00		245.00	377
12.25		12.25			
16.00		16.00			
20.25		20.25			
25.00		25.00			
36.00		36.00			
49.00		49.00			
120.00		120.00			
240.00		240.00			
580.00		580.00			
1430.00	435	1470.00	670		

TABLE F-13 SINGLE INCRUMENT CONSOLIDATION DATA

Sludge U-3-4
initial water content 302%
initial void ratio 5.64
wt dry specimen 23.1 gm

Sludge U-3-6 initial water content? initial void ratio 5.48 wt. dry specimen 23.7 gms.

wt. dry spe	Cliffell 23.1 gills.	wt. dry spec	current 25. 7 gills.
load 0 24	$kg/cm^2$ 3/23/72	load 024 k	$g/cm^2$ $3/25/72$
time	dial reading	time	dial reading
min.	in. x 10 <sup>4</sup>	min.	in. x 10 <sup>4</sup>
0.00	0	0.00	0
0.10	1 90	0.10	220
0.25	273	0.25	330
0.50	378	0.50	455
1.00	5 2 0	1.00	630
2. 25	776	2.25	930
4.00	1018	4.00	1185
6.25	1200	6.25	1358
9.00	1328	9.00	1470
12.25	1397	12.25	1520
16.00	1448	16.00	1550
20.25	1472	20.25	1570
25.00	1490	25.00	1585
36.00	1510	36.00	1605
49.00	1518	49.00	1620
120.00	1540	120.00	1648
240.00	1558	240.00	1678
580.00	1570	580.00	1705
1312.00	1597	1440.00	1745

Sludge U-3-5
initial water content 291%
initial void ratio 5.40
wt. dry specimen 24.0 gms.

load 024	$kg/cm^2$	3/24/72
0.00	0	
0.10	265	
0.25	380	
0.50	500	
1.00	680	
2.25	993	
4.00	1258	
6.25	1448	
9.00	1550	
12.25	1610	
16.00	1640	
20.25	1660	
25.00	1673	
36.00	1705	
49.00	1710	
120.00	1737	
240.00	1755	
580.00	1783	
1450.00	1805	

~			1		1																			
SINGLE INCREMENT BISHOP CONSOLIDATION DATA  3 Sludge L-2-4  tent 246% initial water content 266%	2-4 content 266%	oid ratio 5,46 specimen 19,3 ams.	7/26/7	dial re	in. $\times 10^4$	0	350	490	670	930	1370	1750	2000	2160	2250	2295	2320	2340	2360	2380	2415	2440	2470	2510
	Sludge L initial water	initial void ratio 5 wt. dry specimen	0	time	min.	0.00		0.25			2.25		6.25		12.25	16.00	20.25	25.00	36.00	49.00	120.00	240.00	580.00	1510.00
	TABLE F-14 SINGLE INCREN Sludge U-4-3 initial water content $246\%$ initial void ratio 4.43 wt. dry specimen 20.7 gms.	72 2	dial r	in. x 104	0	200	290	3 90	530	755	940	1065	1135	1180	1208	1230	1245	9	1277	1324	1340	1380	1425	
TABLE F-14 SING Sludge U-4-3 initial water content 2 initial void ratio 4.43	initial void	load 0 24	time	min.	00.00	0.10	0.25	0.50	1.00	2.25	4.00	6.25	9.00	12.25	16.00	20.25	25.00	36.00	49.00	120.00	240.00	580.00	1630.00	

TABLE F-14.--continued

	ent	lal void ratio 5.25	wt. dry specimen 18.4 gms.	load 024 kg/cm <sup>2</sup> $5/8/72$	00		25	<b>1.00</b> 690	. 25	1	25 1	00	1	00	25 1	00	00	49.00 1565	20.00	40.00	. 00	. 00	2520.00 1715	.00	00 17	0	
Sludge U-2-1	initial water content 210%	nal void ratio 4.	wt. dry specimen 23, 1 gms.	load 024 kg/cm <sup>2</sup> $\tau/11/72$	00.	10	25		25	00	6.25 1060	00	25 1	00 11	25 1	00 12	00 12	00	00 12	240.00 1275	00 13	1500.00 1330					

TABLE F-15 UNDISTURBED SAMPLE DATA, RAPID LOAD INCREMENTS

Sample B test No. 1 initial water content 237% initial void ratio 4.65 wt. dry specimen 29.5 gms.

Sample B test No. 2 initial water content 234% initial void ratio 4.65 wt. dry specimen 29.5 gms.

load applied	every 25 min. 10/12/72	load applied	every 15 min. 10/17/72
load 2	dial reading	load 2	dial reading
kg/cm <sup>2</sup>	in. x 10 <sup>4</sup>	kg/cm <sup>2</sup>	in. x 10 <sup>4</sup>
0.00	0	0.00	0
0.10	296	0.05	126
0.20	548	0.075	192
0.30	792	0.10	255
0.40	1002	0.15	409
0.60	1382	0.20	500
0.80	1714	0.25	649
1.00	1974	0.30	806
1.50	2450	0.35	919
2.00	2775	0.40	1025
3.00	3213	0.50	1226
4.50	3602	0.60	1396
		0.80	1712
		1.00	<b>1</b> 95 <b>9</b>
		1.50	2422
		2.00	2733
		1.00	2654
		0.40	2427
		1.04	2554
		1.75	2727
		2.24	2893
		3.24	3240
		4.24	3513
		0.40	3000
		0.10	2638

TABLE F-15.--Continued.

Sample F test No. 1 initial water content 165% initial void ratio 3.50 wt. dry specimen 39.4 gms.

Sample F test No. 2 initial water content 168% initial void ratio 3.52 wt. dry specimen 38.8 gms.

load applied	every 15 min. 11/9/72	load applied eve	ery 15 min. 11/15/72
load 2	dial reading	load 2	dial reading
kg/cm <sup>2</sup>	in. x 10 <sup>4</sup>	kg/cm <sup>2</sup>	in. x 10 <sup>4</sup>
0.00	0	0.00	0
0.05	65	0.05	58
0.10	132	0.10	121
0.20	261	0.20	233
0.30	408	0.30	357
0.40	517	0.40	449
0.50	607	0.50	536
0.60	707	0.60	615
0.70	816	0.70	699
0.80	91 <b>9</b>	0.80	796
1.00	1093	1.00	993
1.50	1497	1.50	1414
2.00	1838	2.00	1735
3.00	2272	3.00	2192
4.50	2691	4.50	2625
1.00	2412	1.00	2335
0.10	1904	0.10	1799

TABLE F-16 UNDISTURBED SAMPLE DATA

Sample B test no. 3, initial water content 230%, wt. dry specimen 30.4 oct. 23, 1972 gms

time	dial reading	time	dial reading	time	dial reading
min.	in. x 10 <sup>4</sup>	min.	in. x 10 <sup>4</sup>	min.	in. x 10 <sup>4</sup>
load	$.05 \text{ kg/cm}^2$	load	.40 kg/cm <sup>2</sup>	load	1.6 kg/cm <sup>2</sup>
0.00	0	0.00	0	0.00	0
0.10	43	0.10	74	0.10	93
0.25	54	0.25	107	0.25	133
0.50	66	0.50	145	0.50	178
1.00	78	1.00	195	1.00	245
2.25	90	2.25	259	2.25	351
4.30	96	4.00	300	4.00	431
6.25	99	6.25	32 <b>9</b>	6.25	488
12.25	103	9.00	350	12.25	559
36.00	111	12.25	364	25.00	620
750.00	132	16.00	373	50.00	655
	2	36.00	405	100.00	690
<u>load</u>	.10 kg/cm <sup>2</sup>	100.00	443	720.00	780
0.00	U	720.00	514		2
0.10	32		2	1oad	3.2 kg/cm <sup>2</sup>
0.25	45	<u>load</u>	.80 kg/cm <sup>2</sup>	0.00	0
0.50	60	0.00	U	0.10	91
1.00	78	0.10	<b>9</b> 5	0.25	126
2.25	99	0.25	133	0.50	166
4.00	111	0.50	180	1.00	225
6.50	120	1.00	248	2.25	322
9.00	125	2.25	352	4.00	410
12.25	130	4.00	430	6.25	466
100.00	158	6.25	485	9.00	510
700.00	185	9.00	520	12.25	542
	22 1 / 2	12.25	540	20.00	583
1oad	$.20 \text{ kg/cm}^2$	20.00	591	40.00	630
0.00	0	100.00	664	100.00	660
0.10	48	310.00	720	300.00	706
0.25	68	730.00	749	700.00	738
0.50	92				. 2
1.00	122			<u>load</u>	1.8 kg/cm <sup>2</sup>
2.25	158			0.00	O
4.00	180			720.00	<b>-</b> 259
6.25	194				. 2
9.00	204			load	
12.25	212			0.00	U
36.00	235			375.00	<del>-</del> 575
190.00	270				
710.00	296				

## TABLE F-17 UNDISTURBED SAMPLE DATA

Sample E test no. 4, initial water content 196%, wt. dry specimen 34.7 Nov. 1, 1972

			•		S
time	dial reading	time	dial reading	time	dial reading
min.	in. x 10 <sup>4</sup>	min.	in. x 10 <sup>4</sup>	min.	in. x 10 <sup>4</sup>
load	$.05 \text{ kg/cm}^2$	load	.40 $kg/cm^2$	load	$1.6 \text{ kg/cm}^2$
0.00	0	0.00	0	0.00	0
0.10	33	0.10	48	0.10	77
0.25	44	0.25	66	0.25	106
0.50	55	0.50	87	0.50	138
1.00	69	1.00	104	1.00	183
2.25	85	2.25	122	2.25	260
4.00	96	4.00	139	4.00	331
7.00	106	6.25	154	6.25	393
9.00	109	12.25	167	9.00	446
12.25	113	16.00	173	15.00	542
16.00	116	66.00	203	25.00	603
27.00	121	100.00	214	55.00	680
100.00	133	300.00	226	100.00	720
300.00	142	675.00	236	300.00	770
730.00	149		oad increment)	685.00	782
load	.10 kg/cm <sup>2</sup>	load	.80 kg/cm <sup>2</sup>	1oad	3.2 kg/cm <sup>2</sup>
0.00	0	0.00	0	0.00	0
0.10	12	0.10	100	0.10	72
0.25	20	0.25	140	0.25	44
0.50	27	0.50	185	0.50	132
1.00	38	1.00	256	1.00	170
2.25	52	2.25	352	2.25	239
4.00	65	4.00	429	4.00	298
6.25	75	6.50	506	6.25	350
9.00	81	9.00	553	9.00	<b>397</b>
16.00	90	12.25	602	15.00	464
30.00	98	16.00	638	25.00	520
100.00	115	25.00	693	55.00	588
710.00	138	54.00	765	1.00.00	623
, 10.00		100.00	810	300.00	691
load	$.20 \text{ kg/cm}^2$	300.00	862	720.00	708
0.00	0	735.00	758	720.00	700
0.10	22	733.00	750	1oad	.80 kg/cm <sup>2</sup>
0.25	33			0.00	0
0.50	41			745.00	-228
1.00	65				
2.25	87			load	.10 $kg/cm^2$
4.00	100			0.00	0 kg/cm
6.25	112			670.00	<b>-</b> 503
9.00	122			370.00	-505
15.00	133				
30.00	142				
100.00	153				
300.00	164				
775.00	173				
113.00	1/3				

## TABLE F-18 UNDISTURBED SAMPLE DATA

Sample F test no. 3, initial water content 170%, wt. dry specimen 39.0 Nov. 27, 1972 gms

time	dial reading	time	dial reading	time	dial reading
min.	in. x 10 <sup>4</sup>	min.	in. x 10 <sup>4</sup>	min.	in. x 10 <sup>4</sup>
load	.05 kg/cm <sup>2</sup>	load	.40 kg/cm <sup>2</sup>	load	1.6 kg/cm <sup>2</sup>
0.00	0	0.00	0	0.00	0
0.10	30	0.10	45	0.10	75
0.25	38	0.25	61	0.25	102
0.50	46	0.50	80	0.50	134
1.00	57	1.00	107	1.00	182
2.25	68	2.25	141	2.35	258
4.00	74	4.00	165	4.00	325
6.25	78	6.25	180	6.25	379
9.00	80	9.00	190	9.00	423
12.25	82	12.25	198	12.25	451
100.00	90	32.00	218	20.00	500
830.00	99	100.00	242	40.00	545
	10.1. / 2	700.00	281	100.00	597
load	$.10 \text{ kg/cm}^2$		2	300.00	650
0.00	0	load	.80 kg/cm <sup>2</sup>	730.00	683
0.10	18	0.00	0		•
0.25	23	0.10	67	load	3.2 kg/cm <sup>2</sup>
0.50	29	0.25	92	0.00	0
1.00	36	0.50	119	0.10	79
2.25	45	1.00	154	0.25	108
4.00	50	2.25	206	0.50	143
6.25	54	4.00	242	1.00	196
9.00	56	6.25	268	2.25	287
100.00	73	9.00	287	4.00	368
600.00	86	12.25	302	6.25	437
	201 / 2	40.00	360	9.00	493
1oad	$.20 \text{ kg/cm}^2$	100.00	38 <b>5</b>	12.25	534
0.00	0	200.00	405	30.00	635
0.10	26	720.00	435	50.00	670
0.25	34			110.00	720
0.50	44			275.00	750
1.00	56			750.00	783
2.25	72				•
4.00	82			load	.80 kg/cm <sup>2</sup>
6.25	90			0.00	0
12.25	99			660.00	<del>-</del> 277
113.00	127				
740.00	152			load	.10 kg/cm <sup>2</sup>
				0.00	. 0
				650.00	<b>-</b> 593

TABLE F-19 UNDISTURBED SAMPLE DATA

Sample F test no. 4, initial water content 163%, wt. dry specimen 40.1 pec. 6, 1972 gms

time min.	dial reading in. x 10 <sup>4</sup>	time min.	dial reading in. x 104	time min.	dial reading in. x 10 <sup>4</sup>
	.05 kg/cm <sup>2</sup>		.40 kg/cm <sup>2</sup>		1.6 kg/cm <sup>2</sup>
0.00	0	0.00	0	0.00	0
0.10	28	0.10	28	0.10	75
0.25	34	0.25	37	0.25	99
0.50	40	0.50	48	0.50	126
1.00	47	1.00	62	1.00	167
2.25	57	2.25	84	2.25	239
4.00	63	4.00	100	4.00	305
6.25	67	6.25	112	6.25	354
9.00	70	9.00	121	9.00	395
12.25	71	12.25	127	12.25	426
16.00	73	32.00	145	16.00	450
175.00	82	100.00	163	32.00	500
710.00	87	300.00	180	70.00	548
11	10.1./2	660.00	192	134.00	581
10ad	.10 kg/cm		20 100/002	414.00	624
0.00	0	load	.ou kg/cm	1200.00	668
0.10	16	0.00	0		2 2 1 / 2
0.25	20	0.10	70		3.2 kg/cm
0.50	25	0.25	90	0.00	0
1.00 2.25	30 38	0.50	113	0.10	76
4.00	43	1.00	146	0.25	99
6.25	43	2.25	198	0.50	130
9.00	49	4.00	239	1.00	175
12.25	51	6.25	267	2.25	251
16.00	52	9.00 12.25	291	4.00	323
100.00	64		309	6.25	388
725.00	77	32.00 100.00	350	9.00 12.25	442
723.00		300.00	391 421		482 515
load	$.20 \text{ kg/cm}^2$	740.00	446	16.00 32.00	515 593
$\frac{1000}{0.00}$	0	740.00	440	100.00	665
0.10	23			400.00	725
0.25	29			970.00	723 757
0.50	36			370.00	757
1.00	45			1oad	.80 kg/cm <sup>2</sup>
2.25	58			0.00	0
4.00	67			430.00	-264
6.25	73			.55.00	
9.00	78			load	.10 kg/cm <sup>2</sup>
16.00	84			0.00	0
67.00	99			930.00	<b>-</b> 558
360.00	117				233
710.00	127				

### APPENDIX G

COMPUTER PROGRAM FOR LOAD INCREASING LINEARLY WITH TIME FOLLOWED BY AN INSTANTANEOUS SURCHARGE APPLICATION

```
PROGRAM SLUDGE ( INPUT.OUTPUT)
      DIMENSION P(20.200). TP(20.200), U1(200), U2(200). PP(200). I(200)
     1. TM1(200).TM2(200)
()
C.
      EN = CONTROL CARD (1F=1.0 PROGRAM TERMINATES)
      NCV = COFF. OF COMSOL. X 10**3 IN. **2/MIN. (CVI) INTEGER FORM
C
C
      NH = AVG. THICKNESS OF LAYER (IN.) DURING LINEAR LUADING
      NOT = TOTAL TIME OF LINEAR LUAD IN MIN.
C
\mathcal{C}
       I != INCREMENTS OF TIME SOLVED AFTER SURCHARGE APPLICATION
      CVI = COEF. OF CONSUL. OF LAYER DURING LINEAR EVAULING
      GAMI TO GAMB = UNIT WT. OF MATL + S USED IN LINEAR LUAD SEGMENT
C
      GAM4 = UNIT WT. OF SURCHARGE MAT = L
(
      HI TO H3 = HT. OF MATZLS IN LINEAR LUAD SEGMENT
(
      H4 = HI. OF SURCHARGE MAT≠L
C
      CV2 = COEF. OF CUNSOL. UF LAYER AFTER SURCHARGE LUADING
C
      P(1,M) TO P(9,M) = INITIAL VALUES OF PORE PRESSURE
C
      ULTS = ULTIMATE PRIMARY SETTLEMENT UNDER TOTAL LOAD (IN.)
С
      HN1 = INITIAL THICKNESS OF LAYER (IN.)
C
   50 READ 3. EN
    3 FORMAT (F10.3)
      IF (EN.EU.1.0) 300.40
   40 READ 2.NCV. NH. NOT. I. CVI. GAMI, GAM2. GAM3. GAM4
    2 FORMAT (415,5F13.3)
      READ4.H1.H2.H3.H4.CVZ
    4 FORMAT (5F10.3)
      M = 1
      READ 5. (P(L.M).L=1.9)
    5 FORMAT (9F8.2)
      READ 69.ULTS.HILL
   69 FORMAT(2F10.0)
C
C
      DETERMINE NO. OF INCREMENTS FOR SIEP FUNCTION DETERMINED BY THE
C
      VALUES OF CV+DT+AND H
      NXDT = (4*NCV*NDT*96)/(100C*NH*NH)
      TUXN = TUX
      HN=NH
      Y = GAM] #H1 + GAM2 #H2 + GAM3 #H3
      Z = GAM4#H4
      X = Y/XI)
C
C
      SET HOUNDARY PURE PRESSURES = 0.00 FOR ALL TIMES
C
      DO 7 N = 1.200
      P(1 \bullet N) = 0.00
      P(9*N) = 0.00
      TP(1 \cdot 1) = 0.00
      TP(\neg \bullet \Theta) = 0.00
    7 CONTINUE
```

```
C
      CALCULATE PURE PRESSURES GENERATED BY UNIT INCREASES IN STEP LUAD
C
      (LINEAR LOADING) FOR EACH TIME INCREMENT
C
C
      LXDT = NXDT-1
      DO'6K = 1 \cdot LXDT
      D0!9 L = 2.8
      P(L_{*}K+1) = P(L_{*}K)*2./3.+(P((L+1)_{*}K)+P((L-1)_{*}K))*1./6.+1.00
    9 CONTINUE
    6 CONTINUE
C
      CALCULATE ACTUAL PURE PRESSURES GENERATED AT END OF LINEAR LOADING
C
C
      (IN PSF)
C
      D0: 10 L = 1.9
      PP(L) = X*P(L*NX)T
   10 CONTINUE
C
      CALCULATE PERCENT CONSOLIDATION UNDER THE EXISTING APPLIED STRUSS
C
      FOR THE LINEAR LUADING (USING TRAPEZUIDAL RULE)
С
C
      SUM = 0.00
      XT = 0.00
      DOI 11 K = 1,NXUT
      |XT| = |XT+1.00|
      D0: 12 L = 1.8
      B \models ((2.4xT)-P(L.K)-P((L+1).K))/(16.04xT)
      SUM = SUM + B
   12 CONTINUE
      U_1(K) = SUM * 100.0
      SUM = 0.00
   11 CONTINUE
C
      SET INITIAL VALUES OF PORE PRESSURE FOR SURCHARGE INCREMENTAL
C
      LOADING. HERE Z (OR TP(L.1)) COULD BE MADE EQUAL TO FIELD VALUES
C
C
      D0: 13 L = 2.8
      TP(L+1) = PP(L)+Z
   13 CONTINUE
C
      CALCULATE PURE PRESSURES. PERCENT CONSOLIDATION. AFTER SURCHARGE
C
      APPLICATION
C
      J= I - 1
      DO 15 K= 1.J
      DO 17 L = 2.8
      TP(L+K+1) = TP(L+K)+2./3.+(TP((L+1)+K)+TP((L-1)+K))+1./6.
   17 CONTINUE
   15 CONTINUE
      DSUM = 0.0
      D0 20 K = 1 \cdot I
      DO 21 L = 1.8
      1) = ((Y+Z)*2.-TP(L*K)-TP((L+1)*K))/(16.4*(Y+Z))
      DSUM = DSUM + D
```

```
21 CONTINUE
       U2(K) = D5UM*160.
       DSUM = 0.00
   20 CONTINUE
       T(1) = 0.00
       TMI(1) = 0.0
       TM2(1) = 0.00
       DO 30 N = 2.200
       T(N) = T(N-1)+1./96.
       TM1(N) = (T(N) *HN *HN) / (4.0 *CV1 *1440.)
   30 CONTINUE
       Do 29 N=2.1
       H=HN1-(U2(N)+U2(N-1))/200.4ULTS
       TM2(N) = (T(N) *H*H) / (4.0*CV2*1440.)
  -29 CONTINUE
C
       PRINT JUT VALUES
       PRINT 39 NXDT + CV1 + NH + X + Y + Z
   39 FOHMAT(#14,4NXDT = 4,13,2X,4CV1 = 4,F5,3,1X,4Su. IN./M1N.4,2X,4NH
      1= 4.13.1X.41N.4.2X.4X = 4.F5.2.1X.4PSF/INCHEMENT4.2X.4Y = 4.F6.1.1
     2X, #PSF (LINFAR STRESS) # + 2X, #Z = # + F5 . 1 , 1X , #PSF (SURCHARGE) #)
       PRINT 31
   31 FORMAT(***-331-*PORE PRESSURES* PERCENT COMSOLIDATION* DUE TO LINE
     TAR APPLIED STRESSED
       PRINT 33
   33 FORMAT(#0#+18X+#H=0#+5X+#H/5#+5X+#H/4#+5X+#3H/8#+4X+#H/2#+5X+
      1#5H/9#•4X•#3H/4#•4X•#7H/8#•5X•#H#•8X•#U#•7X•#TIME•DAYS#)
       DO 100 K = 1.000T
       PRIN[ 35 \cdot K \cdot I(K) \cdot (P(L \cdot K) \cdot L = 1 \cdot 9) \cdot UI(K) \cdot [MI(K)
   35 FORMAT(*0**13*1X**T = **F7.5*9F8.2*F8.1*F8.1)
  100 CONTINUE
       PRINT 41 \cdot (PP(L) \cdot L = 1 \cdot 9) \cdot UI(NXDT)
   41 FORMAT(*0*.*PP ( IN PSF )*.1X.10F8.1)
       PRINT 80 + CV2
   80 FORMAT(#0#+15X+#PORE PRESSURES+ PERCENT CONSOLIDATION+ DUE TO SURC
     1HARGE AND LINEAR LOAD++5X++CV2 = ++F5.3+1X++SQ. IN. PER MIN.+)
       PRINT 33
       D0:101 K = 1.1
      PRINT 45 \cdot K \cdot T(K) \cdot (P(L \cdot K) \cdot L = 1 \cdot 9) \cdot U2(K) \cdot TMZ(K)
   45 FORMAT(*0*•13•1X•*1 = *•F7•5•9F8•0•F8•1•F8•1)
  101 CONTINUE
      GO TO 50
  300 CONTINUE
      END
```

#### APPENDIX H

# COMPUTER PROGRAM FOR THE SOLUTION TO THE EQUATIONS IN THE THEORY OF GIBSON AND LO (1961)

```
PROGRAM GIRSON (INPUT. DUTPUT)
      REAL LAMI
      DIMENSION 5 (90)
      I = NO. OF TIMES DESIRED FOR SETTLEMENT COMPUTATION.
C
      00 = APPLIED LUAD (PSI)
C
C
      A = PRIMARY COMPRESSIBILITY (SU. 19./LIG.)
      B = SECONDARY COMPRESSEREETTY (SW.19./LM.)
C
      LAMI = VISCUSITY (LR./50.1N./MIN.)
С
      HI = LAYER THICKNESS (IN.)
C
      CV = COEFFICIENT OF CONSOLIDATION (SW.11./MIN.)
C
C:
      T = TIME (HOURS)
C
      READ PRIMARY DATA
C
      REAU 3.1.400.A.H.LAMI.HI.CV
    3 FORMAT (15.6F10.0)
      L=0
      J=v
      S(0)=0.0
   50 CONTINUE
      M=0
      IF (J.E0.1) 60 TO 43
      H=H1/2.0
      H=H-S(J)/2.0
C'
      READ TIME FOR SETTLE OF AT COMPHIATION
C:
C
      REAU 4.T
    4 FORMAT (F10.0)
      J=J+1
      XM=1.0+8/A
      XM=(H442)/(B4CV4LAN_)
      T1=T#60.
      UL [5=(A+H)#06#H]
      CALCULATE SETTLEMENT AT TIME = 1
      SUM=0.0
      DO 20 N=1.25.2
      11=NY
      XK1=(N*#2#3.1416##2#Cy)/(4.0#H##2)
      ALPHA=(1.6/A+1.5/6)/LA41
      BF [A=1.0/(LAM1+h)
      XT1=((ALPHA+XK1)##2-(A. ***2ETA*XK1))
      T2=504T(XII)
      KI=ALPHA+AKI
```

```
X11 = (R1 + \Gamma 2) / 2.0
       X22=(R1-T2)/2.0
       V3=-1.0*X!]#T!
       V4=-1.0*X22*T1
       V5=EXP(V3)
       V6=EXP(V4)
       X \times 2 = A / (A + H) # X K ]
       E = (XK2 - X11) / (X11 - X22)
       E1=t*V6
       E_{2}=(x_{1}x_{2}-x_{2}x_{2})/(x_{1}x_{1}-x_{2}x_{2})
       E3=E2#V5
       G= (+1-+3)/YH##2
       SUM=5UM+17
   20 CONTINUE
       R=1.0+((8.0/3.1415##4)#5UM)
       S(J)=ULTS#K
       XT=4.0/3.14164((A+H)/A)*44
       L=H/4.U
   18 CONTINUE
C
       CALCULATE PORE PRESSURES OF TIME = I
C^{!}
       SUM1=0.0
       00 22 8=1.51.2
       ZN=V
       XK1=(N**2*3.1416**2*CV)/(4.J*H**2.)
       ALPHA=(1.0/A+1.6/8)/LAH1
       BETA=1.0/(LAM]#H)
       XT1=((ALPH4+XK1) ##2-(4.0#HETA#XK1))
       T2=5QRT(AT1)
       R1=ALPHA+XK1
       X11 = (R1 + T2)/2.3
       X22 = (R1 - L5)/5 \cdot 3
       V1=A/(A+d)-x22/xv1
       V \supset = A / (A + B) - X = I / X B 
       V3=-1.04X114T1
       V4=-1.04X224[]
       Vc=FXP(Y3)
       V6=EXP(V4)
       W1 = (X114V1) / (X11-X22) #V5
       W2=(X22#V2)/(X11-X22)#V5
       W3=(N#3.1416#/)/(2.#m)
       W4=5IN(W3)
       Y=(W1-W2)#84
       Y]=Y/24
       SUMI=5'M1+Y1
    22 CONTINUE
       U=X1#SUM1
       L=L+1
       IF(L.oT.1)60 TO 7
```

```
6 PRINT 80
BC FORMAT (*1*, *TIME (HOURS) *. IOX, *SETTLEMENT (INCHES) *. IOX, *DEPTH (IN
  1.) * . 10 X . * PORE PRESSURE (PS1) * . 10 X . * SUM * . 10 X . * SUM 1 * )
 7 PZ=H/4.0
   IF (Z.EU.PZ) N.13
 6 PRINT 90.1.5 (J) . Z. + U + 5 UM + 5 UM 1
90 FORMAT(#O#+3x+Fb+)+10x+F14+2+14x+F10+1+13x+F10+2+13x+F10+4+5x+F10+
  14)
 9 IF (Z) EQ. PZ) 60 TO 11
1J PRINT 91./.U
91 FORMAT(#0#+49X+F10.1+13X+F10.2)
11 M = M + 1
   IF (M. EQ. 4) GU TO 53
   Z=7+H/4.)
   GO TO 18
40 CONTINUE
   END
```

•

